The Control Valve as a Universal Steam Trap Replacement

by

© Craig Joseph Mercer

A Thesis submitted to the

School of Graduate Studies in partial fulfillment of the requirements for the degree

of

Master of Engineering (M.Eng.)

Faculty of Engineering and Applied Science

Memorial University of Newfoundland

October 2015

St. John's, Newfoundland and Labrador

ABSTRACT

The steam trap is considerably overlooked and unappreciated within the steam and condensate distribution system. Its role is to remove condensate and non-condensables from the primary steam loop. However, the conventional methods used today are the devices developed a century ago. An original study was conducted to evaluate the universal replacement of conventional steam trap technology with control valves. The condensate flowrate is determined by using a standardized steam trap performance test. During experimentation, the mass flowrate is acquired through the utilization of a weigh tank technique. Results indicated that the application of a control valve is feasible and provides remarkable advantages over the traditional approach. Improvements to enhance efficiency and effectiveness are evident through the performance attributes of the control valve, which includes auxiliary prediction and diagnostic capabilities. A response surface methodology successfully validates the use of theoretical models for practical design consideration.

ACKNOWLEDGEMENTS

I would like to thank Dr. Michael Hinchey for his continual support and timely advice. His mentorship was instrumental in both my undergraduate and graduate engineering studies, which enabled me to become proficient as a practicing engineer. I was able to complement academia with a practical applied understanding of thermal sciences. The result has allowed me to identify and pursue research that promoted passion, enjoyment, and a conviction to positively contribute to environmental sustainability.

Throughout my industrial experience, Western Health was fundamental in my personal and professional development; including the exposure to specialized equipment, training, and professionals. The competent and professional leadership of Dr. Susan Gillam, Devon Goulding, and Keith Allen supported my creativity and nurtured a progressive environment to meet the needs of clients, patients, and residents. Sometimes the greatest engineering accomplishments were achieved though unconventional methods. Also, I want to recognize the invaluable knowledge I acquired from Art Munden, Randy King, Jim Rowsell, Con Stacey, Joseph Benoit, and Julian O'Gorman. In many ways they have taught me more about steam and condensate than I could ever learn through literature.

Johnson Controls, Clayton Industries, Maynard Reece, Spirax Sarco, and Honeywell are warrant recognition for advancing my knowledge in the field of thermodynamics. Specific individuals include Paul Tulk, Saeed Baccus, Walter Collier, Bill Walker, and Ray Greene.

The unequivocal support of my family cannot be overstated. The nurturing demeanor of my father, mother, and brother has instilled strong values of education, work ethic, and life philosophies. I am in most part the person I am today because of the love and devotion I received from Ronald Mercer Sr., Barbra Mercer, and Ronald Mercer Jr.. Thank you for being there, being present, and having a profound effect on my life.

For my wife, Crystal Mercer, I would not be complete without your presence in my life. You bring me hope, happiness, and a future full of possibilities. My father said it best during our wedding: “When you see one, you see the other”. The reason is obvious; my wife is also my best friend. Thank you for believing in me and supporting all my endeavors.

Table of Contents

ABSTRACT ii

ACKNOWLEDGEMENTS iii

Table of Contents v

List of Tables x

List of Figures xi

Abbreviations xiv

Nomenclature xv

List of Appendices xvii

-1- Introduction 1-1

1.1 - Problem Statement 1-1

1.2 - Motivation for Study 1-5

1.3 - Objectives and Scope of Work 1-7

1.4 - Outline 1-9

-2- Literature Review 2-1

2.1 - Steam Utilization 2-1

2.2 - Steam Traps 2-3

2.2.1 - Introduction 2-3

2.2.2 - Purpose 2-3

2.2.3 - History 2-4

2.2.4 - Variations 2-5

2.2.4.1 - Mechanical 2-5

2.2.4.2 - Thermostatic 2-6

2.2.4.3 - Thermodynamic 2-7
2.2.4.4 - Orifice Trap 2-7
2.2.4.5 - Emerging 2-9
2.2.5 - Selection 2-9
2.3 - Hazards 2-11
2.3.1 - Introduction 2-11
2.3.2 - Theory 2-12
2.3.3 - Prevention 2-13
2.4 - Plant Efficiency 2-15
2.5 - System Diagnostics 2-16
2.6 - Sustainable Design 2-19
2.7 - Control Valves 2-19
2.8 - Mass Flowrate Prediction Modeling 2-21
2.9 - Summary 2-28
-3- Experimental Procedures 3-1
3.1 - Apparatus 3-1
3.1.1 - Introduction 3-1
3.1.2 - Weigh Tank Technique 3-1
3.1.3 - Physical Description 3-2
3.1.3.1 - Introduction 3-2
3.1.3.2 - Supply and Weigh Tank 3-5
3.1.3.3 - Sensors 3-6
3.1.3.4 - Circulation Pump 3-7

3.1.3.5 - Data Acquisition and Control 3-7
3.1.3.6 - Control Valves and Piping 3-7
3.1.3.7 Testing Fluid 3-8
3.1.4 - Design and Fabrication 3-9
3.1.4.1 – Introduction 3-9
3.1.4.2 - Pipe Network 3-9
3.1.4.3 - Condensate Control Valve 3-10
3.1.4.4 - Supply Reservoir 3-13
3.1.4.5 - Motive Pressure Control Valve 3-13
3.1.4.6 - Control Strategy 3-15
3.1.4.7 - Safety 3-18
3.1.5 - Operation 3-19
3.1.5.1 – Introduction 3-19
3.1.5.2 - Measurement 3-19
3.1.5.3 - General 3-21
3.1.5.4 - System Initialization Test Procedures 3-24
3.1.5.5 - Condensate Preparation Test Procedures 3-24
3.1.5.6 - Experimentation Test Procedures 3-25
3.1.5.7 - Condensate Recovery Test Procedures 3-26
3.1.6 - Operational Issues 3-27
3.1.6.1 - Motive Pressure Control 3-28
3.1.6.2 -Condensation Induced Water Hammer 3-29
3.1.6.3 - Hard-to-Change Factor 3-30

3.2 - Design of Experiment 3-32
3.2.1 - Introduction 3-32
3.2.2 - Factors 3-33
3.2.3 - Levels and Range 3-33
3.2.4 - Design Type 3-35
3.2.5 - Model Validation and Confirmation 3-38
3.3 - Sample Preparation 3-40
3.3.1 - Initial Fill 3-40
3.3.2 - Oxygen Removal 3-41
3.3.3 - Experimental Factors 3-41
3.4 - Mass Flowrate Calculation 3-41
3.4.1 - Introduction 3-41
3.4.2 - Mass Flowrate Methodology 3-42
3.4.3 - Data Fitting 3-42
3.4.3.1 – Introduction 3-42
3.4.3.2 - Regression Model 3-43
3.4.3.3 - Regression Evaluation 3-44
3.5 - Experimental Error and Uncertainty 3-44
3.5.1 - Introduction 3-44
3.5.2 - Mass Flowrate 3-45
3.5.3 - Results 3-48
3.5.4 - Discussion 3-50
3.5.5 - Method of Analysis 3-50

-4- Results and Discussion 4-1
4.1 - Introduction 4-1
4.2 - Mass Flowrate 4-1
4.3 - Discharge Pressure 4-14
4.4 - Flow Visualization 4-28
4.5 - Literature Comparison 4-31
4.5.1 - Introduction 4-31
4.5.2 - Results 4-33
4.5.3 - Discussion 4-37
4.5.3.1 – Prediction Model 4-37
4.5.3.2 – Flowrate Capacity 4-40
4.5.3.4 – Control Valves 4-42
-5- Conclusions and Recommendations 5-1
5.1 - Conclusion 5-1
5.2 - Contribution to Science 5-2
5.3 - Recommendations 5-3
-6- Bibliography 6-1
Appendix A - Physical Experimental Apparatus A-1
Appendix B - Instrumentation Calibration Reports B-1
Appendix C - Uncertainty Analysis C-1
Appendix D - Source Code D-1
Appendix E - Experimental and Confirmation Trial Data (Graphical) E-1
Appendix F - Flow Visualization Apparatus F-1

List of Tables

Table 3-1: Municipal water quality 3-8

Table 3-2: Range and level for experimental design 3-34

Table 3-3: Confirmation trials for experimentally acquired model 3-36

Table 3-4: Experimental trials for response surface methodology 3-37

Table 3-5: Overall and relative uncertainty for experimental trials 3-49

Table 4-1: Mass flowrate response 4-2

Table 4-2: Mass flowrate model summary evaluation 4-3

Table 4-3: Mass flowrate analysis of variance 4-4

Table 4-4: Mass flowrate goodness of fit characteristics 4-4

Table 4-5: Discharge pressure response 4-15

Table 4-6: Discharge pressure model summary evaluation 4-16

Table 4-7: Discharge pressure analysis of variance 4-16

Table 4-8: Discharge pressure goodness of fit characteristics 4-17

Table 4-9: Thermodynamic properties (Lemmon, E. W et al., 2005) 4-32

Table 4-10: Theoretical and empirical prediction models 4-33

Table 4-11: Theoretical and empirical prediction models (modified) 4-35

List of Figures

Figure 1-1: Primary and secondary steam and condensate loop (Spirax Sarco, 2015).... 1-2

Figure 1-2: Steam trap function 1-3

Figure 1-3: Pictorial schematic of application and research intent..... 1-10

Figure 2-1: Reference terminology and phase diagram for an isobar..... 2-2

Figure 2-2: Mechanical steam traps (Paikin, 1981) 2-6

Figure 2-3: Thermostatic steam traps (Paikin, 1981)..... 2-6

Figure 2-4: Thermodynamic steam traps (Paikin, 1981) 2-7

Figure 2-5: Orifice steam traps (Dickman, 1984)..... 2-8

Figure 2-6: Emerging steam trap with diagnostic capabilities (Rebik, 2001) 2-9

Figure 2-7: Ideal flow characteristics for control valves (ASHRAE, 1985)..... 2-20

Figure 3-1: Schematic for experimental apparatus 3-3

Figure 3-2: Graphical user interface for the experimental mode..... 3-22

Figure 3-3: Graphical user interface for the circulation mode..... 3-23

Figure 3-4: Graphical user interface for the purge mode..... 3-23

Figure 3-5: Transient condition for experimental startup 3-28

Figure 3-6: Condensation induced water hammer 3-30

Figure 3-7: Graphical user interface for timing circuit..... 3-31

Figure 3-8: Standard error of response surface design 3-36

Figure 3-9: Experimental and confirmation trials (pressure and temperature)..... 3-39

Figure 3-10: Experimental and confirmation trials (valve position and pressure) 3-39

Figure 3-11: Experimental and confirmation trials (valve position and temperature)... 3-40

Figure 3-12: Sensitivity analysis for mass flowrate (supply pressure) 3-47

Figure 3-13: Sensitivity analysis for mass flowrate (supply temperature) 3-48

Figure 4-1: Mass flowrate normal probability plot 4-5

Figure 4-2: Mass flowrate variance plot 4-6

Figure 4-3: Mass flowrate randomization plot 4-6

Figure 4-4: Mass flowrate prediction 4-7

Figure 4-5: Mass flowrate Box-Cox plot 4-7

Figure 4-6: Mass flowrate variance plot (residuals and block) 4-8

Figure 4-7: Mass flowrate variance plot (residuals and pressure) 4-8

Figure 4-8: Mass flowrate variance plot (residuals and temperature) 4-9

Figure 4-9: Mass flowrate variance plot (residuals and valve position) 4-9

Figure 4-10: Mass flowrate interaction plot (pressure and valve position) 4-12

Figure 4-11: Mass flowrate interaction plot (temperature and valve position) 4-12

Figure 4-12: Mass flowrate cube plot 4-13

Figure 4-13: Mass flowrate perturbation plot 4-14

Figure 4-14: Discharge pressure normal probability plot 4-18

Figure 4-15: Discharge pressure variance plot 4-18

Figure 4-16: Discharge pressure randomization plot 4-19

Figure 4-17: Discharge pressure prediction 4-19

Figure 4-18: Discharge pressure Box-Cox plot 4-20

Figure 4-19: Discharge pressure variance plot (residuals and block) 4-20

Figure 4-20: Discharge pressure variance plot (residuals and pressure) 4-21

Figure 4-21: Discharge pressure variance plot (residuals and temperature)..... 4-21

Figure 4-22: Discharge pressure variance plot (residuals and valve position) 4-22

Figure 4-23: Maximum discharge pressure contour plot (pressure and temperature) ... 4-24

Figure 4-24: Minimum discharge pressure contour plot (pressure and temperature).... 4-25

Figure 4-25: Discharge pressure interaction plot (pressure and valve position) 4-26

Figure 4-26: Discharge pressure interaction plot (temperature and valve position)..... 4-26

Figure 4-27: Discharge pressure cube plot 4-27

Figure 4-28: Discharge pressure perturbation plot 4-28

Figure 4-29: Saturated liquid flow visualization (minimal valve position)..... 4-29

Figure 4-30: Saturated liquid flow visualization (maximum valve position)..... 4-30

Figure 4-31: Condensing two-phase mixture..... 4-30

Figure 4-32: Theoretical and empirical prediction models..... 4-34

Figure 4-33: Mass flowrate contour plot for pressure versus temperature 4-34

Figure 4-34: Theoretical and empirical prediction models (modified)..... 4-35

Figure 4-35: ISA-I model versus EAM model CI/TI (95%)..... 4-36

Figure 4-36: HNE-DS model versus EAM model CI/TI (95%) 4-37

Figure 4-37: Steam trap capacity chart (Armstrong, 2015) 4-41

Figure 4-38: Distribution energy loss for inadequate condensate removal 4-43

Figure 4-39: Energy losses for steam trap failures 4-44

Figure 4-40: Recovery pressure for a subcooled liquid (Hutchison, 1971)..... 4-45

Figure 4-41: Effect of air on heat transfer (Spirax Sarco, 2015) 4-48

Figure 4-42: Effect of air on steam temperature (Spirax Sarco, 2015)..... 4-49

Abbreviations

ANOVA	Analysis of Variance	LC1	Load Cell 1
ASME	American Society of Mechanical Engineers	LEED	Leadership in Energy and Environment Design
BBD	Box-Behnken Design	MAD	Median Absolute Deviation
CCD	Central Composite Design	OFAT	One-Factor-at-a-Time
CFC	Chloral Floral Carbon	PID	Proportional Integral Derivative
DAQ	Data Acquisition	PRV	Pressure Reducing Valve
EAM	Empirical Acquired Model	PT1	Pressure Transducer 1
FSO	Full-Scale Output	PT2	Pressure Transducer 2
HE	Homogenous Equilibrium	R^2	Coefficient of Determination
HF	Homogenous Frozen	RMSE	Root Mean Squared Error
HNE	Homogenous Non-Equilibrium	RTD1	Resistance Temperature Detector 1
HNE-DS	Homogenous Non-Equilibrium Diner & Schmidt	SSE	Error Sum of Squares
I/P	Current to Pressure	TSM	Taylor Series Method
ISA	International Society of Automation	VP1	Valve Position 1

Nomenclature

a	Boiling delay exponent	N_6	Numerical constant
a^*	Wave speed	0	Stagnation
C_P	Specific heat	P	Pressure
C_v	Flow coefficient	P_c	Critical pressure
D	Internal pipe diameter	l	Liquid phase
E	Equilibrium	Pu	Borderline period
F_d	Valve style modifier	P_V	Vapor pressure
F_F	Critical pressure ratio	Q^*	Control signal
F_L	Pressure recovery factor	Q	Volumetric flowrate
F_γ	Specific heat ratio	r	Residuals
G	Mass flux	R	Reaction rate
g	Vapor phase	R^*	Valve lift
h_i	Leverage of residuals	r_{adj}	Adjusted residuals
h	Enthalpy	R_e	Reynolds number
k_p	Proportional gain	s	Entropy
k_u	Borderline gain	T	Temperature
L	Lag time	t	Throat
n	Thermal equilibrium	T_D	Derivative parameter
N	Boiling delay factor	T_I	Integral parameter
N_1	Numerical constant	u	Standardized residuals
N_2	Numerical constant	W	Mass flowrate
N_4	Numerical constant	W^*	Weighting function

x	Vapor quality	ΔU	Velocity differential
X_T	Choked pressure ratio	η	Critical pressure ratio
Y	Expansion factor	ρ_1	Density at PT1 and RDT1
α	Void fraction	ρ_1/ρ_0	Relative density
γ	Isentropic exponent	τ	Valve rangeability
Δh_{fg}	Latent heat of vaporization	υ	Specific volume
ΔP	Pressure differential	ψ	Expansion factor
Δt	Time differential	ω	Compressibility factor

List of Appendices

Appendix A – Physical Experimental Apparatus A-1

Appendix B – Instrumentation Calibration Reports B-1

Appendix C – Uncertainty Analysis C-1

Appendix D – Source Code D-1

Appendix E – Experimental and Confirmation Trial Data (Graphical)..... E-1

Appendix F – Flow Visualization Apparatus F-1

-1- Introduction

1.1 - Problem Statement

Renewable and non-renewable resources are increasingly being depleted due to exponential population growth and demand through contemporary consumerism. Both industry and the general public have a moral obligation to preserve existing resources and protect the earth. Unfortunately environmental damage from the past may be irreversible, but with future considerations and substitutive choices, an alternate course of action can be instituted. The ultimate focus must be on developing sustainability to realize a lasting effect. Resources that are consumed must be done so in an efficient manner. Continuance of status quo practices has to be challenged, and improved methods implemented.

Promoting sustainable development within the steam industry involves recognizing opportunities to reduce environmental resources and pollution, without sacrificing corporate mandates. The author recognizes a significant void to effectively remove condensate and non-condensables from the primary loop. The deficiency is considerable because the primary loop contains steam production, distribution, and point of use processes. Insufficient removal of condensate and non-condensables reduces thermal energy for delivery, while increasing equipment damage, life safety issues, maintenance, and plant start-up. Figure 1-1 presents a generic primary and secondary loop for a steam plant as adapted from Spirax Sarco (2015).

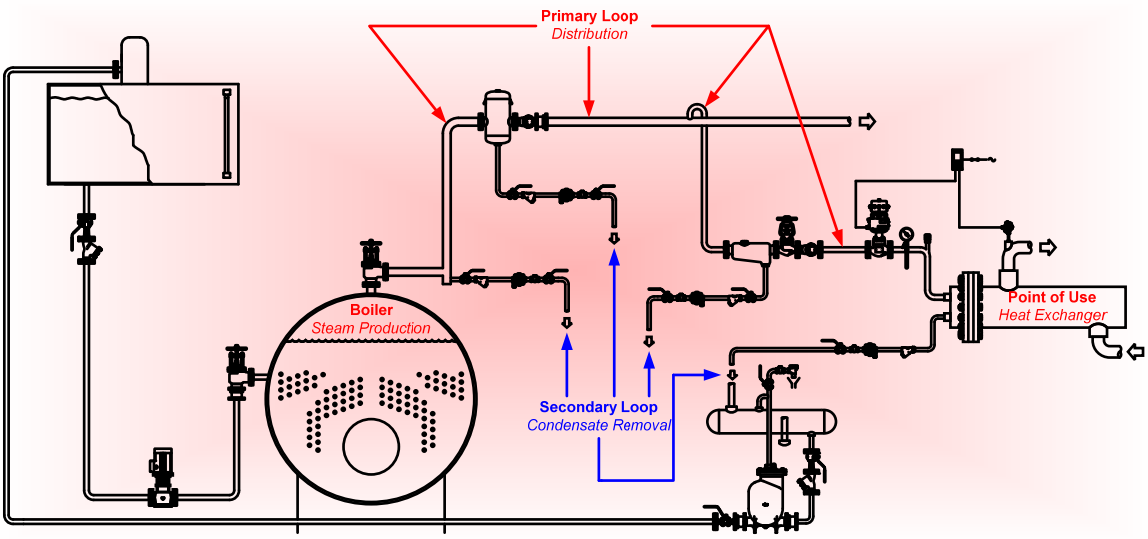

Figure 1-1: Primary and secondary steam and condensate loop (Spirax Sarco, 2015)

The significant loss of energy between steam production and the point of use process decreases enthalpy and reduces the surface area for convection heat transfer. For instance, the presence of condensate will reduce the quality of steam (vapor quality) and thereby reduce the latent thermal energy. Also, the physical presence of condensate within a heat exchanger reduces the volume for the latent heat of condensation. When these two undesirable events occur, increased steam consumption and production are required to satisfy the heat flux requirement. To make matters worse, if increasing the steam capacity does not work, the root of the problem may be masked with larger heat exchangers to provide increased rates of heat transfer.

The damages caused by water hammer (hydraulic, differential, and thermal shock) results in reoccurring and premature failures of equipment/components. The result increases plant downtime, capital and maintenance expenditures. Also, the associated dangers created by water hammer pose serious safety issues. Equipment and components

can rupture, which result in the direct injury or loss of life due to shrapnel or exposure to steam energy.

Rarely accommodated are the condensate flow capacities required during plant start-up. The deficiency increases the time before normal operation can commence. For example, a large facility can take an hour or longer to preheat. Also, excess volume of condensate within the primary loop will cause water hammer.

The device which removes the unwanted condensate from the primary loop is the steam trap. As the name implies, the steam is trapped, however, the removal of condensate is facilitated. Figure 1-2 is a simple representation of the steam trap function.

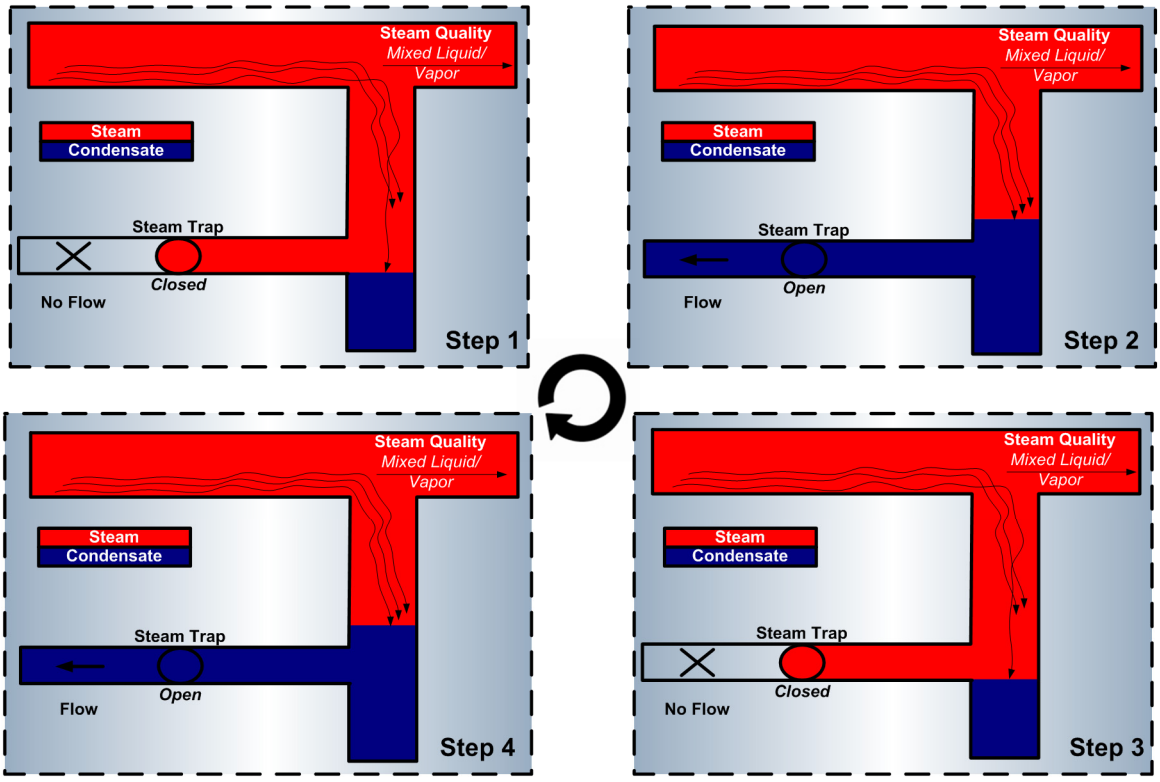

Figure 1-2: Steam trap function

The steam traps used today were developed in the twentieth century, and several deficiencies prevent the adequate removal of condensate. The deficiencies include limited flow capacity, selection, and maintenance.

The physical size, functionality, and condensate flow capacities differ within trap series and between trap types. Excess condensate removal can only be accommodated by the collection leg or orifice size. The limitation transpires because the orifice provides a fixed flowrate at a differential pressure and causes the inability for the steam trap to match the varying load. Also, a fixed orifice size is prone to dirt and debris blocking or impeding flow during operation.

The manufacturers specification serves as an important design element when determining the suitable orifice diameter for selection. However, many trap vendors fail to provide the actual capacity for condensate at saturation temperature, which inherently provides the design engineer with overstated flowrates. Also relevant is whether steam trap manufacturers follow a regulated test standard. The combined effect of both factors makes adequate trap selection complicated and near impossible for comparing alternate manufacturers, should these inconsistencies exist.

The next issue is related to steam trap selection. Several variations of steam traps exist, whereby each trap has a unique niche that makes one type of trap more advantageous over another. Although a recommend trap type is provided by the manufacturers, no standardization exist for selection.

The last issue concerns maintainability. Increased maintenance is caused by incorrect selection of orifice and trap type. Choosing an orifice that is oversized is as problematic as an undersized orifice. An oversized orifice will frequently cycle, thereby

reducing the trap's life expectancy and reliability. An undersized orifice will cause the condensate to back up into the collection leg, process equipment, or distribution piping. The result will increase the probability of corrosion related damage, water hammer, and energy loss.

Several issues exist for having different trap types within a facility. For example, increased stock inventory for parts is required to support several variations of trap types and sizes. Also, increased staff training to maintain and diagnosis steam trap operation is required.

1.2 - Motivation for Study

Professionals within the industry are slowing gaining awareness of the important role steam traps perform within the steam and condensate system. The increased efficiency, effectiveness, reliability, and safety created by the proper removal of condensate contributes significantly to the overall operation.

Condensate removal would benefit from improved methods to redefine steam trap ideology. Existing steam trap technology remains relatively unchanged over the last century and fails to deliver optimal performance. The proposed method includes replacing steam traps with control valves.

Advances in steam trap technology are predominantly in the field of diagnostics. The diagnostic feedback is communicated through an automated process or building control system to allow real-time information. However, technology integration between a control system and monitoring hardware is disjointed, as such, several different vendors are required to complete an installation. Also, providing service can cause havoc due to

the involvement of multiple vendors. This process leads to increased capital/operating cost, confusion, and a gap in communications and reliability. Consequently, the majority of customers have not committed to the implementation of the diagnostic technology, retrofit, or new installation despite the significant advantages.

Control valves are anticipated to provide a diverse range of flow capacity by varying the valve position. Also, the control valve could provide diagnostic information for operational status, performance indicators, and predictive maintenance activities. For instance, sufficient condensate removal, flowrate of condensate removed, and just-in-time service are a few advantages. Furthermore, payback incentives are possible with increased efficiency and energy recovery. The reduced operating budget would offset capital and installation cost.

The seamless and successful use of control valves is prevalent throughout industrial applications. Selection is dependent on operating conditions, desired flow, actuation type, and safety considerations. Two important characteristics a design engineer recognizes when sizing a control valve are the fluid flow and differential pressure. A convenient representation of both process variables and other parameters are characteristic of the flow coefficient. The development and acceptance of the standard equations for single-phase fluid flow are well-known for liquid and gas (American National Standards Institute, 2002). However, only a limited number of multiphase flow throttling adaptations have been validated for practical use. The establishment of a theoretical model best suited to describe the mass flowrate has not been validated for the explicit application. Research is required to develop an experimentally acquired model

for the multiphase flow. Also, the assessment of control valve suitability for deployment within an industrial environment is of vital interest.

It is conceivable that the use of a control valve for modulating the flow of condensate may, in fact, be a universal replacement for all steam traps. TLV (2015) indicates that a manual valve adjustment was initially used to facilitate condensate removal and later replaced with automatic steam traps. Condensate control followed a succession of progressive developments in the early twentieth century. After which, relatively minor changes occurred. At what point in time could the automatic control valve be a viable option? Could it be that such an obvious solution was not so obvious or has the steam trap development satisfied the requirements for condensate removal?

Using control valves to remove condensate can provide benefits not yet realized. Design engineers may be able to adopt familiar valve sizing methods to achieve the intended objective should the valve coefficient predict multiphase flow (condensate and flash steam).

1.3 - Objectives and Scope of Work

Creating a continuous model is possible with response surface methodology. As such, physical research into the governing flow of condensate with control valve utilization has several stipulated goals. The objectives include the following:

1. Determine the significant contributing factors for both flow and discharge pressure.
2. Develop a prediction model for flow and discharge pressure.

3. Confirm the prediction equations through physical trials, where provisional consideration include evaluating the gaps in the experimental design.
4. Conduct flow visualization of the condensate supply and discharge.
5. Evaluate theoretical multiphase models with the experimentally acquired model.
6. Surmise the practical relevance of an automatic control valve for use in industry.

The scope of work required to facilitate the experimental objectives include the following:

1. Design the experimental setup, as given in test standard PTC 39, the performance of steam traps (American National Standards Institute, 2005).
2. Acquire materials for installation and fabrication. Features include mechanical, electrical, and electronic aspects of the design.
3. Use statistical software (Stat-Ease, 2014) to design an experiment and model the response surface.
4. Develop a graphical user interface within LabVIEW (National Instruments, 2013); including programming elements pertinent to the control and acquisition of data.
5. Calibrate pressure, temperature, and load cell transducers.
6. Use Ziegler-Nichols control strategy to tune the proportional and integral gain for pressure control.
7. Conduct physical research based on the response surface methodology.
8. Perform data analysis to ensure that it conforms or exceeds the test standard (American National Standards Institute, 2005).

9. Define models for flow of condensate and discharge pressure through statistical measures. For example, the model development and authentication occur through analysis of variance, goodness of fit, and diagnostic residuals.
10. Validate the experimental model to ensure it adequately represents mass flowrate and discharge pressure of condensate through the control valve.
11. Use a high-speed camera to capture the flow of condensate through glass piping for visual observation and insight into the multiphase flow.

1.4 - Outline

The introduction established the importance of removing condensate from the primary loop and identified steam trap deficiencies. Enhanced performance capabilities, intended research objectives, and scope of work were proposed. The second chapter contains a literature review for matters pertinent to the provision of a suitable background. Also, a review of appropriate experimental work conducted in the development of theoretical prediction models and steam trap performance is presented. The third chapter covers the design, construction, and a debugging segment of the experiment and testing apparatus. Chapter four provides the experimental results, data analysis, and literature comparison between theoretical and experimental models for multiphase flow. The conclusion summarizes the results and experimental discoveries, which includes final remarks and future recommendations.

Figure 1-3 presents typical production and distribution components within a boiler room. Of interest is the steam trap location that connects the collection leg to the steam header, which is recognizable as a critical placement for condensate removal. However,

this is for illustration only, several hundred to several thousand steam traps would be operating throughout an industrial facility (Frank, 2006). The sketch portrays a conceptual approach and research intent for replacement of conventional steam traps with control valves. An experimentally acquired model (EAM) is used to understand the significant contributing factors and physical phenomena of using a control valve to modulate the flow of low-pressure condensate. The experimental model is compared to several theoretical models for predicting multiphase flow. Relevant and reasonable inferences provide knowledge regarding control valve feasibility for universal steam trap replacement.

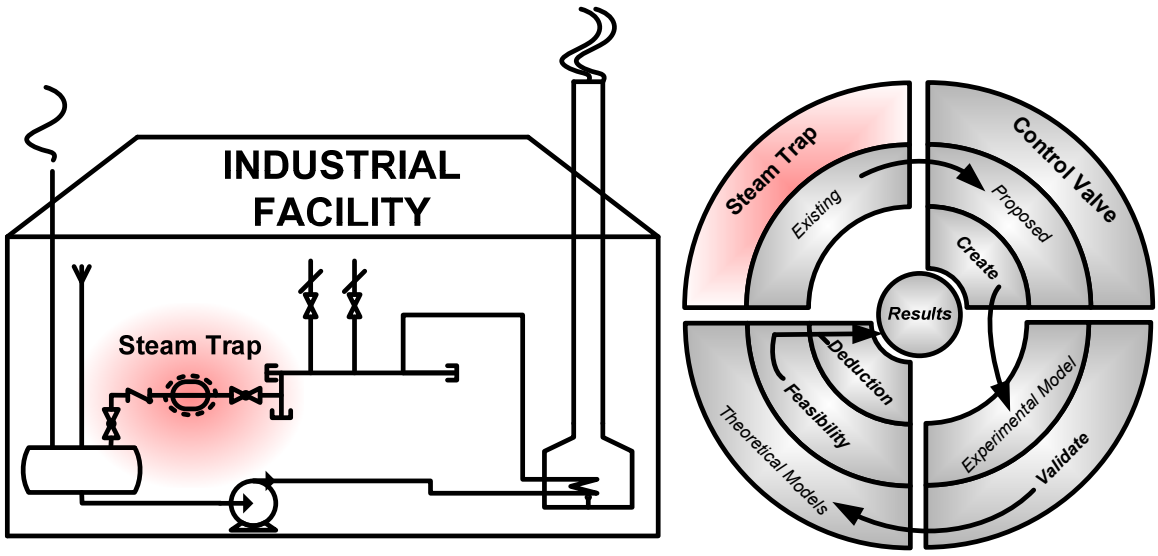

Figure 1-3: Pictorial schematic of application and research intent

-2- Literature Review

2.1 - Steam Utilization

Steam use in industry is prevalent within processing, manufacturing, electrical power production, commercial infrastructure, and healthcare. It has desirable physical properties, succinct temperature control, high deliverable energy content, reduced capital and operating cost, and promotion of hazard prevention. Spirax Sarco (2008) indicates that steam is widely used to harness the latent and sensible thermal energy.

Favorable properties of steam are specific heat capacity, specific volume, and the latent heat of vaporization. The specific heat capacity of steam is higher than most other fluids, which makes it a great medium for thermal energy storage. Also, the specific volume and enthalpy lends itself well to the efficient use of saturated steam; higher pressures allow for increased levels of energy with decreased levels of specific volume. This trait allows smaller pipe transmission sizes for distributing the energy throughout the facility for point of use. The design will keep capital and installation cost lower during construction. Also, the transmission of steam requires no pump and can travel at velocities significantly greater than liquid. The conveyance of large amounts of energy is possible in an efficient manner.

An important function of steam is the relationship between pressure and temperature. Accurate temperature control occurs by fixing pressure at the saturation state. Also, water is more valuable in vapor form because of the enthalpy of evaporation. The stored energy of the saturated vapor is approximately six times greater than saturated liquid at the same temperature per unit mass. Hence, the significant energy capacity is

made available for delivery. Figure 2-1 includes reference terminology and a visual indication of the available energy through a latent heat phase change.

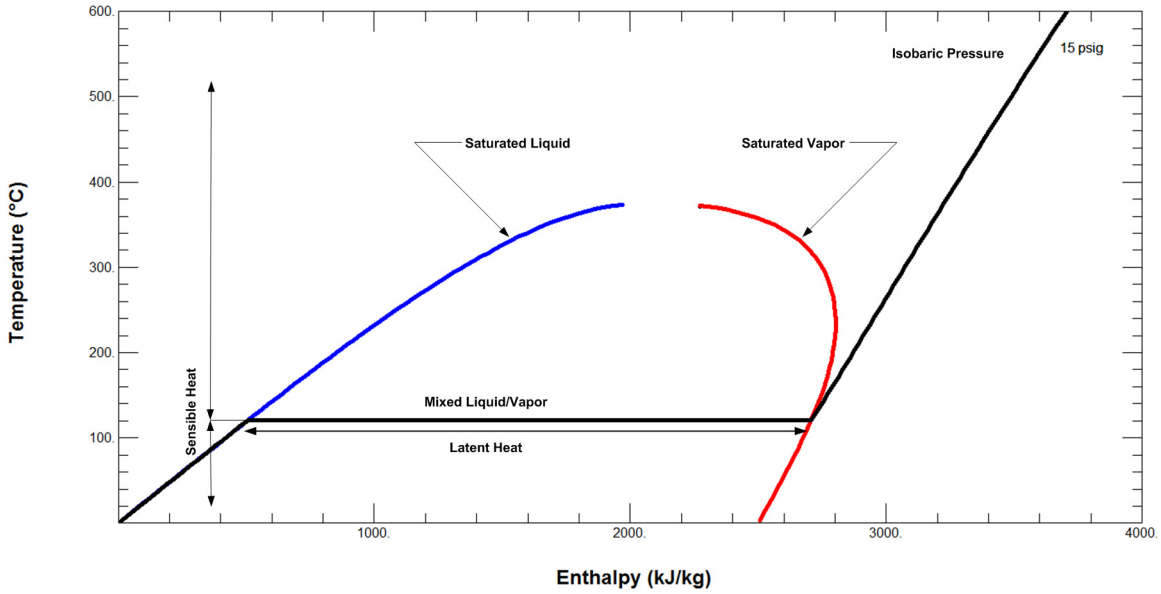

Figure 2-1: Reference terminology and phase diagram for an isobar

Water is a non-hazardous renewable resource. However, water must be chemically treated to prevent corrosion, scaling, and foaming. Therefore, a minor risk of environmental exposure exists. The location of the environmental exposure will determine the adversity of the effect. For steam distribution and condensate return, the only chemical present is the neutralizing amines for corrosion protection. However, should a leak exist within the boiler or feedwater supply, then other chemicals will be present that would cause an undesirable exposure to the environment. Compounds consisting of sulfites, phosphates, and anti-foaming agents inhibit the presence of oxygen, scaling, and foaming. However, the adverse environmental effects generated by chemical exposure is insignificant compared to an oil leak.

2.2 - Steam Traps

2.2.1 - Introduction

Within the steam and condensate distribution system, the steam trap is a critical device that continues to be significantly overlooked and unappreciated. Although gaining recognition within the last forty years as being a vital element, the engineering profession has yet to exploit its potential.

2.2.2 - Purpose

All aspects related to steam production, transmission, and point of use requires the presence of a steam trap. Its primary function consists of facilitating the removal of condensate that has either separated as incomplete vaporization or generated within a system; preventing or restricting the loss of steam. The secondary role of a steam trap is to assist with the removal of air.

Removal of condensate will allow steam to reach its destination in as dry a state as possible to perform its task sufficiently and economically. Failure to properly maintain or select a steam trap will lead to water hammer, premature failure of other system components, reduced sensible/latent heat transfer, and wasted energy. Steam traps are necessary within the steam industry. The quantities vary from plant to plant. Frank (2006) indicates that the contribution of the steam trap is significant despite the cost or size and that several hundred to several thousdands can be present within a plant.

2.2.3 - History

As the use of steam flourished during the Industrial Revolution, a process requiring the removal of condensate was recognized. According to TLV (2015) the first steam trap was a manually operated valve. Depending on the process or function, human interjection would vary the valve position to modulate the restricting orifice. This process would thereby alter the discharge capacity. The method, although rudimentary and human resource intensive, improved steam distribution for point of use. However, should the valve adjustment not be suitable then the condensate would either backup into the system or discharge of steam to the surroundings. Both lead to an inefficient and hazardous operating environment.

As steam production and utilization continued to be a dominating source of energy, opportunities to improve the method of condensate removal were recognized for development. Several patents for steam traps were issued in the late nineteenth to early twentieth century and implemented within industry. The activity of inventors and patents issued peaked during this period with only marginal developments afterward. These advancements are the primary steam traps used within industry today.

The main goal of the inventors was to make the process of phase separation automatic to improve safety and efficiency. Implementing the process of automation was possible through self-governing physical properties. Design characteristics distinguish the phase difference through static and dynamic attributes, which include buoyancy, thermal expansion, or differential pressure. The categorical grouping of steam traps corresponds to the various operation characteristics. The three basic types of steam traps

used extensively in the industry are mechanical, thermostatic, and thermodynamic. However, within the last couple of decades, electronic technologies have been integrated into modern designs.

2.2.4 - Variations

2.2.4.1 - Mechanical

Mechanical steam trap designs differentiate between steam and condensate through fluid density. Included in this category are ball float traps and bucket traps. In a ball float trap, the ball rises in the presence of condensate, allowing the orifice to become exposed to permit the discharge of condensate. Otherwise, the hole will remain closed. The bucket trap position can either be vertical or inverted. The style dictates the functional characteristic of the bucket position. For instance, with the inverted bucket trap, the presence of steam or liquid within the bucket establishes if the discharge orifice is exposed. The calibrated port in the top of the bucket restricts the removal of outgoing steam/condensate to control the action of the operation. When condensate is present, it forces the steam out of a vent port and causes the bucket to sink; exposing an open orifice for the condensate to flow. All primarily function as mechanical fulcrums and levers, with the resultant buoyancy force dictated by the fluid density. Figure 2-2 includes three standard styles of mechanical steam traps.

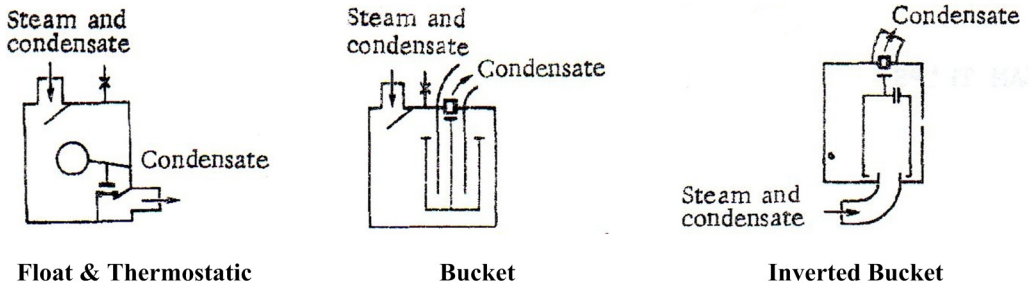

Figure 2-2: Mechanical steam traps (Paikin, 1981)

2.2.4.2 - Thermostatic

Thermostatic steam traps operate with changes in fluid temperature. For example, the temperature of the saturated steam is determined by its pressure. In the steam space, steam gives up its enthalpy of evaporation, producing condensate at steam temperature. As a result of any further heat loss, the temperature of the condensate will decrease. Detection of the sensible temperature change of heat within a thermostatic trap will allow the discharge of condensate. As steam reaches the trap, the temperature increases and the trap will close. Falling under this category are balanced pressure, bimetallic, and liquid expansion steam traps. Figure 2-3 presents three mutual styles of thermostatic steam traps.

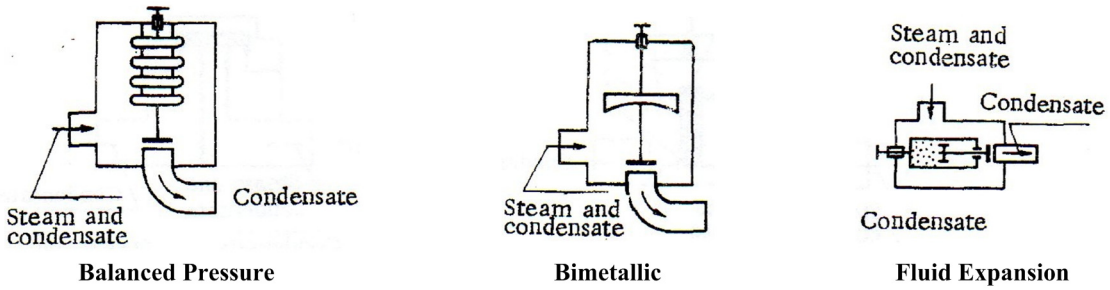

Figure 2-3: Thermostatic steam traps (Paikin, 1981)

2.2.4.3 - Thermodynamic

The operation of a thermodynamic steam trap depends on fluid dynamics and fluid properties. The fluid flow through an orifice creates a low pressure and a high velocity. Based on the corresponding pressure, the fluid will either exhibit a subcooled, mixed, or superheated phase. A subcooled condition will allow the orifice to remain constantly in the open position. However, the presence of excess energy available at the isobaric pressure causes the condensate to form a vapor. For instance, flashing occurs at the top of the disk. When this happens, the force exhibited on the upper part of the disk exceeds the force acting on the bottom. The reason the disk is pushed down, closing the outlet, is related to the increased surface area above. The discharge orifice becomes exposed, and the cycle repeats once the vapor condenses. Included in this group are disc, impulse, and labyrinth steam traps. Figure 2-4 shows four styles of thermodynamic steam traps.

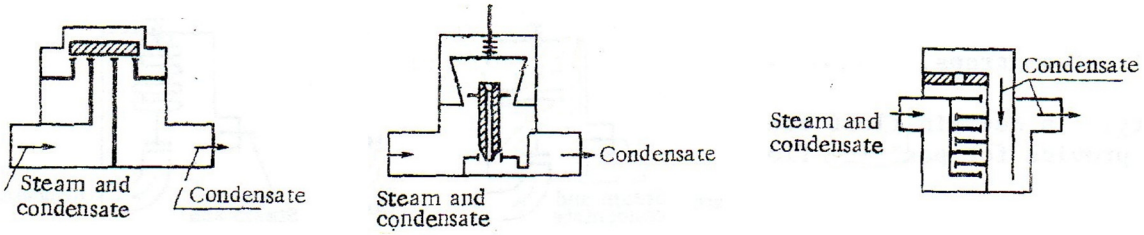

Figure 2-4: Thermodynamic steam traps (Paikin, 1981)

2.2.4.4 - Orifice Trap

The orifice trap has not been universally accepted to belong to any particular category. It has existed since the early twentieth century and is rarely mentioned in the literature. Several debates correspond to the trap's efficiency and effectiveness in

controlling condensate; or if, in fact, it controls the removal at all. However, ASHRAE (2004) classifies the orifice trap as being thermodynamic.

Dickman (1984) produced a convincing article to debunk the myths surrounding a fixed orifice trap. Also, Abu-Halimeh (2004) establishes that the loss of steam from the orifice trap can be significantly less than other steam traps in most operating conditions. However, Abu-Halimeh (2004) ensures the correct orifice size selection to obtain optimal performance. If a larger size orifice trap is used an increase in steam loss will occur.

An orifice trap allows a continual passage for the condensate and steam to pass freely, fueling the debate whether an orifice trap can control the separation between the condensate and steam. Dickman (1984) surmises the fact that sufficient velocity of steam will cause a choked flow and will limit the wastage. Given that the specific volume of steam is much greater than condensate, the wastage is considered to be minimal and acceptable. However, the passing of condensate with lower specific volumes will exhibit a greater capacity of mass flowrates at lower velocities. Also, the excess energy within the condensate will flash dependent upon differential pressure, thereby increasing the resistance for flow capacity. Figure 2-5 shows various orifice trap styles.

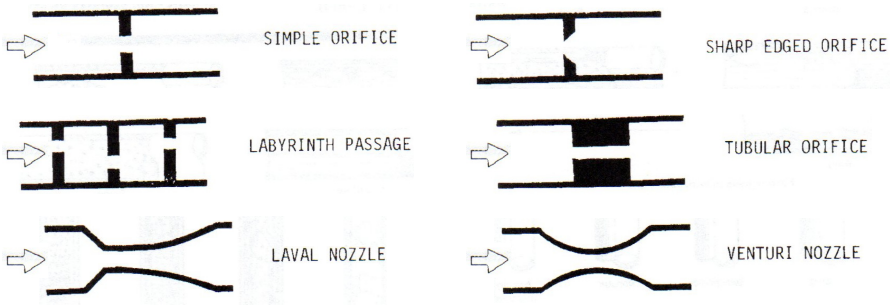

Figure 2-5: Orifice steam traps (Dickman, 1984)

2.2.4.5 - Emerging

The modernization of existing steam traps are evident within the intellectual property agencies. Patents submitted indicate the use of instrumentation to evaluate steam trap function. For instance, sound profiles are notably different between condensate and steam flow. Also, the detection can be made between each phase with changes in conductivity. However, condensate removal still depends on the basic principles of the trap type. Figure 2-6 shows a float and thermostatic steam trap that is capable of temperature and pressure detection; providing diagnostic feedback to a computerized maintenance management system. The schematic is an approved patent and owned by Fisher Controls International LLC.

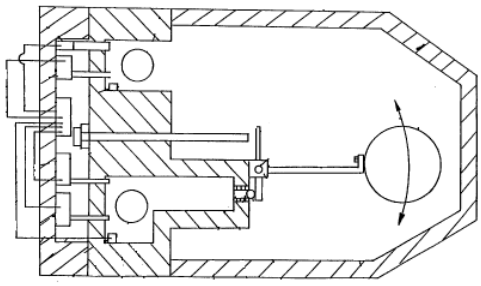

Figure 2-6: Emerging steam trap with diagnostic capabilities (Rebik, 2001)

2.2.5 - Selection

With the existence of several variations of steam trap categories and then several options of available traps, a design engineer has a daunting task to ensure an adequate choice. Trap selection depends on the engineer's experience of steam and condensate system design and the manufacturer's recommendation tables. Literature indicates that

no universal steam trap exists for the selection and deployment of a particular type or size (ASHRAE, 2004).

Several common applications require a steam trap within a steam and condensate system. For example, steam production, distribution, and point of use equipment. Should the selection of the incorrect steam trap occur, several unwanted events will transpire depending on the application. For example, placement of a float and thermostatic steam trap on a coil tube boiler will produce an unsuitable environment for the hollow stainless steel float. Vacuum and pressure conditions will cause damage to the float and create a non-functional trap, causing a carry-over of condensate within the steam distribution system. The life expectancy of applying this steam trap to the above application will be excessively short. The other attributes related to the improper operation of a steam trap are expressively evident throughout the thesis.

Determination of the steam trap capacity is based on manufacturer reported data, theoretical calculation, and/or through physical measurement. The appropriate selection of the required steam trap is determined by a quantitative estimate, the differential pressure across the trap, and a factor of safety. Paffel (2013) recommends a factor of safety of three for all traps except float and thermostatic. However, Spirax Sarco (1992) suggests a factor of safety of two on everything except temperature controlled air heater coils/converters, and siphon applications. For these, a factor of three is advisory.

2.3 - Hazards

2.3.1 - Introduction

Unsteady fluid flow occurs within many systems. Several names exist to describe the severe dangers associated with the incident, i.e., water hammer, pressure surge, or pressure transients are all synonymous. In theory, the sudden change in velocity corresponding to a fluids density and wave propagation speed correlate to a maximum or minimum pressure deviation (Wylie and Streeter, 1978). The pressure transient is recognizable as Joukowsky's pressure rise or pressure drop. These pressure changes are detrimental when they occur because they cause equipment damage, loss of life, and other adverse operational conditions. Subsequent banging and hammering noises are prevalent during the event.

The possibility of water hammer occurring depends on several variables and characteristic attributes. A few well known contributing conditions are sudden valve opening, sudden valve closing, pump start-up, pump shutdown, and fluid column separation. However, three general conditions are known contributors enabling the formation of water hammer: hydraulic shock, thermal shock, and differential shock (McCauley, 1995).

Hydraulic shock relies predominately on the fluid's bulk modulus, which is the ability for the fluid to compress (Wylie and Streeter 1978). In reality, all fluids are compressible, however for practical use, the degree of compressibility is virtually non-existent for some fluids. It is when the fluid flow is abruptly interrupted that compressibility creates the pressure transient.

Thermal shock occurs in the presence of two-phase fluid (steam and condensate). Depending on the state of the gas phase, it will have a specific volume larger than that of the liquid. If the temperature between phases is considerable, then the rate of change of heat transfer will dominate the severity of the transient and collapse the vapor space.

Differential shock exists in the formation of a slug, encapsulated condensate, which is representative of a mass having substance and propelled with significant steam velocities (Risko, 2013). The damages conveyed by this method relies on the kinetic energy dissipation of the slug with the sudden change of direction, i.e., straight pipe transition to an elbow.

Water hammer creates a significant risk to human life, the environment, and operations. The occurrence of condensation induced water hammer events has caused 11 fatalities worldwide according to Dirndorfer, Doerfler, Kulisch, and Malcherek (2012). Other consequences include the loss of production through direct damage of infrastructure, which require significant capital investments and remediation (Risko, 2013).

Industries are slowing becoming aware of condensation induced water hammer. Recognized institutions are highlighting the dangers and potential audits required to identify dutifully, address and resolve any problematic incident (U.S. Nuclear Regulatory Commission, 1996).

2.3.2 - Theory

Joukowsky's derived formula for pressure surge (ΔP) is given in Equation 2.1 (Wylie and Streeter, 1978) and is representative of hydraulic and thermal shock.

$$\Delta P = \rho a^{*} \Delta U \quad (2.1)$$

Where the pressure magnitude is dependent upon the fluid's density (ρ), acoustic wave speed (a^{*}), and a sudden change in velocity (ΔU).

The wave's acoustic velocity is highly dependent upon the fluid, the existence of more than one phase, and elastic properties of the piping. One cycle consists of four transient waves, i.e., surge, backflow, suction, and inflow (Wylie and Streeter, 1978).

2.3.3 - Prevention

The natural formation of hydraulic, thermal, and differential shock is avoidable within a steam and condensate loop. Correctly applied design features include pipe diameter, pipe grading, drainage, collection leg width/height, flash steam recovery, and control of subcooled condensate (ASHRAE, 2004).

The pipe diameter is relevant to ensure adequate fluid velocities are maintained. Excessive velocities within a saturated steam environment will cause premature wear of piping, fittings, and valves due to the presence of liquid molecules within the mixed phase. The substantial magnitude of high velocity saturated steam, and the presence of condensate causes an excitation of the fluid to create a wave formation. When this wave joins the bottom and top of the piping, a seal is formed and the generation of a differential shock occurs. One method to reduce the forming of the seal is the implementation of an adequate pipe diameter.

The grade of piping and the location of drainage is necessary when removing condensate from the system. Inclined distribution allows gravity to direct the condensate to low-level sites for drainage. Further localities of drainage are headers, separators, and

point of use equipment. Reducing the presence of condensate eliminates the formation of all three water hammer scenarios.

Collection legs of the correct width and height allow the collection of condensate. If the width is insufficient, then a low pressure is developed at the entrance and prevents the collection of condensate (ASHRAE, 2004). The height of the collection leg will allow the system to act as a buffer or accumulator for changing load conditions. An inadequate design of the collection points will enable the formation of all three water hammer scenarios.

Excess energy not controlled through condensate return can facilitate thermal and differential shock. The probability of flash steam and subcooled condensate generates an elongated bubble, and rapid heat transfer will likely create thermal shock. Depending on the condensate return diameter and backpressure, an increased amount of condensate can prospectively bridge the piping to form the differential shock (Gorelick, 2010). The addition of heat recovery flash vessels can alleviate the formation of both water hammer events occurring. The excess energy from the condensate return system would be removed from the flash vessel and utilized for another energy transfer purpose. Controlling subcooled condensate below isobaric saturation temperature or lower sensible thermal energy requires the careful arrangement of piping to prevent the formation of thermal shock.

Understanding the fundamental principles that create water hammer is important to recognize and avoid during engineering design. Also, it is just as important to identify and resolve water hammer transients during operating conditions. The presence of the event will be audibly evident and likely include a visual indication, i.e., pipe movement,

fitting/component failure, or reduced life expectancy. The appropriately selected and efficiently operating steam trap is the most important element in any steam system. With the condensate removed properly from the system, as is the primary function of the steam trap, the most severe events will be avoided within the primary and secondary loop.

2.4 - Plant Efficiency

As the energy cost to produce steam continues to rise, so does the responsibility of an organization to ensure an optimally performing system. The expense related to the improper maintenance and inadequate initial design of the system is considerable. Furthermore, the environmental cost of not ensuring an optimal system may be more concerning. Greenhouse gas emissions, the consumption of non-renewable resources and the excessive use of valuable renewable resources will continue to contribute adversely to the global ecosystem. Also, organizations have a moral responsibly to preserve earth's resources while maintaining the natural habitat through environmental stewardship. The first step to ensure system efficiency is through conservation of current resources, thereby minimizing environmental impacts while increasing system reliability and decreasing the operating cost.

The only component to universally improve the effectiveness of the steam plant through production, distribution, and point of use is the steam trap. Steam traps perform a significant role in increasing plant effectiveness, safety, and efficiency. Incorrect stream trap size or type, along with inadequate maintenance may result in operational failure.

The removal of condensate from the primary loop will make certain that excess energy is not wasted. For example, the delivery of high steam quality will ensure that the

latent heat extracted through the process will provide greatest efficiency. Also, removing condensate when it forms during a process event will ensure a maximum surface area for heat transfer. Otherwise the heating surfaces will reduce the available heat flux that can be given to the intended convection process.

There are indirect costs associated with increased maintenance and/or replacement of system components. For instance, not removing the condensate from process applications will cause decreased life expectancy. Pressure surges can create instantaneous failure or failure through exposure to chronic repetitive incidence. Furthermore, although condensate is chemically treated to protect against the formation of carbonic acid, the subcooled environment increases the probability of an acidic condition occurring. For this scenario, either the carbonic acid will form to cause corrosive damage or an increased usage of chemical treatment is required to prevent deterioration from occurring.

2.5 - System Diagnostics

Recognition within the associated professions of the industry understands the importance to be able to identify adequate and timely steam trap failure. Both conventional and modern methods exist to facilitate detection. Regardless of the method, the operating condition of the steam trap has three potential modes of operation: fail closed (no flow), fail open (steam flow), or function correctly (intermitted or continuous condensate flow without the loss of steam).

The conventional method of identifying the three operating modes include utilizing either sound or temperature technology. Ultrasonic equipment can detect the

difference between condensate and steam. The distinct sound made by the velocity of steam creates a high frequency and intensity as compared to condensate. Also, the meter displays an analog feedback of the sound to aid the examiner in diagnostics. By no means is this method definitive in the detection of trap operation. As the diagnostics pertain to the use of one's senses, a variation exists between examiners. Also, the operating environment has a significant impact on the ability to differentiate between the two phases. For instance, the presence of rotating equipment and steam provide frequencies that transmit through the pipe network (primary and secondary) that are detected by the sound equipment.

Measurement of steam trap temperature or temperature differential between the inlet and outlet of the trap can provide insight into the functional operation. Either infrared thermometers, pyrometric crayons, and/or touch are primary modes of temperature detection. Obvious failure detection occurs when the steam trap is cold with respect to the operating environment. Trap failure is evident because the condensate is not being discharged from the orifice, thereby stabilizing at the residual ambient temperature (failed close). Diagnosing a hot trap requires more knowledge on behalf of the examiner. Should the examiner know the operating condition, i.e., operating pressure, then they could compare the isobaric pressure with the saturation temperature. Consideration of deviations between the actual temperature of the condensate and trap housing is a factor that has to be considered by the examiner. The reason is that the measured surface (external housing) is undergoing several forms of heat transfer to provide a lower temperature then the condensate. For conditions where an uninsulated trap is located in an extreme ambient temperature, the difference between the condensate

and housing will be greater. After considering the bias in the temperature, an evaluation of trap functionality is possible. For instance, a couple of degrees difference between the inlet and outlet of the steam trap would establish a functioning trap. It is when there is no difference between the inlet and outlet of the trap that steam loss is occurring, resulting in an open trap failure.

The issue with manual diagnostics is the time required to perform the preventative or routine maintenance necessary to ensure an effective and efficient drainage of condensate. A matter that further complicates the process is the ability of the examiner to conduct appropriate diagnostics of the steam trap. Should the examiner misdiagnose a properly functioning steam trap, then the labor, replacement part and loss production cost will contribute to an inefficient use of resources. When completing maintenance, the effect may cause improper trap operation. The reason is that the replacement part may be faulty or incorrectly installed based on the skillset and knowledge of the maintenance personnel.

Temperature and sound technology continue to be the modern diagnostic approach for determining the operating condition of the steam trap. The difference between conventional and modern methods is that instrumentation within the steam trap design provides feedback of the process. For example, integration within a control system provides instantaneous monitoring status through a building management maintenance system. The advantage is the ability for immediate diagnostic detection of steam trap failure. When commissioning the steam trap monitoring system, careful attention must be applied to ensure an adequate detection signal is valid for the given process and environment. A valid detection signal is possible only through individual calibration of

the motioning system for each steam trap. The systematic effects from equipment and adjacent steam lines are imperative considerations during the threshold initiation.

2.6 - Sustainable Design

The American Society of Heating, Refrigerating, and Air-Conditioning Engineers (2006) define sustainability as "providing for the needs of the present without detracting from the ability to fulfill the needs of the future". Before the embargo oil crisis of 1973, sustainable and green design were factors of insignificant consequence. Earth's natural resources were providing for global consumption and any adverse impacts on the environment were not evident or implicit. The World Commission on Environment and Development (1987) published the Brundtland Report titled *Our Common Future* to address antagonistic issues that relate to poverty and the environment. The report was able to assist and establish worldwide recognition of the ensuing crisis. The publication was the first to provide a simple and succinct definition of sustainable development as "development that meets the needs of the present without compromising the ability of future generations to meet their own needs" (World Commission on Environment and Development, 1987). Today, attributes of sustainable and green design remain in stages of infancy and are rapidly developing.

2.7 - Control Valves

Control valves are prevalent within industrial applications. The ability to control fluid is a crucial processing requirement, whereby the selection of an incorrectly sized valve will decrease reliability, effectiveness, and efficiency. There are several design

types with varying attributes and characteristics, including a butterfly, globe, and ball valve.

Flow characteristics change depending on the style of valve design or trim type. Established are three ideal flow characteristics for design purposes, which include fast opening, linear, and equal percentage (ASHRAE, 1985). Each characteristic defines the flow of fluid in conjunction with the movement of the valve position. Figure 2-7 shows the valve travel operating position versus flow.

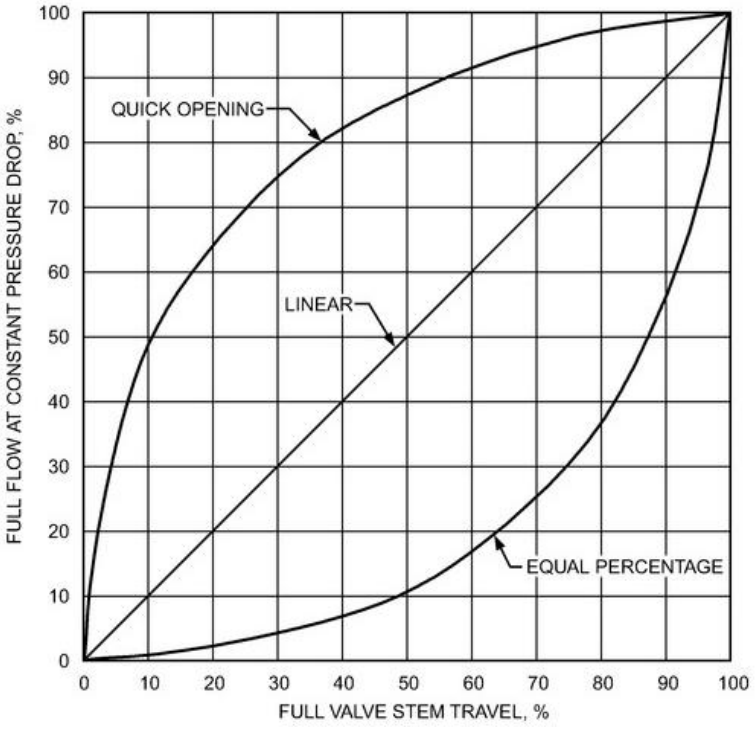

Figure 2-7: Ideal flow characteristics for control valves (ASHRAE, 1985)

The ideal flow characteristics are used for design purposes. However, the installed flow characteristics prevent the flow response from achieving the desired effect. According to ASHRAE (1985), the pressure drop during actual field operation does not remain constant and causes the discrepancy from the ideal case.

Rangeability is the maximum controllable flow to the minimum controllable flow (Spirax Sarco, 2004) and is an important design characteristic. A high rangeability will produce high-resolution control near the low and middle range valve stem travel.

However, one of the most important terms to help with the selection of a control valve is the manufacturers flow coefficient. Performing capacity test procedures, IEC 60534-2-3, provide the flow coefficient for the valve (American National Standards Institute, 2002). This value corrects for contraction of the fluid stream through the valve and corresponding frictional pressure losses (Hutchison, 1971). The flow coefficient is used within standard equations to determine the flowrate of the fluid.

2.8 - Mass Flowrate Prediction Modeling

The International Society of Automation (ISA) incompressible model is useful for evaluating the experimentally acquired response (American National Standards Institute, 2002). The method applies to a single-phase flow with considerations for choked conditions. Both incompressible and compressible models as stated within the ISA standard are considered the primary resource for selecting an adequate sized control valve (Diener and Schmidt, 2005). Alternative models were evaluated to determine which could best describe the mass flowrate and critical pressure ratio. Included were the homogeneous equilibrium (HE), homogeneous frozen (HF), homogeneous non-equilibrium (HNE), and homogeneous non-equilibrium Diener and Schmidt (HNE-DS).

The incompressible model was first selected to evaluate how well it could predict the experimental response for a saturated stagnation state. Consideration of flashing and cavitation are part of the method and adjusts for the decrease of valve efficiency. The

ISA volumetric flowrate prediction equations are given in Equation 2.2 and 2.3 (American National Standards Institute, 2002).

$$Q = \frac{N_1 \cdot C_v}{\sqrt{\frac{\rho_1}{\rho_0 \Delta P}}} \qquad \left[Applicable \text{ if } \Delta P < F_L^2 \left(P_1 - F_F P_V \right) \right] \tag{2.2}$$

Where the magnitude of the volumetric flowrate (Q) is dependent upon the flow coefficient for the valve (C_v), the relative density (ρ_1/ρ_0), and the differential pressure (ΔP) between PT1 and PT2. A numerical constant (N_1) accounts for formulae units, i.e., metric or imperial.

$$Q = \frac{N_1 \cdot C_v}{\sqrt{\frac{\rho_1}{\rho_0 \left(P1 - F_F P_V \right)}}} \qquad \left[Applicable \text{ if } \Delta P \geq F_L^2 \left(P_1 - F_F P_V \right) \right] \tag{2.3}$$

The additional change between Equation 2.2 and 2.3 is the accommodation of the choke flow parameter. The inlet pressure (P_1), vapor pressure (P_V), and the critical pressure ratio (F_F) define the limiting constriction at the vena contracta.

Several methods have been adapted to predict the mass flow for multiphase mixtures (liquid/vapor, liquid/gas) that are suitable for throttling devices. Notable work completed by Sheldon and Shuder (1965), Henry and Fauske (1971), Leung (1986), and Diener and Schmidt (2005) helped to lead the movement for acquiring an adequate formulation. Some models include first principles while all make simplified assumptions for practical use. Suitable performing models are applied and evaluated against the experimentally obtained model. Each of the theoretical models assumes a homogenous mixture between each phase.

The HE method is a common model. It used first principles and was simplified based on several assumptions. The assumptions include that the fluid is undergoing isentropic expansion, maintains equilibrium between the liquid and gas phase and that the average velocities of each phase are equal (Henry and Fauske, 1971). The mass flux (G) prediction equation is representative of Equation 2.4.

$$G = \frac{\left(2\left[h_g - \left(1 - x_E\right)h_{lE} - x_E h_{gE}\right]\right)^{\frac{1}{2}}}{\left(1 - x_E\right)v_{lE} + x_E v_{gE}} \tag{2.4}$$

Where x defines the vapor quality, υ expresses the specific volume of the fluid, and h represents the enthalpy. Subscripts g, l, and E are representative of the vapor, liquid, and equilibrium phase, respectively.

Another method is the HF model. As was the case for the HE model, assumptions are made regarding the average velocities of each phase and that the process undergoes an isentropic expansion. However, this model fundamentally deviates because there is no consideration of momentum, heat, or mass transfer between phases (Henry and Fauske, 1971). Also, the HF model is primarily vapor dominated. The gas-dynamic relationship limits the critical flowrate. The mass flux (G) prediction equation is represented by Equation 2.5.

$$G = \frac{1}{v}\left(2x_0 v_{g0} P_0 \left(\frac{\gamma}{\gamma - 1}\right)\left(1 - \eta^{\frac{(\gamma-1)}{\gamma}}\right)\right)^{\frac{1}{2}} \tag{2.5}$$

Where x represents the vapor quality, v is the specific volume, P signifies the supply pressure, and γ is the isentropic exponent for the vapor. The subscript *0* indicates the stagnation state and *g* signifies the vapor phase.

The transcendental equation requiring resolution is the critical pressure ratio (η), which is illustrative of Equation 2.6.

$$\frac{(1-x_0)v_{l0}}{x_0 v_{g0}}(1-\eta)+\frac{\gamma}{\gamma-1}\left(1-\eta^{\frac{(\gamma-1)}{\gamma}}\right)=\left(\frac{(1-x_0)v_{l0}}{x_0 v_{g0}}+\eta^{-\frac{1}{\gamma}}\right)\left(\frac{\gamma}{2}\right)\eta^{\frac{(\eta+1)}{\gamma}} \tag{2.6}$$

Where x characterizes the vapor quality, υ denotes the specific volume, and γ is the isentropic exponent for the vapor. Subscripts *0*, *g,* and *l* represent stagnation state, vapor, and liquid phase, respectively.

The HNE and HNE-DS models are a combination of several works of literature. For instance, the method by Henry and Fauske (1971), compressibility factor for void fraction and phase change from Leung (1986), and the addition of the boiler delay factor from Diener and Schmidt (2004) contribute to nonequilibrium model development. The formulations that describe the critical mass flux (G) and the critical pressure ratio (η) for HNE methods are given in Equations 2.7 and 2.8 (Diener and Schmidt, 2005).

$$G=\psi\sqrt{\frac{2P_0}{v_0}} \tag{2.7}$$

$$\eta^2+\left(\omega^2-2\omega\right)(1-\eta)^2+2\omega^2\ln(\eta)+2\omega^2(1-\eta)=0 \tag{2.8}$$

Where P is representative of the supply pressure, η indicates the critical pressure ratio, and υ denotes the specific volume of the fluid at the stagnation state (*0*). The expansion

factor (ψ) is given in Equation 2.9 and the compressibility factor (ω) is shown in Equation 2.10.

$$\psi = \frac{\sqrt{\omega \ln\left(\frac{1}{\eta}\right) - (\omega - 1)(1 - \eta)}}{\left(\omega\left(\frac{1}{\eta} - 1\right) + 1\right)} \tag{2.9}$$

$$\omega = \frac{x \cdot vg0}{v_0} + C_{Pl0} T_0 P_0 \left(\frac{\left(v_{g0} - v_{l0}\right)^2}{\Delta h_{fg}^2 0} \right) N \tag{2.10}$$

Where C_P signifies the specific heat at constant pressure, T symbolizes the supply temperature, and Δh is the latent heat of vaporization. Additionally, the boiling delay factor (N) is given in Equation 2.11, which includes the boiling delay exponent (a) and the critical pressure ratio (η).

$$N = \left(x_0 + C_{Pl0} T_0 P_0 \left(\frac{\left(v_{g0} - v_{l0}\right)}{\Delta h_{fg0}^2} \right) \ln\left(\frac{1}{\eta}\right) \right)^a \tag{2.11}$$

The method of Henry and Fauske (1971) and the method of Leung (1986) for determining the critical pressure ratio (G) and critical mass flux (η) are indicated in Equation 2.12 through 2.19 and 2.20 through 2.23, respectively.

$$G^2 = \left[\frac{x_o v_g}{nP} + \left(v_g - v_{lo}\right) \left\{ \frac{\left(1 - x_0\right)\left(\frac{x_E}{0.14}\right)}{s_{gE} - s_{lE}} \frac{ds_{lE}}{dP} - \frac{x_0 c P_g \left(\frac{1}{n} - \frac{1}{\gamma}\right)}{P\left(s_{g0} - s_{l0}\right)} \right\} \right]_t^{-1} \tag{2.12}$$

Where the thermal equilibrium polytropic exponent (n) is provided in Equation 2.13 and the critical pressure ratio (η) is given in Equation 2.14. Entropy is defined by s, while the

rate of change with respect to pressure (*ds/dP*) is available from thermodynamic data. The subscript *t* represents the throat position within the valve (vena contracta).

$$n = \frac{\left((1-x)\left(\frac{C_{Pl}}{C_{Pg}} \right) + 1 \right)}{\left((1-x)\left(\frac{C_{Pl}}{C_{Pg}} \right) + \frac{1}{\gamma} \right)} \tag{2.13}$$

$$\eta = \left\{ \frac{\left(\frac{\left(1-\alpha_0\right)}{\alpha_0}(1-\eta) + \frac{\gamma}{\gamma-1} \right)}{\frac{1}{2\beta\alpha_t^2} + \frac{\gamma}{\gamma-1}} \right\}^{\frac{\gamma}{\gamma-1}} \tag{2.14}$$

Where the quality is characterized by *x*, C_P is the specific heat at constant pressure, and γ represents the isentropic exponent. Subscripts *0* and *t* represent stagnation state and throat, respectively. Equations 2.15 to 2.19 define the parameters of Equation 2.14 for the transcendental expression. N^* is an experimental parameter and describes the partial phase change of the fluid (Henry and Fauske, 1971). The void fraction (α) and specific volume (υ) for the throat/stagnation state are described.

$$\eta = \frac{P_t}{P_0} \tag{2.15}$$

$$\beta = \left| \frac{1}{n} + \left(1 - \frac{v_{l0}}{v_{g0}} \right) \left(\frac{\left(1-x_0\right) N^* P_t}{x_g\left(s_{gE} - s_{lE}\right)} \frac{ds_{lE}}{dP} \right)_t - \frac{cP_g\left(\frac{1}{n} - \frac{1}{\gamma} \right)}{\left(s_{g0} - s_{l0}\right)} \right| \tag{2.16}$$

$$\alpha_0 = \frac{x_0 v_{g0}}{\left(1-x_0\right) v_{l0} + x_0 v_{g0}} \tag{2.17}$$

$$\alpha_t = \frac{x_0 v_{gt}}{(1 - x_0) v_{l0} + x_0 v_{gt}} \tag{2.18}$$

$$v_{gt} = v_{g0}\left(\eta^{-\frac{1}{\gamma}}\right) \tag{2.19}$$

The method of Leung (1986) provides a convenient formulation to determine the mass flux (G) and critical pressure ratio (η) as indicated in Equation 2.20, 2.21, and 2.23.

$$G = \frac{\left[0.6055 + 0.1356(\ln(\omega)) - 0.0131(\ln(\omega)^2)\right]}{\omega^{0.5}} \cdot \sqrt{\frac{P_0}{v_0}} \qquad [Applicable \text{ if } \omega \geq 4] \tag{2.20}$$

$$G = \frac{066}{\omega^{0.39}} \cdot \sqrt{\frac{P_0}{v_0}} \qquad [Applicable \text{ if } \omega < 4] \tag{2.21}$$

The compressibility factor (ω) is given in Equation 2.22, where the first group of terms represent the void fraction and the second group denote the phase change. Once the compressibility factor is available, the transcendental Equation 2.23 for critical pressure ratio (η) can be determined.

$$\omega = \frac{x \cdot v_{g0}}{v_0} + cP_{l0}T_0P_0\left(\frac{(v_{g0} - v_{l0})^2}{\Delta h_{fg}^2 0}\right) \tag{2.22}$$

$$\eta^2 + (\omega^2 - 2\omega)(1 - \eta)^2 + 2\omega^2 \ln(\eta) + 2\omega^2(1 - \eta) = 0 \tag{2.23}$$

The correction factor used to adapt the incompressible and compressible models of Sheldon and Shuder (1965) were not evaluated based on inadequate performance as stipulated by Diener and Schmidt (2005). The method of Henry and Fauske (1971) was also not provided due to the experimental model's lack of conformance to HE and HF.

2.9 - Summary

Steam utilization will continue in the future to be an effective mode for delivering high quantities of thermal energy through the use of a non-hazardous and renewable resource. Generation, distribution, and steam use must occur efficiently to ensure optimization of existing resources through promoting environmental stewardship and sustainability. Adequate condensate removal eliminates pressure transients, improves reliability, reduces operating cost, and increases the energy deliverables to the point of use processes. However, existing steam traps have several deficiencies that prevent the optimal removal of condensate. It is conceivable the best solution to modulate the flow of fluid is through the use of a control valve, which is the focus of the experimental research. Also, several theoretical prediction models are evaluated to determine suitability.

Recognizing the shortcomings of existing steam traps provide an opportunity for improvement. Not only could the process become more reliable, safer, efficient, and effective, but the reduction of greenhouse gasses and harmful emissions will be reduced to promote sustainability. A thorough understanding of concepts related to improving thermal energy use and delivery is derived from the literature review. The application of mass flowrate prediction modeling provides the capability to evaluate theoretical and experimental model performance.

-3- Experimental Procedures

3.1 - Apparatus

3.1.1 - Introduction

The mass flowrate of condensate through a control valve is the primary interest. Three potential methods exist to determine the result, which include either a weigh tank, flowmeter, or volumetric tank. Recognizing the importance of utilizing a standard test procedure is crucial for an accurate comparison of the steam trap and control valve.

The most direct method to determine mass flowrate is to use a flow meter. However, the vast span of expected values prevented an adequate selection. The meters have a specified range of operation and deviations outside the range provide unreliable data. Although the other two options are viable for the experimental work, selection of a weigh tank was chosen based on available instrumentation and equipment.

Using a standardized performance assessment allows comparable results for equivalent operating conditions. The standard chosen was from the American National Standards Institute (2005), performance test code PTC 39, revision and designation of the ASME PTC 39.1-1980 standard. The test standard was reaffirmed in 2010. The research is concerned with determining the mass flowrate of condensate through a control valve for various supply temperatures, supply pressures, and valve positions.

3.1.2 - Weigh Tank Technique

Collecting condensate in a containment tank for a known amount of time will provide the desired response of mass flowrate (unit of mass per unit of time). The initial

mass of the containment unit and subcooled condensate are tared before experimentation. Two techniques are conducted to ensure accurate weight collection during experimentation. The first is using subcooled condensate within the tank to collapse flash steam. Secondly, a vacuum breaker is installed at the top of the discharged line to eliminate condensate from being pulled up the piping.

3.1.3 - Physical Description

3.1.3.1 - Introduction

The physical layout includes storage and condensate preparation, distribution piping, control, weigh tank, and graphical user interface. Figure 3-1 depicts the experimental apparatus, while Appendix A contains several pictures of the physical equipment.

The storage and condensate preparation components consist of several items. Included are a supply reservoir, immersion heating element, pneumatic control valve, pneumatic pressure regulator valve (PRV), current to pressure transducer (I/P), supply/ discharge pressure sensor (PT1/PT2), supply temperature sensor (RTD1), circulation pump, and a manual vent valve. The supply reservoir is adequately insulated to minimize the effects of heat loss while the 1500 W immersion element heats the condensate to the desired test condition.

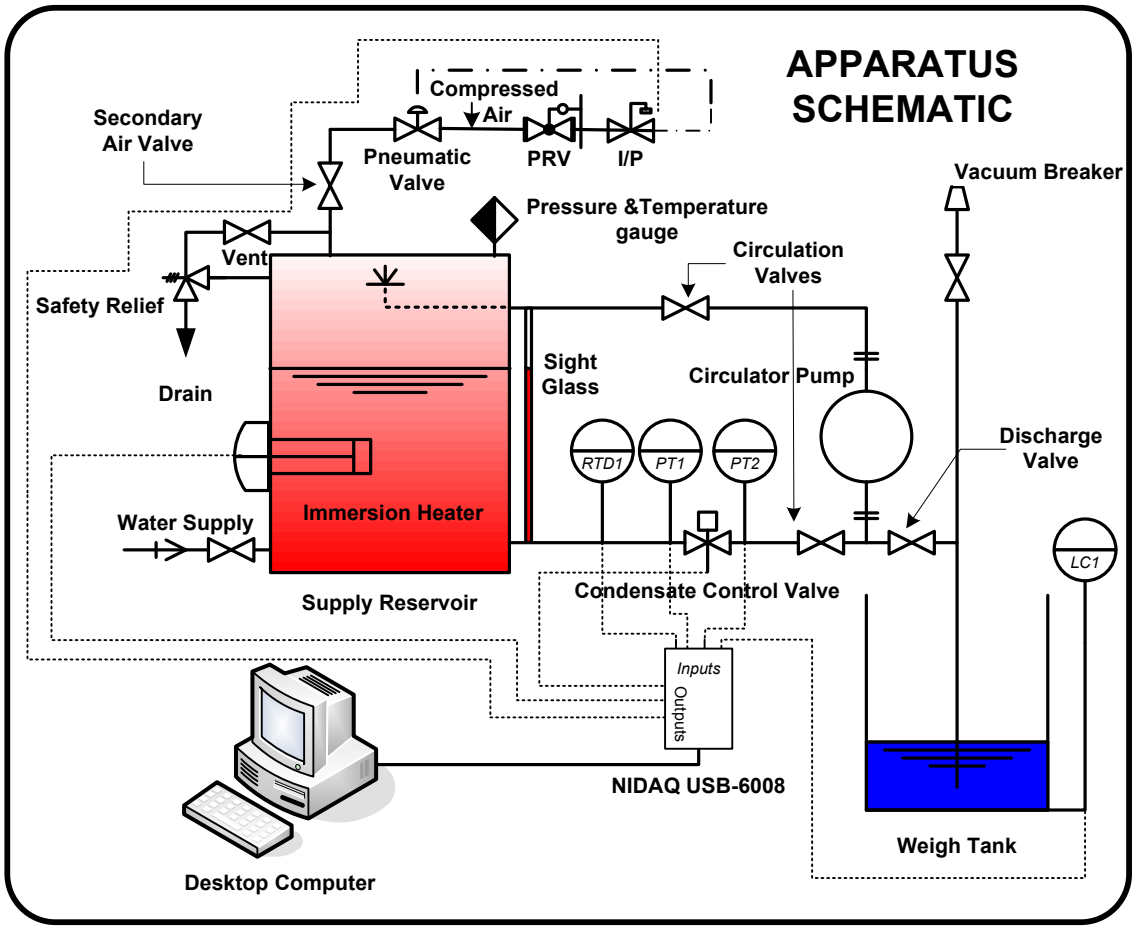

Figure 3-1: Schematic for experimental apparatus

A circulation pump enables a homogeneous temperature distribution by thoroughly mixing the condensate between the supply reservoir and distribution piping. Upon re-entry into the tank, condensate is sprayed through a nozzle to remove air and promote sufficient mixing. The manual vent valve provides a release of entrained oxygen from the supply reservoir when heating the condensate. The supply/discharge pressure and temperature sensors provide an analog input as feedback to the controller. A pneumatic control valve provides the necessary supply pressure for the experimental test via the current to pressure transducer.

The pipe network consists of a circulation loop and an experimental section. The circulation loop exists between the pump and the supply reservoir. All piping is adequately insulated to minimize the effects of heat loss. One benefit of the circuit is to provide a thorough mixing process of the temperature throughout the condensate. Another advantage is related to preheating the distribution piping, which establishes experimental conditions within the pipe and control valve. The preliminary piping includes the lateral section of the circulation loop and an intersecting tee to allow for alternate connections. For instance, the top of the tee permits the connection of a vacuum breaker during experimentation or pump priming during the purge cycle. The bottom of the tee directs condensate into the weigh tank during experimentation or the connection of a check valve for pump priming during the purge cycle. Piping is also present to connect the manual vent valve and safety relief valve to drain. To utilize pneumatic air, a series of piping connects the compressed air source to the supply reservoir and the current to pressure transducer. Finally, as required upon initial fill, piping connects a water source to the supply tank.

Several components enable the suitable control of condensate supply pressure, supply temperature, and valve actuation position. The placement of the majority of components is in an electrical enclosure. They include the NIDAQ controller, low voltage solid state and reed relays, AC transformer, DC power supply, RTD1 signal conditioning module, and a current to pressure transducer. Externally, RTD1 and PT1 provide feedback signals for control. An electric control actuator positions the condensate control valve while a pneumatic actuator regulates the supply pressure. The

manual control of several ball valves influences the direction of flow or the removal of fluid.

The weigh tank is plastic with a metal base and an open top. The base accepts a one button compressive load cell and two load cell imitations. The hole placements are equally spaced and drilled to a depth appropriate for the proper function of the load cell. The geometric center of the tank is concentric with the circle pattern for load cells and the metal jig fixed to the base of the weigh tank. The load cell provides a modified signal to the controller through an AC powered signal conditioner.

A graphical user interface provides operating control of the experimental apparatus and is facilitated by a desktop computer, LabVIEW (National Instruments, 2013), and monitor. A sight glass provides visual identification of liquid level during preconditioning of condensate.

3.1.3.2 - Supply and Weigh Tank

A 17.1 Gal electric water heater is the supply tank. The steel tank was adequate to facilitate the experimental operating conditions for pressure (0.5 - 14.5 psig) and temperature (194 - 248.3°F). The tank was well insulated, contained an immersion heater, and provided adequate national pipe thread fittings for auxiliary components and piping. However, modifications were required to prepare the tank for use. A certified pressure safety relief valve (15 psig) replaces the integrated pressure and temperature safety relief valve. Replacement of the manufacturer provided immersion heater (3000 W) with a 1500 W element allows operation within the laboratory space. The cathodic

protection device was removed to make use of the tank connection. Finally, the manufacturer temperature control was removed.

The weigh tank is a high impact, cross-linked polymer with an approximate volume of 22 Gal. The excess volume as compared to the supply tank is adequate for the provision of a subcooled liquid buffer to collapse any excess flash steam; ensuring an accurate collection of condensate for mass measurement.

3.1.3.3 - Sensors

The three types of sensors required to conduct experimentation included pressure, temperature, and load cell. The location of two pressure sensors (PX209-015G5V) are before and after the condensate control valve, a temperature sensor (PR-20-2-100-3/16-2-E-T) on the condensate supply line, and a load cell (LC304-100) on the weigh tank. The sensors are provided an excitation voltage to produce a calibrated response. Converting the response into engineering units facilitates the convenient utilization of high-level programming, visual representation within the graphical user interface, and data acquisition.

Only one load cell is used to provide measurement, although the capacity has equal distribution for three contact points. Two equivalent sized replicas of the cells have displacement about 360° and each is located such that the geometric center corresponds to the weigh tank's center of gravity. The load cell was calibrated to represent the total mass of condensate instead of the actual 1/3 distributed contribution.

The detailed performance specifications relevant to each sensor are presented in a later measurement section.

3.1.3.4 - Circulation Pump

A multiple speed circulator pump (Grundfos UPS 15-58 FC) delivered the necessary pressure differential for condensate recovery (6.5 GPM) and condensate preparation (8 GPM). Although the operating conditions for the pump exceeded the recommended maximum liquid temperature for several trials, the pump functioned as required during experimentation.

3.1.3.5 - Data Acquisition and Control

A National Instruments DAQ USB-6008 device and LabVIEW (National Instruments, 2013) program was used for control and data acquisition. A graphical approach provides the controlling attributes instead of a language based program, i.e., FORTRAN or C. LabVIEW is a software tool that provides a foundation for instrument and computer integration, programming, and graphical user interface. These two elements enabled instrumentation signals to be converted into machine code. The machine code is transformed into units of engineering measurement through calibration. Storage, control, and/or post-processing is possible once data conversion is successful. MathWorks (2015) was chosen for the exportation and post-processing of data.

3.1.3.6 - Control Valves and Piping

Two control valves facilitate experimentation. The condensate control valve (VG1245BN) is the focus of study while the motive control valve (VG7441CT) modulates the compressed air. Type L copper provides the distribution piping for conveying the fluid.

The two-way condensate control valve has a forged brass body and stainless steel components for serviceability of 15 psig at saturation temperature. The equal percentage ball valve has an electric actuator (M9106-GGC-2) that provides a feedback signal for valve location. During the experimental trials, the valve could be rotated precisely to the desired position. A linkage kit (M9000-520) couples the valve and actuator for application relevant to high operating service temperatures.

The two-way motive control valve has a cast bronze body and is rated as class 250. It is considerably higher than the operating pressure and temperature of the compressed air service. Accompanying the equal percentage globe valve is a pneumatic actuator (3008D0). As the performance of the control valve in maintaining the supply pressure was critical, a fast acting actuator was required.

3.1.3.7 Testing Fluid

Domestic cold water is the source fluid for experimental research. Table 3-1 provides a municipal sample for tap water quality in public water supplies (Conservation and Environment, 2014). Included in the table are pertinent physical parameters for water collected in December 2014. The quality is representative of pre-experimental trials.

Table 3-1: Municipal water quality

Water Quality					
Alkalinity	Color	Conductivity	Hardness	pH	TDS
21.0	2.0	116.0	22.0	7.3	75.0

3.1.4 - Design and Fabrication

3.1.4.1 – Introduction

The conceptual design of the experimental apparatus adheres to PTC39 performance test standard (American National Standards Institute, 2005). Modifications include the use of compressed air for the supply pressure and an immersion heating element to control condensate temperature.

To reduce financial cost and alleviate delays due to manufacturing, original equipment manufacturer components were acquired for assembly. Furthermore, all fabrication work for the experimental setup was completed by the author. The only exception consisted of the fabrication and installation of glass piping for flow visualization.

Guiding references utilized during the construction of the pipe network included the use of the Copper Development Association (1960) handbook. The pressure-temperature relationship for soldered joints and safe operating conditions were considered. Furthermore, methods related to plumbing were followed, i.e., measuring and cutting, reaming, cleaning, applying flux, assembly and support, heating, soldering, cooling and cleaning, and testing.

3.1.4.2 - Pipe Network

The choice of pipe diameter was equivalent to the size of the control valve and alleviated the need to install reducing fittings. Additional concentric or eccentric reducers would have added complications to maintaining the performance standard's maximum

allowable placement for instrumentation. Also, the joints would add minor losses that would have to be accounted during the development of the correction factor.

The difference between the inside diameter of the experimental piping versus the inside diameter of the industrial piping is approximately 45 thousands of an inch. The deviation has an insignificant impact on experimental results.

Schedule 80 black iron piping is predominately the industrial choice for condensate piping. The piping provides greater protection to the inherently corrosive environment because of the increased pipe thickness; as compared to schedule 40. However, this material was not used for experimentation as undesirable oxidation and corrosion would have occurred without chemical treatment. Instead, Type L copper was used to fulfill the piping requirement. It is corrosion-resistant, economic, and provides ease of workmanship. The frictional impact between the coefficient of friction for pipe material over the exceedingly short distance is minimal.

3.1.4.3 - Condensate Control Valve

Choosing a condensate control valve entailed the consideration of several factors: price, flow characteristics, operating specifications, actuator, and flow capacity.

Comparisons between equivalent valve types indicated that the most cost-effective selection was the ball valve. Other auxiliary expenses for consideration are the operating and maintenance cost. The ball valve provides low maintenance design features, i.e., simplistic, compact, and minimal moving parts. Also, an attribute relevant for control valve selection is rangeability, which is the ratio of the maximum to minimum flowrate (Spirax Sarco, 2008). The valve selected included a high rangeability of 500:1. The

rangeability of other valve types were less desirable, i.e., the rangeability of globe valves are typically 50:1. Finally, the class rating of the ball valve provided a tight shutoff (200 psig).

The potential choices for valve flow characteristics included fast opening, linear, or equal percentage (ASHRAE, 1985). The desired flow characteristic for the ball valve is equal percentage. Each increment in valve rotation increases the flowrate by a certain proportion of the previous flow. The resulting relationship provides a desirable logarithmic response for purposes of control. Equation 3.1 represents the theoretical volumetric flowrate (Q) through a valve for a given rotation (R^*); where 0 indicates a valve fully closed and 1 describes a fully open valve (Spirax Sarco, 2008).

$$Q = \frac{e^{\ln(\tau \cdot R^*)} Q_{\max}}{\tau} \tag{3.1}$$

Where the parameter τ represents rangeability and the subscript *max* references the greatest flow possible through the valve.

The ball valve must be able to sustain operation at a high temperature and harsh environment. The pressure range and corresponding saturation temperature include 0 - 15 psig and 212.0 - 249.7°F. A stainless steel ball, trim, and stem assembly were required to ensure the valve could operate within the specified condition.

Relevant criteria for selecting the actuator was valve position feedback and adaptation to the stem of the control valve. For the experimental design, process control of the valve was irrelevant because the valve position resides in a stationary location for each trial. Therefore, concerns related to the control valve having a non-spring return

actuator or a minimum rotation time of 60 s did not impact characteristics relevant to practical use. Cheaper actuators exist for adequate use, but accurate valve position feedback is required for experimentation.

Prediction of the flow capacity for various conditions deemed to be significant include valve position, supply pressure, and supply temperature. The ability to determine a general guideline for selecting a flow coefficient is one of the primary goals of conducting the experimentation. A choked flow condition for the fluid can be validated and established through Equation 3.2; according to the physical parameters of the valve and flow conditions. The American National Standards Institute (2002) provide the valve recovery factor and formulation.

$$\Delta P \geq F_L^2\left(P_1 - F_F P_V\right) \tag{3.2}$$

$$F_F = 0.96 - 0.28\sqrt{\frac{P_v}{P_c}} \tag{3.3}$$

Where the expression for liquid critical pressure ratio (F_F) is given in Equation 3.3. The valve recovery factor (F_L), vapor pressure (P_V), supply pressure (P_1), and thermodynamic critical pressure (P_c) are key parameters for establishing a choked flow condition.

A maximum volumetric flowrate (Q) of 10 GPM produced a flow coefficient (C_v) of 10.59 by using Equation 3.4.

$$Q = \frac{N_1 \cdot C_v}{\sqrt{\frac{\rho_1}{\rho_0\left(P1 - F_F P_V\right)}}} \tag{3.4}$$

Where the relative density is characterized by ρ_1/ρ_0. A suitable choice of control valve that would meet or exceed the design parameters resulted in the selection of $C_v = 11.7$, which produces a flowrate of 11 GPM.

The Reynolds number (R_e) was confirmed to be turbulent through Equation 3.5. The result ($R_e = 496{,}388$) was compared against a threshold ($R_e \geq 10{,}000$) and validated for justification and use of Equation 3.4. The American National Standards Institute (2002) provides the valve style modifier (F_d), recovery factor (F_L), and unit formulae modifiers (N_x's).

$$R_e = \frac{N_4 \cdot F_d \cdot Q}{v\sqrt{c_v F_L}} \left(\frac{F_L^2 C_v^2}{N_2 \mathrm{D}^4} + 1 \right)^{\frac{1}{4}} \tag{3.5}$$

Where D is the inside pipe diameter and v represents the specific volume.

3.1.4.4 - Supply Reservoir

After having established the maximum flowrate, the pressure vessel volume was determined based on a collection time of 90 s. The resultant volume is approximately 17 Gal.

3.1.4.5 - Motive Pressure Control Valve

The original testing utilized a manual flow regulator, but adequate regulation of the supply pressure was inconsistent and at times failed to maintain PT1 $\leq \pm$ 1 psig (experimental control standard). Several steps to establish the necessary flow coefficient for the compressible fluid entailed identifying the required mass flowrate for air.

Determination of the flow condition is possible through the use of one out of four recommended ISA models (American National Standards Institute, 2002).

An estimate for the mass flowrate of air (15 lbm/h) comes from previous experimental trials, which produced the largest response. The pressure differential ratio factor (X_T) for an equal percentage globe valve was acquired from ISA (American National Standards Institute, 2002) to match the desired style of the control valve. Establishment of the specific heat ratio factor (F_γ) is through Equation 3.6 and is dependent upon the specific heat ratio (γ^*).

$$F_\gamma = \frac{\gamma^*}{1.40} \tag{3.6}$$

At ambient temperate and pressure, the specific heat ratio (γ^*) for air is determined and the expression, as indicated by Equation 3.7, confirms the presence of a choked and turbulent flow through the control valve.

$$\frac{\Delta P}{P_1} \geq F_\gamma X_T \tag{3.7}$$

Where X_T is the pressure differential ratio factor, ΔP is the differential pressure between supply and discharge pressure, F_γ is the specific heat ratio factor, and P_1 is the supply pressure.

A turbulent model for a compressible fluid with choked flow was chosen to determine and approximate the flow coefficient (C_v) for valve selection with Equation 3.8.

$$C_V = \frac{W}{Y \cdot N_6 \sqrt{F_\gamma X_T P_1 \rho_1}} \tag{3.8}$$

Where W is the mass flowrate of air, Y represents the expansion factor, N_6 is the unit formulae modifier, and ρ is the fluid density.

Comparing the result ($C_v = 0.31$) against a manufacturer vendor catalog provides the next available coefficient of flow for selection ($C_v = 0.73$). The new flow coefficient provides a maximum flowrate of 34.9 lbm/h. The Reynolds number was confirmed to be turbulent through Equation 3.5. The result ($R_e = 48{,}232$) was compared against a threshold ($R_e \geq 10{,}000$) and confirmed the appropriate use of Equation 3.8. The valve style modifier and valve recovery factor was attained from the American National Standards Institute (2002).

3.1.4.6 - Control Strategy

The motive pressure valve requires a control strategy to provide a desirable and stable response for experimentation. The goal was to use proportional, integral, and derivate control (PID). Ziegler-Nichols empirical methodology was applied to determine controller gains. The control signal (Q) and gain parameters (k_p, T_I, T_D) suggested by Ziegler-Nichols is representative of Equation 3.9 (Franklin, Powell and Emami, 2002). All future reference of control formulation and methodology is provided by Franklin et al. (2002).

$$Q = k_p\left(1 + \frac{1}{T_I} + T_D\right) \tag{3.9}$$

Two methods provide a way to achieve the best response. The first method entailed utilizing the ultimate sensitivity method within a closed loop. In this case, the system is made to become borderline stable through actuation of the control valve in

response to supply pressure. To achieve a borderline unstable system the operator changes the proportional gain to different values while observing the pressure response. During this process, the integral and derivative gains are 0. Two channels are invoked in LabVIEW (National Instruments, 2013) program to measure the pressure and I/P response voltage. The proportional gain producing a borderline instability is noted and the corresponding period for several cycles are measured and averaged. The values are entered into a series of formulas to determine the optimal gains; depending upon the desired control strategy. The gains for the controller are changed, and the response analyzed to verify conformance with the desired attributes, i.e., minimal overshoot and settling time.

For proportional control (k_p), the borderline gain (k_u) will establish the necessary parameter with Equation 3.10.

$$k_p = 0.5\, k_u \tag{3.10}$$

For proportional and integral control, borderline gain (k_u) and borderline period (P_u) will establish the necessary parameters by using Equations 3.11 and 3.12. The integral portion of the control strategy is represented by T_I.

$$k_p = 0.45\, k_u \tag{3.11}$$

$$T_I = \frac{P_u}{1.2} \tag{3.12}$$

The borderline gain (k_u) and borderline period (P_u) will establish the necessary parameters with Equations 3.13, 3.14, and 3.15 for proportional (k_p), integral (T_I), and derivative (T_D) control parameters.

$$k_p = 0.6\,k_u \tag{3.13}$$

$$T_I = 0.5\,P_u \tag{3.14}$$

$$T_{\mathrm{D}} = 0.125\,P_u \tag{3.15}$$

The second method consists of investigating the system response within a closed system (quarter decay). In this case, the control block is changed to provide a step unit input for a predetermined duration. The controller parameters remain the same as the ultimate sensitivity method, but with the addition of lag time (L) as well as the corresponding reaction rate (R). The data and a series of formulas achieve a set of possible parameters for a stable system response. The gains go into the source code once calculated, and a desired control strategy determined.

For proportional control (k_p), acquiring the lag time (L) and reaction rate (R) provides the necessary gain by using Equation 3.16.

$$k_p = \frac{1}{RL} \tag{3.16}$$

For proportional (k_p) and integral (T_I) control parameters, acquiring the lag time (L) and reaction rate (R) provides the necessary parameters with Equations 3.17 and 3.18.

$$k_p = \frac{0.9}{RL} \tag{3.17}$$

$$T_I = \frac{L}{0.3} \tag{3.18}$$

Acquiring the lag time (L) and reaction rate (R) provides the necessary parameters by using 3.19, 3.20, and 3.21 for proportional (k_p), integral (T_I), and derivative (T_D) control parameters.

$$k_p = \frac{1.2}{RL} \tag{3.19}$$

$$T_I = 2L \tag{3.20}$$

$$T_D = 0.5L \tag{3.21}$$

The gains for each method are evaluated within the control system to provide a desired response, i.e., minimal overshoot and settling time. After having completed both methods, the ultimate sensitivity procedure provided improved system performance for experimentation. The proportional and integral (k_p= 4.75, T_I = 3 s) control strategy provided the best response.

3.1.4.7 - Safety

Installing a safety relief valve limits the maximum condensate temperature within the supply reservoir. The system protection is for 15 psig and can provide a maximum temperature of 248.3°F. Electrical safety was possible through the use of primary fuses and a secondary breaker. Consideration of the supply reservoir volume was sized appropriately to alleviate the potential of the weigh tank overflowing. A pressure regulating valve is required to limit the maximum allowable pressure for the actuator. Furthermore, to protect failures related to operator involvement, safety checks were programmed into the graphical user interface. Also, the addition of a universal power

supply prevented the loss of power to the controller and desktop computer during preconditioning and experimental trials.

3.1.5 - Operation

3.1.5.1 – Introduction

The role of the experimental apparatus is to facilitate the delivery and control of supply pressure, supply temperature, and valve position to determine the mass flowrate of condensate. To maintain PTC 39-2005 performance test standard (American National Standards Institute, 2005), the supply pressure and temperature must be within ±1 psig and ± 5°F, respectively.

3.1.5.2 - Measurement

An IEC Class A sensor (RTD1) provides the condensate supply temperature. It is a PR-20 series resistance transducer acquired from Omega Engineering Inc. The particular model is SCM7B34-03D and distinguished by serial number 99637-1. A three wire construction was selected to provide a temperature range of 32 - 392°F. The standard maintains a high-accuracy 100 Ω DIN platinum element as per IEC751 (α = 0.00385 Ω/ Ω/°C). Included in Appendix B is the manufacturer 5-point NIST calibration certificate.

The temperature sensor exceeds the minimum stipulation as required through the performance test standard (American National Standards Institute, 2005). RTD1 has a minimum accuracy of ±0.25°F.

Two electronic transmitters (PT1 and PT2) measure the supply and discharge pressure of the condensate before and after the control valve. Each sensor is certified to be a 0.1% accuracy class, with a 0.25% combined accuracy specification that includes linearity, hysteresis, and repeatability. The PX209 series sensor is a product from Omega Engineering Inc. The particular model is PX209-015G5V and distinguished by serial numbers 99719 (condensate supply pressure) and 97399 (condensate discharge pressure). A three wire construction provides a pressure range of 0 - 15 psig. Included in Appendix B is the manufacturer 5-point NIST calibration certificates.

The pressure sensors exceed the minimum stipulation as required through the performance test standard (American National Standards Institute, 2005). PT1 and PT2 has an overall accuracy of 0.25% (±0.04 psig).

A compression load cell (LC1) is calibrated to measure the mass of condensate. The sensor is certified to have a combined accuracy of 0.5% full-scale output that includes linearity, hysteresis, and repeatability. The LC304 series sensor is a product from Omega Engineering Inc. The explicit model is LC304-100 and serial number 208927. A four wire construction provided an excitation voltage of 15 VDC, including signal amplification to produce a suitable range for experimentation. The load cell ratings are 100 lb with a safe overload of 150 lb and an ultimate overload of 300 lb. The manufacturer 5-point NIST calibration certificates are included in Appendix B.

The load cell meets the minimum stipulation as required through the performance test standard (American National Standards Institute, 2005). LC1 has an overall uncertainty of 0.5% (±0.5 lbm).

Data acquisition (DAQ) is used to collect sensory information based on the physical characteristics of pressure, temperature, and mass. The timing accuracy of the device is specified to be 100 ppm of the actual sample rate. The DAQ is a USB series from National Instruments. The model is NIDAQ USB-6008 and serial number 0X19BEB99.

Measurement of the timing interval exceeds the minimum stipulation as required through the performance test standard (American National Standards Institute, 2005). The DAQ has an overall accuracy of ±0.1 s for a sample rate of 1000 Hz.

3.1.5.3 - General

Four distinct procedures are required for experimental research. They include system initialization, condensate preparation, experimentation, and condensate recovery. Adherence of the performance test standard (American National Standards Institute, 2005) occurs during development and testing. Conservatory measures were implemented to preserve energy efficiency and aid in reducing the time required to conduct physical trials. Condensate recovery increases temperature and reduces the solubility of oxygen. The reduced levels of oxygen promoted conditions favorable in the prevention of corrosion. Also, an increased fluid temperature reduced the electrical energy and time required for condensate preparation.

Figure 3-2 provides a visual representation of the graphical user interface (GUI); including the three experimental factors for altering the pressure, temperature, and valve position. Depicted are the physical components of the apparatus that portray the mode of

operation and instrumentation signals. Three modes of operation include experimental, circulation, and purge.

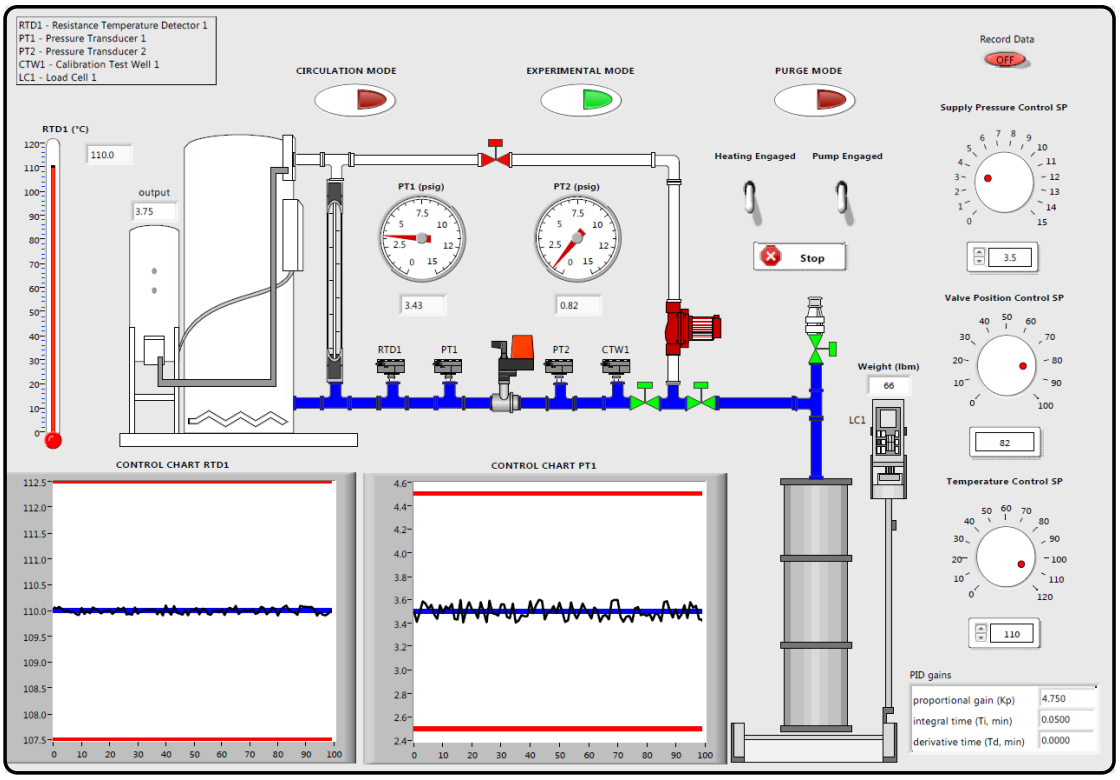

Figure 3-2: Graphical user interface for the experimental mode

Figure 3-2, Figure 3-3, and Figure 3-4 present the experimental, circulation, and purge modes, respectively. Furthermore, the control charts establish if the experiment adheres to meeting the test standard (American National Standards Institute, 2005) for supply temperature and pressure variation.

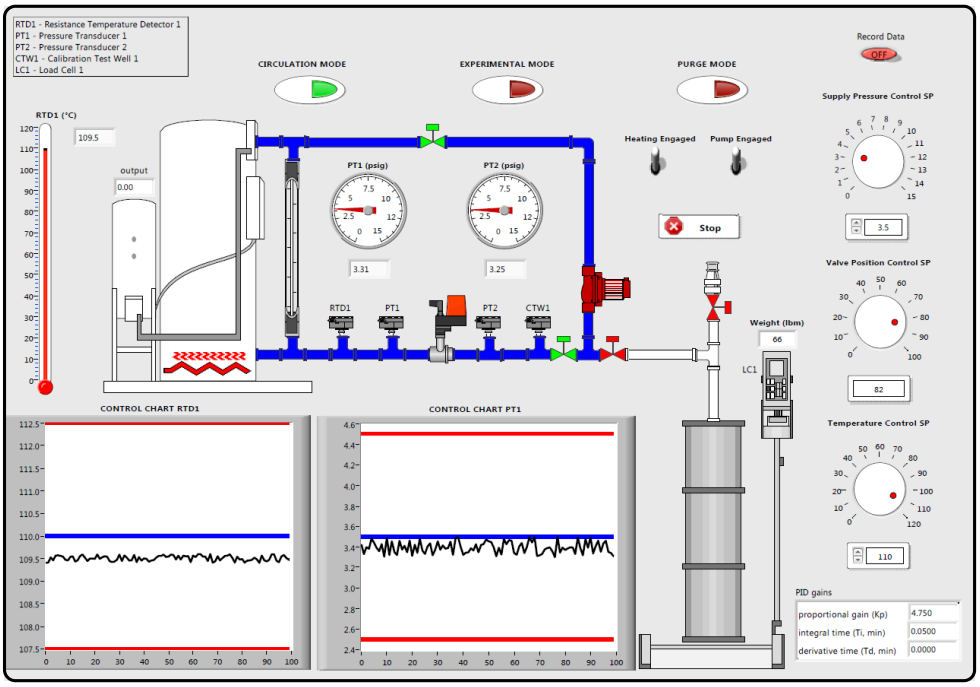

Figure 3-3: Graphical user interface for the circulation mode

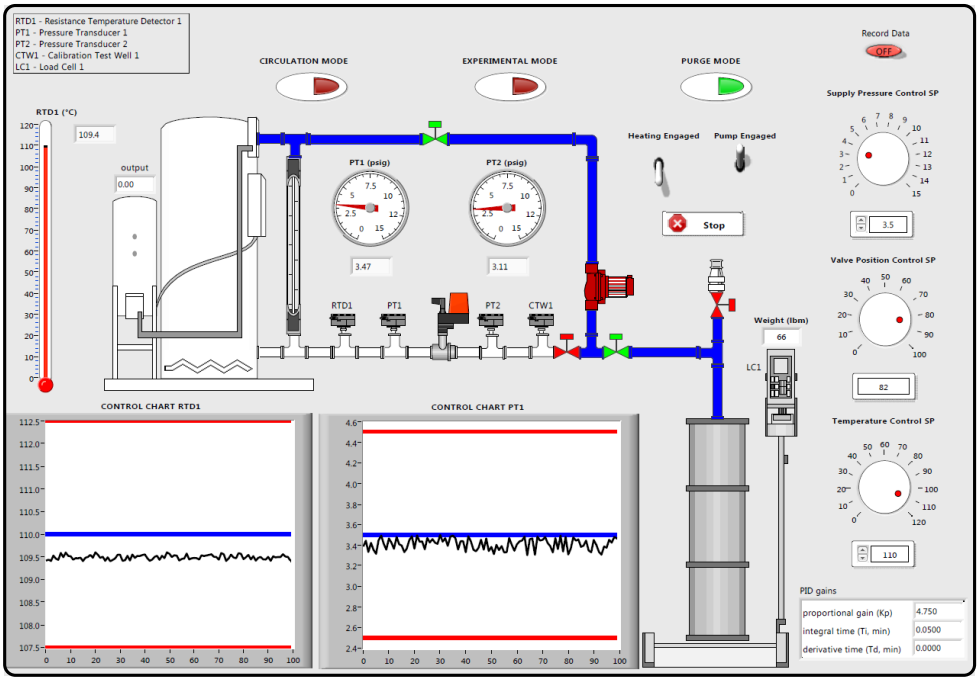

Figure 3-4: Graphical user interface for the purge mode

3.1.5.4 - System Initialization Test Procedures

System initialization includes enabling localized resources for experimentation, i.e., domestic water, electrical services, pneumatic services, and graphical user interface. The procedural steps for system initialization include:

1. Prepare computer station, primary air supply valve, and graphical user interface. Set temperature control, pressure control, and valve position control to 0°C, 0 psig, and 100%, respectively. Activate program and energize instrument panel.
2. Ensure secondary air supply valve is closed. Open the air vent valve. Ensure both circulation valves are open and discharge valve is closed.
3. Securely connect stainless steel braided hose to a domestic cold water source. Open both level indicator valves. Completely open tank filling valve. Then slowly open the water supply valve to fill supply reservoir to desired level. The water level must be greater than the immersion element. When the water level is suitable, close water supply valve and close tank filling valve. Disconnect stainless steel braided hose from the water source. Close top circulation valve, shut the air vent valve, and close both level indicator valves.
4. Fill weigh tank until the discharge line is a few inches below the water surface.

3.1.5.5 - Condensate Preparation Test Procedures

The preparation of condensate before each experimental trial requires the stabilization of temperature to within ± 2°F. Furthermore, removal of excess oxygen and other non-condensables produces the desired experimental conditions.

The procedural steps to procure condensate preparation include:

1. Set temperature control, pressure control, and valve position control to 0°C, 0 psig, and 100%, respectively within GUI. Run program.
2. Ensure secondary air supply valve is closed. Open air vent valve slowly. Confirm both circulation valves are open and discharge valve is closed.
3. Prepare circulation circuit within GUI. Verify circuit manipulation before engaging the pump control switch.
4. Set temperature control to the desired value. Engage heater control switch. When the temperature is at setpoint and stable within ± 2°F, disengage heater control and pump switch.
5. Record initial condensate temperature and initial air/steam temperature.

3.1.5.6 - Experimentation Test Procedures

Upon completion of condensate preparedness, the experimental apparatus must be readied for experimentation. The procedural steps for experimentation include:

1. Set temperature control, pressure control, and valve position control to 0°C, 0 psig, and 100%, respectively within GUI. Run program.
2. Open secondary air pressure valve. Close air vent valve. Close top circulatory valve. Open bottom circulatory valve. Install vacuum breaker and remove check valve (foot valve). Open ball valve adjacent to the vacuum breaker.
3. Initialize experimental circuit within the graphical user interface. Verify circuit manipulation. Set pressure, temperature, and valve position controls to desired value.

4. Enter appropriate trial run in text box. Commence data acquisition with toggle switch (record data) within GUI.
5. Open discharge valve. During experimentation, observe temperature and pressure control charts to ensure adherence to test standard. Close the discharge valve when sufficient condensate is collected in the weigh tank.
6. Turn off 'record data' toggle switch. Inspect data to ensure pressure and temperature are within the prescribed ranges (± 1 psig and ± 5°F).
7. Record ambient temperature, barometric pressure, air/steam pressure and temperature. The initial and final supply pressure (PT1/PT2), the mass of condensate (LC1), supply temperature (RTD1), and time interval are for steady state conditions. Determination of the initial and final mass of the condensate requires post processing.

3.1.5.7 - Condensate Recovery Test Procedures

The temperature of the weigh tank and supply reservoir are observed upon completion of the experiment. Relevant conditions within the supply reservoir are excess energy and pressurization. Usually, a small amount of condensate is left over from the experimental trial and requires caution before opening up the vent valve. Should excess thermal energy exist inside the supply reservoir, it will cause the condensate to flash and become discharged through the air vent. Also, the pressure within the supply reservoir must be reduced to a minimum of 4 psig to allow the circulator pump to function in purge mode. The procedural steps for condensate recovery include:

1. Set temperature control, pressure control, and valve position control to 0°C, 0 psig, and 100%, respectively within GUI. Run program.
2. Ensure secondary air supply valves are closed. Open the air vent valve. Confirm top circulation valve is open. Close bottom circulation valve. Open the discharge valve once there is no pressure within the supply reservoir.
3. Uninstall union and remove pipe. Remove vacuum breaker. Install check valve (foot valve). Reinstall union. Open vacuum breaker valve. Securely connect the clear hose to a water source and place the other end in the top of the open pipe (prime pump). Open water supply valve slowly. Close the water supply valve when the water reaches the upper part of the pipe. Remove the clear hose and place in weigh tank. Close vacuum breaker valve.
4. Initialize purge circuit within the graphical user interface. Verify circuit manipulation before turning on the pump. Turn off the pump when the water level is a few inches above the foot valve. Close the air vent valve.
5. Shut the discharge valve. Open the vacuum breaker valve. Push check valve open to remove water in the pipe. Uninstall union and remove pipe. Install vacuum breaker. Remove check valve (foot valve). Reinstall union. Open bottom circulatory valve. Close top circulatory valve.

3.1.6 - Operational Issues

Although considerable efforts go into the conceptual and final design, unforeseen problems can be expected. Three issues arose that required remedial action: motive

pressure control, condensation induced water hammer, and a hard-to-change factor (temperature). Determination of the mass flowrate was adversely impacted.

3.1.6.1 - Motive Pressure Control

As the method to determine the mass flowrate of condensate depends on the weigh tank, concerns related to the measurement of time and mass are crucial. The performance standard relies on the pre-experimental mass, post mass, and time interval to determine the flowrate. The test standard (American National Standards Institute, 2005) sets limitations upon an acceptable supply pressure and temperature deviation to ensure the flowrate uncertainty conforms to a 95% confidence interval. However, during experimentation it was noted that the transient pressure exceed the imposed limitation. Figure 3-5 shows the transient and steady-state conditions.

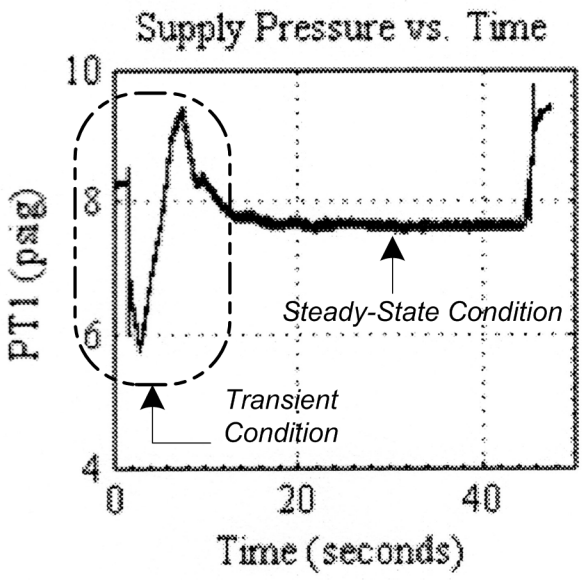

Figure 3-5: Transient condition for experimental startup

Failure to meet the limitation is due to the manual intervention for adjusting the motive pressure valve. The first applied solutions consisted of replacing the manual pressure valve with a solenoid valve and then to an automatic control valve. Although a significant improvement, the larger magnitude flowrates still exceeded the threshold.

The second solution consisted of integrating a load cell into the data acquisition system to accommodate for the presence of the pressure transient. This process replaced using the manual scale and stopwatch. The ability to electronically record the experimental factors in conjunction with mass and time measurement enabled conformance to the performance test standard (American National Standards Institute, 2005). The transient pressure variation that commences within the first 10 s, depending on the trial, does not matter when steady-state conditions are collected. Within the retrieved data set, the steady state conditions are established and the initial mass, final mass, and corresponding time interval determines the mass flowrate.

3.1.6.2 -Condensation Induced Water Hammer

The phenomena known as condensation induced water hammer occurs within the weigh tank for experimental trials above saturation temperature at atmospheric pressure. The effect causes a high-frequency oscillatory signal. The magnitude of oscillation seemed to increase for increased discharge temperatures and flowrates. The excess energy collapses within the subcooled liquid to produce an undesirable vibration. Figure 3-6 is an example of the oscillation effect due to condensation induced water hammer.

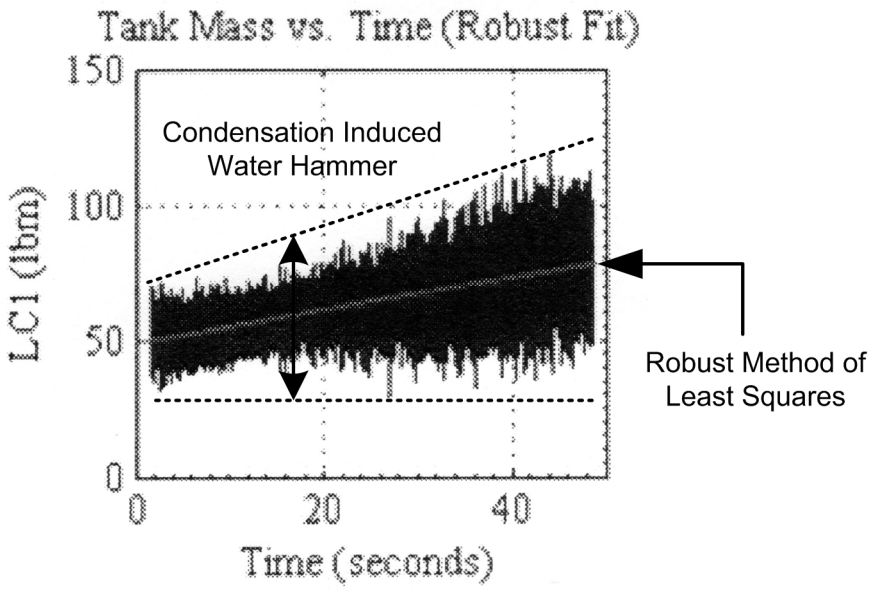

Figure 3-6: Condensation induced water hammer

Polyurethane isolation materials of different spring constant were placed under the weigh tank contact points. However, this provided minimal impact in reducing the magnitude of vibration. As the physical effect could not be altered at the time of experimentation, a reasonable solution was the use of post signal processing. A robust method of least squares was applied to evaluate goodness of fit. Various polynomial models and statistical indicators were assessed to ensure selection of the best fitting coefficients. Examples of statistical indicators include the R-squared, root mean squared error (RMSE), physical observation, and analysis of the residuals.

3.1.6.3 - Hard-to-Change Factor

The only factor that caused havoc during the research was temperature. The issue was with the available generation capacity of heat flux. For example, it would take approximately 60 min to increase the temperature 68°F. Each day the experiment

commenced with a fresh supply of domestic water and an average temperature of 46.4°F. Given the minimum experimental temperature was 194°F, the shortest initial preparation time of condensate was approximately 2 h. Reducing the fluid temperature was not an issue as rapid cooling commenced when entering the subcooled liquid within the weigh tank.

Reducing the time delay was possible through the addition of a software automation timing circuit. The program initiated each morning to preheat the test fluid to the correct temperature, which corresponded to the initial experimental trial. This change allowed increased number of trial runs per day. Figure 3-7 includes the graphical user interface for the timing circuit.

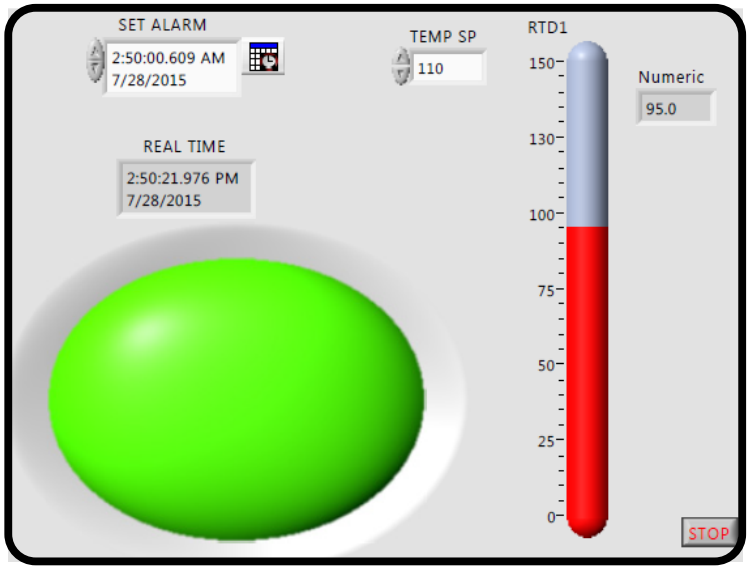

Figure 3-7: Graphical user interface for timing circuit

3.2 - Design of Experiment

3.2.1 - Introduction

Concerns related to the experimental acuity and objectivity can pose serious deficiencies should the improper design strategy and planning not be applied. For instance, interaction effects become invalidated, and the size of experimental design can become large for a one-factor-at-a-time (OFAT) experiment. Furthermore, experiments that do not incorporate a completely randomized design, replication, and blocking will inherently jeopardize the legitimacy of the results (Montgomery, 2013). The outcome of a proper experimental strategy is a true representation of the physical response, which is unbiased and scientifically accepted.

A randomized design reduces the random errors that inherently occur during experimentation, where deviations from the true value are negated. Replication allows for the evaluation of variability within the measured response. The closer the repeated measurements are to each other, the lower the error term produced. Removing systematic errors during experimentation is possible through blocking, which facilitates obtaining the true value of the response. Other experimental design methods are impractical because a continuous (response surface) model is desired.

Several aspects of the experimental design are important within the planning stages. Investigating the selection of experimental factors, levels, ranges, design type, and response variables are critical for successful results. The conceptual development and analysis for the design of experiment method is obtained through specialty software

(Stat-Ease, 2014). The program is intuitive to use and provides comprehensive statistical information.

3.2.2 - Factors

Three experimental factors are significant in the development of an empirical formulation for the mass flowrate of low-pressure condensate through a control valve. These include supply pressure, supply temperature, and valve position. Selection is due to experience, theory, and/or inferred throughout the literature review. The supply pressure provides flow potential, the valve position alters the flow path, and the temperature affects the flow characteristics of the fluid. For instance, the supply pressure provides a force on the surface of the condensate and produces an increased pressure differential with respect to the atmosphere. The valve position would create a pressure drop within the valve and would effectively reduce the flow potential. Changes in supply temperature causes the volume to increase while promoting flash formation at or above saturation temperature. Essentially the variables are selected because each experimental factor is thought to influence the experimental responses, i.e., mass flowrate of condensate and discharge pressure.

3.2.3 - Levels and Range

A response surface model requires a low and high level for each factor, where continuous data exist for the range of values between each level. The choice of ranges are important to ensure the results are measurable, but far enough apart to observe evident changes in the response variable. The information for each factor is as follows:

1. Pressure - The range represents a feasible spread of data for a low-pressure steam system. Values below 0.5 psig cannot be obtained as the test fluid's head pressure corresponds to this minimum pressure. The upper level was 14.5 psig, which was 0.5 psig below the safety relief valve.

2. Temperature - A minimum level of 203°F was required by the performance test standard (American National Standards Institute, 2005). The top level for temperature corresponded to the equation of state for maximum experimental pressure (248.3°F).

3. Valve position – A minimum level of 25% rotation provides the smallest measurable flow. There are no restrictions for the upper level and the selection of the maximum rotation is 100%. Table 3-2 provide the associated ranges and levels for each experimental factor.

Table 3-2: Range and level for experimental design

Name	Units	Type	Subtype	Minimum	Maximum	Coded Values		Mean	Std. Dev.
Pressure	psig	Numeric	Continuous	0.5	14.5	-1.000=0.50	1.000=14.50	7.81	5.05
Temperature	°C	Numeric	Continuous	90	120.17	-1.000=90.00	1.000=120.44	100.76	8.87
Valve Position	% Open	Numeric	Continuous	25	100	-1.000=25.00	1.000=100.00	59.9	25.74

3.2.4 Experimental Response

There are two measured responses of interest, which include the mass flowrate of condensate (lbm/h) and the discharge pressure (psig). The mass flowrate is required to evaluate the performance of control valves and the discharge pressure is needed for the theoretical prediction models.

3.2.4 - Design Type

Several different experimental design types and variations exist. Selection is dependent upon the goal of the experimentation. For instance, a screening experiment reduces cost and number of trials before commencing advanced experimentation.

For this research, a response surface method is desirable to predict the mass flowrate of condensate and discharge pressure. Although several options are available within the experimental design type, only one adequately serves to provide the best model. For example, classical methods include central composite design (CCD) and Box-Behnken design (BBD). However, problems arise with the equation of state, as the design produces factor combinations that are physically impossible to conduct. The condensate temperature must be at or below saturation temperature. Incomplete experimental trials result if this condition is not satisfied.

The response surface method that can facilitate the equation of state constraint is the optimal design. Applying this method to the experimental research produces a range of factor combinations that satisfy the equation of state. Figure 3-8 give a contour plot for standard error with the pressure and temperature constraint for saturated conditions. As Design Expert (Stat-Ease, 2014) can only create linear constraints, the actual non-linear relationship has to be estimated. This approximation is reasonable in developing the experimental design. Another benefit for optimal design is the ability to model higher than a quadratic function. The third order polynomial was selected and the result was beneficial and necessary to produce an adequate fit for the experimental data.

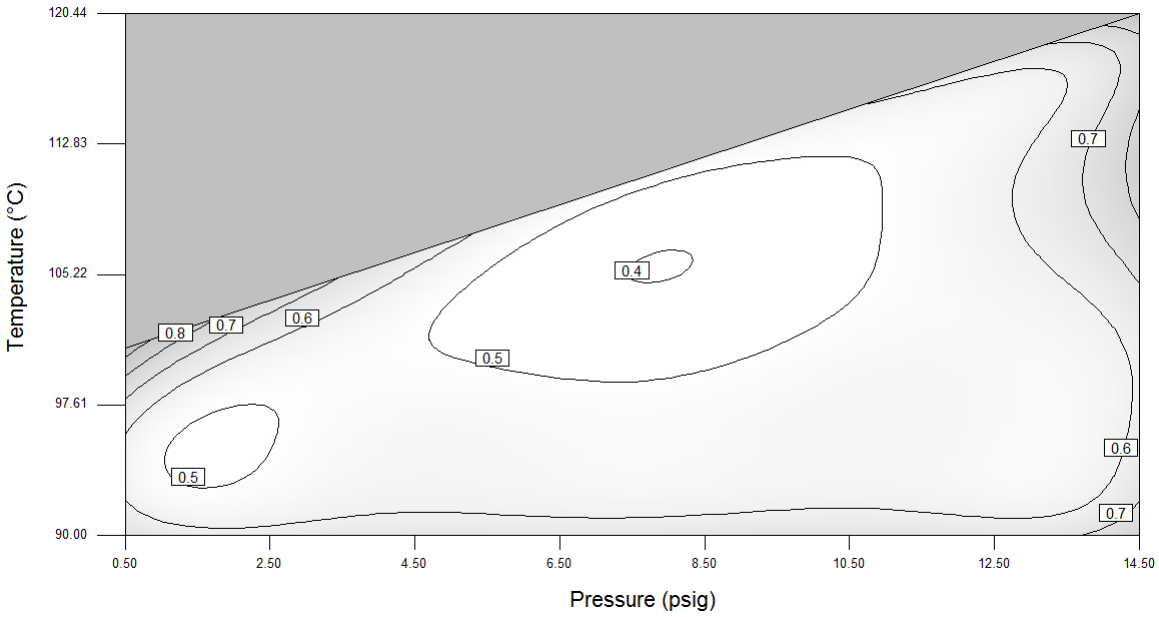

Figure 3-8: Standard error of response surface design

Table 3-3 and Table 3-4 show the confirmation and experimental design for response surface methodology.

Table 3-3: Confirmation trials for experimentally acquired model

Block	Run	Factor 1 A:Pressure	Factor 2 B:Temperature	Factor 3 C:Valve Position
		psig	*°C*	*% Open*
Block IV	37	14.5	90.0	50
Block IV	38	12.8	113.6	87
Block IV	39	4.0	99.3	37
Block IV	40	4.0	94.0	87
Block IV	41	8.0	98.0	62
Block IV	42	7.5	105.5	50
Block IV	43	12.7	105.0	62
Block IV	44	3.3	104.0	42
Block IV	45	3.3	104.0	29
Block IV	46	3.3	104.0	72

Table 3-4: Experimental trials for response surface methodology

Block	Run	Factor 1 A:Pressure	Factor 2 B:Temperature	Factor 3 C:Valve Position
		psig	*°C*	*% Open*
Block I	1	9.5	112.8	100
Block I	2	9.2	90.0	25
Block I	3	14.5	97.6	75
Block I	4	9.2	90.0	25
Block I	5	0.5	92.0	54
Block I	6	0.5	92.0	54
Block I	7	14.5	97.6	75
Block II	8	4.6	106.6	25
Block II	9	14.5	90.0	100
Block II	10	3.8	105.6	79
Block II	11	11.6	96.7	49
Block III	12	14.5	109.9	100
Block III	13	5.1	97.9	43
Block III	14	11.0	90.0	75
Block III	15	0.5	90.0	99
Block IV	16	10.2	114.5	49
Block IV	17	10.2	114.5	49
Block IV	18	0.5	90.0	76
Block IV	19	0.5	99.1	100
Block IV	20	4.7	90.0	100
Block V	21	10.7	98.1	100
Block V	22	4.9	99.6	82
Block V	23	14.5	112.7	49
Block V	24	4.5	90.0	47
Block VI	25	14.5	120.4	25
Block VI	26	14.5	100.1	25
Block VI	27	11.6	110.3	72
Block VI	28	5.8	98.2	42
Block VII	29	10.7	106.9	25
Block VII	30	0.5	100.9	48
Block VII	31	14.5	90.0	37
Block VII	32	0.5	90.8	25
Block VIII	33	14.5	120.4	86
Block VIII	34	7.6	103.5	84
Block VIII	35	5.9	108.5	55
Block VIII	36	1.2	100.2	25

3.2.5 - Model Validation and Confirmation

Analyzing the residuals for the regression models, mass flowrate, and discharge pressure validates the model's acceptability. The analysis of variance assumptions was validated. The data is normal, has constant variance, was conducted in a random fashion, and the predicted and actual values are in agreement with each other. Once the experimental analysis is complete and valid, confirmation trials make sure that the experimental model can predict actual responses.

A minimum of three confirmation trials should be conducted to evaluate the prediction model (National Institute of Standards and Technology, 2003). These trials are ideally at locations that represent gaps in the experimental design, as locations near the design points are known to be good approximations. Figures 3-9, 3-10, and 3-11 show confirmation and experimental trials of various factor combinations. For example, the check marked boxes located within each representation illustrates the confirmation trials while all other boxes represent experimental trials. The colours of the boxes are irrelevant and represents the order for which the trials was completed.

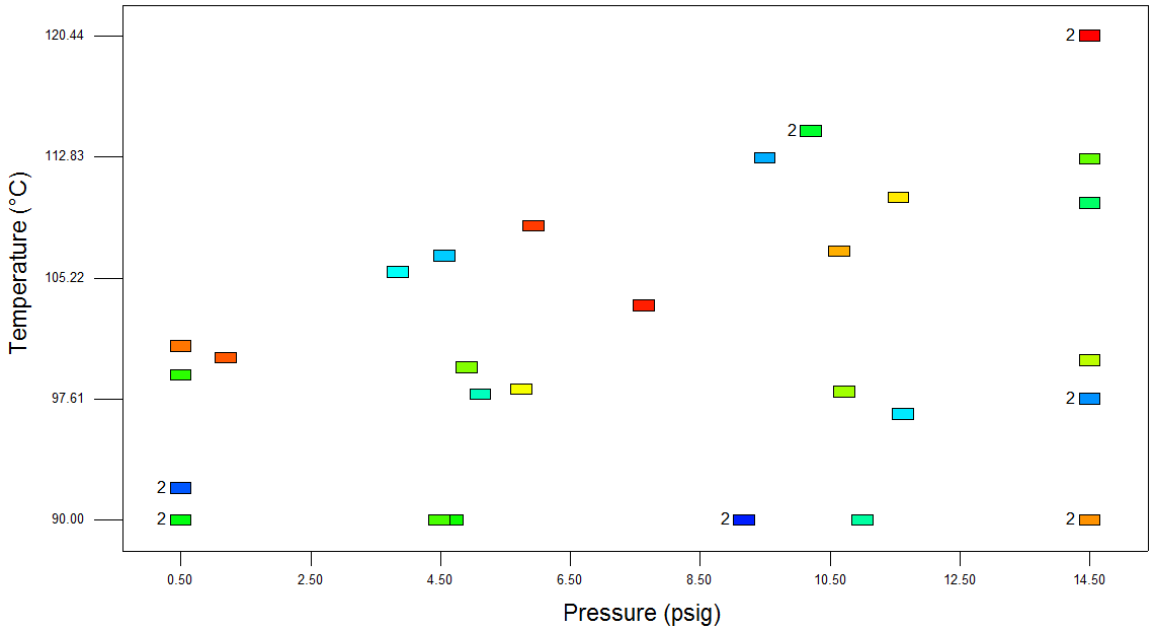

Figure 3-9: Experimental and confirmation trials (pressure and temperature)

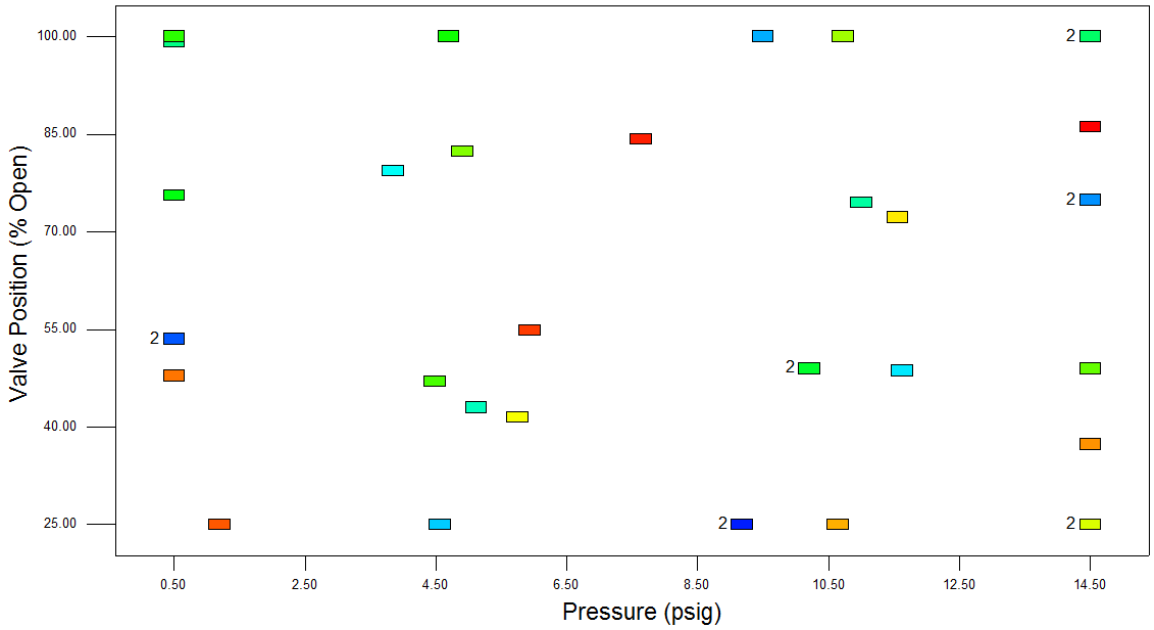

Figure 3-10: Experimental and confirmation trials (valve position and pressure)

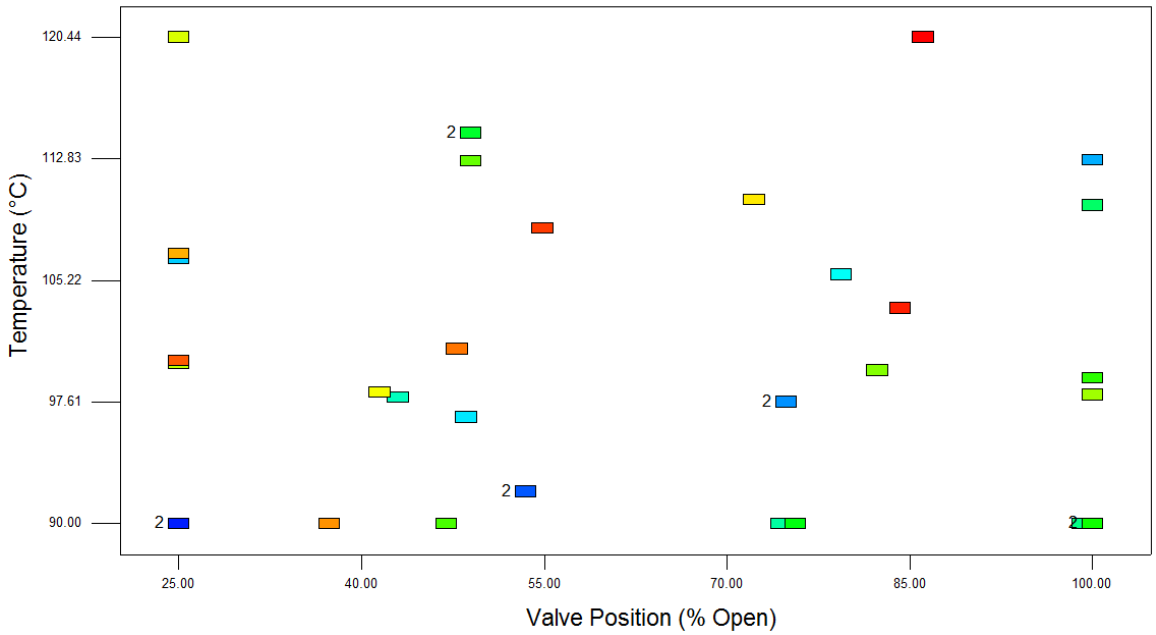

Figure 3-11: Experimental and confirmation trials (valve position and temperature)

3.3 - Sample Preparation

A systematic approach was taken when preparing each block and trial. Included are the initial fill, oxygen removal, and the establishment of the experimental factors.

3.3.1 - Initial Fill

Filtered domestic cold water is used to flush the supply tank, piping distribution, and weigh tank each day. The intent is to remove any deposits that resided from fabrication or past experimentation. Once completed, the remaining water is returned to the supply reservoir from the weigh tank. The sight glass displays the water level within the supply reservoir and piping when preparing experimental conditions. Allocation of space within the supply reservoir is required for thermal expansion and the removal of non-condensables such as oxygen and nitrogen.

3.3.2 - Oxygen Removal

The presence of oxygen is undesirable as it promotes a suitable environment for corrosion. Furthermore, the experimental conditions require the reduction of oxygen to reflect industrial conditions.

As domestic water contains a significant quantity of oxygen, a deaerator was utilized to decrease the amount present. The process causes the removal of oxygen due to the lack of solubility at increased temperature. A manual venting valve eliminates the excess oxygen and other non-condensables to the external environment.

3.3.3 - Experimental Factors

The first factor established during the preparation of condensate is temperature. The fluid is circulated through the piping and the desired supply temperature is maintained within ±2°F. Next, the valve is rotated and fixed at the desired position. Compressed air fills the space above the condensate to provide the supply pressure. After the preparation test procedures and experimentation, no further changes are made until the trial run is completed.

3.4 - Mass Flowrate Calculation

3.4.1 - Introduction

Determining the mass flowrate of condensate for each trial run requires the collection and manipulation of data.

3.4.2 - Mass Flowrate Methodology

As the mass flowrate of condensate was not measured directly with a flow meter, two measurements in conjunction with weighted least-squares regression provide the response. The initial time and corresponding mass are established as the process reaches a steady state condition. During the experiment, the control measures for pressure (± 1 psig) and temperature (±5°F) deviations are observed. Establishment of the final mass and time are determined when the weigh tank has reached the maximum volume or a sufficient lapse of time has occurred. After this, the operator will cease experimentation. All process variables are sampled at one-kilohertz frequency and stored within data acquisition for analysis and post-processing.

The noise detected from the load cell was minimal when the temperature was below saturation. When above, the noise produced substantially larger oscillatory vibrations. For all trials, a data fitting scheme was applied to produce a best fit response.

3.4.3 - Data Fitting

3.4.3.1 – Introduction

Sampling only occurs for discrete mass measurements. However, it is necessary that a continuous model be developed from the discrete data. The best method to represent the general trend of data is to apply a weighted least-squares regression. The method minimizes the discrepancy between the fit of the data and the original data. When the model is developed, it can predict a mass value. The statistical assumptions for regression analysis include normal distribution, independently distributed, random experimentation, and constant variance (Montgomery, 2013).

The software program, MathWorks (2015), has a specialized application for curve fitting and facilitates robust least-square regression analysis.

3.4.3.2 - Regression Model

Gaussian, exponential, and polynomial models were evaluated. The polynomial model produced the best fitting results.

The goal of least-squares regression analysis is to minimize the sum of squares of the residuals (r_i) between the measured and actual response. This facilitates obtaining the model coefficients (a_n). The squares of the residuals (S_r) are given in Equation 3.22, which includes the weighing function (W^*).

$$S_r = \sum_{i=1}^{n} W^* r_i^2 = \sum_{i=1}^{n} W^* \left(y_{i,\,measured} - y_{i,\,model} \right)^2 \tag{3.22}$$

To determine model coefficients, the sum of the squares of the residuals are differentiated with respect to each coefficient and set to a minimum (0).

Although the data is assumed to be normal, an added measure was taken to reduce the error of the residuals by the presence of outliers. Outliers cause an adverse effect on the distribution and fit of the data. For instance, a normal distribution can be skewed with outliers that invalidate statistical assumptions. Also, the presence of outliers cause the data fit to become a misrepresentation of the general trend. The algorithm consists of utilizing an iterative least squares with a bisquare weighting function.

The weighted function provides a parameter that scales the relative magnitude of each data point. The range consists of $0 \leq W^* \leq 1$, with the value of the weighted function effectively determining the data point's contribution.

The weighting function and least-squares determines the coefficients. However, as the iteration progresses, the weighting function will change depending on the presence of outliers. The adjusted standardized residuals are used within the bisquare function to acquire the weighted quantity. Data points compared to previous predictions are assigned a weight (W^*) based on the bisquare function and the adjusted standardized residuals. Then the model coefficients and intercept are determined through the use of the weighted least-squares method. The process continues until the coefficient estimates converge within a given tolerance (MathWorks, 2015).

3.4.3.3 - Regression Evaluation

Two indicators are used to determine the best fit polynomial. They include the sum of squared errors (SSE) and the coefficient of determination (R^2). The SSE represents the error between the measured and predicted values. The R^2 quantifies the variation of the model, i.e., the variation between the actual and predicted values. For instance, R^2 equal to 1 is ideal and is representative of the fitted model exactly predicting the experimental data. The model that had the lowest SSE and greatest R^2 was selected.

3.5 - Experimental Error and Uncertainty

3.5.1 - Introduction

It is important to distinguish the true value when obtaining experimental data. Given that the true value is somewhat elusive, determining the mean of the data becomes the best estimate (Coleman and Steele, 2009). The true value resides within a 95% confidence interval and is representative of the uncertainty.

Estimation of uncertainties are either characterized by statistical (type A) or non-statistical (type B) methods. Statistical methods quantify the scatter about the mean while non-statistical methods include manufacturer provided specifications (Kirkup and Frenkel, 2006). Although type A and type B are segregated, they are combined using a Taylor Series Method (TSM). This model will allow for the propagation of uncertainties and the determination of the overall result. Identifying the instrumentation accuracy and sensitivity are essential steps when developing the TSM.

The TSM model, given in Equation 3.23, represents instrument uncertainty $\left(u_i^{'s}\right)$ and is mutually uncorrelated.

$$U_x = \sqrt{\left(\frac{\partial}{\partial a}x\right)^2 \cdot u_a^2 + \left(\frac{\partial}{\partial b}x\right)^2 \cdot u_b^2 + \left(\frac{\partial}{\partial c}x\right)^2 \cdot u_c^2 + \ldots} \tag{3.23}$$

Where U_x is the overall uncertainty and the partial derivative represents the sensitivity of the function to each factor.

The International Organization for Standardization's *Guide to the Expression of Uncertainty in Measurement* (Coleman and Steele, 2009) applies to the uncertainty analysis. It provides a reasonable and practical representation of uncertainties in individual measurements.

3.5.2 - Mass Flowrate

The foundation for uncertainty analysis is from the American National Standards Institute (2005) performance test standard. The mass flowrate (W) of low-pressure liquid is determined with mass and time measurement, as given in Equation 3.24.

$$W = \frac{3600\,\Delta W}{\Delta t} \tag{3.24}$$

As evident from the capacity formula, the change in tank mass (ΔW) and time (Δt) are quantities that contribute to mass flow uncertainty. The partial derivative with respect to the contributing variable can determine small changes in that variable. However, two other significant factors contribute to the overall uncertainty, as established through the analysis of variance. They include supply pressure (PT1) and the supply temperature (RTD1). Although valve position (VP1) is a significant factor, it is not included in the uncertainty analysis. The valve position remains constant and represents a fixed orifice.

The prediction equation for mass flowrate is utilized to generate a series of data points over a suitable range of inlet pressures. The relationship between the mass flowrate (W) and the supply pressure (P) can be estimated with Equation 3.25.

$$W = a \cdot P^6 + b \cdot P^5 + c \cdot P^4 + d \cdot P^3 + e \cdot P^2 + f \cdot P + g \tag{3.25}$$

The limitations are supply pressure and equation of state. These restrictions correspond to the range utilized in the development of the prediction equations and ensure that the temperature and pressure relationship is satisfied to maintain a saturated or subcooled liquid (condensate).

The partial derivative of mass flowrate (W) with respect to supply pressure (P) produces the governing sensitivity contribution. Figure 3-12 presents the least-squares regression model, corresponding residuals, and the inlet pressure sensitivity for Trial 1. Careful inspection of the residuals indicate a random trend and an acceptable goodness of fit.

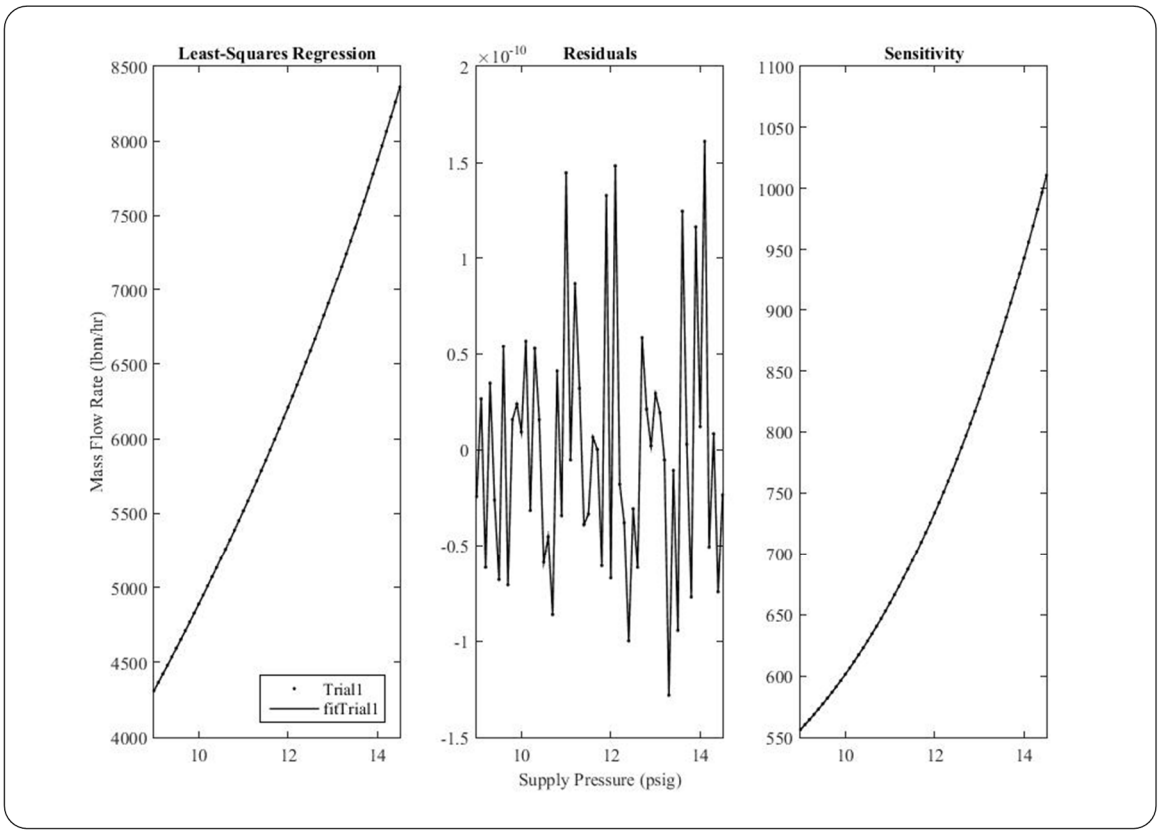

Figure 3-12: Sensitivity analysis for mass flowrate (supply pressure)

The prediction equation for mass flowrate (W) is utilized to generate a series of data points over a suitable range of condensate temperatures (T). The functional relationship can be estimated with Equation 3.26.

$$W = a \cdot T^6 + b \cdot T^5 + c \cdot T^4 + d \cdot T^3 + e \cdot T^2 + f \cdot T + g \tag{3.26}$$

One of the limitations imposed on the range of subcooled temperatures includes a lower and upper level (194 - 248.3°F) for the experimental design. The restriction corresponds to the range utilized to develop the prediction equations. The second constraint is the equation of state. It is necessary to ensure that the relationship between

the supply temperature and supply pressure are satisfied to maintain a saturated or subcooled liquid (condensate).

The partial derivative of mass flowrate (W) with respect to temperature (T) produces the governing sensitivity contribution. Figure 3-13 shows the least-squares regression model, corresponding residuals, and the supply temperature sensitivity for Trial 1. Careful inspection of the residuals indicate a random trend and an acceptable goodness of fit.

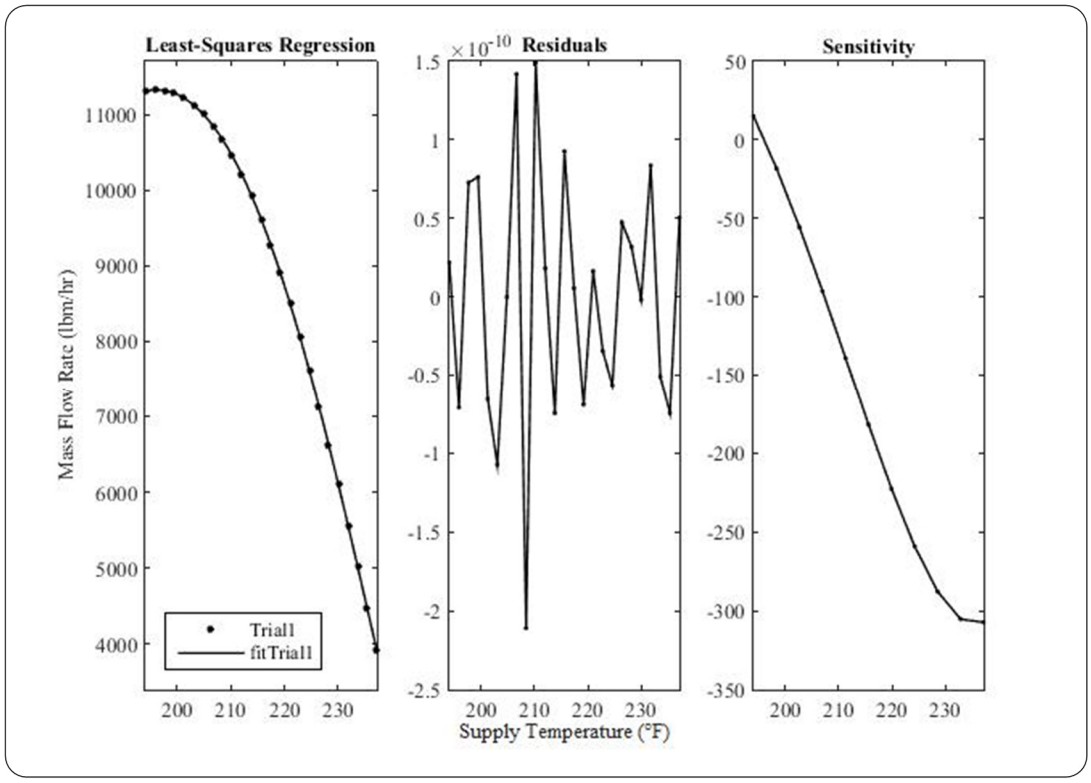

Figure 3-13: Sensitivity analysis for mass flowrate (supply temperature)

3.5.3 - Results

The expanded TSM of the overall uncertainty (U_W) for mass flowrate (W) sensitivity and instrumentation (u) are given in Equation 3.27. The uncertainty analysis

for each trial is shown in Table 3-5. Both the overall uncertainty and relative uncertainty are included for each experimental trial.

$$U_W = \sqrt{\left(\frac{\partial W}{\partial \Delta W}\right)^2 \cdot u^2_{\Delta W} + \left(\frac{\partial W}{\partial \Delta t}\right)^2 \cdot u^2_{\Delta t} + \left(\frac{\partial W}{\partial P}\right)^2 \cdot u^2_{P} + \left(\frac{\partial W}{\partial T}\right)^2 \cdot u^2_{T}} \tag{3.27}$$

Detailed uncertainty analysis is included in Appendix C.

Table 3-5: Overall and relative uncertainty for experimental trials

Experimental Uncertainty							
	Relative Contribution						
Trial	Mass Measurement	Time Interval	Pressure Measurement	Temperature Measurement	Mass Flow (lb/hr)	Overall (lbm/hr)	Relative (%)
1	0.1363	0.0014	0.2863	0.5760	3,847.4	102.15	2.66
2	0.9557	0.0002	0.0032	0.0408	385.0	25.59	6.65
3	0.8119	0.0019	0.1848	0.0015	11,985.0	278.17	2.32
4	0.9420	0.0003	0.0040	0.0536	401.1	21.78	5.43
5	0.9880	0.0010	0.0077	0.0033	776.8	24.09	3.1
6	0.9934	0.0004	0.0044	0.0017	690.9	33.11	4.79
7	0.7130	0.0025	0.2823	0.0022	11,340.0	226.87	2
8	0.9829	0.0002	0.0107	0.0062	244.7	17.73	7.25
9	0.6887	0.0033	0.3078	0.0002	14,728.0	257.63	1.75
10	0.5279	0.0049	0.2051	0.2621	4,105.1	58.65	1.43
11	0.8547	0.0026	0.1375	0.0052	3,716.4	73.41	1.98
12	0.4538	0.0021	0.4106	0.1335	10,896.0	235.99	2.17
13	0.7941	0.0036	0.1733	0.0291	1,605.1	26.76	1.67
14	0.7372	0.0073	0.2553	0.0002	10,869.0	127.42	1.17
15	0.9039	0.0194	0.0273	0.0494	3,783.9	27.14	0.72
16	0.4513	0.0019	0.2759	0.2708	1,938.8	44.37	2.29
17	0.5986	0.0017	0.1975	0.2022	2,084.3	50.66	2.43
18	0.9870	0.0042	0.0085	0.0004	3,061.3	47.17	1.54
19	0.8921	0.0043	0.0077	0.0960	3,196.1	49.03	1.53
20	0.6205	0.0125	0.3665	0.0005	7,798.9	69.63	0.89
21	0.4113	0.0098	0.4833	0.0956	11,549.0	116.9	1.01
22	0.5054	0.0122	0.3516	0.1309	7,311.5	66.31	0.91
23	0.2581	0.0019	0.6552	0.0848	3,429.9	78.94	2.3
24	0.9283	0.0014	0.0628	0.0074	2,202.3	58.27	2.65
25	0.9371	0.0000	0.0541	0.0088	295.3	50.82	17.21
26	0.9934	0.0001	0.0061	0.0004	523.4	42.74	8.17
27	0.3294	0.0041	0.4534	0.2132	7,210.5	112.95	1.57
28	0.9710	0.0005	0.0239	0.0045	1,571.0	68.38	4.35
29	0.9961	0.0002	0.0013	0.0024	361.2	29.29	8.11
30	0.9872	0.0004	0.0046	0.0078	585.4	28.64	4.89
31	0.9401	0.0019	0.0562	0.0018	1,963.2	45.07	2.3
32	0.8436	0.0000	0.0000	0.1563	79.8	67.42	84.52
33	0.0590	0.0007	0.6162	0.3241	4,459.5	167.24	3.75
34	0.5038	0.0070	0.3162	0.1730	8,270.2	98.6	1.19
35	0.6947	0.0020	0.1387	0.1646	2,198.3	48.83	2.22
36	0.9966	0.0001	0.0031	0.0003	145.4	16.26	11.18

3.5.4 - Discussion

American National Standards Institute (2005) suggests a post-test uncertainty of 10% for mass flow less than 200 lbm/h and 5% for mass flow greater than 200 lbm/h. As can be seen from the results, approximately three-quarters of the trails adhere to the test standard (American National Standards Institute, 2005). However, only trial 32 warrants removal from the experimental analysis. The other experimental trials that exceeded the suggested target range are considered to be reasonable. The reason is related to the magnitude of the mass flowrate and the boundary that segregates the 5% from the 10% limit, which coincides with the low condensate capacities.

Within the uncertainty analysis, the dominating term is mass measurement. In particular, the mass sensitivity and the time variable are the significant governing parameters. Increasing the time interval will reduce the uncertainty, but the quantity of condensate and volume of the weigh tank create limitations. However, the uncertainty for these trials are more than acceptable and do not need further investigation. It is the low mass flowrates that would benefit through increased collection time.

3.5.5 - Method of Analysis

A MathWorks (2015) programming script (m-file) was created to acquire the necessary variables and generate an array of data. The source codes are in Appendix D.

The polynomial model for temperature or pressure versus mass flowrates provided the best fit as compared to other models. These include exponential, Fourier, Gaussian, and power. Also, the selection of the sixth order polynomial provided the lowest order function having suitable residuals and goodness of fit characteristics.

-4- Results and Discussion

4.1 - Introduction

Design Expert (Stat-Ease, 2014) was utilized to analyze the experimental model and produce prediction equations for system responses. Each response is investigated within the summary to see how the model fits the data, including adjusted and predicted R^2. Once complete, the best model is selected for analysis of variance (ANOVA) with a 95% confidence interval. Significant factors are shown in the ANOVA tables. Diagnostics of the residuals illustrate conformance of the model to being normal, having constant variance, and producing a satisfactory fit.

4.2 - Mass Flowrate

Table 4-1 includes the observational responses for the mass flowrate of condensate. The response range encompasses a significant portion of industrial operating conditions. Mass flowrates above 10,000 lbm/h represent a significant and less common operating capacity. However, the ability to showcase the range potential of a control valve in the pursuit of a universal steam trap replacement shows promise. The lowest and highest flowrates observed were 79.9 lbm/h and 14,727.6 lbm/h, respectively. The experimental data (graphical) is included in Appendix E.

Table 4-1: Mass flowrate response

Block	Run	Factor 1 A:Pressure	Factor 2 B:Temperature	Factor 3 C:Valve Position	Response 2 Mass Flowrate
		psig	*°C*	*% Open*	*psig*
Block I	1	9.5	112.8	100	3,847.4
Block I	2	9.2	90.0	25	385.5
Block I	3	14.5	97.6	75	11,985.3
Block I	4	9.2	90.0	25	401.1
Block I	5	0.5	92.0	54	776.8
Block I	6	0.5	92.0	54	690.9
Block I	7	14.5	97.6	75	11,340.2
Block II	8	4.6	106.6	25	244.8
Block II	9	14.5	90.0	100	14,727.6
Block II	10	3.8	105.6	79	4,105.8
Block II	11	11.6	96.7	49	3,716.4
Block III	12	14.5	109.9	100	10,896.2
Block III	13	5.1	97.9	43	1,605.1
Block III	14	11.0	90.0	75	10,868.8
Block III	15	0.5	90.0	99	3,783.9
Block IV	16	10.2	114.5	49	1,938.8
Block IV	17	10.2	114.5	49	2,084.3
Block IV	18	0.5	90.0	76	3,061.3
Block IV	19	0.5	99.1	100	3,196.1
Block IV	20	4.7	90.0	100	7,798.9
Block V	21	10.7	98.1	100	11,548.5
Block V	22	4.9	99.6	82	7,311.5
Block V	23	14.5	112.7	49	3,429.9
Block V	24	4.5	90.0	47	2,202.4
Block VI	25	14.5	120.4	25	295.4
Block VI	26	14.5	100.1	25	523.3
Block VI	27	11.6	110.3	72	7,210.4
Block VI	28	5.8	98.2	42	1,571.0
Block VII	29	10.7	106.9	25	361.2
Block VII	30	0.5	100.9	48	585.4
Block VII	31	14.5	90.0	37	1,963.2
~~Block VII~~	~~32~~	~~0.5~~	~~90.8~~	~~25~~	~~79.7~~
Block VIII	33	14.5	120.4	86	4,459.5
Block VIII	34	7.6	103.5	84	8,270.3
Block VIII	35	5.9	108.5	55	2,198.2
Block VIII	36	1.2	100.2	25	145.4

A transformation (square root) of the response data was necessary to produce normal probability. Included in the analysis is the ability to compare the models with statistical information, i.e., p-values, lack of fit, and R^2 values. The transform is

supported by theory; as the flow of fluid tends to vary with the square root of pressure. Table 4-2 provides a summary of statistical indicators for model selection.

Table 4-2: Mass flowrate model summary evaluation

Summary					
Source	**Sequential p-value**	**Lack of Fit p-value**	**Adjusted R-Squared**	**Predicted R-Squared**	
Linear	< 0.0001	0.0002	0.8343	0.6894	
2FI	0.006	0.0004	0.8939	0.7462	
Quadratic	0.0001	0.0024	0.9604	0.884	
Cubic	< 0.0001	0.2176	0.9972	0.9319	Suggested
Quartic	0.2176		0.9983		Aliased

Several model reduction methods were assessed. The method that produced the best fit, adjusted and predicted R^2 was chosen to eliminate unnecessary terms from the model. The methods include backward, forward, stepwise, and all hierarchical. Table 4-3 provides the analysis of variance table.

Insignificant terms are removed from the model. The only exceptions are the inclusion of hierarchical terms. The hierarchical principle indicates that for significant high-order terms, the low-order terms must also be present. Although models are known to work well without including the hierarchical terms (Montgomery, 2013), it was decided that they would remain. The inclusion of the hierarchical terms produces an adequate model for predicting the mass flowrate of condensate through a control valve.

Table 4-3: Mass flowrate analysis of variance

ANOVA for Response Surface Reduced Cubic model Analysis of variance table [Partial sum of squares - Type III]					
Source	Sum of Squares	df	Mean Square	F Value	p-value Prob > F
Block	6,690.3	7.0	955.8		
Model	28,394.1	15.0	1,892.9	887.3	< 0.0001
A-Pressure	560.3	1.0	560.3	262.6	< 0.0001
B-Temperature	430.2	1.0	430.2	201.7	< 0.0001
C-Valve Position	3,161.7	1.0	3,161.7	1482.0	< 0.0001
AB	4.2	1.0	4.2	2.0	0.1876
AC	849.9	1.0	849.9	398.4	< 0.0001
BC	882.6	1.0	882.6	413.7	< 0.0001
A^2	38.4	1.0	38.4	18.0	0.0011
B^2	274.6	1.0	274.6	128.7	< 0.0001
C^2	1,011.7	1.0	1,011.7	474.2	< 0.0001
A^2B	8.8	1.0	8.8	4.1	0.0651
AC^2	121.4	1.0	121.4	56.9	< 0.0001
B^2C	173.9	1.0	173.9	81.5	< 0.0001
A^3	23.3	1.0	23.3	10.9	0.0063
B^3	10.7	1.0	10.7	5.0	0.0446
C^3	318.7	1.0	318.7	149.4	< 0.0001
Residual	25.6	12.0	2.1		
Lack of Fit	18.5	8.0	2.3	1.3	0.4256
Pure Error	7.1	4.0	1.8		
Cor Total	35,110.1	34.0			

Key elements that determine how the predicted model compares to the measured response are analysis of variance table and the goodness of fit characteristics (Table 4-4).

Table 4-4: Mass flowrate goodness of fit characteristics

Goodness of Fit Characteristics			
Std. Dev.	1.46	R-Squared	0.9991
Mean	57.18	Adj R-Squared	0.9980
C.V. %	2.55	Pred R-Squared	0.9895
PRESS	297.23	Adeq Precision	92.0

The analysis of variance table indicates that the model is significant and provides an adequate fit. The measured data and predicted data are in reasonable agreement as indicated by goodness of fit. These are desirable features, as the intention is to produce a

model that emulates the response of the mass flowrate. The ability of the model to predict future responses is vital, otherwise there is no practical benefit.

The studentized residuals[1] and normal probability plot indicate that the analysis of variance is valid. Figure 4-1 shows the probability plot for normal distribution. Figure 4-2 presents the variance plot, indicating constant variance. Figure 4-3 provides confirmation that the experiment is random. The final step involves the evaluation of how well the measured data coincides with the predicted data. Figure 4-4 shows that the actual response is well represented with the experimental model. The model is valid based on the statistical principles.

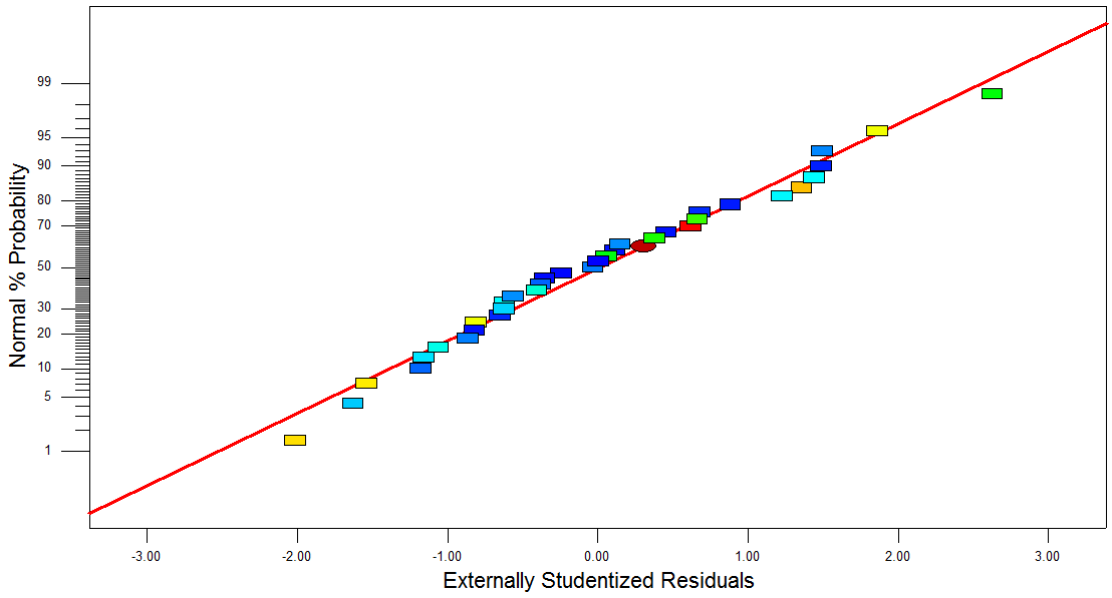

Figure 4-1: Mass flowrate normal probability plot

[1] Studentized residuals represent the difference between the actual and predicted values, including the division of the residuals by the estimate of its standard deviation.

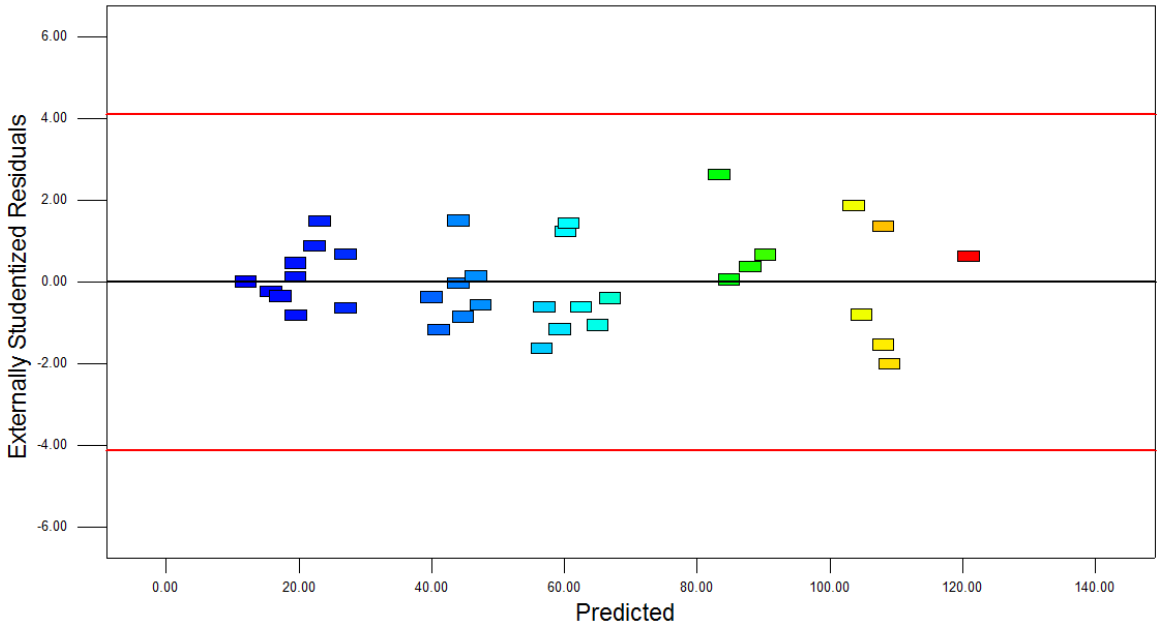

Figure 4-2: Mass flowrate variance plot

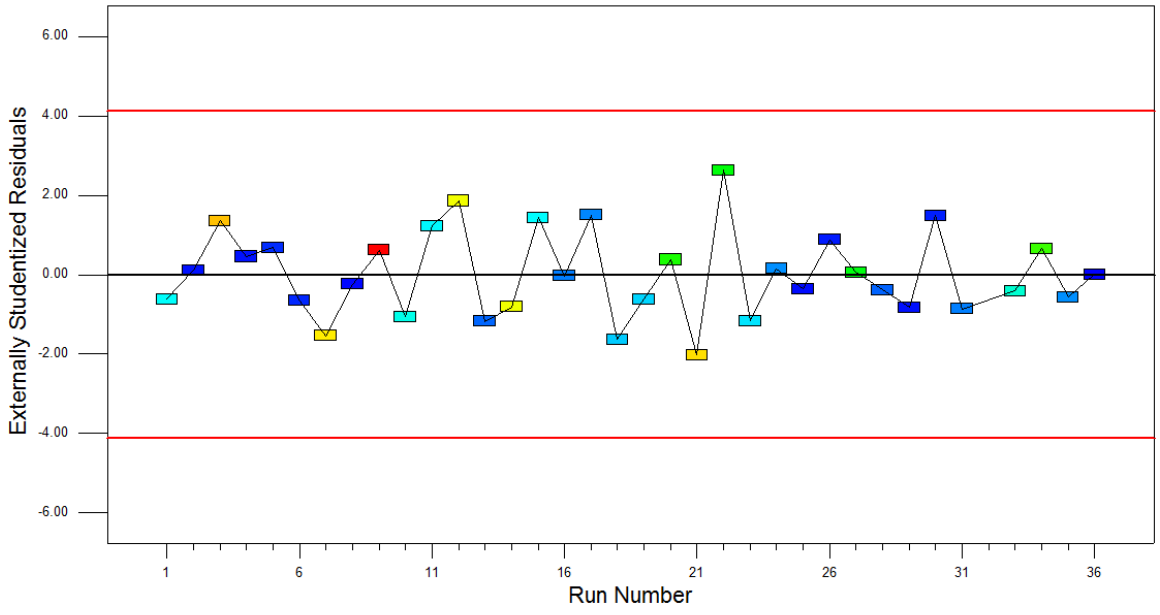

Figure 4-3: Mass flowrate randomization plot

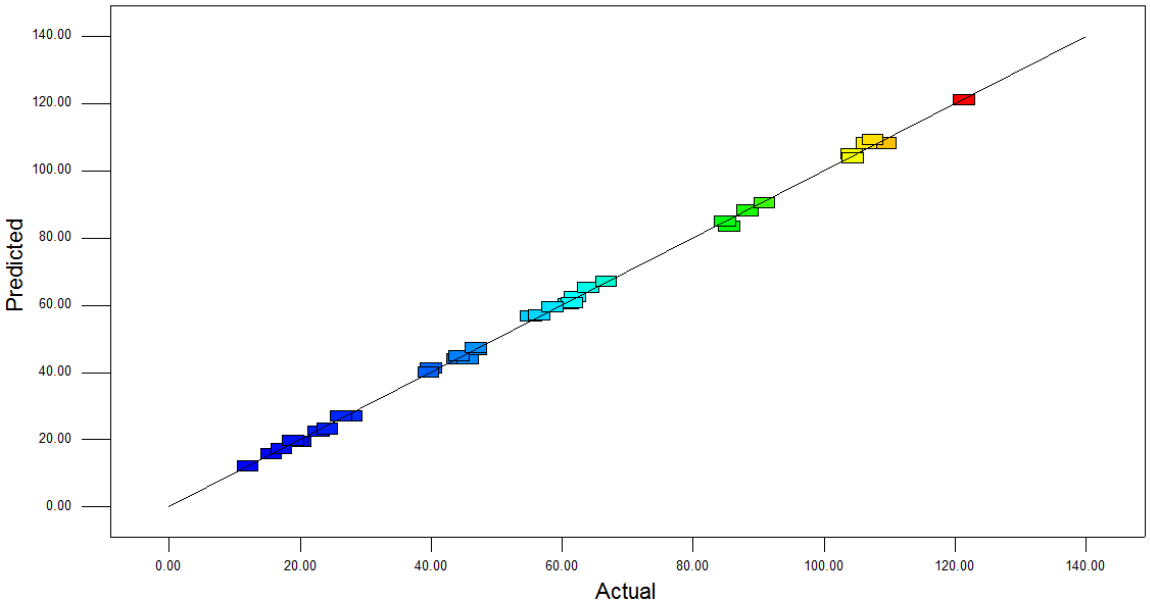

Figure 4-4: Mass flowrate prediction

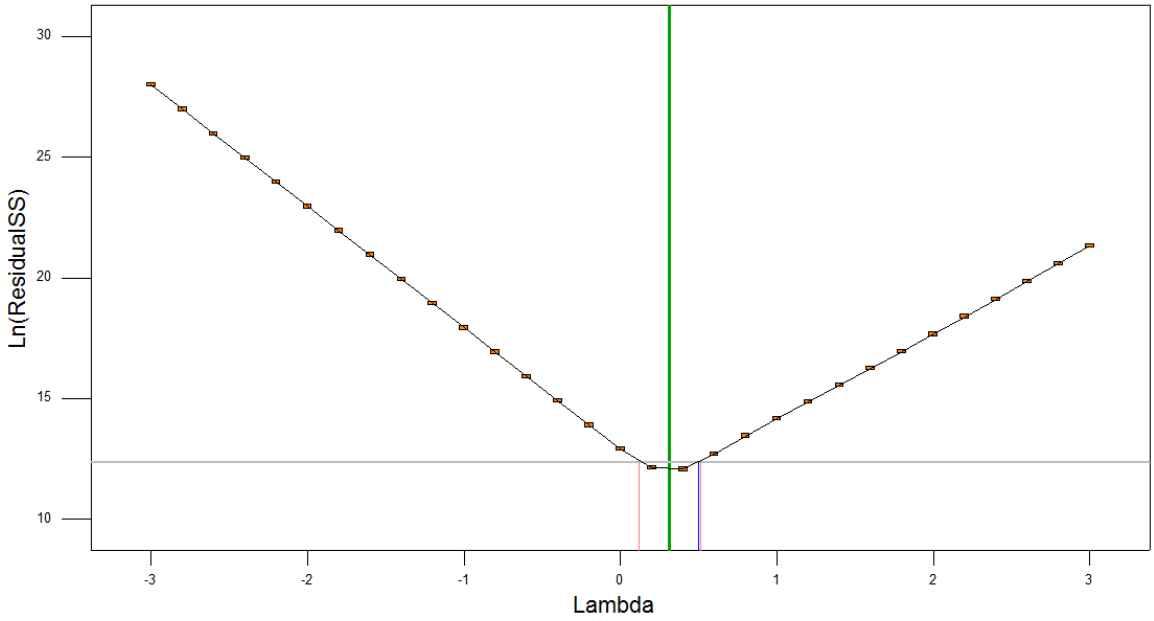

Figure 4-5: Mass flowrate Box-Cox plot

Figure 4-5 presents the Box-Cox plot for an appropriate square root transform. Other transforms were evaluated, but the square root was the best choice. Figures 4-6 to

4-9 show that the model's random scatter is not different for various levels. Random scatter indicates independence.

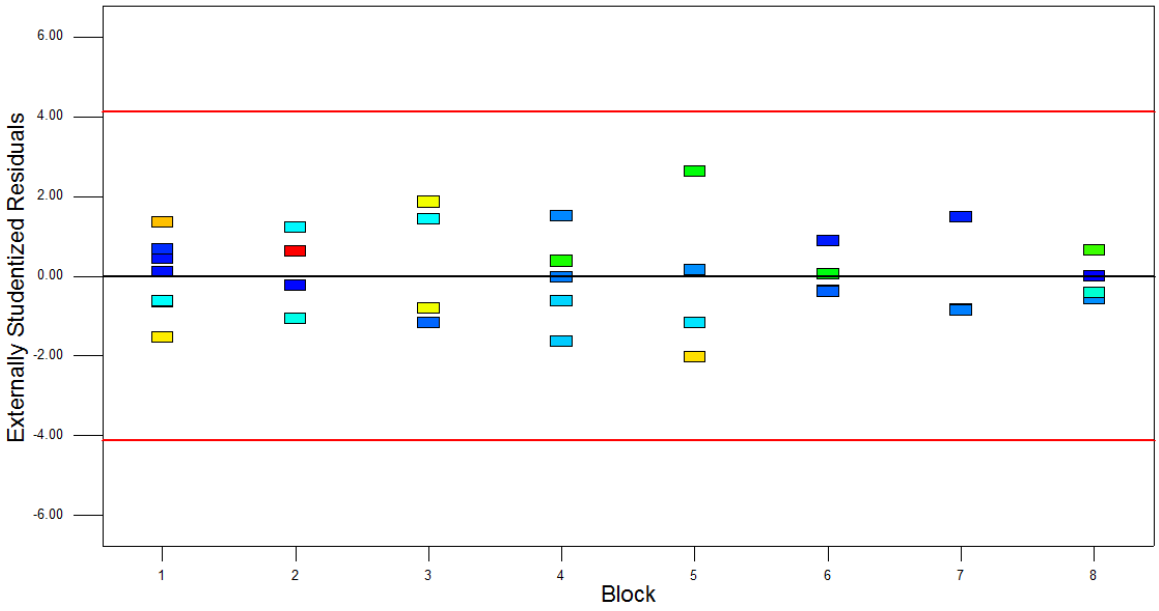

Figure 4-6: Mass flowrate variance plot (residuals and block)

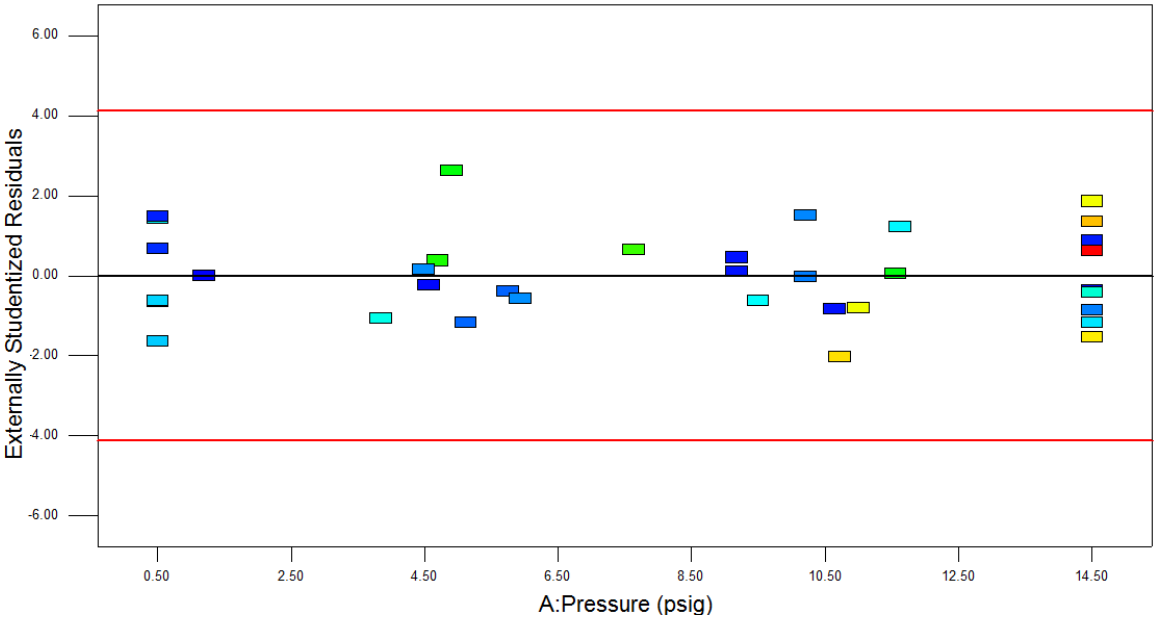

Figure 4-7: Mass flowrate variance plot (residuals and pressure)

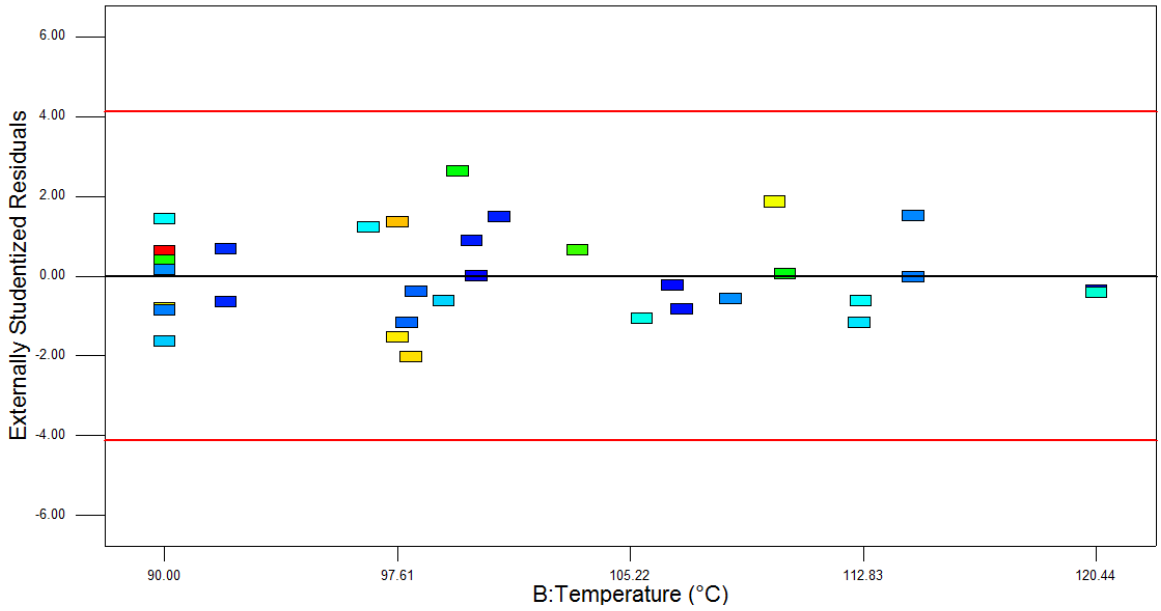

Figure 4-8: Mass flowrate variance plot (residuals and temperature)

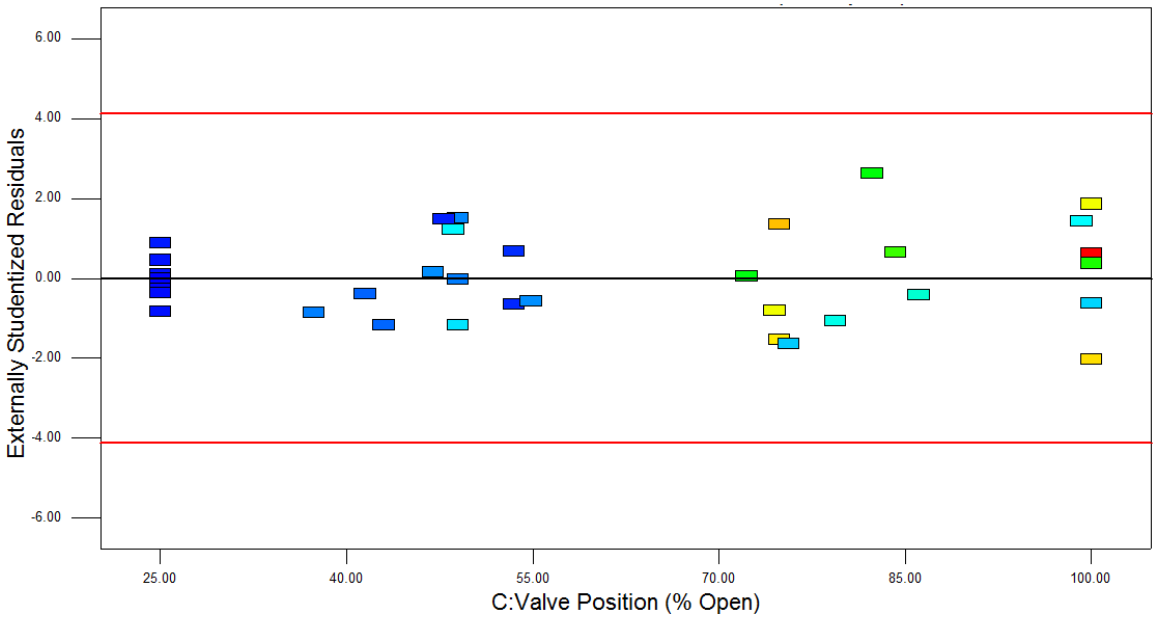

Figure 4-9: Mass flowrate variance plot (residuals and valve position)

A prediction equation can be generated that adequately explains the measured response. Equations 4.1 and Equations 4.2 show the prediction model for coded units and actual units, respectively. The difference between each prediction equation is the minor

change in magnitude through either inclusion or exclusion of trial 32. It is important to note that the significant factors remain the same and the relative effects are consistent.

Final Equation with Trial 32 Included

$$Sqrt(Mass\,Flow) = 66.83 + 23.10A - 20.27B + 47.58C + 1.27AB + 13.47AC - 15.68BC - 4.36A^2 - 13.97B^2 - 15.18C^2 + 4.36A^2B - 7.20AC^2 - 10.50B^2C + 4.36A^3 - 3.92B^3 - 15.65C^3$$

Final Equation without Trial 32 Included

$$Sqrt(Mass\,Flow) = 66.75 + 23.56A - 20.45B + 48.08C + 2.19AB + 13.92AC - 15.64BC - 4.85A^2 - 13.97B^2 - 14.90C^2 + 3.46A^2B - 7.83AC^2 - 11.22B^2C + 4.68A^3 - 3.70B^3 - 15.99C^3 \quad (4.1)$$

Final Equation with Trial 32 Included

$$Sqrt(Mass\,Flow) = 1.4 \times 10^{3} + 8.7 \times 10^{0}\,Pressure - 3.9 \times 10^{1}\,Temperature - 1.2 \times 10^{1}\,Valve\,Position - 7.6 \times 10^{-2}\,Pressure\,Temperature + 1.4 \times 10^{-1}\,Pressure\,Valve\,Position + 2.3 \times 10^{-1}\,Temperature\,Valve\,Position - 9.9 \times 10^{-1}\,Pressure^2 + 3.7 \times 10^{-1}\,Temperature^2 + 5.0 \times 10^{-2}\,Valve\,Position^2 + 5.8 \times 10^{-3}\,Pressure^2\,Temperature - 7.3 \times 10^{-4}\,Pressure\,Valve\,Postion^2 - 1.2 \times 10^{-3}\,Temperature^2\,Valve\,Position + 1.3 \times 10^{-2}\,Pressure^3 - 1.1 \times 10^{-3}\,Temperature^3 - 3.0 \times 10^{-4}\,Valve\,Postion^3$$

Final Equation without Trial 32 Included

$$Sqrt(Mass\,Flow) = 1.4 \times 10^{3} + 5.9 \times 10^{0}\,Pressure - 3.9 \times 10^{1}\,Temperature - 1.4 \times 10^{1}\,Valve\,Position - 4.9 \times 10^{-2}\,Pressure\,Temperature + 1.5 \times 10^{-1}\,Pressure\,Valve\,Position + 2.4 \times 10^{-1}\,Temperature\,Valve\,Position - 9.0 \times 10^{-1}\,Pressure^2 + 3.5 \times 10^{-1}\,Temperature^2 + 5.2 \times 10^{-2}\,Valve\,Position^2 + 4.6 \times 10^{-3}\,Pressure^2\,Temperature - 8.0 \times 10^{-4}\,Pressure\,Valve\,Position^2 - 1.3 \times 10^{-3}\,Temperature^2\,Valve\,Position + 1.4 \times 10^{-2}\,Pressure^3 - 1.0 \times 10^{-3}\,Temperature^3 - 3.0 \times 10^{-4}\,Valve\,Position^3 \quad (4.2)$$

The coded equation provides valuable information related to the magnitude of the coefficients because it does not have to adjust for differences in range or measurement scale. The removal of engineering units facilitates an unbiased comparison of coefficients to determine the contribution of each factor.

As evident from the coded prediction equation, the valve position variable is the most important contributing parameter affecting the mass flowrate of condensate through the control valve. Also evident are that the main effects are larger than the interaction effects. However, the interaction effect of temperature and valve position and pressure and valve position are almost as important as the pressure and temperature main effects. The valve position is approximately twice as important as the other factors and is a contributing term for both interaction effects. Failure to produce the correct experimental design would have resulted in a model that would not adequately represent the mass flowrate. Figure 4-10 and Figure 4-11 shows the effect that high and low valve position has on the mass flowrate. The interaction effect between pressure and valve position is for a temperature of 194°F, while the interaction effect between temperature and valve position is for a pressure of 14.5 psig.

A distinct deviation of sensitivity occurs for temperatures at or above the saturation temperature. The rate of change increases with increasing temperatures above atmospheric pressure. Supply pressure produces a proportional relationship while supply temperature produces an inversely proportional relationship. As one factor increases, the corresponding mass flowrate will either increase or decrease. Low valve position produces relatively minuscule changes in the response to both pressure and temperature.

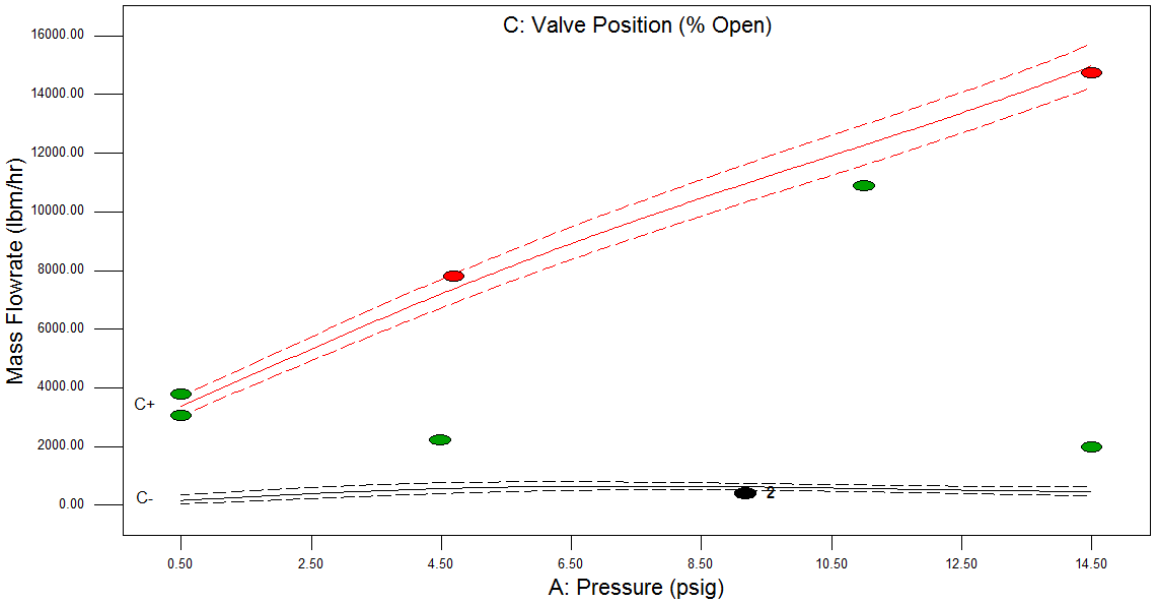

Figure 4-10: Mass flowrate interaction plot (pressure and valve position)

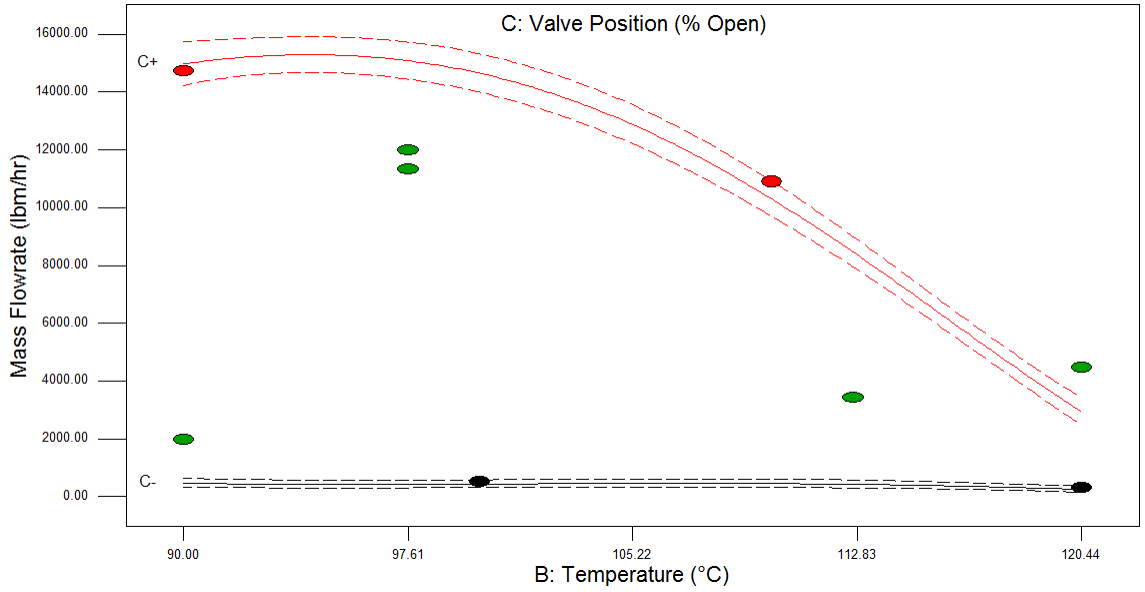

Figure 4-11: Mass flowrate interaction plot (temperature and valve position)

Figure 4-12 presents the cube plot for mass flowrate. The plot shows the high and low factor combinations for the experimental model. As discussed, the combination of high temperature and low pressure violates the equation of state and are not represented by the cube plot. The general trend among the factor combinations are:

1. Decreased mass flowrate with increased temperature
2. Increased mass flowrate with increased pressure
3. Increased mass flowrate with increased valve position

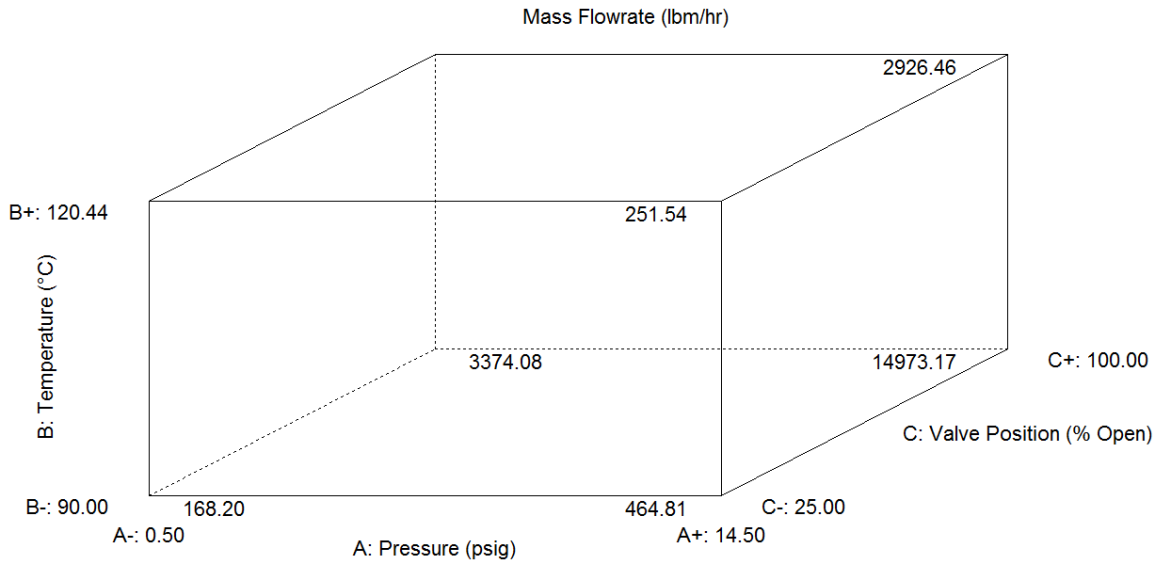

Figure 4-12: Mass flowrate cube plot

Figure 4-13 shows the perturbation plot for the model and represents the effect of all factors at a distinct location.

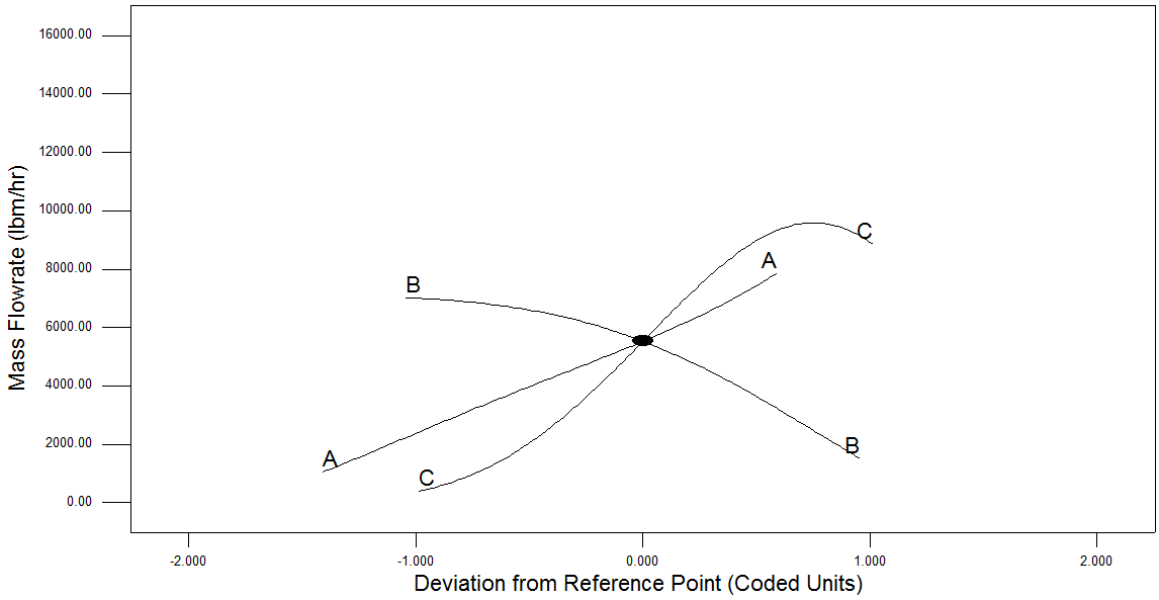

Figure 4-13: Mass flowrate perturbation plot

The mass flowrate peaked due to the overextended rotation of the valve body. Instead of being fully open, the valve body rotated past 100% by an estimated 4°. The estimate was made possible by removing of the valve. The position considered to be 100% during experimentation was established as a reference datum and the valve was rotated to the true 100% position. For each position, points were inscribed and a protractor was used to estimate the angle.

4.3 - Discharge Pressure

The purpose of modulating a valve position is to alter the flow characteristics of condensate. Valve modulation achieves a varying range of mass flowrate. The model of the discharge pressure will help to understand and describe the dynamic phenomena occurring within the control valve. All factors are considered, and the response is observed through instrumentation measurement.

Table 4-5 provides the discharge pressure response for each experimental trial. The lowest and highest observed discharge pressures are 0 psig and 12.63 psig, respectively. Appendix E includes the experimental data (graphical).

Table 4-5: Discharge pressure response

Block	Run	Factor 1 A:Pressure	Factor 2 B:Temperature	Factor 3 C:Valve Position	Response 2 Discharge Pressure
		psig	*°C*	*% Open*	*psig*
Block I	1	9.5	112.8	100	7.76
Block I	2	9.2	90.0	25	0.11
Block I	3	14.5	97.6	75	3.52
Block I	4	9.2	90.0	25	0.07
Block I	5	0.5	92.0	54	0.1
Block I	6	0.5	92.0	54	0.15
Block I	7	14.5	97.6	75	3.71
Block II	8	4.6	106.6	25	0.08
Block II	9	14.5	90.0	100	7.06
Block II	10	3.8	105.6	79	2.25
Block II	11	11.6	96.7	49	0.03
Block III	12	14.5	109.9	100	9.93
Block III	13	5.1	97.9	43	0.14
Block III	14	11.0	90.0	75	1
Block III	15	0.5	90.0	99	0
Block IV	16	10.2	114.5	49	3.52
Block IV	17	10.2	114.5	49	3.59
Block IV	18	0.5	90.0	76	0
Block IV	19	0.5	99.1	100	0.06
Block IV	20	4.7	90.0	100	2.23
Block V	21	10.7	98.1	100	5.19
Block V	22	4.9	99.6	82	2.37
Block V	23	14.5	112.7	49	5.46
Block V	24	4.5	90.0	47	0
Block VI	25	14.5	120.4	25	1.32
Block VI	26	14.5	100.1	25	0.13
Block VI	27	11.6	110.3	72	6.18
Block VI	28	5.8	98.2	42	0.2
Block VII	29	10.7	106.9	25	0.24
Block VII	30	0.5	100.9	48	0.29
Block VII	31	14.5	90.0	37	0.08
~~Block VII~~	~~32~~	~~0.5~~	~~90.8~~	~~25~~	~~0.07~~
Block VIII	33	14.5	120.4	86	12.63
Block VIII	34	7.6	103.5	84	4.5
Block VIII	35	5.9	108.5	55	2.28
Block VIII	36	1.2	100.2	25	0.15

A transformation (square root) of the response data was necessary to adhere to a normal probability. The analysis includes the ability to compare the models with statistical information, i.e., p-values, lack of fit and R-squared values. Table 4-6 provides a summary of the statistical measures regarding model selection.

Table 4-6: Discharge pressure model summary evaluation

Summary					
Source	Sequential p-value	Lack of Fit p-value	Adjusted R-Squared	Predicted R-Squared	
Linear	< 0.0001	0.0001	0.853	0.7036	
2FI	0.0014	0.0004	0.9184	0.8264	
Quadratic	0.5453	0.0003	0.9152	0.7469	
Cubic	< 0.0001	0.1992	0.9977	0.9502	Suggested
Quartic	0.1992		0.9987		Aliased

Several model reduction methods were assessed. The method that produced the best fit, adjusted and predicted R^2 was chosen to eliminate unnecessary terms from the model. The methods include backward, forward, stepwise, and all hierarchical. Table 4-7 shows the analysis of variance table. Terms that are not significant are not in the model.

Table 4-7: Discharge pressure analysis of variance

ANOVA for Response Surface Reduced Cubic model Analysis of variance table [Partial sum of squares - Type III]					
Source	Sum of Squares	df	Mean Square	F Value	p-value Prob > F
Block	4.28	7	0.61		
Model	31.36	17	1.84	822.55	< 0.0001
A-Pressure	0.043	1	0.043	19.37	0.0013
B-Temperature	1.16	1	1.16	515.88	< 0.0001
C-Valve Position	1.69	1	1.69	754.66	< 0.0001
AB	0.16	1	0.16	71.22	< 0.0001
AC	1.81	1	1.81	805.93	< 0.0001
BC	0.038	1	0.038	16.86	0.0021
A^2	0.093	1	0.093	41.65	< 0.0001
B^2	0.15	1	0.15	69.05	< 0.0001
C^2	0.53	1	0.53	234.39	< 0.0001
A^2B	0.03	1	0.03	13.59	0.0042
A^2C	0.31	1	0.31	138.45	< 0.0001
AB^2	0.17	1	0.17	75.91	< 0.0001
AC^2	0.18	1	0.18	81.98	< 0.0001
BC^2	0.97	1	0.97	432.16	< 0.0001
A^3	0.14	1	0.14	61.04	< 0.0001
B^3	0.28	1	0.28	123.45	< 0.0001
C^3	0.11	1	0.11	47.92	< 0.0001
Residual	0.022	10	2.24E-03		
Lack of Fit	0.016	6	2.71E-03	1.75	0.3068
Pure Error	6.20E-03	4	1.55E-03		
Cor Total	35.67	34			

Key elements that determine how the predicted model compares to the measured response are analysis of variance table and the goodness of fit characteristics (Table 4-8).

Table 4-8: Discharge pressure goodness of fit characteristics

Goodness of Fit Characteristics			
Std. Dev.	0.05	R-Squared	0.9993
Mean	1.20	Adj R-Squared	0.9981
C.V. %	3.94	Pred R-Squared	0.9882
PRESS	0.37	Adeq Precision	88.0

The analysis of variance table indicates that the model is significant and provides an adequate fit. The measured data and predicted data are in reasonable agreement as indicated by goodness of fit. These are desirable features, as the intention is to produce a model that emulates the response of the discharge pressure. The ability of the model to predict future responses is vital, otherwise there is no practical benefit.

The residuals and normal probability plot indicate that the analysis of variance is valid. Figure 4-14 shows the probability plot for normal distribution. Figure 4-15 presents the variance plot, indicating constant variance. Figure 4-16 provides confirmation that the experiment is random. The final step involves the evaluation of how the measured data coincides with the predicted data. Figure 4-17 shows that the actual response is well represented with the experimental model. The model is valid based on the statistical principles.

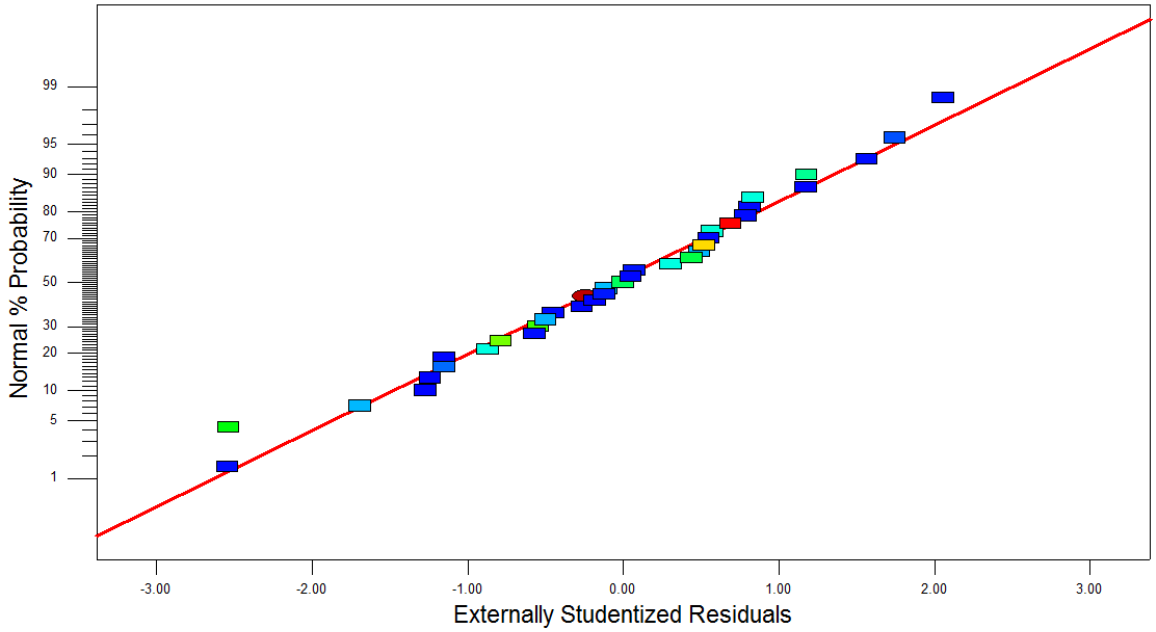

Figure 4-14: Discharge pressure normal probability plot

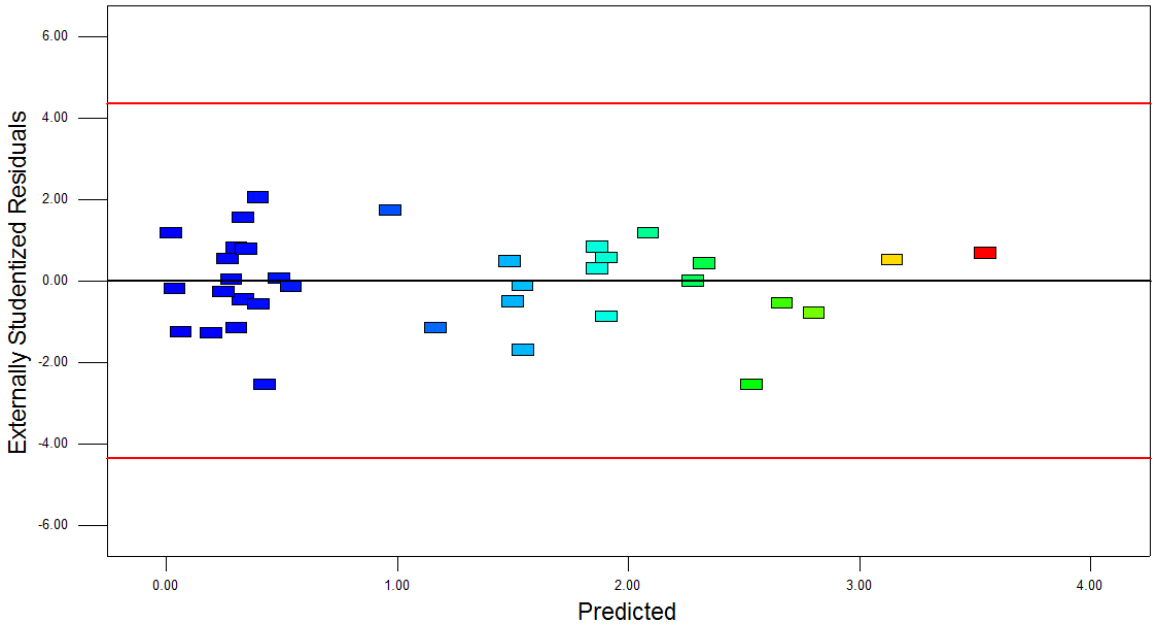

Figure 4-15: Discharge pressure variance plot

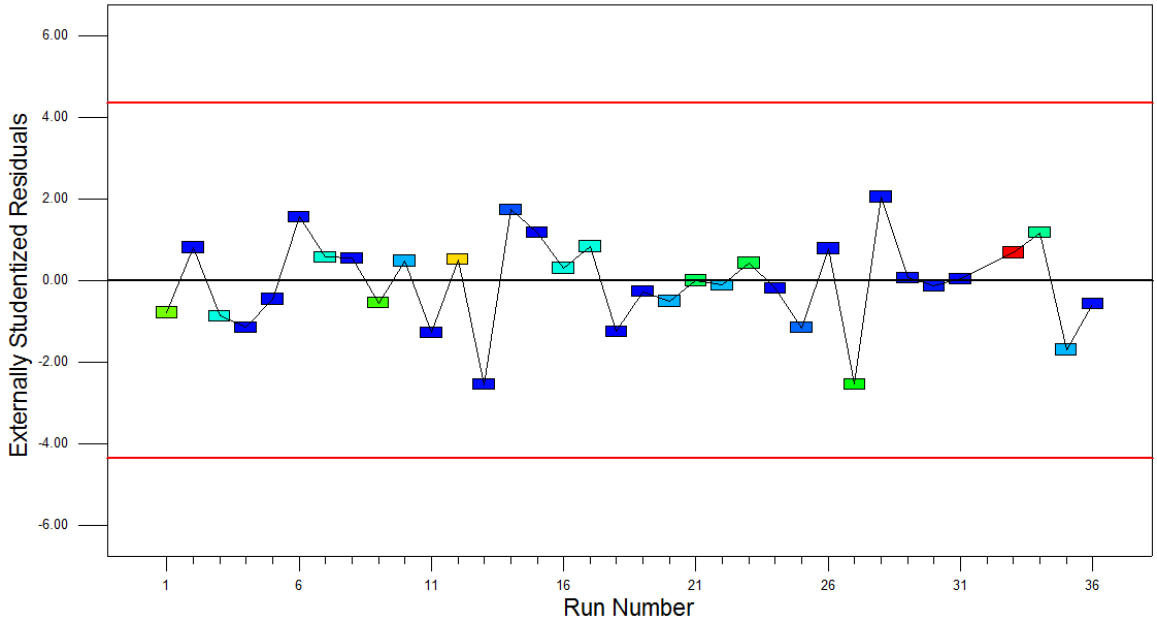

Figure 4-16: Discharge pressure randomization plot

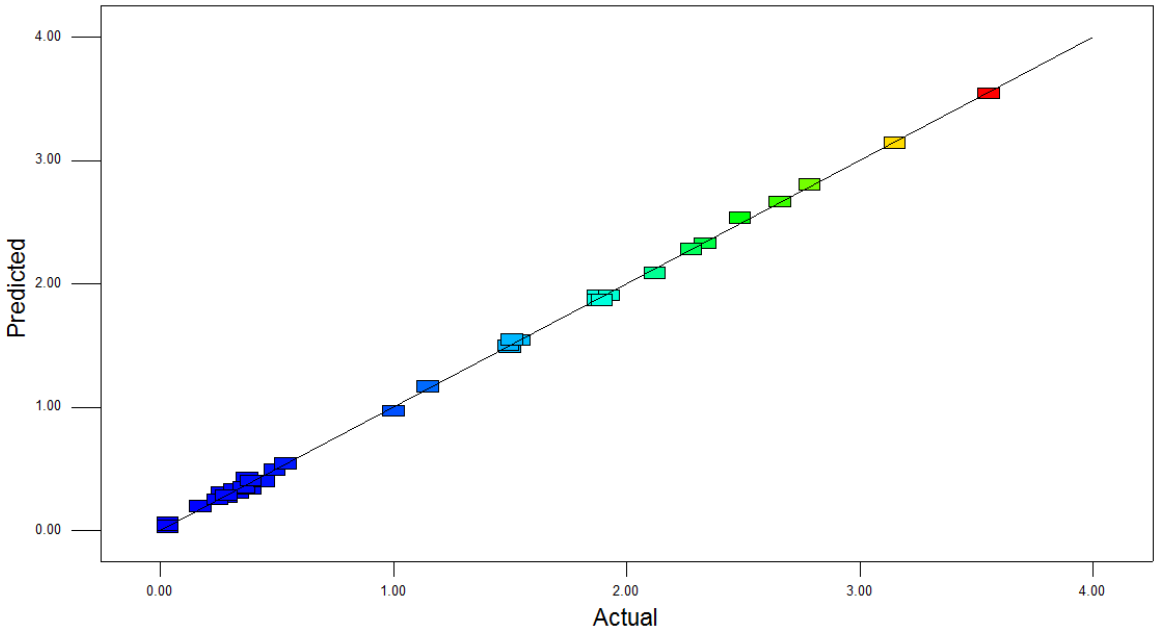

Figure 4-17: Discharge pressure prediction

Figure 4-18 presents the Box-Cox plot for an appropriate square root transform.

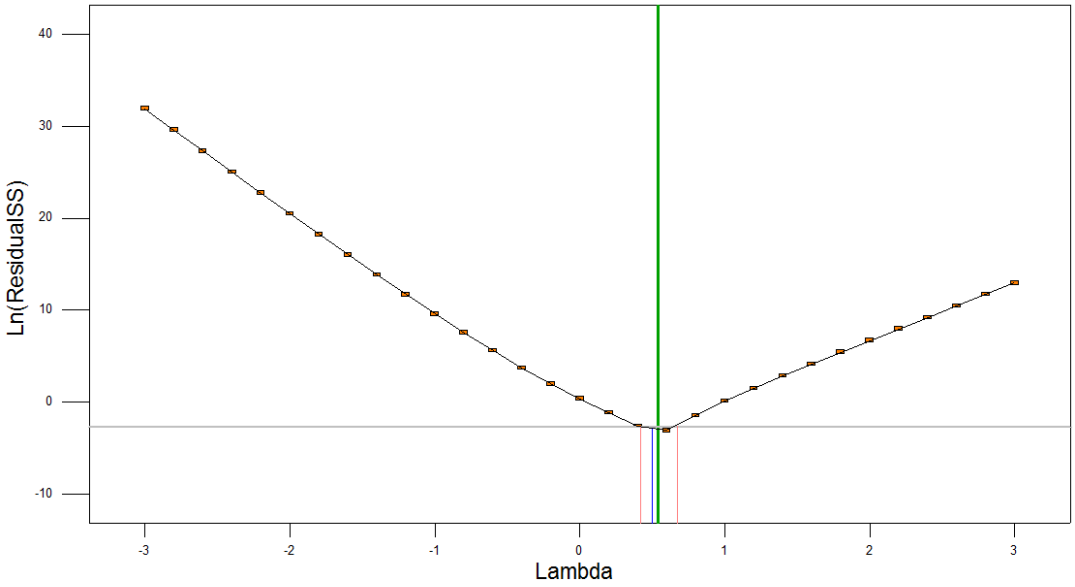

Figure 4-18: Discharge pressure Box-Cox plot

Other transforms were evaluated, but the square root was the best possible choice. Figures 4-19 to 4-22 shows that the model's random scatter is not different for various levels. Random scatter indicates independence.

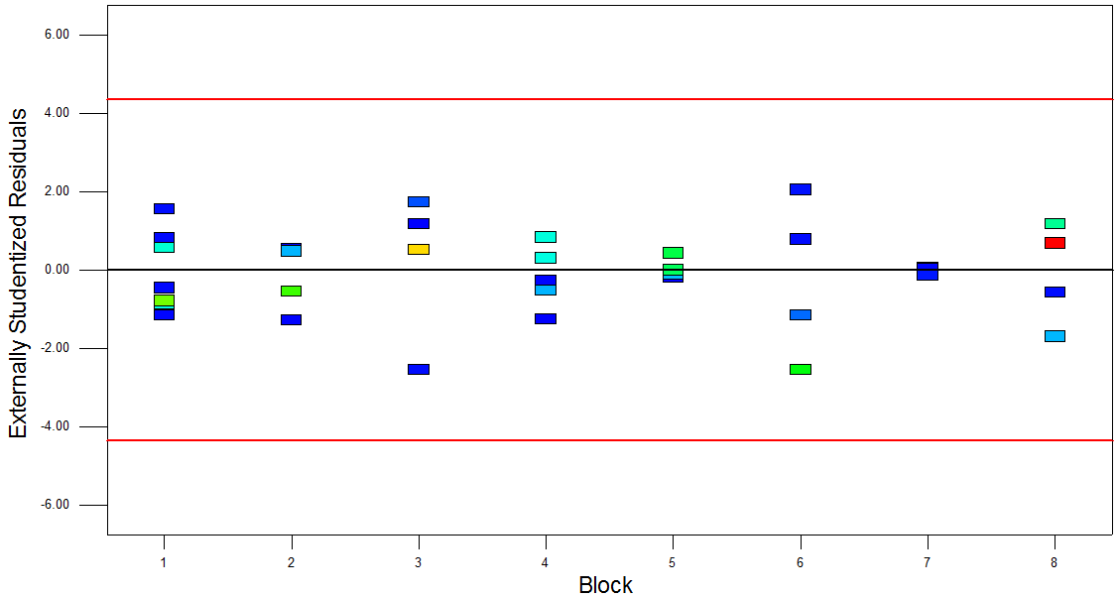

Figure 4-19: Discharge pressure variance plot (residuals and block)

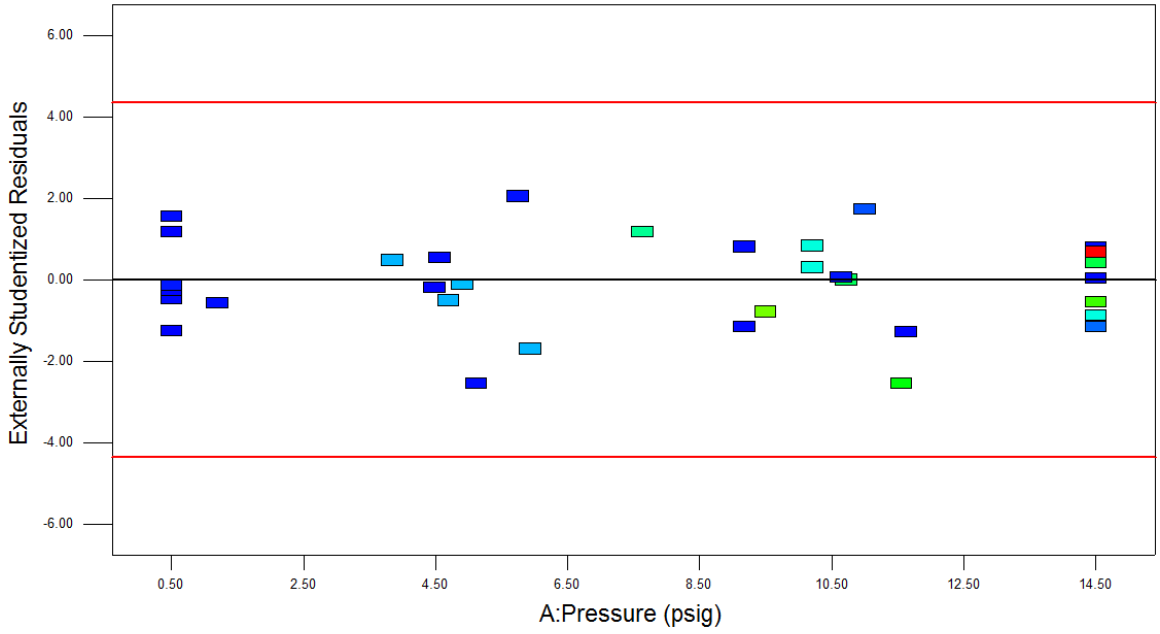

Figure 4-20: Discharge pressure variance plot (residuals and pressure)

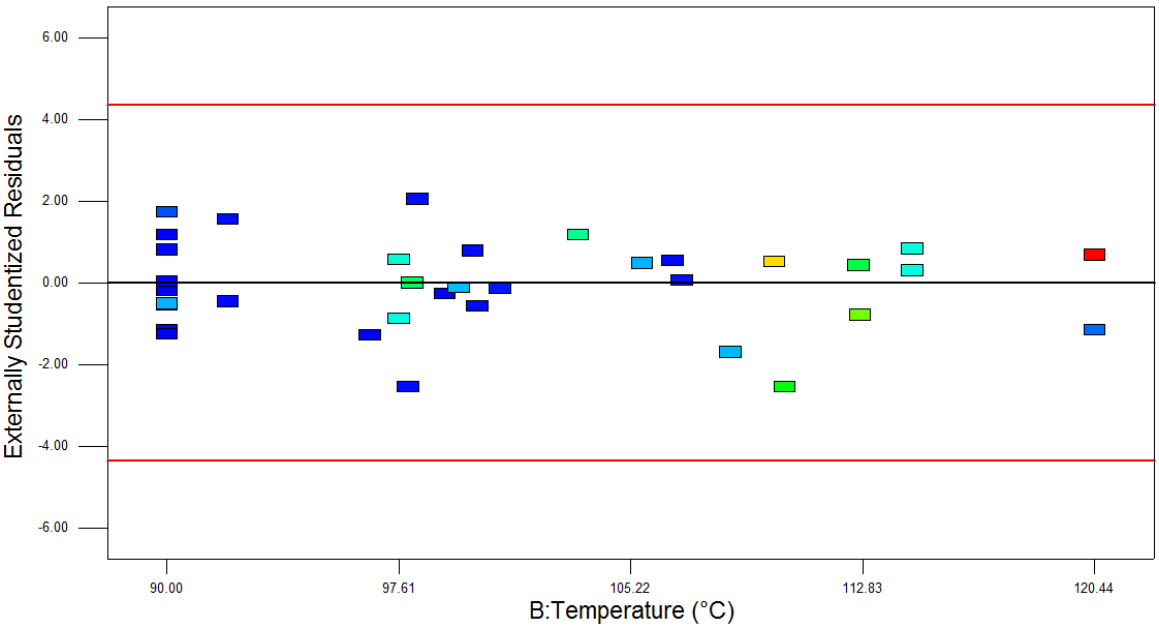

Figure 4-21: Discharge pressure variance plot (residuals and temperature)

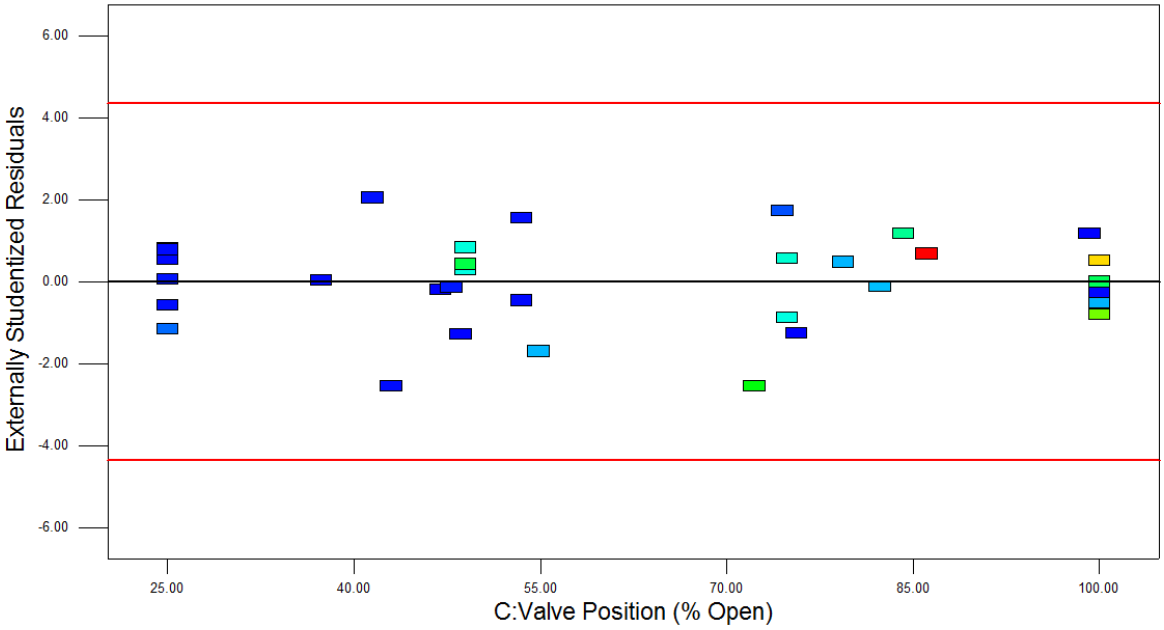

Figure 4-22: Discharge pressure variance plot (residuals and valve position)

A prediction equation can be generated that adequately explains the measured response. Equations 4.3 and Equations 4.4 show the prediction model for both coded and actual units, respectively.

Final Equation with Trial 32 Included

$$Sqrt(Discharge\,Pressure) = 1.70 + .22A + 1.20B + 1.20C + 1.00AB + .62AC - .09BC - .33A^2 - .83B^2 - .38C^2 - .28A^2B - .43A^2C + .92AB^2 + .28AC^2 - .94BC^2 + .36A^3 - .79B^3 - .32C^3$$

Final Equation without Trial 32 Included

$$Sqrt(Discharge\,Pressure) = 1.70 + .21A + 1.24B + 1.18C + 1.03AB + .60AC - .10BC - .32A^2 - .85B^2 - .39C^2 - .26A^2B - .41A^2C + .94AB^2 + .30AC^2 - .92BC^2 + .36A^3 - .81B^3 - .30C^3 \quad (4.3)$$

Final Equation with Trial 32 Included

$$\begin{aligned} Sqrt(Discharge\ Pressure) = {} & 2.0 \times 10^{2} + 4.9 \times 10^{0}\ Pressure - 6.1 \times 10^{0}\ Temperature - 5.5 \\ & \times 10^{-1}\ Valve\ Position - 1.1 \times 10^{-1}\ Pressure\ Temperature + 1.9 \\ & \times 10^{-3}\ Pressure\ Valve\ Position + 5.2 \times 10^{-3}\ Temperature\ Valve\ Position + 2.1 \\ & \times 10^{-2}\ Pressure^{2} + 6.5 \times 10^{-2}\ Temperature^{2} + 5.1 \times 10^{-3}\ Valve\ Position^{2} - 3.5 \\ & \times 10^{-4}\ Pressure^{2}\ Temperature - 2.2 \times 10^{-4}\ Pressure^{2}\ Valve\ Position + 5.8 \\ & \times 10^{-4}\ Pressure\ Temperature^{2} + 3.0 \times 10^{-5}\ Pressure\ Valve\ Position^{2} - 4.3 \\ & \times 10^{-5}\ Temperature\ Valve\ Position^{2} + 1.0 \times 10^{-3}\ Pressure^{3} - 2.3 \times 10^{-4}\ Temperature^{3} \\ & - 5.7 \times 10^{-6}\ Valve\ Position^{3} \end{aligned}$$

Final Equation without Trial 32 Included

$$\begin{aligned} Sqrt(Discharge\ Pressure) = {} & 1.9 \times 10^{2} + 4.7 \times 10^{0}\ Pressure - 6.0 \times 10^{0}\ Temperature - 5.7 \\ & \times 10^{-1}\ Valve\ Position - 1.0 \times 10^{-1}\ Pressure\ Temperature + 2.3 \\ & \times 10^{-3}\ Pressure\ Valve\ Position + 5.3 \times 10^{-3}\ Temperature\ Valve\ Position + 2.3 \\ & \times 10^{-2}\ Pressure^{2} + 6.3 \times 10^{-2}\ Temperature^{2} + 5.3 \times 10^{-3}\ Valve\ Position^{2} - 3.7 \\ & \times 10^{-4}\ Pressure^{2}\ Temperature - 2.3 \times 10^{-4}\ Pressure^{2}\ Valve\ Position + 5.7 \\ & \times 10^{-4}\ Pressure\ Temperature^{2} + 2.9 \times 10^{-5}\ Pressure\ Valve\ Position^{2} - 4.4 \\ & \times 10^{-5}\ Temperature\ Valve\ Position^{2} + 1.1 \times 10^{-3}\ Pressure^{3} - 2.2 \times 10^{-4}\ Temperature^{3} \\ & - 6.0 \times 10^{-6}\ Valve\ Position^{3} \end{aligned} \quad (4.4)$$

The difference between each prediction equation is the minor change in magnitude through either the inclusion or exclusion of trial 32. It is important to note that the significant factors remain the same and that the relative effects are consistent.

The coded equation provides an extra fragment of valuable information related to the magnitude of the coefficients. The reason is that it does not have to adjust for differences in range or measurement scale. The removal of engineering units allows magnitude comparison for evaluating the relative importance of effects.

As evident from the coded prediction equation, the supply temperature variable is the most important contributing parameter effecting the discharge pressure. However, the relative magnitude of the valve position is close to the supply temperature coefficient. The relative magnitude of the interaction effect between the supply pressure and supply

temperature is considerable. Even through all main effects are present, including the interaction effects, the contributions are less than half the relative magnitude.

Failure to produce the correct experimental design would have resulted in a model that would not adequately represent the discharge pressure. Figures 4-23 and 4-24 present a cross section of the surface plot (high and low valve position) to visualize sensitivity, complexity, and the extreme limits of pressure and temperature for discharge pressure. A high valve position has increased sensitivity to the rate of change of factors, and results in producing a maximum pressure. The low valve position produces a decreased sensitivity to the rate of change of factors, and produces a minimum pressure.

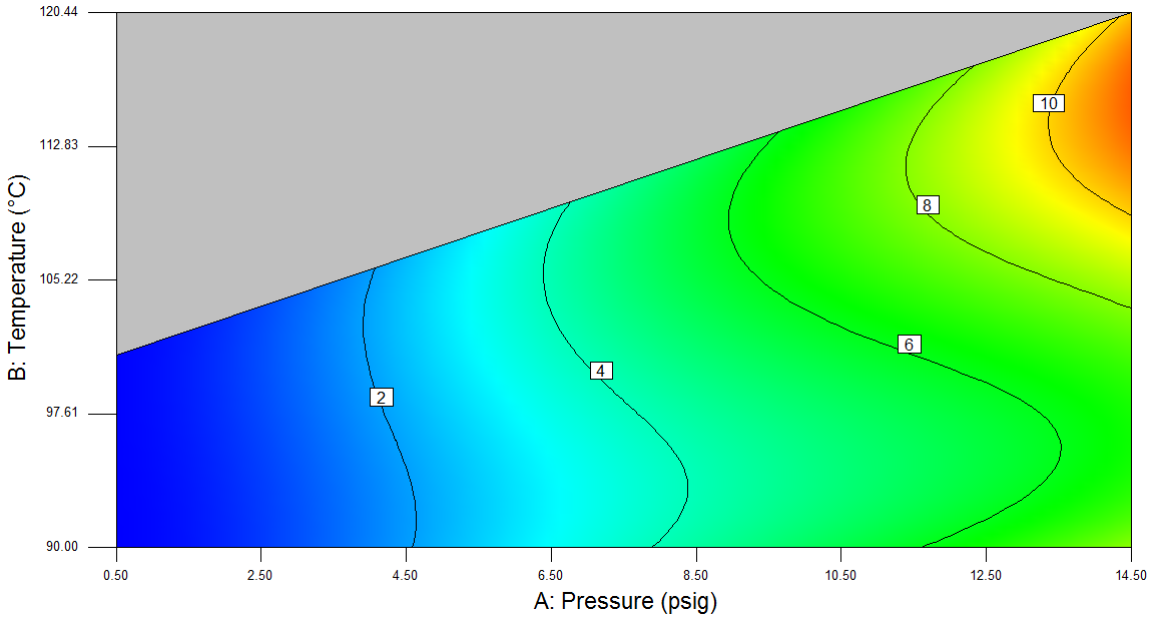

Figure 4-23: Maximum discharge pressure contour plot (pressure and temperature)

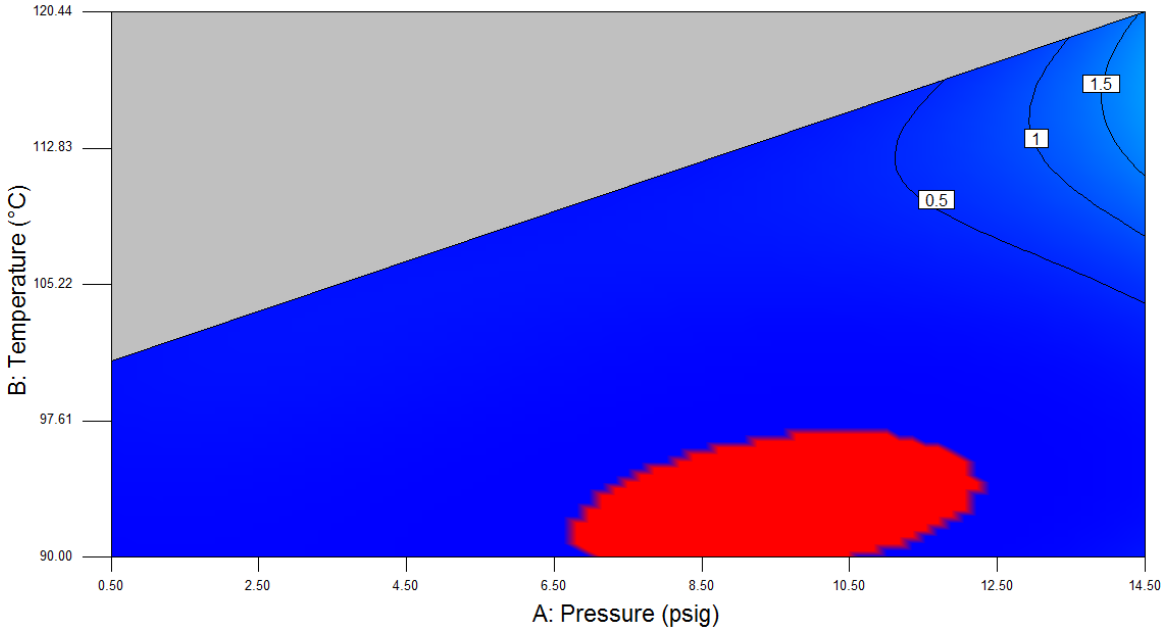

Figure 4-24: Minimum discharge pressure contour plot (pressure and temperature)

The next significant interaction effect is between the supply pressure and the valve position. Although the contribution is approximately half the magnitude of the interaction effect, it remains highly sensitive to a fully open valve position. Figure 4-25 shows the interaction effect for the case of low temperature. However, for other ranges of temperature, the sensitivity trend remains relatively constant. The tendency is for the pressure to shift with the corresponding saturation temperature.

Figure 4-26 presents the last significant interaction effect for a 14.5 psig supply pressure. The trend remains constant for low levels of temperature. An interesting transition occurs around the saturation temperature. For instance, the general trend illustrates that an increased rate of discharge pressure produces a decreased rate of mass flowrate.

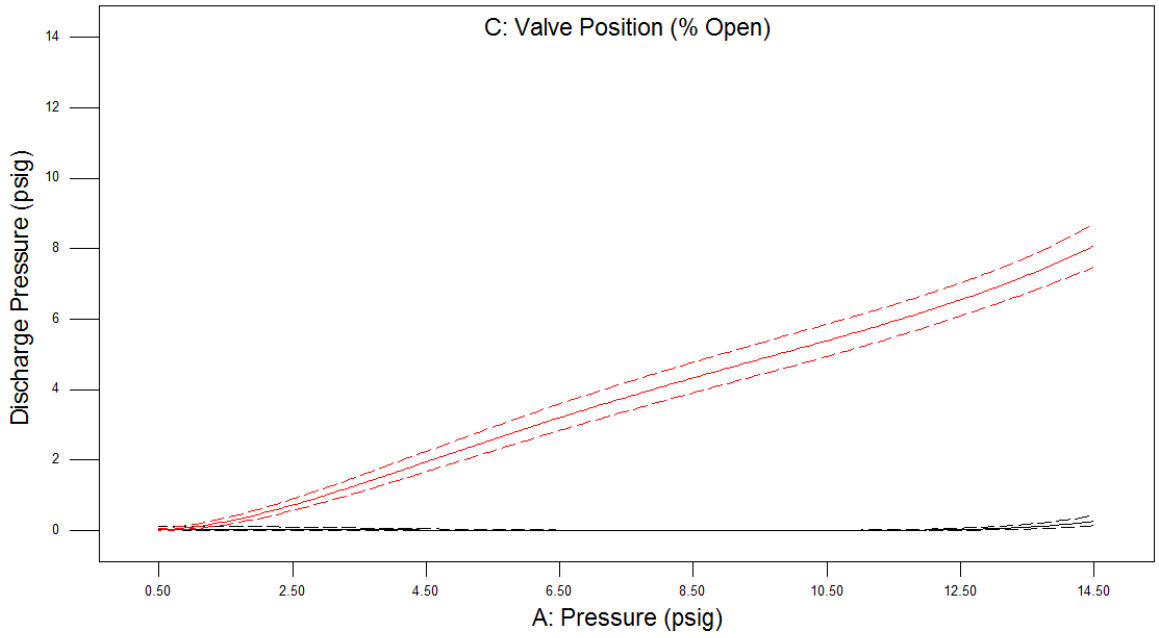

Figure 4-25: Discharge pressure interaction plot (pressure and valve position)

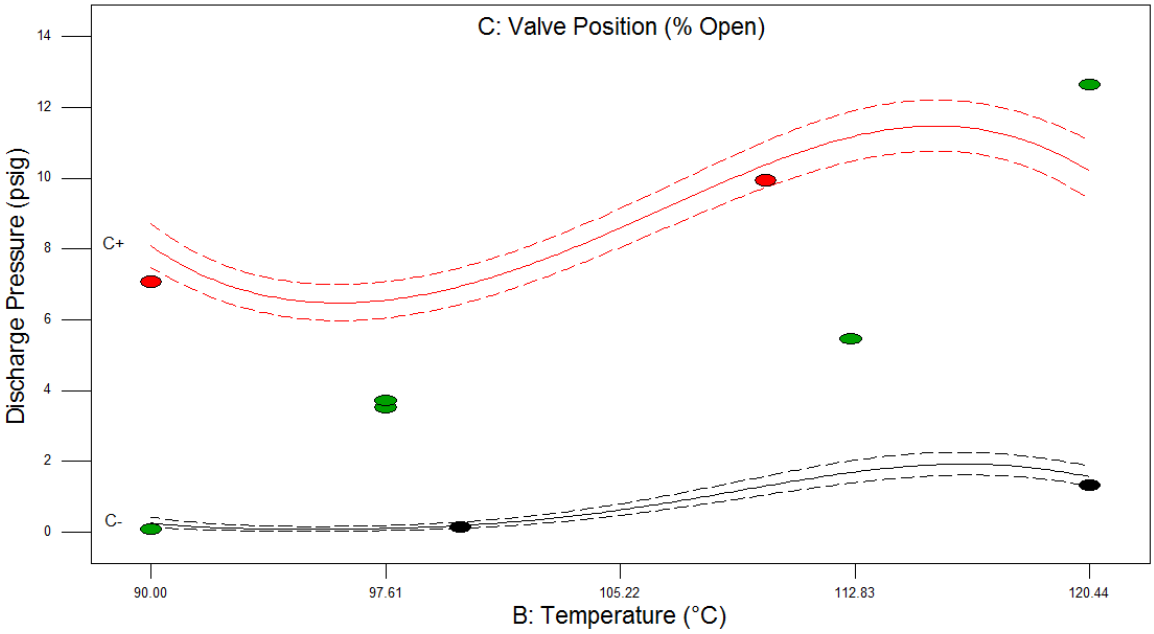

Figure 4-26: Discharge pressure interaction plot (temperature and valve position)

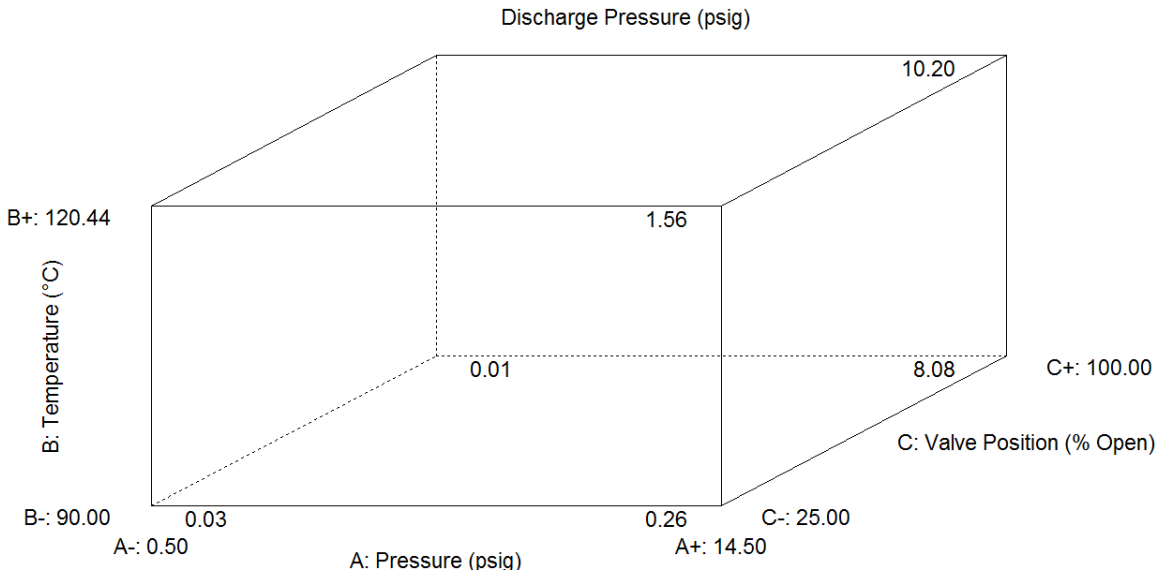

Figure 4-27: Discharge pressure cube plot

Figure 4-27 presents the cube plot for mass flowrate. The predicted values from the actual model indicate the high and low factor combinations. As discussed, the combination of high temperature and low pressure violates the equation of state and are not represented by the cube plot. The general trend among the coded factors for discharge pressure are as follows:

1. Increased discharge pressure with increased supply temperature
2. Increased discharge pressure with increased supply pressure
3. Increased discharged pressure with increased valve position

Figure 4-28 shows the perturbation plot for the model and represents the effect of all factors at a distinct location.

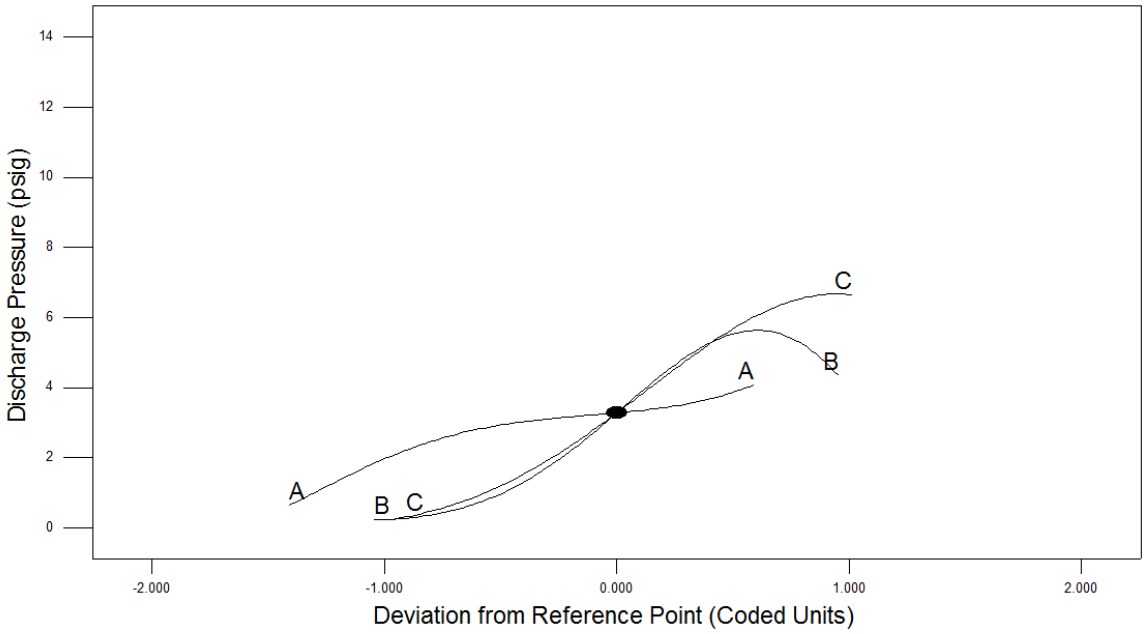

Figure 4-28: Discharge pressure perturbation plot

The discharge pressure peaked due to an overextended rotation of the valve body. Increased mass flowrate produces an increased discharged pressure, and the reduction of the mass flowrate occurs during the overextension. Also, the supply temperature and valve position are predominant contributors to the discharge pressure.

4.4 - Flow Visualization

High and low flow operating conditions provide an opportunity to visualize the presence of liquid and vapor within the glass test apparatus. The low condition consisted of a saturated liquid at 3.5 psig stagnation pressure and a valve position of 25%. Once the process reached a steady state, a partially stratified, wavy liquid and vapor phase occurred immediately after the discharge of the valve. The vapor phase was observed to be varying sizes of small 'bubbles' (0.100 – 0.180"). The vapor was not continuous but may have presented a periodic presence. Further downstream, a completely stratified flow

existed and maintained a wavy profile. The wavy profile was just below the middle of the pipe, with the maximum peak occurring just above the middle of the pipe. The presence of vapor bubbles could be seen to condense and produce a homogeneous liquid and vapor stream. Figure 4-29 shows an image from a high-speed camera immediately after the valve discharge.

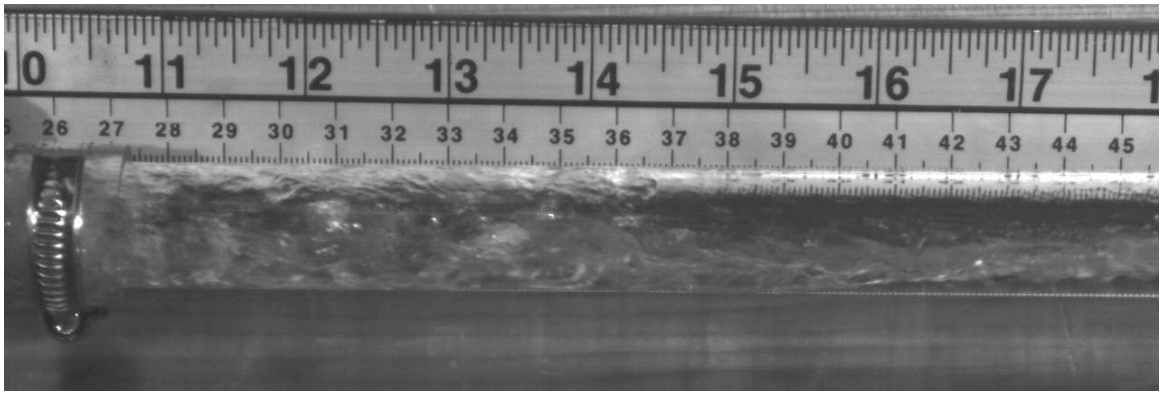

Figure 4-29: Saturated liquid flow visualization (minimal valve position)

The high condition consisted of a saturated liquid at 14.5 psig stagnation pressure and a valve position of 82%. The discharge of the valve could be described as a violent mixture of liquid and vapor. Further downstream, no stratification of the fluid or vapor occurs. The violent mixture somewhat ceases and the coagulation of vapor bubbles seems to be occurring. Figure 4-30 represents an image from a high-speed camera immediately after the valve discharge.

The flow visualization before the valve provides confirmation that the fluid is either subcooled or saturated as the fluid was without any voids or bubbles. The flow visualization after the valve provides confirmation that the fluid is a mixed liquid/vapor.

No air is present before or after the trial. For instance, when the discharge valve is closed, the mixed liquid/vapor condenses and returns to a homogeneous liquid phase.

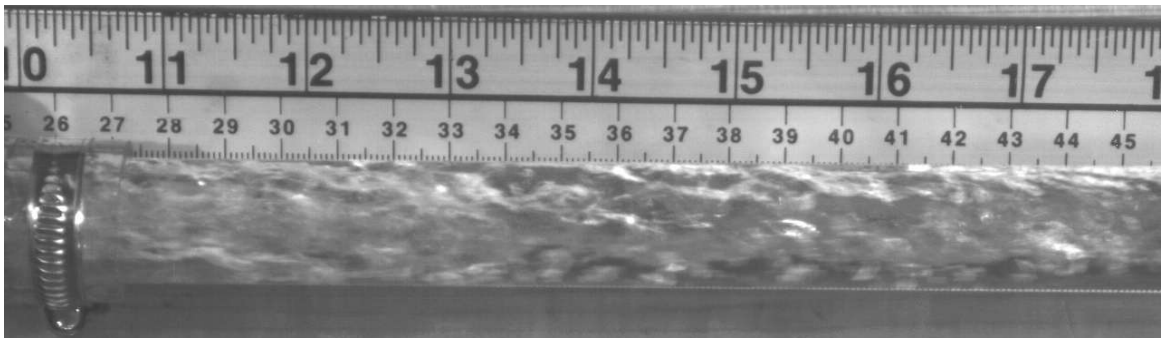

Figure 4-30: Saturated liquid flow visualization (maximum valve position)

Figure 4-31 illustrates the change of state upon the completion of a flow visualization trial. Appendix F presents the glass setups for flow visualization.

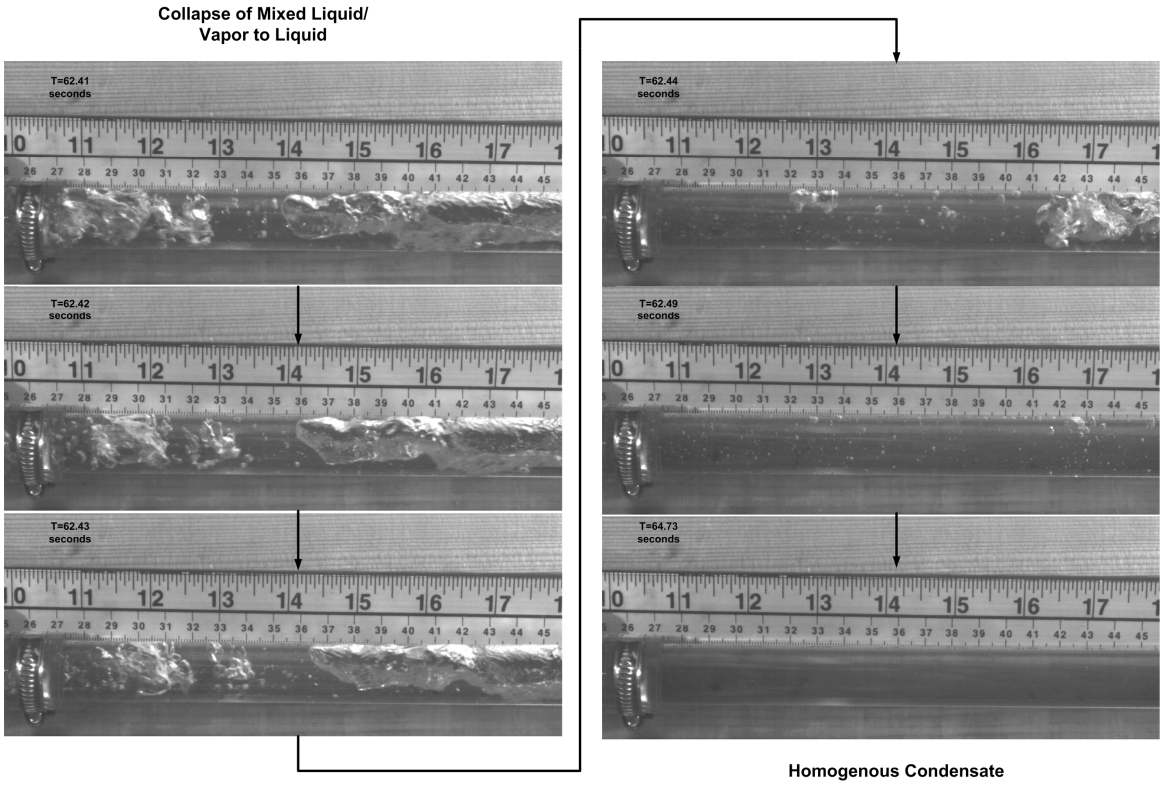

Figure 4-31: Condensing two-phase mixture

4.5 - Literature Comparison

4.5.1 - Introduction

Theories concerned with the sizing of control valves for both incompressible and compressible fluid flow are well understood and provide reasonable predictions (Hutchison, 1971). However, these models poorly predict mixed-phase fluid flow (Diener and Schmidt, 2005). For this reason, several methods have been proposed to provide suitable flowrate prediction.

All methods attempt to mathematically describe the relationship between the theoretical and actual flowrates. Such a model would be desirable for inclusion in an international standard. However, not all the methods analyzed are acceptable for adequately predicting the mass flowrate of condensate through a control valve.

The differences between the models vary based on fundamental principles. For instance, some models are reduced for simplicity and take liberal assumptions concerning the system, surroundings, and boundary interaction. Others attempt to formulate a more realistic approach to represent the physical phenomena.

The experimentally acquired model (EAM) is used when sizing a valve for low-pressure condensate control. The goal is to compare and evaluate potentially relevant models (ISA-I, HE, HF, HNE, HNE-DS) to the EAM for saturated inlet conditions, while considering flashing and choked flow. The saturated liquid is representative of the state in which a steam trap generally operates to efficiently harness latent thermal energy, increase plant reliability, reduce operating cost, and enable a safe working environment. Accompanying Appendix D are the MathWorks (2015) source code files for several

models (ISA-I, HE, HF, HNE, HNE-DS). Also, the thermodynamic properties are located in Table 4-9 (Lemmon, E. W., Mclinden, M. O., and Huber, M. L., 2005).

Another potentially useful method was presented by Henry and Fauske (1971), with the flexibility to describe either the subcooled, saturated, or a mixed-phase stagnation state. The model is creditable for vapor quality above 10% and large stagnation pressures. However, successfully using the method requires the critical pressure that occurs within the vena contracta, which was not included in the experimental scope of work.

Table 4-9: Thermodynamic properties (Lemmon, E. W et al., 2005)

Thermodynamic Properties												
Temperature *(°C)*	Pressure *(psig)*	Liquid Density *(kg/m^3)*	Vapor Density *(kg/m3)*	Liquid Enthalpy *(kJ/kg)*	Vapor Enthalpy *(kJ/kg)*	Liquid Entropy *(kJ/kg·K)*	Vapor Entropy *(kJ/kg·K)*	Liquid Specific Heat *(kJ/kg·K)*	Vapor Specific Heat *(kJ/kg·K)*	Liquid Kin. Viscosity *(cm^2/s)*	Vapor Kin. Viscosity *(cm2/s)*	Vapor Isentropic Exp.
100.46	0.5	958.02	0.6074	421.1	2,676.3	1.3124	7.3486	4.2162	2.0819	0.0029267	0.20225	1.315
102.29	1.5	956.69	0.64531	428.82	2,679.2	1.333	7.3269	4.2184	2.0895	0.0028756	0.19134	1.3146
104.03	2.5	955.42	0.68307	436.16	2,681.9	1.3525	7.3065	4.2205	2.097	0.0028287	0.18163	1.3143
105.68	3.5	954.2	0.72069	443.15	2,684.4	1.3709	7.2873	4.2226	2.1043	0.0027854	0.17294	1.3139
107.26	4.5	953.02	0.75817	449.82	2,686.9	1.3885	7.2691	4.2246	2.1114	0.0027452	0.16511	1.3136
108.77	5.5	951.88	0.79553	456.22	2,689.2	1.4053	7.2519	4.2266	2.1185	0.0027079	0.15801	1.3133
110.22	6.5	950.78	0.83276	462.36	2,691.4	1.4213	7.2356	4.2286	2.1254	0.002673	0.15154	1.313
111.62	7.5	949.71	0.86989	468.27	2,693.5	1.4367	7.22	4.2306	2.1323	0.0026404	0.14562	1.3126
112.96	8.5	948.67	0.90691	473.96	2,695.5	1.4514	7.2051	4.2326	2.139	0.0026097	0.14019	1.3123
114.26	9.5	947.66	0.94382	479.46	2,697.5	1.4656	7.1908	4.2345	2.1457	0.0025808	0.13518	1.312
115.51	10.5	946.68	0.98065	484.77	2,699.3	1.4793	7.1772	4.2364	2.1523	0.0025535	0.13054	1.3117
116.73	11.5	945.72	1.0174	489.92	2,701.1	1.4925	7.164	4.2382	2.1588	0.0025276	0.12624	1.3115
117.9	12.5	944.79	1.054	494.91	2,702.9	1.5052	7.1514	4.2401	2.1652	0.0025031	0.12224	1.3112
119.04	13.5	943.88	1.0906	499.75	2,704.5	1.5176	7.1393	4.2419	2.1715	0.0024797	0.1185	1.3109
120.15	14.5	942.99	1.1271	504.45	2,706.1	1.5295	7.1275	4.2438	2.1778	0.0024575	0.115	1.3106

The maximum mass flowrate is determined at saturation temperature for a fully open valve position (100% open to the flow condition). This valve position provides a standard condition for establishing criteria related to engineering design and valve selection.

4.5.2 - Results

The two best models have an approximate error of 10 and 14% (HNE-DS, ISA-I), while the worst model approaches 120% (HF) from the experimental model. Table 4-10 provides a comparison between the proposed models and the experimentally acquired model. Figure 4-32 presents a visual representation of all methods. Figure 4-33 shows the EAM contour plot for mass flowrate through a fully opened valve position.

An inconsistency exists between the EAM and all the corresponding models for the lowest stagnation pressure. The EAM inherently includes a measure of error. Table 4-11 gives the proposed models and the adjusted experimentally acquired model. Figure 4-34 shows a visual representation of all methods.

Table 4-10: Theoretical and empirical prediction models

Saturated Liquid: T=Tsat, V.P.=100%

Supply Pressure, PT1 (psig)	0.5	1.5	2.5	3.5	4.5	5.5	6.5	7.5	8.5	9.5	10.5	11.5	12.5	13.5	14.5	
ΔP (psig)	0.12	0.53	0.79	1.00	1.20	1.41	1.65	1.90	2.14	2.35	2.50	2.53	2.40	2.05	1.45	
Models (lbm/hr)																**Overall (%)**
ISA-I	2025	3357	3476	3592	3706	3817	3926	4034	4139	4243	4345	4446	4545	4643	4740	
error (%)	46.7	5.5	15.3	21.4	24.4	24.6	22.9	19.9	16.0	11.8	7.7	4.1	1.3	0.3	0.6	*14.8*
HE	1359	1701	1802	1891	1979	2065	2151	2236	2320	2403	2486	2568	2649	2730	2801	
error (%)	118.6	108.2	122.4	130.7	132.9	130.3	124.3	116.3	107.0	97.4	88.3	80.2	73.8	69.5	68.1	*104.5*
HF	674	1391	1665	1837	1974	2101	2234	2357	2461	2537	2575	2547	2438	2213	1825	
error (%)	340.4	154.6	140.7	137.4	133.4	126.3	116.0	105.1	95.1	86.9	81.8	81.6	88.8	109.2	158.0	*130.4*
HNE	1964	4123	5030	5655	6191	6707	7251	7776	8248	8638	8905	8954	8717	8053	6771	
error (%)	51.3	14.1	20.3	22.9	25.6	29.1	33.5	37.8	41.8	45.1	47.4	48.3	47.2	42.5	30.5	*35.8*
HNE-DS																
a=3/5	1938	3907	4669	5178	5608	6013	6428	6822	7174	7472	7688	7773	7670	7257	6310	
error (%)	53.3	9.3	14.1	15.8	17.8	20.9	24.9	29.1	33.1	36.5	39.1	40.5	40.0	36.2	25.4	*29.1*
a=2/5	1880	3502	4047	4405	4704	4982	5259	5521	5755	5964	6138	6253	6279	6126	5589	
error (%)	57.9	1.2	1.0	1.0	2.0	4.6	8.3	12.4	16.6	20.5	23.7	26.0	26.7	24.5	15.7	*16.1*
a =best est. (0.35)	1853	3337	3811	4121	4382	4625	4866	5091	5296	5481	5643	5763	5818	5731	5315	
error (%)	60.3	6.2	5.2	5.8	5.1	2.8	0.8	5.0	9.3	13.5	17.0	19.7	20.9	19.3	11.4	*13.5*
Experimental																
95% T.I low of populaiton	2282	2765	3260	3582	3806	3940	3997	3989	3939	3867	3797	3749	3735	3758	3803	
95% C.I low for mean	2663	3191	3723	4067	4305	4448	4507	4497	4439	4359	4283	4231	4216	4240	4281	
mean mass flowrate (lbm/hr)	2970	3542	4008	4362	4608	4755	4825	4835	4802	4743	4681	4627	4604	4628	4709	
95% C.I high for mean	3263	3751	4302	4669	4922	5074	5149	5168	5150	5109	5057	5009	4985	5021	5175	
95% T.I high of populaiton	3712	4240	4827	5216	5483	5644	5721	5739	5716	5668	5610	5559	5534	5571	5726	
95% T.I low of populaiton	0.13	0.59	1.22	1.91	2.62	3.30	3.97	4.60	5.24	5.91	6.66	7.55	8.62	9.94	11.52	
95% C.I low for mean	0.23	0.80	1.51	2.27	3.03	3.77	4.47	5.15	5.82	6.52	7.30	8.23	9.35	10.72	12.35	
mean discharge (psig)	0.38	0.97	1.71	2.50	3.30	4.09	4.85	5.60	6.36	7.15	8.00	8.97	10.10	11.45	13.05	
95% C.I high for mean	0.46	1.11	1.90	2.75	3.60	4.41	5.19	5.95	6.72	7.52	8.39	9.36	10.51	11.93	13.79	
95% T.I high of populaiton	0.64	1.38	2.26	3.18	4.08	4.94	5.77	6.56	7.36	8.20	9.10	10.12	11.31	12.78	14.69	

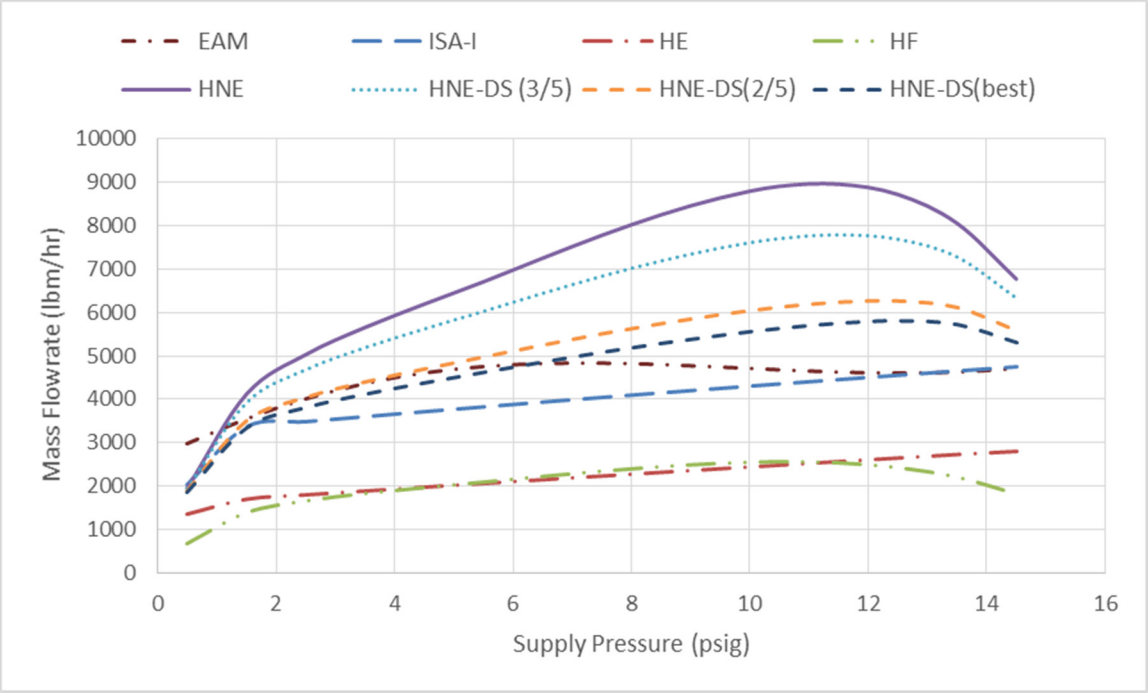

Figure 4-32: Theoretical and empirical prediction models

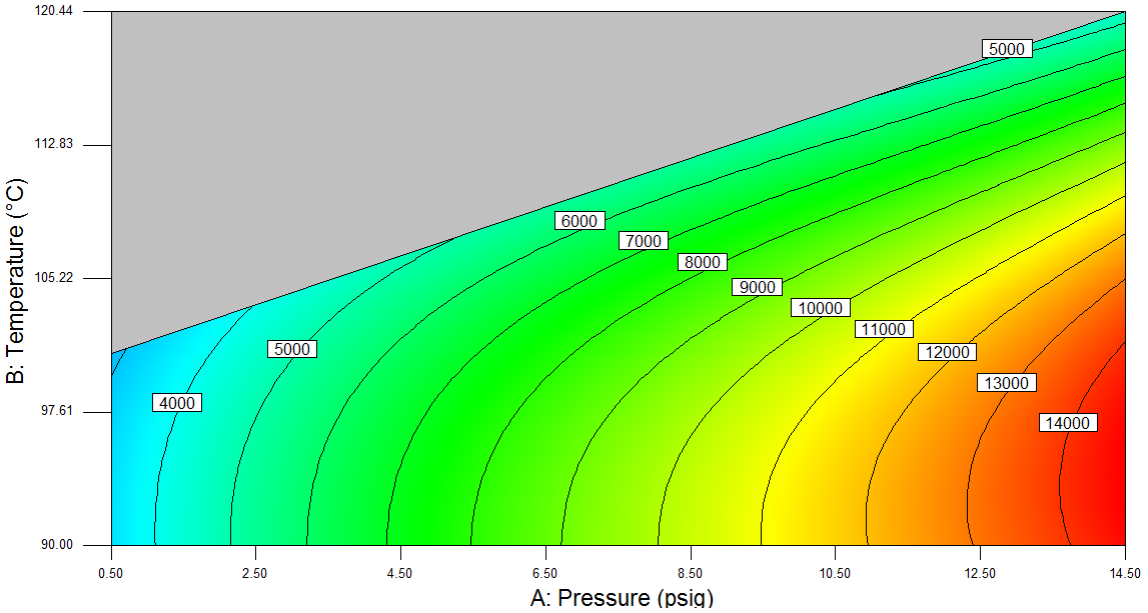

Figure 4-33: Mass flowrate contour plot for pressure versus temperature

Table 4-11: Theoretical and empirical prediction models (modified)

Saturated Liquid: T=Tsat, V.P.=100%

Supply Pressure, PT1 (psig)	0.5	1.5	2.5	3.5	4.5	5.5	6.5	7.5	8.5	9.5	10.5	11.5	12.5	13.5	14.5	
ΔP (psig)	0.22	0.53	0.79	1.00	1.20	1.41	1.65	1.90	2.14	2.35	2.50	2.53	2.40	2.05	1.45	
Models (lbm/hr)																**Overall (%)**
ISA-I	2025	3357	3476	3592	3706	3817	3926	4034	4139	4243	4345	4446	4545	4643	4740	
error (%)	33.5	5.5	15.3	21.4	24.3	24.6	22.9	19.9	16.0	11.8	7.7	4.1	1.3	0.3	0.7	*13.9*
HE	1512	1701	1802	1891	1979	2065	2151	2236	2320	2403	2486	2568	2649	2730	2801	
error (%)	78.7	108.2	122.4	130.7	132.9	130.2	124.3	116.3	107.0	97.3	88.3	80.2	73.8	69.5	68.1	*101.9*
HF	914	1391	1665	1837	1974	2101	2234	2357	2461	2537	2575	2547	2438	2213	1825	
error (%)	195.5	154.6	140.7	137.4	133.4	126.3	116.0	105.1	95.2	86.9	81.8	81.6	88.8	109.2	158.0	*120.7*
HNE	2659	4123	5030	5655	6191	6707	7251	7776	8248	8638	8905	8954	8717	8053	6771	
error (%)	1.6	14.1	20.3	22.9	25.6	29.1	33.5	37.8	41.8	45.1	47.4	48.3	47.2	42.5	30.5	*32.5*
HNE-DS																
a=3/5	2595	3907	4669	5178	5608	6013	6428	6822	7174	7472	7688	7773	7670	7257	6310	
error (%)	4.1	9.3	14.1	15.8	17.8	20.9	24.9	29.1	33.1	36.5	39.1	40.5	40.0	36.2	25.4	*25.8*
a=2/5	2460	3502	4047	4405	4704	4982	5259	5521	5755	5964	6138	6253	6279	6126	5589	
error (%)	9.9	1.2	1.0	1.0	2.0	4.6	8.3	12.4	16.6	20.5	23.7	26.0	26.7	24.5	15.8	*12.9*
a ≈best est.(0.35)	2398	3337	3811	4121	4382	4625	4866	5091	5296	5481	5643	5763	5818	5731	5315	
error (%)	12.7	6.2	5.2	5.8	5.1	2.8	0.8	5.0	9.3	13.5	17.1	19.7	20.9	19.3	11.4	*10.3*
Experimental																
*mean mass flowrate (lbm/hr)**	2702	3542	4008	4362	4608	4755	4825	4835	4802	4743	4681	4627	4604	4628	4709	
*mean discharge (psig)**	0.28	0.97	1.71	2.50	3.30	4.09	4.85	5.60	6.36	7.15	8.00	8.97	10.10	11.45	13.05	

**Except adj.95%C.I low for 0.5*

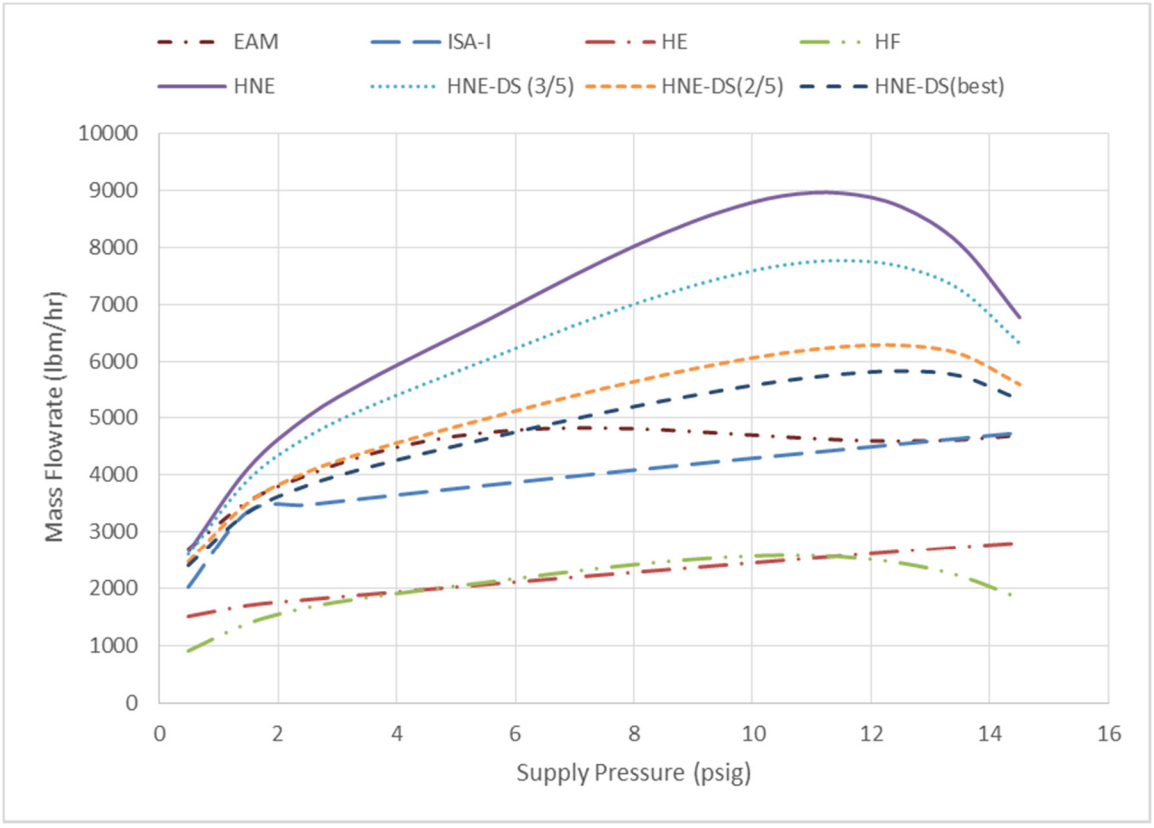

Figure 4-34: Theoretical and empirical prediction models (modified)

The optimal performance of the ISA-I (American National Standards Institute, 2002) and HNE-DS (Diener and Schmidt, 2005) prediction models are apparent over the

range for low-pressure saturation. The 95% confidence and tolerance interval provides an upper and lower boundary as developed by the EAM. For instance, the confidence interval boundary represents the flowrate variation expected with the experimental setup. However, tolerance interval represents the flowrate variation for all population outcomes occurring outside of the experimental setup. Figure 4-35 and Figure 4-36 presents the average response for each of the ISA-I (American National Standards Institute, 2002) and HNE-DS (Diener and Schmidt, 2005) models with the EAM confidence/tolerance intervals. It is important to note the dependency of each model on the discharge pressure.

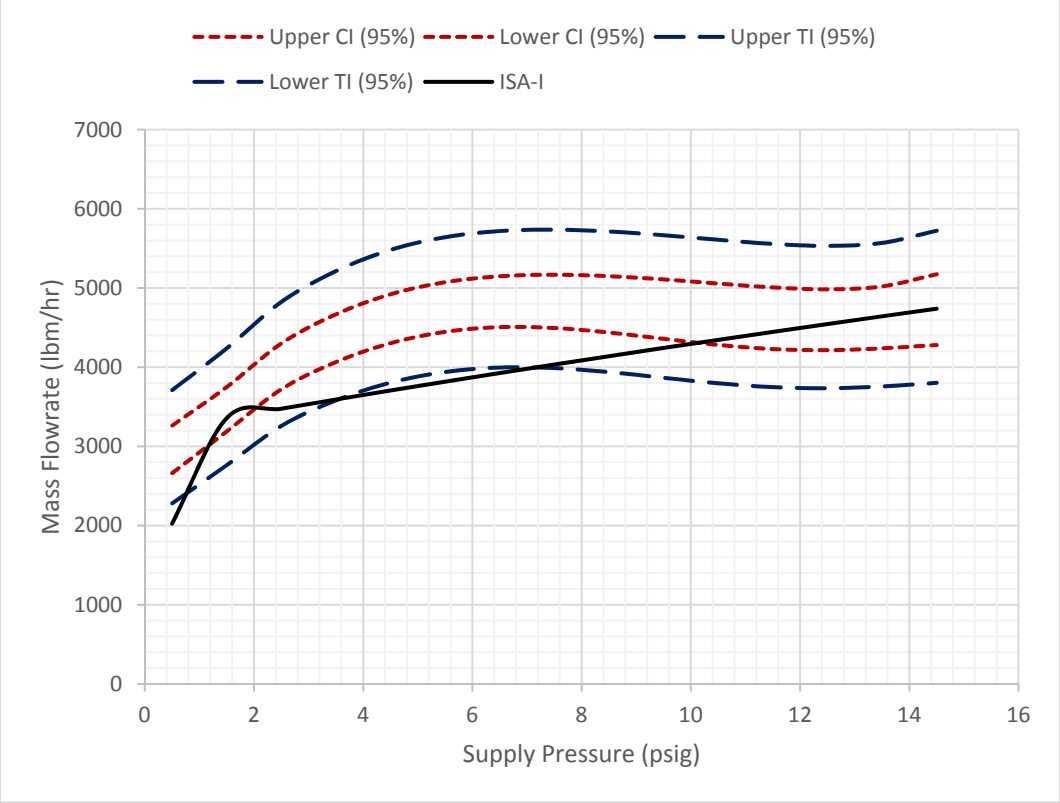

Figure 4-35: ISA-I model versus EAM model CI/TI (95%)

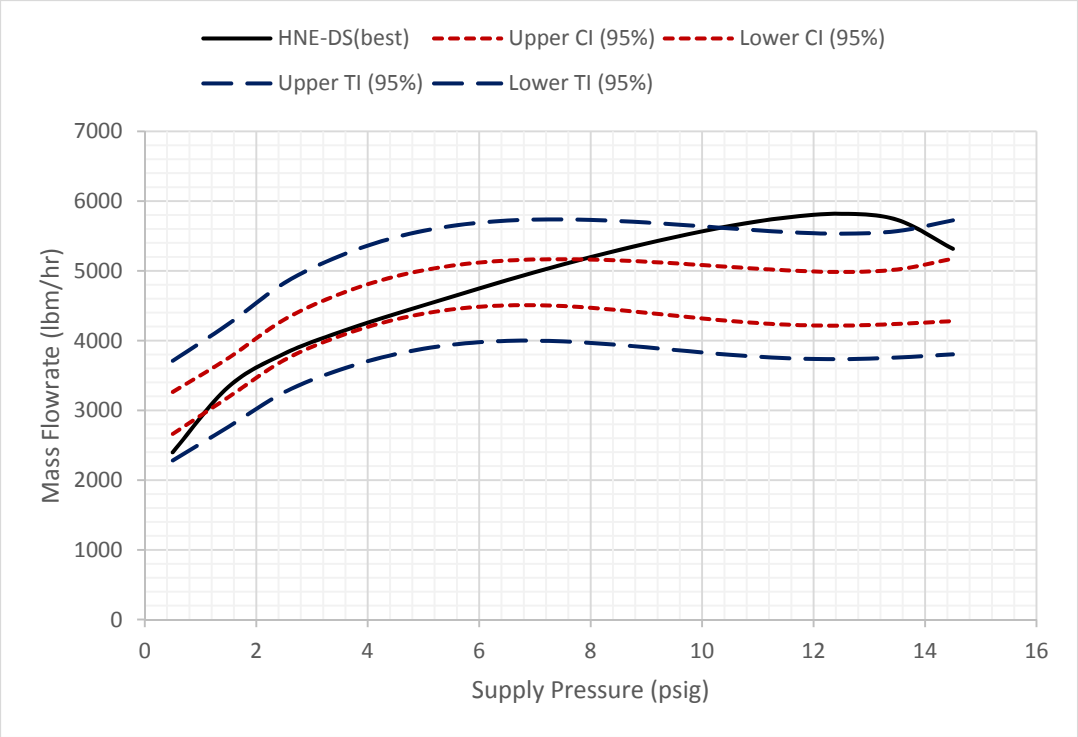

Figure 4-36: HNE-DS model versus EAM model CI/TI (95%)

For instance, an increased discharge pressure will reduce the mass flowrate of each model and vice versa. The tendency will shift the model. For the purpose of the illustration, the mean is acceptable for determining the suitably of a model when selecting a valve to control condensate.

4.5.3 - Discussion

4.5.3.1 – Prediction Model

The model that best describes the mean account of the experimental behavior is the HNE-DS (Diener and Schmidt, 2005) model. It produced an average error of approximately 10%. The ISA-I (American National Standards Institute, 2002) model is also acceptable with 14% error.

The average error between all models at each stagnation pressure remained relatively constant (45%). The result for the ISA-I model is similar to the work completed with R-12 refrigerant, which produced an approximate error of 20% for a low-quality liquid/vapor mix (Hutchison, 1971). The literature indicates that within this model further reduction in flowrate is usually not observed with further increases in differential pressure (Hutchison, 1971).

The Homogenous Non-Equilibrium model tends to over-predict while the Homogenous Frozen and Homogenous Equilibrium models tend to under-predict (Diener and Schmidt, 2005). Also, the method proposed by Henry and Fauske (1971) predicts between the HE and HF models (Yoon, Ishii and Revankar, 2006), and would not provide an improvement over the ISA-I and HNE-DS models.

Each of the HNE models and the HF model follows the transitional changes of the EAM. For instance, two distinct transitions occur within each model. The first occurs at a lower stagnation pressure and the second near the upper stagnation value. Each model type predicts the initiation of the critical pressure, which results in choked flow. It is the second transitional offset that fails to follow the mean of the EAM. The range of error within the EAM model could easily explain the deviation of the second transition. In fact, the improved model prediction can be realized within the 95% confidence interval for mass flowrate and discharge pressure. These methods adequately represent the critical pressure ratio.

The boiling delay exponent is a critical term for the HNE-DS (Diener and Schmidt, 2004) method. Estimation of the exponent was established to produce the mass flowrate that would best represent EAM. This was a reverse engineering approach to

produce the best theoretical fit to the experimental model. Experimental comparisons were conducted between EAM and HNE-DS (Diener and Schmidt, 2004) for the recommended exponent coefficients. These include 3/5 (orifices, control valves, short nozzles), 2/5 (safety valves, high lift control valves), and 0.0001 (long nozzles, orifice with large area ratios) exponent coefficients. Diener and Schmidt (2004) suggest these coefficients work reasonably well for representing the flowrate. A scientific method to acquire the exponent exists and consists of first estimating the critical mass flux from Henry and Fauske (1971). Based on the mass flux and critical pressure ratio, the compressibility constant can be determined. With the homogenous non-equilibrium compressibility constant and the compressibility constant for a homogenous equilibrium flow, the power coefficient can be estimated (Diener and Schmidt, 2004).

Through reverse engineering, the HNE-DS (Diener and Schmidt, 2005) model allows for the identification of an exponent that best represents the physical characteristics of the valve and environment (a=0.35). Given that the recommended values for the exponent were not optimal, it was noted that further investigations of other valve types may provide opportunities for model improvement (Diener and Schmidt, 2004). In particular, long nozzles, venturi, or orifices with large area ratios were noted. The ball valve simulates a venturi when functioning in the fully open flow position. Given the physical geometry of the valve, it would be expected to deviate from the 3/5 power and gravitate closer to the 2/5 power, as observed within the reverse engineering approach. Based on the fact that the boiling delay exponent is critical for the actual response, valve manufacturers could establish this coefficient to satisfy design requirements. This concept would not be original, as valve manufacturers currently

perform standard testing to develop the flow coefficient. The development of testing standards to acquire the boiling delay factor would require development should the HNE-DS (Diener and Schmidt, 2005) model become universally accepted for international use.

The critical pressures generated within the valve provide the necessary information to determine flash formation, which includes vapor quality. For the instituted ball valve and the low-pressure condensate system (saturated liquid stagnation quality), the vapor quality produced within the valve is low. For instance, the vapor quality would be less than 1% at vena contracta. Prediction with low-quality vapor is not ideal for multiphase (liquid/vapor or liquid/gas) models. An increase in error is evident for cases with vapor conditions below 10%. After 10%, most of the proposed models converge, producing a minimal error.

4.5.3.2 – Flowrate Capacity

The use of a valve to control the flow of condensate is ascertained to be a feasible, versatile, and preferred option. The potential range of mass flowrate for control valves exceeds existing steam trap technology. The highest supply pressure (14.5 psig) produces an average flowrate range of 260 - 4,708 lbm/h, while the lowest supply pressure (0.5 psig) produces an average flowrate range of 77 - 2,977 lbm/h. The range of high and low mass flowrates correspond to a change of valve position, i.e., 82% and 25%, respectively. These values occur at the saturation liquid state for the corresponding supply pressures.

As indicated in Figure 4-37, differential pressure and orifice size will determine the actual capacity capable of the inverted bucket steam trap. The most important consideration is to notice that a fixed pressure produces a fixed flowrate. Trap model 214

illustrates that 6 psig and a 1/2” orifice can provide a condensate capacity of 4000 lbm/h. The only way for the steam trap to provide higher or lower condensate capacities is to change the orifice, i.e., 5/8” or 3/8” diameter. This is critical information as the control valve operating at saturation temperature and a differential pressure of 6 psig can produce an average flow capacity between 298 - 4,813 lbm/h. To produce the rated range of flowrate, several orifices would have to be implemented to match the performance of the control valve; a process that would be impractical and unfeasible during operation.

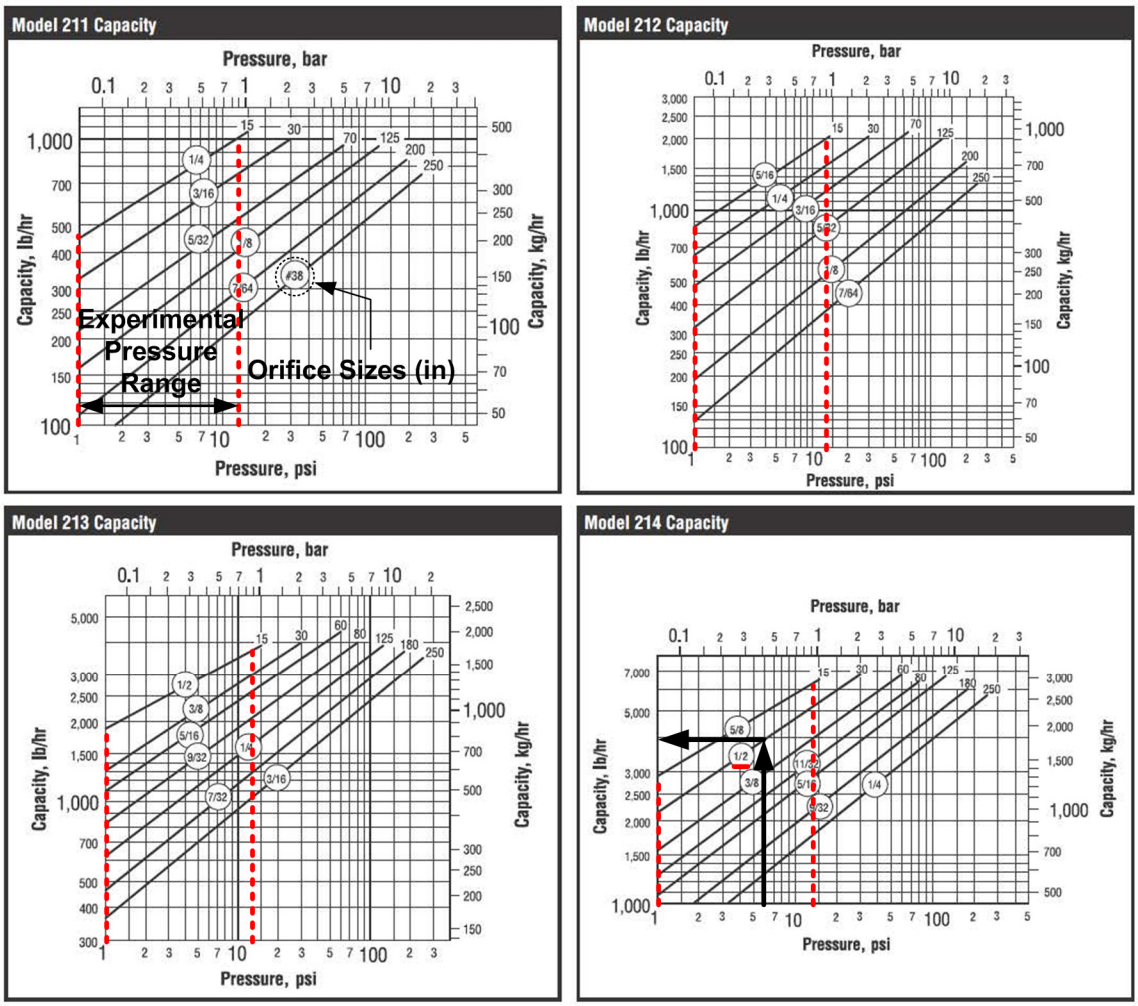

Figure 4-37: Steam trap capacity chart (Armstrong, 2015)

A major problem is sizing the steam trap. Start-up loads within the primary loop and point of use process vary significantly and the magnitude could be significantly larger than the trap capacity. Undersized steam traps results in increased inefficiency and pose dangerous and damaging effects; predominately differential and thermal shock. The addition of increased trapping stations to reduce the hazard during start-up requires an increased capital and operating cost for installation and maintenance. Steam traps that have been sized to handle the start-up load or peak operational load will be oversized during normal operation. A rapid cycle operation of the trap will increase the likelihood of failure; increasing maintenance cost related to labor and parts. The majority of existing steam traps operate via an on and off behavior to perform condensate removal and steam trapping. The exception consist of the venturi trap and float type traps that can provide a steady discharge. In practice, the condensate load is never constant, which causes the venturi/float trap to function in a cyclic behavior. Conversely, the condensate control valve can match the peak load to maintain a relatively steady state operation.

4.5.3.4 – Control Valves

Control valves are capable of delivering increased latent/sensible thermal energy to the point of use process and for reprocessing purposes. Several descriptions and illustrations are used to support the corresponding statement in the subsequent paragraphs. Steam quality indicates the amount of vapor present at saturation temperature. High vapor quality provides increased latent energy for heating applications, which is the most valuable energy. However, a decreased vapor quality will occur if the condensate is improperly removed.

Figure 4-38 represents several processes for steam production, distribution, and point of use. Two separate processes (3a to 4a and 3b to 4b) illustrate the loss of energy for inadequate condensate removal during distribution.

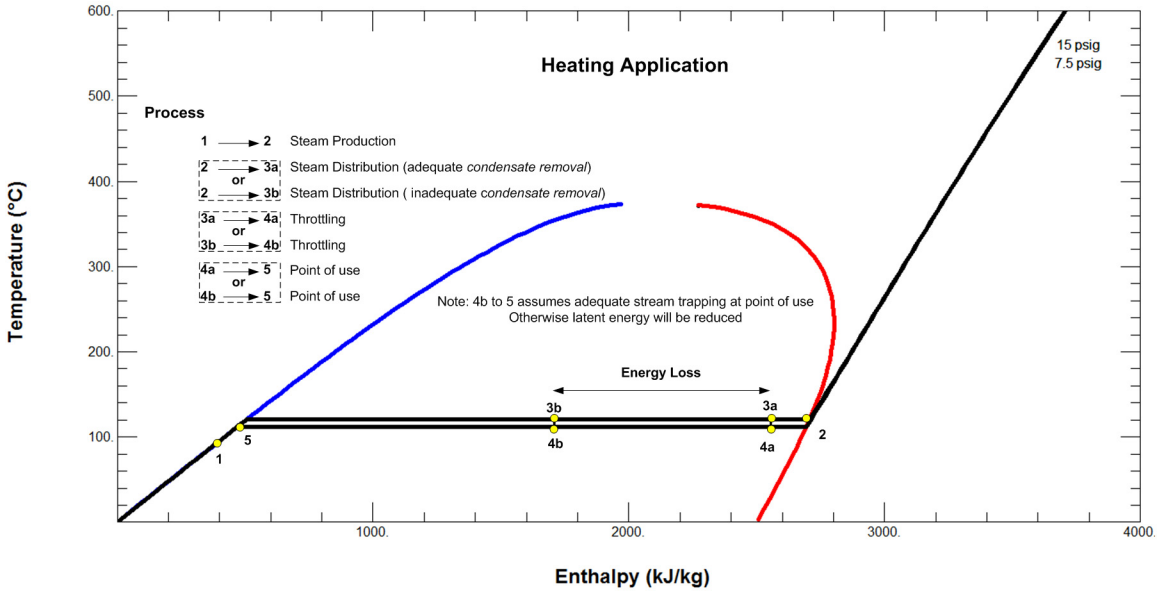

Figure 4-38: Distribution energy loss for inadequate condensate removal

Figure 4-39 shows the energy loss that occurs at the point of use for a failed steam trap (open or close position). Each condition causes inefficient energy extraction for latent heat of condensation. Steam traps fail because of an obstructed orifice, mechanical failure, or water hammer damage. All three failures are not a concern for control valves. For example, an obstructed orifice would result in the control valve opening further to dislodge the debris. Also, the control valve has minimal moving parts and is resistant to harsh operating environments.

Sensible thermal energy increases when subcooling occurs. Only a select number of steam traps can provide this capability. However, engineering judgement is required to determine where this application is suitable.

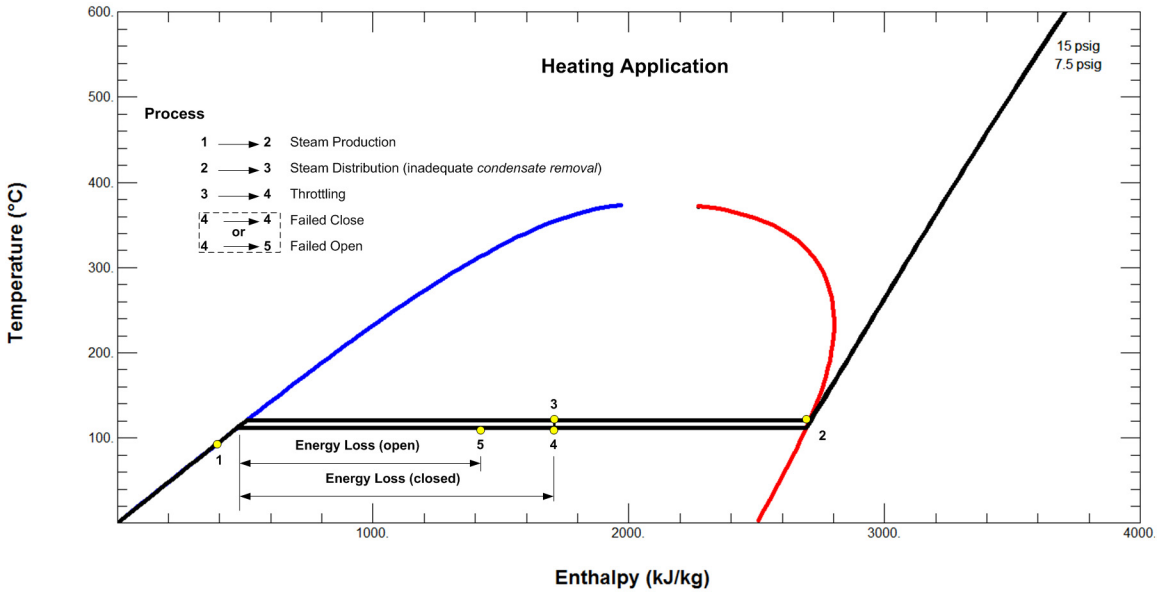

Figure 4-39: Energy losses for steam trap failures

Reprocessing is a concept that involves making use of condensate and flash steam. The fluid is preheated, chemically treated, and contains potential energy for reuse. Increased temperatures will reduce pipeline corrosion, water hammer, and energy loss.

The use of ball valves indicates an advantage over other valve types, i.e., globe valves. The reason is related to cost and pressure recovery of the valve, which is the downstream discharge pressure. Increased pressures allow for increased temperatures, which means that more of the energy will be delivered for steam production by reducing flash steam. Also, reducing the flash steam will allow smaller condensate return lines.

Figure 4-40 provides the pressure profile for vena contracta and recovery pressure. The depiction is representative of the saturated condition where P_1 is P_v. The ball valve (top) produces an increased pressure recovery versus the globe valve (bottom).

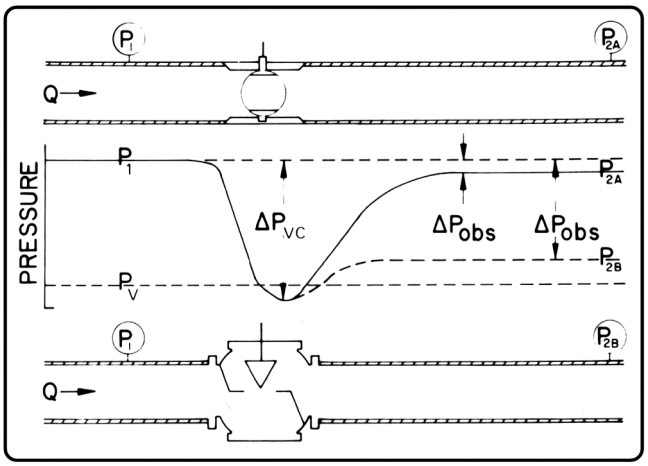

Figure 4-40: Recovery pressure for a subcooled liquid (Hutchison, 1971)

Another advantage of the control valve is the steady state flow conditions through condensate return lines. The consistent removal of condensate reduces corrosion related damage and water hammer. Unnecessary energy loss does not occur within the collection leg. For example, most steam traps have intervals where the condensate remains in the collection leg before being periodically removed.

Consideration for predictive maintenance, performance indicators, diagnostic operation, control strategy, and material can provide increased reliability and efficiency.

Predictive maintenance is considered just-in-time service. The idea is that maintenance is completed as needed to minimize unnecessary labor, material and part cost. This service generally has a high capital investment that could detract potential customers. The use of automatic control valves inherently has the capability to be used for predictive maintenance. For instance, the valve is relatively maintenance free and failure can be predicted based on performance indicators or operational hours. This results in the maximum use of resources.

Performance indicators are extremely important determinants for plant engineers. Decisions are based on operational requirements and problems can be identified immediately for resolution. A flow meter is an example of a performance indicator. However, the high cost of flow meters results in limited installations. Fortunately, each control valve is capable of functioning as a flowmeter.

Sufficient information to provide mass flowrate requires knowledge of the supply pressure, valve position, and supply temperature. This provides a consumption map for the whole facility, which offers valuable insight for decision making. For example, the mass flowrate from steam production equipment informs the operator of changes within the process. Recognizing the deficiency will allow the operator to address the issue immediately to ensure efficiency and effectiveness. Other opportunities for performance indicators are possible, i.e., use the control valve as a calorimeter.

Diagnostic capabilities inform the engineer of operational status. For example, if a valve is functioning correctly. Supply temperature, pressure, valve position, and condensate level are key elements that would determine functional status. The information can immediately resolve a deficiency related to condensate removal.

Control strategy of existing steam traps can remove condensate at saturation temperature or below, but not both. However, the strategy for control valves can use both methods. For instance, the control valve can provide extra energy extraction through subcooling (sensible heat), but should the condensate level take precedence, the valve would open for condensate removal. The included instrumentation is sufficient to perform temperature and level control. Another consideration for control includes redundancy and increased flowrate capacity. For example, even though the range of

mass flowrate capacity is comprehensive, the selection of a 1/3 and 2/3 valve capacity provides further capabilities for control. The overlap of both valves provides lower and higher capacities for design considerations.

Damage related to cavitation is of primary concern for two-phase flows when the supply pressure is equal to or less than the vapor pressure. Cavitation occurs due to the extreme low-pressure location of the valve (vena contracta), and upon the recovery of downstream pressure the void collapses to produce physical damage (Hutchison, 1971). However, cavitation is not a concern when valves are used to control condensate.

The flash mixture can cause damage depending upon the body material and flow passage of the valve, where higher velocities promote an erosive environment (Hutchison, 1971). However, the adverse impact of erosion can be negated by adequate material selection, valve style, and size. The differences between erosion and cavitation are that erosion causes a smooth wear pattern while cavitation causes a pitted wear pattern (Hutchison, 1971). Between the two types of effect, cavitation is substantially more damaging than erosion.

When the steam system undergoes a cooling process, air is pulled into the steam production, distribution, and point of use equipment. This occurs because the volume of steam is magnitudes larger than condensate (liquid). When the steam cools, a reduction of volume will create a lower than atmospheric pressure and cause a vacuum of air into the system. Provision of vacuum breakers are necessary to prevent system damage. However, the air that is now entrained has to be removed upon start-up. The reason is twofold. First, the presence of air provides insulation characteristics within a heat transfer process. Second, only with the removal of air can the heating fluid travel to its

desired destination. Figure 4-41 and Figure 4-42 shows the adverse effect air creates through heat transfer and steam energy.

It is important to highlight that not all existing steam traps are capable of removing air. This is significant, as less available locations to purge air will cause the existing air removal devices to be burdened. However, the expiated removal of air occurs through control valves because they have an increased operating capacity and function as air removal devices.

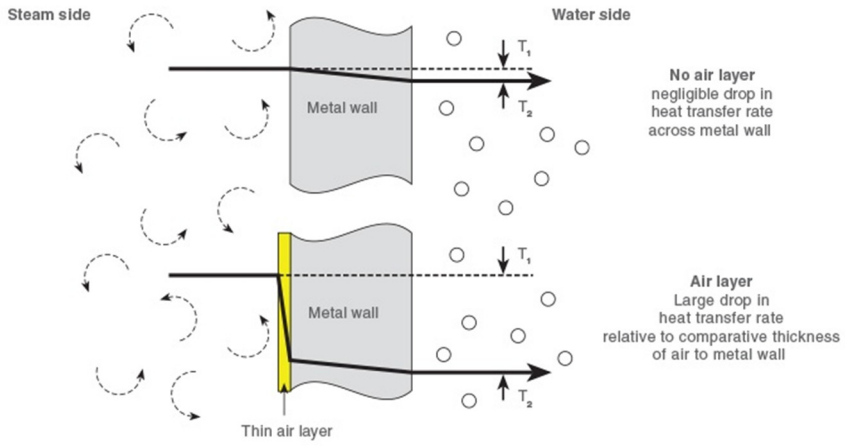

Figure 4-41: Effect of air on heat transfer (Spirax Sarco, 2015)

The capital cost of ball valves are comparable to available steam traps, which includes the additional instrumentation for integration within existing infrastructure. The exact cost for the tested ball valve, rotary actuator, and linkage kit is $270.80 before taxes. The instrumentation cost for the pressure, temperature, and two level sensors (conductivity probes) are $337. The cost of a comparable steam trap capacity (5300 lbm/hr) and operating pressure from Bell and Gossett is $622.78 before taxes (Mfr#: FT015H-6), while the illustrated Armstrong bucket trap (214) cost $785.00. However, the operational cost for valves are lower because of efficiency gains, reduced inventory,

just-in-time maintenance, and the diagnostic performance capabilities. Overall, the control valve is more cost effective than steam traps and enhances sustainability.

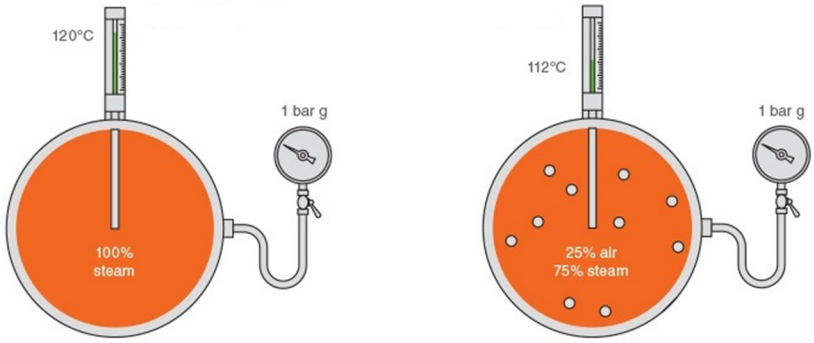

Figure 4-42: Effect of air on steam temperature (Spirax Sarco, 2015)

How is the use of a control valve an unusual consideration for such an obvious solution to efficiently and effectively remove condensate and non-condensables from production, distribution, and point of use processes? Based on professional experience, it is the opinion of the author that the natural progression of steam trap development occurred before the feasible implementation of instrumentation technology. Also, the financial and environmental need was unsubstantiated. Either the technology did not exist, or if it did, the financial cost would negate the practical consideration. Much of the research work concerning steam and condensate originated during the twentieth century. During this time, energy efficiency or environmental concerns were not a contention within the industry. The availability of energy was abundant and the monetary and environment cost of production insignificant. However, after the 1970 embargo oil crisis, there was a fundamental shift towards sustainability and efficient use of resources. The next several decades did provide the right combination of conditions to implement the control valve for the universal replacement of steam traps, but the reality was not recognized until the present.

-5- Conclusions and Recommendations

5.1 - Conclusion

The removal of condensate from a saturated steam system provides increased latent thermal energy while decreasing equipment damage, safety issues, maintenance, and plant start-up. Limited flow capacity, selection, and increased maintenance are deficiencies present within existing steam traps. The universal replacement of all steam traps with control valves was proposed.

The response surface methodology produces prediction equations for the mass flowrate and discharge pressure. The equations help to establish the best theoretical model (HNE-DS) for sizing a control valve. The margin of error is within 10%, and comparable to single phase flow equations (American National Standards Institute, 2002). However, the accuracy is critically dependent upon the boiling delay coefficient.

The mass flowrate model indicates that an increased supply pressure, increased valve position, and reduced temperature provides the greatest capacity. A choked flow condition was observed whereby a further increase in pressure produced no increase in mass flowrate. In particular, an increase in differential pressure and temperature produces flow restricting characteristics that adversely affect the capacity. The discharge model shows that increased supply pressure, increased valve position, and increased temperature produced the greatest discharge pressure.

Physical observation, experimental modeling, and flow visualization establishes several improvements for replacing steam traps with control valves. The advantages are as follows:

1. Increased flowrate capacity (≈ 20% greater than illustration).
2. A continuous range of flow for fixed pressure conditions.
3. Decreased flowrate capacity (≈ 93% lower than illustration).
4. Increased removal of non-condensables.
5. Reduced time for plant start-up.
6. Performance indicators, i.e., flowrate.
7. Diagnostic capabilities, i.e., verify operating status.
8. Predictive capabilities, i.e., just-in-time service.
9. Reduced maintenance.
10. Steady state discharge characteristics.
11. Decreased operational cost.
12. Increased efficiency.

The use of the performance standard (American National Standards Institute, 2005) ensures comparable testing conditions between steam traps and control valves.

5.2 - Contribution to Science

The research supports the proposed condensate removal method and provides an innovative solution to enhance industrial and sustainable development. Distinct items of contribution include:

1. Robust experimental models for mass flowrate and discharge pressure.
2. Confirmation of an acceptable theoretical model for sizing control valves.

To the best of the author's knowledge, the proposed use of control valves as a universal replacement of steam traps are a concept not published within literature or applied within industry.

5.3 - Recommendations

An item that could improve the development of the experimentally acquired model (mass flowrate) would be the elimination of condensation induced vibration. It is highly recommended that the volumetric tank method be used instead of the weigh tank method. Additionally, a continuous level measurement device should be used.

Only one type of valve and flow coefficient was tested, but others should be evaluated. This includes observing the responses for a high-pressure system. The results could then be compared to the HNE-DS model to verify if it is an adequate predictor of flowrate. This is important because a theoretical model is required for designers to size the control valve.

Further experimentation should include pressure measurement at vena contracta to provide the exact critical pressure ratio. The verification could improve theoretical prediction models. Ideally, the margin of error would be less than 10% for predicting the flow. A model to determine the boiling delay coefficient should be developed, otherwise the valve manufacturers would have to provide the coefficient.

An attempt should be made to reduce the excess volume of the collection leg. Control valves have a significant range potential for varying the flow of condensate, and further gains in efficiency may be obtained by reducing the energy loss. Also, it is suggested that computational fluid dynamics be utilized to provide details impractical to obtain from experimentation.

-6- Bibliography

Allen, W. F., Jr. (1951). Flow of a flashing mixture of water and steam through pipes and valves. *Trans. ASME.*

American National Standards Institute., ISA--The Instrumentation, Systems, and Automation Society., and Global Engineering Documents (Firm). (2002). Flow equations for sizing control valves. Research Triangle Park, N.C: ISA.

American National Standards Institute., and American Society of Mechanical Engineers. (2005). *Steam Traps: Performance Test Codes*. New York, NY: American Society of Mechanical Engineers.

American Society of Heating, Refrigerating and Air-Conditioning Engineers. (2006).*ASHRAE greenguide: The design, construction, and operation of sustainable buildings*. Atlanta, GA: American Society of Heating, Refrigerating, and Air-conditioning Engineers.

American Society of Heating, Refrigerating and Air-Conditioning Engineers. (1985).*ASHRAE handbook, 1985 fundamentals*. Atlanta, GA: American Society of Heating, Refrigerating and Air-conditioning Engineers.

American Society of Heating, Refrigerating and Air-Conditioning Engineers. (2004).*2004 ASHRAE handbook: Heating, ventilating, and air-conditioning systems and equipment*. Atlanta, Ga: ASHRAE.

American Society of Mechanical Engineers. (2006). *Test uncertainty*. New York, N.Y.: American Society of Mechanical Engineers.

Armstrong. (2015). Product literature. Retrieved from https://armstronginternational.com /products-systems/steam-condensate/steam-trapping-and-steam-tracing-equipment/steam-traps/inverted-bucket/200-series-inverted-bucket-steam-traps

Barna, I. F., Imre, A. R., Baranyai, G., and Ézsöl, G. (2010). Experimental and theoretical study of steam condensation induced water hammer phenomena. *Nuclear Engineering and Design, 240*(1), 146-150.

Benjamin, M. W., and Miller, J. G. (1941). Fluid flow of saturated water through throttling orifices. *Trans. ASME, 63*, 419-429.

Chun, M. (2000). A parametric study and a guide chart to avoid condensation-induced water hammer in a horizontal pipe. Nuclear Engineering and Design, 201(2-3), 239-257.

Chun, M., and Yu, S. (2000). Effect of steam condensation on countercurrent flow limiting in nearly horizontal two-phase flow. Nuclear Engineering and Design, 196(2), 201-217.

Coleman, H. W., and Steele, W. G. (2009). *Experimentation, validation, and uncertainty analysis for engineers* (3rd ed.). Hoboken, N.J: John Wiley and Sons.

Conservation and Environment. (2014). Tap water quality for public water supplies. Retrieved from http://maps.gov.nl.ca/water/

Copper Development Association. (1960). *Copper tube handbook for plumbing, heating, air conditioning and refrigeration*. New York: Copper Development Association.

Dickman, F. (1984). The elimination of steam traps - the most cost effective move for 1985. *Proceedings of the Eighth Annual Industrial Energy Technology Conference,* Houston, TX. 768-775.

Diener, R., and Schmidt, J. (2004). Sizing of throttling device for gas/liquid two-phase flow part 1: Safety valves. *Process Safety Progress, 23*(4), 335-344.

Diener, R., and Schmidt, J. (2005). Sizing of throttling device for gas/liquid two-phase flow part 2: Control valves, orifices, and nozzles. *Process Safety Progress, 24*(1), 29-37.

Dirndorfer, S., Doerfler, M., Kulisch, H.,Malcherek, A. (2012). Condensation induced water hammer. *KT Kerntechnik, 77*(2), 122-127.

Fauske, H,Argone National Lab., Ill.,. (1971). Two-phase critical flow of one-component mixtures in nozzles, orifices, and short tubes. *J.Heat Transfer 93*(2), 179-87.

Franklin, G. F., Powell, J. D., and Emami-Naeini, A. (2002). *Feedback control of dynamic systems*. Reading, Mass: Addison-Wesley.

Ghosh, M. K., Sen, S., and Mukhopadhyay, S. (2008). *Measurement and instrumentation: Trends and applications*. Boca Raton; New Delhi: CRC/Taylor and Francis.

Gorelick, B., and Bandes, A. (2010). *Troubleshooting steam traps*. Don Mills: Business Information Group.

Hutchison, J. W., and Instrument Society of America. Process Measurement and Control Division. Final Control Elements Committee. (1971). *ISA handbook of control valves*. Pittsburgh: Instrument Society of America.

Ishigai, S. (1999). *Steam power engineering: Thermal and hydraulic design principles*. Cambridge, U.K.; New York: Cambridge University Press.

Kirkup, L., and Frenkel, R. B. (2006). An introduction to uncertainty in measurement using the GUM (guide to the expression of uncertainty in measurement). Cambridge, UK; New York: Cambridge University Press.

Kremers, J. (1983). Avoid water hammer. *Hydrocarbon Process. 62:3*, 67-68.

Kubba, S. (2012). Handbook of green building design and construction: LEEDS, BREEAM, and green globes Elsevier Science.

Lemmon, E. W., Mclinden, M. O., and Huber, M. L. (2005). *Standard reference database* (12th ed.) National Institute of Standards and Technology.

Leung, J. C. (1986). A generalized correlation for one-component homogeneous equilibrium flashing choked flow. *AIChE J.AIChE Journal, 32*(10), 1743-1746.

Leung, J. C. (1990). Similarity between flashing and non-flashing two-phase flows. *AIChE Journal, 36*, 797-800.

MathWorks, Inc. (2015). *MATLAB and statistics toolbox release 2015a*. Natick, Massachusetts, United States of America.

Martinez, W. L., and Martinez, A. R. (2008). *Computational statistics handbook with MATLAB* (2nd ed.). Boca Raton, FL: Chapman and Hall/CRC.

McCauley, J. F. (1995). *The steam trap handbook*. Lilburn, GA; Upper Saddle River, NJ: Fairmont Press.

Montgomery, D. C. (2013). *Design and analysis of experiments*. Hoboken, NJ: John Wiley and Sons, Inc.

National Institute of Standards and Technology (U.S.),International SEMATECH.,. (2003). Engineering statistics handbook.

National Instruments. (2013). *LabVIEW*. Austin, Texas, United States of America.

Paffel K. (2013). How to properly size a steam trap. *Chem.Eng.Chemical Engineering (United States), 120*(9), 58-61.

Paikin, I. K. (1981). Classification of steam traps. *Chemical and Petroleum Engineering, 17*(2), 106-110.

Risko, J. (2013). Beware of the dangers of cold traps. *Chemical Engineering Progress, 109*(2), 50-53.

Frank, S. J. (2006). Selecting the right steam trap - In addition to the type, consider the installation, maintenance and wasted energy costs during its operating life. *Hydrocarbon Processing*, 79.

Rebik, T. R. (2001). *Steam trap instrument module* (CA 2460056). United States of America: WO2003/033958.

Sheldon, C. W., and Schuder, C. B. (1965). Sizing control valves for liquid-gas mixtures. *Instruments and Control Systems, 38*, 134-137.

Sobolev, V. V., and Proskunov, I. G. (1973). Design of standard steam traps. *Chemical and Petroleum Engineering, 9*(4), 317-321.

Spirax Sarco. (1992). *Design of fluid systems: hook-ups*. Allentown, PA: Spirax Sarco.

Spirax Sarco. (2015). Steam engineering tutorials. Retrieved from http://spiraxsarco.com/resources/pages/steam-engineering-tutorials.aspx

Spirax Sarco. (2008) *The Steam and condensate loop*. Cheltenham: Spirax-Sarco limited.

Stat-Ease, Inc. (2014). *Design-expert version 9.0.5.1*. Minneapolis, Minnesota, United States of America.

TLV. (2015). The history of steam traps. Retrieved from http:// tlv.com/global/TI/steam-theory/history-of-steam-traps-pt1.html

Van, D., Stone and Webster Engineering Corporation., and Electric Power Research Institute. (1993). *Water hammer prevention, mitigation and accommodation*. Palo Alto, Calif: EPRI.

World Commission on Environment and Development. (1987). *Our common future*. Oxford; New York: Oxford University Press.

Wylie, E. B., and Streeter, V. L. (1978). *Fluid transients*. New York: McGraw-Hill International Book Co.

Yeoh, G. H., and Tu, J. (2009). *Modeling subcooled boiling flows*. New York: Nova Science Publishers.

U.S. Nuclear Regulatory Commission Office of Nuclear Reactor Regulation. (1996). Assurance of equipment operability and containment integrity during design-basis accident conditions.

Appendix A

Physical Experimental Apparatus

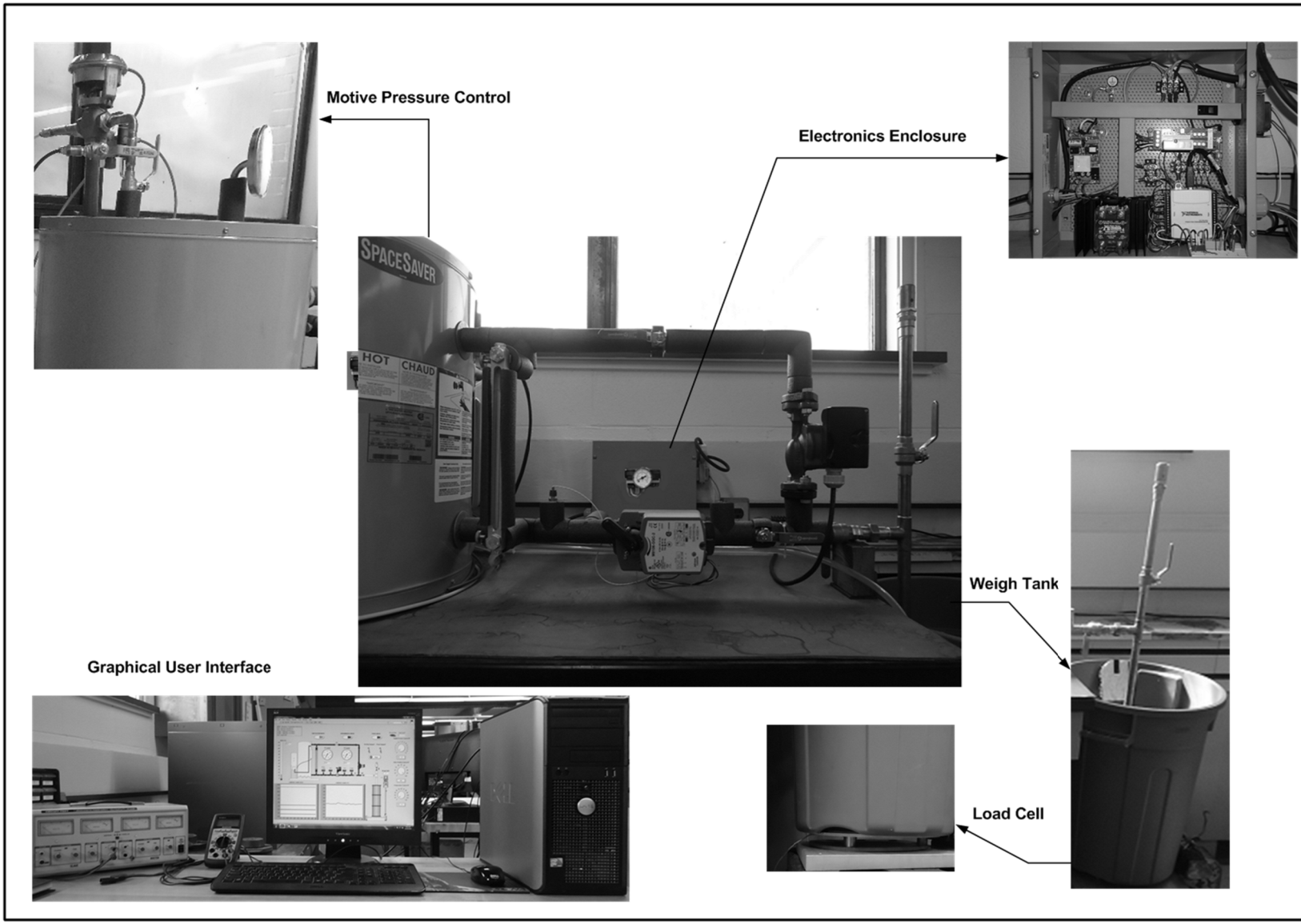
Motive Pressure Control
Electronics Enclosure
SPACESAVER
HOT CHAUD
Weigh Tank
Graphical User Interface
Load Cell

Appendix B

Instrumentation Calibration Reports

Omegadyne Inc.
PX209/219 Final Calibration Report

Serial #	97399	Model	PX209-015G5V
Job #	RMLS10237	Range	15
Date	7/18/2011		

Final Calibration Data

	Data	Theoretical	Error	PASS/FAIL	Required	+/-
Zero	-0.0001	0.0027	-0.0028	PASS	0.0000	0.1000
1/2 Scale	2.5018	2.5006	0.0012			
Full Scale	4.9955	4.9984	-0.0028		5.0000	
1/2 Scale	2.5037	2.5006	0.0031			
Zero	-0.0004	0.0027	-0.0031	PASS		
Sensitivity	4.9956	4.9956		PASS	5.0000	0.0750

Linearity	Hysteresis	Combined		Combined Accuracy Spec.	
0.0410	0.0380	-0.0631	PASS	0.25	%FS

This Calibration was performed using Instruments and Standards that are traceable to the United States National Institute of Standards Technology. This transducer is tested to and meets published specifications. After final calibration our products are stored in a controlled stock room and considered in bonded storage. Depending on environment and severity of use factory calibration is recommended every one to three years after initial service installation date.

Wiring Chart -

PX209/PXM209		PX219/PXM219	
Voltage Units	Current Units	Voltage Units	Current Units
Red = +Excitation	Red = + Excitation	Pin 1 = + Excitation	Pin 1 = + Excitation
Black = Common	Black = - Excitation	Pin 2 = Common	Pin 2 = - Excittation
White = + Output		Pin 3 = + Output	

Omegadyne Inc.
PX209/219 Final Calibration Report

Serial #	99719	Model	PX209-015G5V
Job #	RMLS10544	Range	15
Date	10/6/2011		

Final Calibration Data

	Data	Theoretical	Error	PASS/FAIL	Required	+/-
Zero	-0.0025	-0.0004	-0.0021	PASS	0.0000	0.1000
1/2 Scale	2.5041	2.5039	0.0002			
Full Scale	5.0061	5.0082	-0.0021		5.0000	
1/2 Scale	2.5060	2.5039	0.0021			
Zero	0.0008	-0.0004	0.0012	PASS		
Sensitivity	5.0086	5.0086		PASS	5.0000	0.0750

Linearity	Hysteresis	Combined		Combined Accuracy Spec.	
0.0230	0.0659	0.0419	PASS	0.25	%FS

This Calibration was performed using Instruments and Standards that are traceable to the United States National Institute of Standards Technology. This transducer is tested to and meets published specifications. After final calibration our products are stored in a controlled stock room and considered in bonded storage. Depending on environment and severity of use factory calibration is recommended every one to three years after initial service installation date.

Wiring Chart -

PX209/PXM209

Voltage Units	Current Units
Red = +Excitation	Red = + Excitation
Black = Common	Black = - Excitation
White = + Output	

PX219/PXM219

Voltage Units	Current Units
Pin 1 = + Excitation	Pin 1 = + Excitation
Pin 2 = Common	Pin 2 = - Excittation
Pin 3 = + Output	

TEST DATA SHEET

Date: 09-10-2014
Model: SCM7B34-03D
SN: 99637-1

ACCURACY TEST

Temp. (C)	Calculated Vout (V)	Measured Vout (V)*	Error (%)	Status
-2.06	-0.1027	-0.1002	+0.025	PASS
+47.22	+2.3610	+2.3614	+0.003	PASS
+98.30	+4.9154	+4.9155	+0.001	PASS
+148.23	+7.4116	+7.4118	+0.002	PASS
+197.79	+9.8898	+9.8892	-0.006	PASS

FINAL TEST RESULTS

Parameter	Measured Value*	Specification	Status
Supply Current	16.0 mA	< 30 mA	PASS
Linearity/Conformity	0.008 %	+/-.035 %	PASS
Accuracy	0.025 %	+/-.1 %	PASS
100kHz Output Noise	111 uVrms	< 1000 uVrms	PASS
30Hz Attenuation	57 dB	57 +/- 6 dB	PASS
120VAC Withstand			PASS
Hi-Pot			PASS

Packing Check List

Module Appearance: V
Mounting Screw: V
Pins Straight: V
Module Header: V
Tested by: JY.
QC: QA 10

It is hereby certified that the above product is in conformance with all requirements to the extent specified. This product is not authorized or warranted for use in life support devices and/or systems.

* NIST traceable calibration certificates support Measured Value data. Calibration services are available through ANSI/NCSL Z540-1 and ISO Guide 25 Certified Metrology Labs.

O M E G A D Y N E I N C.
An Affiliate of Omega Engineering, Inc.

LOAD CELL
FINAL CALIBRATION

0.00 - 100.00 LBS
Excitation 10.000 Vdc

Job: MLS6234 Serial: 208927
Model: LC304-100 Tested By: AH
Date: 11/12/2014 Temperature Range: +60 to +160 F
Calibrated: 0.00 - 100.00 LBS Specfile: LC304

Force LBS	Unit Data mVdc	Normalized Data
0.00	0.030	0.000
50.00	8.927	8.897
100.00	17.849	17.819
50.00	8.981	8.951
0.00	0.032	0.002

Balance	0.030	mVdc
Sensitivity	17.819	mVdc
In Resist	376.60	Ohms
Out Resist	351.90	Ohms

Calibration Factors:
Sensitivity = 1.782 mV/V

ELECTRICAL LEAKAGE: PASS
ELECTRICAL WIRING/CONNECTOR: RED = +INPUT (EXC)
BLACK = -INPUT (EXC)
GREEN = +OUTPUT
WHITE = -OUTPUT

This Calibration was performed using Instruments and Standards that are traceable to the United States National Institute of Standards Technology.

S/N	Description	Range	Reference	Cal Cert
Station 3	100lb Dead-Weights	0 - 100.00 LBS	C-2691	C-2691
N/A	Data from Panel Mete	Unit Under Test	N/A	N/A

Q.A. Representative :_____ Date: _____

This transducer is tested to & meets published specifications. After final calibration our products are stored in a controlled stock room & considered in bonded storage. Depending on environment & severity of use factory calibration is recommended every one to three years after initial service installation date.
COMMENTS: FINAL.

Omegadyne Inc., 149 Stelzer Court, Sunbury, OH 43074 (740) 965-9340
http://www.omegadyne.com email: info@omegadyne.com (800) USA-DYNE

Appendix C

Uncertainty Analysis

Condensate Capacity Test with Uncertainty Analysis

General Data

1. Trial no. 1 PT1=9.50 psig, RTD1=112.76 °C, VP1=100.00 % 2. Test date Feb. 25, 2015 @ 10:23 AM
3. Manufacturer's name Johnson Controls Incorporated
4. Type of trap/actuator VG1245BN/M9106-GGC-2
5. Serial no. T250F RY21430 6. Size 3/4, in.
7. Tested by C. Mercer 8. Calculation by C. Mercer
9. Scales description LC304-100 (serial 208927) NIST calibrated reference & certification - 2691

Test Data		Observed Value
10. Pressure at steam trap inlet, PT1, start	psig	9.57
11. Pressure at steam trap outlet, PT2, start	psig	7.84
12. Saturation temperature at PT1, start	◦F	238.47
13. Temperature of condensate, RTD1, start	◦F	235.28
14. Temperature difference, saturation temperature & RTD1, start	◦F	3.19
15. Mass of condensate plus barrel, start	lbm	52.98
16. Pressure at steam trap inlet, finish	psig	9.40
17. Pressure at steam trap outlet, finish	psig	7.66
18. Saturation temperature at PT1, finish	◦F	238.04
19. Temperature of condensate, finish	◦F	235.10
20. Temperature difference, saturation temperature & RTD1, finish	◦F	2.94
21. Mass of condensate plus barrel, finish	lbm	89.25
22. Time interval	sec	33.94

Capacity and General Calculations

23. Average differential pressure	psig	1.73
24. Average subcooling	◦F	3.07
25. Capacity	lbm/hr	3847.40
26. Average inlet pressure	psig	9.48
27. Average condensate temperature	◦F	235.19

Uncertainty Calculations

28. Mass measurement sensitivity		106.07
29. Mass measurement uncertainty		0.3556
30. Mass measurement contribution (Term 1)		1422.50
31. Time interval sensitivity		113.36
32. Time interval uncertainty		0.0339
33. Time interval contribution (Term 2)		14.80
34. Inlet pressure sensitivity		576.43
35. Inlet pressure measurement uncertainty		0.0948
36. Inlet pressure contribution (Term 3)		2987.14
37. Subcooling sensitivity		-308.56
38. Subcooling measurement uncertainty		0.2513
39. Subcooling contribution (Term 4)		6010.67
40. Summation of terms		10435.11
41. Overall uncertainty	lbm/hr	102.15
42. Relative overall uncertainty	%	2.66

Condensate Capacity Test with Uncertainty Analysis

General Data

1. Trial no. 2 PT1=9.18 psig, RTD1=90.00 °C, VP1=25.00 % 2. Test date Feb. 25, 2015 @ 11:12 AM
3. Manufacturer's name Johnson Controls Incorporated
4. Type of trap/actuator VG1245BN/M9106-GGC-2
5. Serial no. T250F RY21430 6. Size 3/4, in.
7. Tested by C. Mercer 8. Calculation by C. Mercer
9. Scales description LC304-100 (serial 208927) NIST calibrated reference & certification - 2691

Test Data		Observed Value
10. Pressure at steam trap inlet, PT1, start	psig	9.18
11. Pressure at steam trap outlet, PT2, start	psig	0.13
12. Saturation temperature at PT1, start	◦F	237.55
13. Temperature of condensate, RTD1, start	◦F	188.91
14. Temperature difference, saturation temperature & RTD1, start	◦F	48.64
15. Mass of condensate plus barrel, start	lbm	51.18
16. Pressure at steam trap inlet, finish	psig	9.18
17. Pressure at steam trap outlet, finish	psig	0.07
18. Saturation temperature at PT1, finish	◦F	237.55
19. Temperature of condensate, finish	◦F	192.57
20. Temperature difference, saturation temperature & RTD1, finish	◦F	44.98
21. Mass of condensate plus barrel, finish	lbm	55.28
22. Time interval	sec	38.30

Capacity and General Calculations

23. Average differential pressure	psig	9.08
24. Average subcooling	◦F	46.81
25. Capacity	lbm/hr	385.03
26. Average inlet pressure	psig	9.18
27. Average condensate temperature	◦F	235.19

Uncertainty Calculations

28. Mass measurement sensitivity		94.00
29. Mass measurement uncertainty		0.2661
30. Mass measurement contribution (Term 1)		625.84
31. Time interval sensitivity		10.05
32. Time interval uncertainty		0.0383
33. Time interval contribution (Term 2)		0.15
34. Inlet pressure sensitivity		-15.85
35. Inlet pressure measurement uncertainty		0.0918
36. Inlet pressure contribution (Term 3)		2.12
37. Subcooling sensitivity		-20.68
38. Subcooling measurement uncertainty		0.2500
39. Subcooling contribution (Term 4)		26.73
40. Summation of terms		654.83
41. Overall uncertainty	lbm/hr	25.59
42. Relative overall uncertainty	%	6.65

Condensate Capacity Test with Uncertainty Analysis

General Data

1. Trial no. 3 PT1=14.50 psig, RTD1=97.61 °C, VP1=74.88 % 2. Test date Feb. 25, 2015 @ 1:11 PM
3. Manufacturer's name Johnson Controls Incorporated
4. Type of trap/actuator VG1245BN/M9106-GGC-2
5. Serial no. T250F RY21430 6. Size 3/4, in.
7. Tested by C. Mercer 8. Calculation by C. Mercer
9. Scales description LC304-100 (serial 208927) NIST calibrated reference & certification - 2691

Test Data		Observed Value
10. Pressure at steam trap inlet, PT1, start	psig	14.31
11. Pressure at steam trap outlet, PT2, start	psig	3.67
12. Saturation temperature at PT1, start	◦F	248.44
13. Temperature of condensate, RTD1, start	◦F	207.60
14. Temperature difference, saturation temperature & RTD1, start	◦F	40.83
15. Mass of condensate plus barrel, start	lbm	111.26
16. Pressure at steam trap inlet, finish	psig	14.42
17. Pressure at steam trap outlet, finish	psig	3.11
18. Saturation temperature at PT1, finish	◦F	248.64
19. Temperature of condensate, finish	◦F	207.42
20. Temperature difference, saturation temperature & RTD1, finish	◦F	41.22
21. Mass of condensate plus barrel, finish	lbm	141.47
22. Time interval	sec	9.08

Capacity and General Calculations

23. Average differential pressure	psig	10.97
24. Average subcooling	◦F	41.02
25. Capacity	lbm/hr	11985.00
26. Average inlet pressure	psig	14.36
27. Average condensate temperature	◦F	235.19

Uncertainty Calculations

28. Mass measurement sensitivity		396.69
29. Mass measurement uncertainty		0.6318
30. Mass measurement contribution (Term 1)		62821.00
31. Time interval sensitivity		1320.70
32. Time interval uncertainty		0.0091
33. Time interval contribution (Term 2)		143.65
34. Inlet pressure sensitivity		832.49
35. Inlet pressure measurement uncertainty		0.1436
36. Inlet pressure contribution (Term 3)		14298.97
37. Subcooling sensitivity		-42.61
38. Subcooling measurement uncertainty		0.2508
39. Subcooling contribution (Term 4)		114.16
40. Summation of terms		77377.78
41. Overall uncertainty	lbm/hr	278.17
42. Relative overall uncertainty	%	2.32

Condensate Capacity Test with Uncertainty Analysis

General Data

1. Trial no. 4 PT1=9.18 psig, RTD1=90.00 °C, VP1=25.00 % 2. Test date Feb. 25, 2015 @ 2:23 PM
3. Manufacturer's name Johnson Controls Incorporated
4. Type of trap/actuator VG1245BN/M9106-GGC-2
5. Serial no. T250F RY21430 6. Size 3/4, in.
7. Tested by C. Mercer 8. Calculation by C. Mercer
9. Scales description LC304-100 (serial 208927) NIST calibrated reference & certification - 2691

Test Data		Observed Value
10. Pressure at steam trap inlet, PT1, start	psig	9.12
11. Pressure at steam trap outlet, PT2, start	psig	0.08
12. Saturation temperature at PT1, start	◦F	237.42
13. Temperature of condensate, RTD1, start	◦F	189.64
14. Temperature difference, saturation temperature & RTD1, start	◦F	47.78
15. Mass of condensate plus barrel, start	lbm	44.25
16. Pressure at steam trap inlet, finish	psig	9.12
17. Pressure at steam trap outlet, finish	psig	0.09
18. Saturation temperature at PT1, finish	◦F	237.40
19. Temperature of condensate, finish	◦F	192.57
20. Temperature difference, saturation temperature & RTD1, finish	◦F	44.83
21. Mass of condensate plus barrel, finish	lbm	48.65
22. Time interval	sec	39.56

Capacity and General Calculations

23. Average differential pressure	psig	9.04
24. Average subcooling	◦F	46.30
25. Capacity	lbm/hr	401.05
26. Average inlet pressure	psig	9.12
27. Average condensate temperature	◦F	191.11

Uncertainty Calculations

28. Mass measurement sensitivity		91.01
29. Mass measurement uncertainty		0.2323
30. Mass measurement contribution (Term 1)		446.73
31. Time interval sensitivity		10.14
32. Time interval uncertainty		0.0396
33. Time interval contribution (Term 2)		0.16
34. Inlet pressure sensitivity		-15.18
35. Inlet pressure measurement uncertainty		0.0912
36. Inlet pressure contribution (Term 3)		1.92
37. Subcooling sensitivity		-20.08
38. Subcooling measurement uncertainty		0.2511
39. Subcooling contribution (Term 4)		25.42
40. Summation of terms		474.22
41. Overall uncertainty	lbm/hr	21.78
42. Relative overall uncertainty	%	5.43

Condensate Capacity Test with Uncertainty Analysis

General Data

1. Trial no. 5 PT1=0.50 psig, RTD1=92.01 °C, VP1=53.50 % 2. Test date Feb. 25, 2015 @ 2:35 PM
3. Manufacturer's name Johnson Controls Incorporated
4. Type of trap/actuator VG1245BN/M9106-GGC-2
5. Serial no. T250F RY21430 6. Size 3/4, in.
7. Tested by C. Mercer 8. Calculation by C. Mercer
9. Scales description LC304-100 (serial 208927) NIST calibrated reference & certification - 2691

Test Data		Observed Value
10. Pressure at steam trap inlet, PT1, start	psig	0.49
11. Pressure at steam trap outlet, PT2, start	psig	0.12
12. Saturation temperature at PT1, start	◦F	213.66
13. Temperature of condensate, RTD1, start	◦F	196.42
14. Temperature difference, saturation temperature & RTD1, start	◦F	17.23
15. Mass of condensate plus barrel, start	lbm	50.03
16. Pressure at steam trap inlet, finish	psig	0.48
17. Pressure at steam trap outlet, finish	psig	0.07
18. Saturation temperature at PT1, finish	◦F	213.62
19. Temperature of condensate, finish	◦F	197.16
20. Temperature difference, saturation temperature & RTD1, finish	◦F	16.46
21. Mass of condensate plus barrel, finish	lbm	58.87
22. Time interval	sec	40.93

Capacity and General Calculations

23. Average differential pressure	psig	0.39
24. Average subcooling	◦F	16.85
25. Capacity	lbm/hr	776.83
26. Average inlet pressure	psig	0.48
27. Average condensate temperature	◦F	196.79

Uncertainty Calculations

28. Mass measurement sensitivity		87.95
29. Mass measurement uncertainty		0.2722
30. Mass measurement contribution (Term 1)		573.32
31. Time interval sensitivity		18.98
32. Time interval uncertainty		0.0409
33. Time interval contribution (Term 2)		0.60
34. Inlet pressure sensitivity		437.56
35. Inlet pressure measurement uncertainty		0.0048
36. Inlet pressure contribution (Term 3)		4.46
37. Subcooling sensitivity		-5.47
38. Subcooling measurement uncertainty		0.2523
39. Subcooling contribution (Term 4)		1.90
40. Summation of terms		580.29
41. Overall uncertainty	lbm/hr	24.09
42. Relative overall uncertainty	%	3.10

Condensate Capacity Test with Uncertainty Analysis

General Data

1. Trial no. 6 PT1=0.50 psig, RTD1=92.01 °C, VP1=53.50 % 2. Test date Feb. 25, 2015 @ 2:38 PM
3. Manufacturer's name Johnson Controls Incorporated
4. Type of trap/actuator VG1245BN/M9106-GGC-2
5. Serial no. T250F RY21430 6. Size 3/4, in.
7. Tested by C. Mercer 8. Calculation by C. Mercer
9. Scales description LC304-100 (serial 208927) NIST calibrated reference & certification - 2691

Test Data		Observed Value
10. Pressure at steam trap inlet, PT1, start	psig	0.49
11. Pressure at steam trap outlet, PT2, start	psig	0.18
12. Saturation temperature at PT1, start	◦F	213.66
13. Temperature of condensate, RTD1, start	◦F	196.61
14. Temperature difference, saturation temperature & RTD1, start	◦F	17.05
15. Mass of condensate plus barrel, start	lbm	63.38
16. Pressure at steam trap inlet, finish	psig	0.51
17. Pressure at steam trap outlet, finish	psig	0.15
18. Saturation temperature at PT1, finish	◦F	213.62
19. Temperature of condensate, finish	◦F	197.16
20. Temperature difference, saturation temperature & RTD1, finish	◦F	16.46
21. Mass of condensate plus barrel, finish	lbm	70.38
22. Time interval	sec	36.48

Capacity and General Calculations

23. Average differential pressure	psig	0.34
24. Average subcooling	◦F	16.75
25. Capacity	lbm/hr	690.88
26. Average inlet pressure	psig	0.50
27. Average condensate temperature	◦F	196.89

Uncertainty Calculations

28. Mass measurement sensitivity		98.69
29. Mass measurement uncertainty		0.3344
30. Mass measurement contribution (Term 1)		1089.00
31. Time interval sensitivity		18.94
32. Time interval uncertainty		0.0365
33. Time interval contribution (Term 2)		0.48
34. Inlet pressure sensitivity		438.32
35. Inlet pressure measurement uncertainty		0.0050
36. Inlet pressure contribution (Term 3)		4.84
37. Subcooling sensitivity		-5.48
38. Subcooling measurement uncertainty		0.2512
39. Subcooling contribution (Term 4)		1.90
40. Summation of terms		1096.22
41. Overall uncertainty	lbm/hr	33.11
42. Relative overall uncertainty	%	4.79

Condensate Capacity Test with Uncertainty Analysis

General Data

1. Trial no. 7 PT1=14.50 psig, RTD1=97.61 °C, VP1=74.88 % 2. Test date Feb. 25, 2015 @ 4:29 PM
3. Manufacturer's name Johnson Controls Incorporated
4. Type of trap/actuator VG1245BN/M9106-GGC-2
5. Serial no. T250F RY21430 6. Size 3/4, in.
7. Tested by C. Mercer 8. Calculation by C. Mercer
9. Scales description LC304-100 (serial 208927) NIST calibrated reference & certification - 2691

Test Data		Observed Value
10. Pressure at steam trap inlet, PT1, start	psig	14.57
11. Pressure at steam trap outlet, PT2, start	psig	3.93
12. Saturation temperature at PT1, start	◦F	248.94
13. Temperature of condensate, RTD1, start	◦F	207.60
14. Temperature difference, saturation temperature & RTD1, start	◦F	41.34
15. Mass of condensate plus barrel, start	lbm	107.93
16. Pressure at steam trap inlet, finish	psig	14.24
17. Pressure at steam trap outlet, finish	psig	4.12
18. Saturation temperature at PT1, finish	◦F	248.29
19. Temperature of condensate, finish	◦F	207.42
20. Temperature difference, saturation temperature & RTD1, finish	◦F	40.87
21. Mass of condensate plus barrel, finish	lbm	145.43
22. Time interval	sec	11.90

Capacity and General Calculations

23. Average differential pressure	psig	10.39
24. Average subcooling	◦F	41.11
25. Capacity	lbm/hr	11340.00
26. Average inlet pressure	psig	14.41
27. Average condensate temperature	◦F	207.51

Uncertainty Calculations

28. Mass measurement sensitivity		302.44
29. Mass measurement uncertainty		0.6334
30. Mass measurement contribution (Term 1)		36698.00
31. Time interval sensitivity		952.70
32. Time interval uncertainty		0.0119
33. Time interval contribution (Term 2)		128.60
34. Inlet pressure sensitivity		836.77
35. Inlet pressure measurement uncertainty		0.1441
36. Inlet pressure contribution (Term 3)		14531.05
37. Subcooling sensitivity		-42.61
38. Subcooling measurement uncertainty		0.2508
39. Subcooling contribution (Term 4)		114.17
40. Summation of terms		51471.82
41. Overall uncertainty	lbm/hr	226.87
42. Relative overall uncertainty	%	2.00

Condensate Capacity Test with Uncertainty Analysis

General Data

1. Trial no. 8 PT1=4.57 psig, RTD1=106.60 °C, VP1=25.00 % 2. Test date Feb. 26, 2015 @ 9:05 AM
3. Manufacturer's name Johnson Controls Incorporated
4. Type of trap/actuator VG1245BN/M9106-GGC-2
5. Serial no. T250F RY21430 6. Size 3/4, in.
7. Tested by C. Mercer 8. Calculation by C. Mercer
9. Scales description LC304-100 (serial 208927) NIST calibrated reference & certification - 2691

Test Data		Observed Value
10. Pressure at steam trap inlet, PT1, start	psig	4.61
11. Pressure at steam trap outlet, PT2, start	psig	0.07
12. Saturation temperature at PT1, start	◦F	226.09
13. Temperature of condensate, RTD1, start	◦F	221.35
14. Temperature difference, saturation temperature & RTD1, start	◦F	4.73
15. Mass of condensate plus barrel, start	lbm	37.62
16. Pressure at steam trap inlet, finish	psig	4.52
17. Pressure at steam trap outlet, finish	psig	0.08
18. Saturation temperature at PT1, finish	◦F	225.86
19. Temperature of condensate, finish	◦F	221.17
20. Temperature difference, saturation temperature & RTD1, finish	◦F	4.69
21. Mass of condensate plus barrel, finish	lbm	40.33
22. Time interval	sec	39.91

Capacity and General Calculations

23. Average differential pressure	psig	4.49
24. Average subcooling	◦F	4.71
25. Capacity	lbm/hr	244.71
26. Average inlet pressure	psig	4.56
27. Average condensate temperature	◦F	221.26

Uncertainty Calculations

28. Mass measurement sensitivity		90.21
29. Mass measurement uncertainty		0.1949
30. Mass measurement contribution (Term 1)		309.10
31. Time interval sensitivity		6.13
32. Time interval uncertainty		0.0399
33. Time interval contribution (Term 2)		0.06
34. Inlet pressure sensitivity		40.22
35. Inlet pressure measurement uncertainty		0.0456
36. Inlet pressure contribution (Term 3)		3.37
37. Subcooling sensitivity		-5.55
38. Subcooling measurement uncertainty		0.2515
39. Subcooling contribution (Term 4)		1.95
40. Summation of terms		314.48
41. Overall uncertainty	lbm/hr	17.73
42. Relative overall uncertainty	%	7.25

Condensate Capacity Test with Uncertainty Analysis

General Data

1. Trial no. 9 PT1=14.50 psig, RTD1=90.00 °C, VP1=100.00 % 2. Test date Feb. 26, 2015 @ 11:09 AM
3. Manufacturer's name Johnson Controls Incorporated
4. Type of trap/actuator VG1245BN/M9106-GGC-2
5. Serial no. T250F RY21430 6. Size 3/4, in.
7. Tested by C. Mercer 8. Calculation by C. Mercer
9. Scales description LC304-100 (serial 208927) NIST calibrated reference & certification - 2691

Test Data		Observed Value
10. Pressure at steam trap inlet, PT1, start	psig	14.38
11. Pressure at steam trap outlet, PT2, start	psig	6.99
12. Saturation temperature at PT1, start	◦F	248.57
13. Temperature of condensate, RTD1, start	◦F	194.04
14. Temperature difference, saturation temperature & RTD1, start	◦F	54.53
15. Mass of condensate plus barrel, start	lbm	103.62
16. Pressure at steam trap inlet, finish	psig	14.38
17. Pressure at steam trap outlet, finish	psig	7.09
18. Saturation temperature at PT1, finish	◦F	248.56
19. Temperature of condensate, finish	◦F	193.86
20. Temperature difference, saturation temperature & RTD1, finish	◦F	54.70
21. Mass of condensate plus barrel, finish	lbm	146.73
22. Time interval	sec	10.54

Capacity and General Calculations

23. Average differential pressure	psig	7.34
24. Average subcooling	◦F	54.62
25. Capacity	lbm/hr	14728.00
26. Average inlet pressure	psig	14.38
27. Average condensate temperature	◦F	193.95

Uncertainty Calculations

28. Mass measurement sensitivity		341.62
29. Mass measurement uncertainty		0.6259
30. Mass measurement contribution (Term 1)		45714.00
31. Time interval sensitivity		1397.60
32. Time interval uncertainty		0.0105
33. Time interval contribution (Term 2)		216.91
34. Inlet pressure sensitivity		993.99
35. Inlet pressure measurement uncertainty		0.1438
36. Inlet pressure contribution (Term 3)		20427.59
37. Subcooling sensitivity		15.52
38. Subcooling measurement uncertainty		0.2510
39. Subcooling contribution (Term 4)		15.17
40. Summation of terms		66373.67
41. Overall uncertainty	lbm/hr	257.63
42. Relative overall uncertainty	%	1.75

Condensate Capacity Test with Uncertainty Analysis

General Data

1. Trial no. 10 PT1=3.84 psig, RTD1=105.60 °C, VP1=79.38 % 2. Test date Feb. 26, 2015 @ 1:04 PM
3. Manufacturer's name Johnson Controls Incorporated
4. Type of trap/actuator VG1245BN/M9106-GGC-2
5. Serial no. T250F RY21430 6. Size 3/4, in.
7. Tested by C. Mercer 8. Calculation by C. Mercer
9. Scales description LC304-100 (serial 208927) NIST calibrated reference & certification - 2691

Test Data		Observed Value
10. Pressure at steam trap inlet, PT1, start	psig	3.90
11. Pressure at steam trap outlet, PT2, start	psig	2.36
12. Saturation temperature at PT1, start	◦F	224.12
13. Temperature of condensate, RTD1, start	◦F	218.79
14. Temperature difference, saturation temperature & RTD1, start	◦F	5.33
15. Mass of condensate plus barrel, start	lbm	86.10
16. Pressure at steam trap inlet, finish	psig	3.89
17. Pressure at steam trap outlet, finish	psig	2.27
18. Saturation temperature at PT1, finish	◦F	224.10
19. Temperature of condensate, finish	◦F	218.97
20. Temperature difference, saturation temperature & RTD1, finish	◦F	5.14
21. Mass of condensate plus barrel, finish	lbm	140.73
22. Time interval	sec	47.91

Capacity and General Calculations

23. Average differential pressure	psig	1.59
24. Average subcooling	◦F	5.23
25. Capacity	lbm/hr	4105.10
26. Average inlet pressure	psig	3.90
27. Average condensate temperature	◦F	218.88

Uncertainty Calculations

28. Mass measurement sensitivity		75.15
29. Mass measurement uncertainty		0.5671
30. Mass measurement contribution (Term 1)		1815.90
31. Time interval sensitivity		85.69
32. Time interval uncertainty		0.0479
33. Time interval contribution (Term 2)		16.85
34. Inlet pressure sensitivity		681.53
35. Inlet pressure measurement uncertainty		0.0390
36. Inlet pressure contribution (Term 3)		705.54
37. Subcooling sensitivity		-119.40
38. Subcooling measurement uncertainty		0.2515
39. Subcooling contribution (Term 4)		901.50
40. Summation of terms		3439.80
41. Overall uncertainty	lbm/hr	58.65
42. Relative overall uncertainty	%	1.43

Condensate Capacity Test with Uncertainty Analysis

General Data

1. Trial no. 11 PT1=11.63 psig, RTD1=96.68 °C, VP1=48.63 % 2. Test date Feb. 26, 2015 @ 1:56 PM
3. Manufacturer's name Johnson Controls Incorporated
4. Type of trap/actuator VG1245BN/M9106-GGC-2
5. Serial no. T250F RY21430 6. Size 3/4, in.
7. Tested by C. Mercer 8. Calculation by C. Mercer
9. Scales description LC304-100 (serial 208927) NIST calibrated reference & certification - 2691

Test Data		Observed Value
10. Pressure at steam trap inlet, PT1, start	psig	11.66
11. Pressure at steam trap outlet, PT2, start	psig	0.00
12. Saturation temperature at PT1, start	◦F	243.02
13. Temperature of condensate, RTD1, start	◦F	205.95
14. Temperature difference, saturation temperature & RTD1, start	◦F	37.07
15. Mass of condensate plus barrel, start	lbm	103.48
16. Pressure at steam trap inlet, finish	psig	11.94
17. Pressure at steam trap outlet, finish	psig	0.00
18. Saturation temperature at PT1, finish	◦F	243.62
19. Temperature of condensate, finish	◦F	206.87
20. Temperature difference, saturation temperature & RTD1, finish	◦F	36.75
21. Mass of condensate plus barrel, finish	lbm	136.30
22. Time interval	sec	31.80

Capacity and General Calculations

23. Average differential pressure	psig	11.80
24. Average subcooling	◦F	36.91
25. Capacity	lbm/hr	3716.40
26. Average inlet pressure	psig	11.80
27. Average condensate temperature	◦F	206.41

Uncertainty Calculations

28. Mass measurement sensitivity		113.22
29. Mass measurement uncertainty		0.5995
30. Mass measurement contribution (Term 1)		4606.10
31. Time interval sensitivity		116.88
32. Time interval uncertainty		0.0318
33. Time interval contribution (Term 2)		13.81
34. Inlet pressure sensitivity		230.73
35. Inlet pressure measurement uncertainty		0.1180
36. Inlet pressure contribution (Term 3)		741.11
37. Subcooling sensitivity		-21.11
38. Subcooling measurement uncertainty		0.2509
39. Subcooling contribution (Term 4)		28.06
40. Summation of terms		5389.09
41. Overall uncertainty	lbm/hr	73.41
42. Relative overall uncertainty	%	1.98

Condensate Capacity Test with Uncertainty Analysis

General Data

1. Trial no. 12 PT1=14.50 psig, RTD1=109.94 °C, VP1=100.00 % 2. Test date Feb. 27, 2015 @ 10:06 AM
3. Manufacturer's name Johnson Controls Incorporated
4. Type of trap/actuator VG1245BN/M9106-GGC-2
5. Serial no. T250F RY21430 6. Size 3/4, in.
7. Tested by C. Mercer 8. Calculation by C. Mercer
9. Scales description LC304-100 (serial 208927) NIST calibrated reference & certification - 2691

Test Data		Observed Value
10. Pressure at steam trap inlet, PT1, start	psig	14.49
11. Pressure at steam trap outlet, PT2, start	psig	9.99
12. Saturation temperature at PT1, start	◦F	248.79
13. Temperature of condensate, RTD1, start	◦F	229.97
14. Temperature difference, saturation temperature & RTD1, start	◦F	18.82
15. Mass of condensate plus barrel, start	lbm	88.15
16. Pressure at steam trap inlet, finish	psig	14.31
17. Pressure at steam trap outlet, finish	psig	9.90
18. Saturation temperature at PT1, finish	◦F	248.43
19. Temperature of condensate, finish	◦F	229.78
20. Temperature difference, saturation temperature & RTD1, finish	◦F	18.64
21. Mass of condensate plus barrel, finish	lbm	124.61
22. Time interval	sec	12.05

Capacity and General Calculations

23. Average differential pressure	psig	4.46
24. Average subcooling	◦F	18.73
25. Capacity	lbm/hr	10896.00
26. Average inlet pressure	psig	14.40
27. Average condensate temperature	◦F	229.88

Uncertainty Calculations

28. Mass measurement sensitivity		298.88
29. Mass measurement uncertainty		0.5319
30. Mass measurement contribution (Term 1)		25272.00
31. Time interval sensitivity		904.64
32. Time interval uncertainty		0.0120
33. Time interval contribution (Term 2)		118.73
34. Inlet pressure sensitivity		1050.10
35. Inlet pressure measurement uncertainty		0.1440
36. Inlet pressure contribution (Term 3)		22868.97
37. Subcooling sensitivity		-343.81
38. Subcooling measurement uncertainty		0.2508
39. Subcooling contribution (Term 4)		7432.99
40. Summation of terms		55692.69
41. Overall uncertainty	lbm/hr	235.99
42. Relative overall uncertainty	%	2.17

Condensate Capacity Test with Uncertainty Analysis

General Data

1. Trial no. 13 PT1=5.12 psig, RTD1=97.92 °C, VP1=43.00 % 2. Test date Feb. 27, 2015 @ 11:04 AM
3. Manufacturer's name Johnson Controls Incorporated
4. Type of trap/actuator VG1245BN/M9106-GGC-2
5. Serial no. T250F RY21430 6. Size 3/4, in.
7. Tested by C. Mercer 8. Calculation by C. Mercer
9. Scales description LC304-100 (serial 208927) NIST calibrated reference & certification - 2691

Test Data		Observed Value
10. Pressure at steam trap inlet, PT1, start	psig	5.23
11. Pressure at steam trap outlet, PT2, start	psig	0.03
12. Saturation temperature at PT1, start	◦F	227.78
13. Temperature of condensate, RTD1, start	◦F	205.77
14. Temperature difference, saturation temperature & RTD1, start	◦F	22.01
15. Mass of condensate plus barrel, start	lbm	37.03
16. Pressure at steam trap inlet, finish	psig	5.11
17. Pressure at steam trap outlet, finish	psig	0.00
18. Saturation temperature at PT1, finish	◦F	227.44
19. Temperature of condensate, finish	◦F	208.15
20. Temperature difference, saturation temperature & RTD1, finish	◦F	19.29
21. Mass of condensate plus barrel, finish	lbm	52.02
22. Time interval	sec	33.61

Capacity and General Calculations

23. Average differential pressure	psig	5.15
24. Average subcooling	◦F	20.65
25. Capacity	lbm/hr	1605.10
26. Average inlet pressure	psig	5.17
27. Average condensate temperature	◦F	206.96

Uncertainty Calculations

28. Mass measurement sensitivity		107.11
29. Mass measurement uncertainty		0.2226
30. Mass measurement contribution (Term 1)		568.59
31. Time interval sensitivity		47.76
32. Time interval uncertainty		0.0336
33. Time interval contribution (Term 2)		2.58
34. Inlet pressure sensitivity		215.41
35. Inlet pressure measurement uncertainty		0.0517
36. Inlet pressure contribution (Term 3)		124.06
37. Subcooling sensitivity		-18.15
38. Subcooling measurement uncertainty		0.2514
39. Subcooling contribution (Term 4)		20.82
40. Summation of terms		716.05
41. Overall uncertainty	lbm/hr	26.76
42. Relative overall uncertainty	%	1.67

Condensate Capacity Test with Uncertainty Analysis

General Data

1. Trial no. 14 PT1=11.00 psig, RTD1=90.00 °C, VP1=74.50 % 2. Test date Feb. 27, 2015 @ 11:18 AM
3. Manufacturer's name Johnson Controls Incorporated
4. Type of trap/actuator VG1245BN/M9106-GGC-2
5. Serial no. T250F RY21430 6. Size 3/4, in.
7. Tested by C. Mercer 8. Calculation by C. Mercer
9. Scales description LC304-100 (serial 208927) NIST calibrated reference & certification - 2691

Test Data		Observed Value
10. Pressure at steam trap inlet, PT1, start	psig	10.86
11. Pressure at steam trap outlet, PT2, start	psig	0.90
12. Saturation temperature at PT1, start	◦F	241.30
13. Temperature of condensate, RTD1, start	◦F	194.77
14. Temperature difference, saturation temperature & RTD1, start	◦F	46.53
15. Mass of condensate plus barrel, start	lbm	87.32
16. Pressure at steam trap inlet, finish	psig	11.08
17. Pressure at steam trap outlet, finish	psig	0.79
18. Saturation temperature at PT1, finish	◦F	241.78
19. Temperature of condensate, finish	◦F	194.59
20. Temperature difference, saturation temperature & RTD1, finish	◦F	47.19
21. Mass of condensate plus barrel, finish	lbm	145.02
22. Time interval	sec	19.11

Capacity and General Calculations

23. Average differential pressure	psig	10.12
24. Average subcooling	◦F	46.86
25. Capacity	lbm/hr	10869.00
26. Average inlet pressure	psig	10.97
27. Average condensate temperature	◦F	194.68

Uncertainty Calculations

28. Mass measurement sensitivity		188.35
29. Mass measurement uncertainty		0.5808
30. Mass measurement contribution (Term 1)		11969.00
31. Time interval sensitivity		568.66
32. Time interval uncertainty		0.0191
33. Time interval contribution (Term 2)		118.13
34. Inlet pressure sensitivity		586.98
35. Inlet pressure measurement uncertainty		0.1097
36. Inlet pressure contribution (Term 3)		4144.75
37. Subcooling sensitivity		-7.09
38. Subcooling measurement uncertainty		0.2509
39. Subcooling contribution (Term 4)		3.17
40. Summation of terms		16235.05
41. Overall uncertainty	lbm/hr	127.42
42. Relative overall uncertainty	%	1.17

Condensate Capacity Test with Uncertainty Analysis

General Data

1. Trial no. 15 PT1=0.50 psig, RTD1=90.00 °C, VP1=99.25 % 2. Test date Feb. 27, 2015 @ 12:23 PM
3. Manufacturer's name Johnson Controls Incorporated
4. Type of trap/actuator VG1245BN/M9106-GGC-2
5. Serial no. T250F RY21430 6. Size 3/4, in.
7. Tested by C. Mercer 8. Calculation by C. Mercer
9. Scales description LC304-100 (serial 208927) NIST calibrated reference & certification - 2691

Test Data		Observed Value
10. Pressure at steam trap inlet, PT1, start	psig	0.51
11. Pressure at steam trap outlet, PT2, start	psig	0.00
12. Saturation temperature at PT1, start	◦F	213.73
13. Temperature of condensate, RTD1, start	◦F	190.92
14. Temperature difference, saturation temperature & RTD1, start	◦F	22.80
15. Mass of condensate plus barrel, start	lbm	46.09
16. Pressure at steam trap inlet, finish	psig	0.41
17. Pressure at steam trap outlet, finish	psig	0.00
18. Saturation temperature at PT1, finish	◦F	213.39
19. Temperature of condensate, finish	◦F	193.86
20. Temperature difference, saturation temperature & RTD1, finish	◦F	19.54
21. Mass of condensate plus barrel, finish	lbm	99.44
22. Time interval	sec	50.75

Capacity and General Calculations

23. Average differential pressure	psig	0.46
24. Average subcooling	◦F	21.17
25. Capacity	lbm/hr	3783.90
26. Average inlet pressure	psig	0.46
27. Average condensate temperature	◦F	192.39

Uncertainty Calculations

28. Mass measurement sensitivity		70.93
29. Mass measurement uncertainty		0.3638
30. Mass measurement contribution (Term 1)		665.94
31. Time interval sensitivity		74.55
32. Time interval uncertainty		0.0508
33. Time interval contribution (Term 2)		14.32
34. Inlet pressure sensitivity		974.12
35. Inlet pressure measurement uncertainty		0.0046
36. Inlet pressure contribution (Term 3)		20.11
37. Subcooling sensitivity		23.91
38. Subcooling measurement uncertainty		0.2522
39. Subcooling contribution (Term 4)		36.36
40. Summation of terms		736.72
41. Overall uncertainty	lbm/hr	27.14
42. Relative overall uncertainty	%	0.72

Condensate Capacity Test with Uncertainty Analysis

General Data

1. Trial no. 16 PT1=10.21 psig, RTD1=114.47 °C, VP1=49.00 % 2. Test date Mar. 2, 2015 @ 10:48 AM
3. Manufacturer's name Johnson Controls Incorporated
4. Type of trap/actuator VG1245BN/M9106-GGC-2
5. Serial no. T250F RY21430 6. Size 3/4, in.
7. Tested by C. Mercer 8. Calculation by C. Mercer
9. Scales description LC304-100 (serial 208927) NIST calibrated reference & certification - 2691

Test Data		Observed Value
10. Pressure at steam trap inlet, PT1, start	psig	10.25
11. Pressure at steam trap outlet, PT2, start	psig	3.58
12. Saturation temperature at PT1, start	◦F	239.97
13. Temperature of condensate, RTD1, start	◦F	237.30
14. Temperature difference, saturation temperature & RTD1, start	◦F	2.67
15. Mass of condensate plus barrel, start	lbm	52.18
16. Pressure at steam trap inlet, finish	psig	10.32
17. Pressure at steam trap outlet, finish	psig	3.48
18. Saturation temperature at PT1, finish	◦F	240.13
19. Temperature of condensate, finish	◦F	238.22
20. Temperature difference, saturation temperature & RTD1, finish	◦F	1.91
21. Mass of condensate plus barrel, finish	lbm	72.45
22. Time interval	sec	37.63

Capacity and General Calculations

23. Average differential pressure	psig	6.76
24. Average subcooling	◦F	2.29
25. Capacity	lbm/hr	1938.80
26. Average inlet pressure	psig	10.29
27. Average condensate temperature	◦F	237.76

Uncertainty Calculations

28. Mass measurement sensitivity		95.66
29. Mass measurement uncertainty		0.3116
30. Mass measurement contribution (Term 1)		888.40
31. Time interval sensitivity		51.52
32. Time interval uncertainty		0.0376
33. Time interval contribution (Term 2)		3.76
34. Inlet pressure sensitivity		226.52
35. Inlet pressure measurement uncertainty		0.1029
36. Inlet pressure contribution (Term 3)		543.08
37. Subcooling sensitivity		-92.00
38. Subcooling measurement uncertainty		0.2510
39. Subcooling contribution (Term 4)		533.13
40. Summation of terms		1968.37
41. Overall uncertainty	lbm/hr	44.37
42. Relative overall uncertainty	%	2.29

Condensate Capacity Test with Uncertainty Analysis

General Data

1. Trial no. 17 PT1=10.21 psig, RTD1=114.47 °C, VP1=49.00 % 2. Test date Mar. 2, 2015 @ 10:55 AM
3. Manufacturer's name Johnson Controls Incorporated
4. Type of trap/actuator VG1245BN/M9106-GGC-2
5. Serial no. T250F RY21430 6. Size 3/4, in.
7. Tested by C. Mercer 8. Calculation by C. Mercer
9. Scales description LC304-100 (serial 208927) NIST calibrated reference & certification - 2691

Test Data		Observed Value
10. Pressure at steam trap inlet, PT1, start	psig	10.13
11. Pressure at steam trap outlet, PT2, start	psig	3.64
12. Saturation temperature at PT1, start	◦F	239.70
13. Temperature of condensate, RTD1, start	◦F	236.57
14. Temperature difference, saturation temperature & RTD1, start	◦F	3.14
15. Mass of condensate plus barrel, start	lbm	80.17
16. Pressure at steam trap inlet, finish	psig	10.12
17. Pressure at steam trap outlet, finish	psig	3.48
18. Saturation temperature at PT1, finish	◦F	239.67
19. Temperature of condensate, finish	◦F	237.30
20. Temperature difference, saturation temperature & RTD1, finish	◦F	2.37
21. Mass of condensate plus barrel, finish	lbm	104.75
22. Time interval	sec	42.46

Capacity and General Calculations

23. Average differential pressure	psig	6.57
24. Average subcooling	◦F	2.75
25. Capacity	lbm/hr	2084.30
26. Average inlet pressure	psig	10.13
27. Average condensate temperature	◦F	236.94

Uncertainty Calculations

28. Mass measurement sensitivity		84.78
29. Mass measurement uncertainty		0.4623
30. Mass measurement contribution (Term 1)		1536.30
31. Time interval sensitivity		49.09
32. Time interval uncertainty		0.0425
33. Time interval contribution (Term 2)		4.34
34. Inlet pressure sensitivity		222.39
35. Inlet pressure measurement uncertainty		0.1013
36. Inlet pressure contribution (Term 3)		507.00
37. Subcooling sensitivity		-90.70
38. Subcooling measurement uncertainty		0.2511
39. Subcooling contribution (Term 4)		518.90
40. Summation of terms		2566.54
41. Overall uncertainty	lbm/hr	50.66
42. Relative overall uncertainty	%	2.43

Condensate Capacity Test with Uncertainty Analysis

General Data

1. Trial no. 18 PT1=0.50 psig, RTD1=90.00 °C, VP1=75.63 % 2. Test date Mar. 2, 2015 @ 11:18 AM
3. Manufacturer's name Johnson Controls Incorporated
4. Type of trap/actuator VG1245BN/M9106-GGC-2
5. Serial no. T250F RY21430 6. Size 3/4, in.
7. Tested by C. Mercer 8. Calculation by C. Mercer
9. Scales description LC304-100 (serial 208927) NIST calibrated reference & certification - 2691

Test Data		Observed Value
10. Pressure at steam trap inlet, PT1, start	psig	0.49
11. Pressure at steam trap outlet, PT2, start	psig	0.00
12. Saturation temperature at PT1, start	◦F	213.67
13. Temperature of condensate, RTD1, start	◦F	193.86
14. Temperature difference, saturation temperature & RTD1, start	◦F	19.82
15. Mass of condensate plus barrel, start	lbm	56.48
16. Pressure at steam trap inlet, finish	psig	0.50
17. Pressure at steam trap outlet, finish	psig	0.00
18. Saturation temperature at PT1, finish	◦F	213.71
19. Temperature of condensate, finish	◦F	194.04
20. Temperature difference, saturation temperature & RTD1, finish	◦F	19.67
21. Mass of condensate plus barrel, finish	lbm	78.52
22. Time interval	sec	25.93

Capacity and General Calculations

23. Average differential pressure	psig	0.50
24. Average subcooling	◦F	19.74
25. Capacity	lbm/hr	3061.30
26. Average inlet pressure	psig	0.50
27. Average condensate temperature	◦F	193.95

Uncertainty Calculations

28. Mass measurement sensitivity		138.85
29. Mass measurement uncertainty		0.3375
30. Mass measurement contribution (Term 1)		2195.80
31. Time interval sensitivity		118.07
32. Time interval uncertainty		0.0259
33. Time interval contribution (Term 2)		9.37
34. Inlet pressure sensitivity		870.63
35. Inlet pressure measurement uncertainty		0.0050
36. Inlet pressure contribution (Term 3)		18.84
37. Subcooling sensitivity		3.54
38. Subcooling measurement uncertainty		0.2523
39. Subcooling contribution (Term 4)		0.80
40. Summation of terms		2224.81
41. Overall uncertainty	lbm/hr	47.17
42. Relative overall uncertainty	%	1.54

Condensate Capacity Test with Uncertainty Analysis

General Data

1. Trial no. 19 PT1=0.50 psig, RTD1=99.13 °C, VP1=100.00 % 2. Test date Mar. 2, 2015 @ 12:54 PM
3. Manufacturer's name Johnson Controls Incorporated
4. Type of trap/actuator VG1245BN/M9106-GGC-2
5. Serial no. T250F RY21430 6. Size 3/4, in.
7. Tested by C. Mercer 8. Calculation by C. Mercer
9. Scales description LC304-100 (serial 208927) NIST calibrated reference & certification - 2691

Test Data		Observed Value
10. Pressure at steam trap inlet, PT1, start	psig	0.48
11. Pressure at steam trap outlet, PT2, start	psig	0.07
12. Saturation temperature at PT1, start	◦F	213.62
13. Temperature of condensate, RTD1, start	◦F	210.35
14. Temperature difference, saturation temperature & RTD1, start	◦F	3.27
15. Mass of condensate plus barrel, start	lbm	58.12
16. Pressure at steam trap inlet, finish	psig	0.53
17. Pressure at steam trap outlet, finish	psig	0.06
18. Saturation temperature at PT1, finish	◦F	213.80
19. Temperature of condensate, finish	◦F	210.35
20. Temperature difference, saturation temperature & RTD1, finish	◦F	3.45
21. Mass of condensate plus barrel, finish	lbm	82.36
22. Time interval	sec	27.30

Capacity and General Calculations

23. Average differential pressure	psig	0.44
24. Average subcooling	◦F	3.36
25. Capacity	lbm/hr	3196.10
26. Average inlet pressure	psig	0.51
27. Average condensate temperature	◦F	210.35

Uncertainty Calculations

28. Mass measurement sensitivity		131.86
29. Mass measurement uncertainty		0.3512
30. Mass measurement contribution (Term 1)		2144.60
31. Time interval sensitivity		117.07
32. Time interval uncertainty		0.0273
33. Time interval contribution (Term 2)		10.22
34. Inlet pressure sensitivity		850.63
35. Inlet pressure measurement uncertainty		0.0051
36. Inlet pressure contribution (Term 3)		18.51
37. Subcooling sensitivity		-60.22
38. Subcooling measurement uncertainty		0.2522
39. Subcooling contribution (Term 4)		230.70
40. Summation of terms		2404.02
41. Overall uncertainty	lbm/hr	49.03
42. Relative overall uncertainty	%	1.53

Condensate Capacity Test with Uncertainty Analysis

General Data

1. Trial no. 20 PT1=4.70 psig, RTD1=90.00 °C, VP1=100.00 % 2. Test date Mar. 2, 2015 @ 1:12 PM
3. Manufacturer's name Johnson Controls Incorporated
4. Type of trap/actuator VG1245BN/M9106-GGC-2
5. Serial no. T250F RY21430 6. Size 3/4, in.
7. Tested by C. Mercer 8. Calculation by C. Mercer
9. Scales description LC304-100 (serial 208927) NIST calibrated reference & certification - 2691

Test Data		Observed Value
10. Pressure at steam trap inlet, PT1, start	psig	4.76
11. Pressure at steam trap outlet, PT2, start	psig	2.20
12. Saturation temperature at PT1, start	◦F	226.50
13. Temperature of condensate, RTD1, start	◦F	194.59
14. Temperature difference, saturation temperature & RTD1, start	◦F	31.91
15. Mass of condensate plus barrel, start	lbm	76.36
16. Pressure at steam trap inlet, finish	psig	4.42
17. Pressure at steam trap outlet, finish	psig	2.10
18. Saturation temperature at PT1, finish	◦F	225.57
19. Temperature of condensate, finish	◦F	194.41
20. Temperature difference, saturation temperature & RTD1, finish	◦F	31.16
21. Mass of condensate plus barrel, finish	lbm	160.59
22. Time interval	sec	38.88

Capacity and General Calculations

23. Average differential pressure	psig	2.44
24. Average subcooling	◦F	31.54
25. Capacity	lbm/hr	7798.90
26. Average inlet pressure	psig	4.59
27. Average condensate temperature	◦F	194.50

Uncertainty Calculations

28. Mass measurement sensitivity		92.59
29. Mass measurement uncertainty		0.5924
30. Mass measurement contribution (Term 1)		3008.40
31. Time interval sensitivity		200.58
32. Time interval uncertainty		0.0389
33. Time interval contribution (Term 2)		60.82
34. Inlet pressure sensitivity		918.56
35. Inlet pressure measurement uncertainty		0.0459
36. Inlet pressure contribution (Term 3)		1777.01
37. Subcooling sensitivity		6.00
38. Subcooling measurement uncertainty		0.2515
39. Subcooling contribution (Term 4)		2.28
40. Summation of terms		4848.51
41. Overall uncertainty	lbm/hr	69.63
42. Relative overall uncertainty	%	0.89

Condensate Capacity Test with Uncertainty Analysis

General Data

1. Trial no. 21 PT1=10.72 psig, RTD1=98.07 °C, VP1=100.00 % 2. Test date Mar. 3, 2015 @ 9:16 AM
3. Manufacturer's name Johnson Controls Incorporated
4. Type of trap/actuator VG1245BN/M9106-GGC-2
5. Serial no. T250F RY21430 6. Size 3/4, in.
7. Tested by C. Mercer 8. Calculation by C. Mercer
9. Scales description LC304-100 (serial 208927) NIST calibrated reference & certification - 2691

Test Data		Observed Value
10. Pressure at steam trap inlet, PT1, start	psig	10.34
11. Pressure at steam trap outlet, PT2, start	psig	4.75
12. Saturation temperature at PT1, start	◦F	240.16
13. Temperature of condensate, RTD1, start	◦F	211.64
14. Temperature difference, saturation temperature & RTD1, start	◦F	28.52
15. Mass of condensate plus barrel, start	lbm	72.06
16. Pressure at steam trap inlet, finish	psig	10.43
17. Pressure at steam trap outlet, finish	psig	5.40
18. Saturation temperature at PT1, finish	◦F	240.36
19. Temperature of condensate, finish	◦F	211.82
20. Temperature difference, saturation temperature & RTD1, finish	◦F	28.54
21. Mass of condensate plus barrel, finish	lbm	162.30
22. Time interval	sec	28.13

Capacity and General Calculations

23. Average differential pressure	psig	5.31
24. Average subcooling	◦F	28.53
25. Capacity	lbm/hr	11549.00
26. Average inlet pressure	psig	10.38
27. Average condensate temperature	◦F	211.73

Uncertainty Calculations

28. Mass measurement sensitivity		127.97
29. Mass measurement uncertainty		0.5859
30. Mass measurement contribution (Term 1)		5621.40
31. Time interval sensitivity		410.51
32. Time interval uncertainty		0.0281
33. Time interval contribution (Term 2)		133.37
34. Inlet pressure sensitivity		782.75
35. Inlet pressure measurement uncertainty		0.1038
36. Inlet pressure contribution (Term 3)		6605.36
37. Subcooling sensitivity		-144.00
38. Subcooling measurement uncertainty		0.2510
39. Subcooling contribution (Term 4)		1306.14
40. Summation of terms		13666.27
41. Overall uncertainty	lbm/hr	116.90
42. Relative overall uncertainty	%	1.01

Condensate Capacity Test with Uncertainty Analysis

General Data

1. Trial no. 22 PT1=4.91 psig, RTD1=99.59 °C, VP1=82.38 % 2. Test date Mar. 3, 2015 @ 10:45 AM
3. Manufacturer's name Johnson Controls Incorporated
4. Type of trap/actuator VG1245BN/M9106-GGC-2
5. Serial no. T250F RY21430 6. Size 3/4, in.
7. Tested by C. Mercer 8. Calculation by C. Mercer
9. Scales description LC304-100 (serial 208927) NIST calibrated reference & certification - 2691

Test Data		Observed Value
10. Pressure at steam trap inlet, PT1, start	psig	4.95
11. Pressure at steam trap outlet, PT2, start	psig	2.30
12. Saturation temperature at PT1, start	◦F	227.03
13. Temperature of condensate, RTD1, start	◦F	211.64
14. Temperature difference, saturation temperature & RTD1, start	◦F	15.39
15. Mass of condensate plus barrel, start	lbm	62.00
16. Pressure at steam trap inlet, finish	psig	4.91
17. Pressure at steam trap outlet, finish	psig	2.44
18. Saturation temperature at PT1, finish	◦F	226.90
19. Temperature of condensate, finish	◦F	211.45
20. Temperature difference, saturation temperature & RTD1, finish	◦F	15.45
21. Mass of condensate plus barrel, finish	lbm	140.54
22. Time interval	sec	38.67

Capacity and General Calculations

23. Average differential pressure	psig	2.56
24. Average subcooling	◦F	15.42
25. Capacity	lbm/hr	7311.50
26. Average inlet pressure	psig	4.93
27. Average condensate temperature	◦F	211.55

Uncertainty Calculations

28. Mass measurement sensitivity		93.10
29. Mass measurement uncertainty		0.5064
30. Mass measurement contribution (Term 1)		2222.30
31. Time interval sensitivity		189.08
32. Time interval uncertainty		0.0387
33. Time interval contribution (Term 2)		53.46
34. Inlet pressure sensitivity		797.49
35. Inlet pressure measurement uncertainty		0.0493
36. Inlet pressure contribution (Term 3)		1545.83
37. Subcooling sensitivity		-95.40
38. Subcooling measurement uncertainty		0.2515
39. Subcooling contribution (Term 4)		575.53
40. Summation of terms		4397.12
41. Overall uncertainty	lbm/hr	66.31
42. Relative overall uncertainty	%	0.91

Condensate Capacity Test with Uncertainty Analysis

General Data

1. Trial no. 23 PT1=14.50 psig, RTD1=112.70 °C, VP1=49.00 % 2. Test date Mar. 3, 2015 @ 1:00 PM
3. Manufacturer's name Johnson Controls Incorporated
4. Type of trap/actuator VG1245BN/M9106-GGC-2
5. Serial no. T250F RY21430 6. Size 3/4, in.
7. Tested by C. Mercer 8. Calculation by C. Mercer
9. Scales description LC304-100 (serial 208927) NIST calibrated reference & certification - 2691

Test Data		Observed Value
10. Pressure at steam trap inlet, PT1, start	psig	14.33
11. Pressure at steam trap outlet, PT2, start	psig	5.41
12. Saturation temperature at PT1, start	◦F	248.47
13. Temperature of condensate, RTD1, start	◦F	234.37
14. Temperature difference, saturation temperature & RTD1, start	◦F	14.10
15. Mass of condensate plus barrel, start	lbm	57.94
16. Pressure at steam trap inlet, finish	psig	14.60
17. Pressure at steam trap outlet, finish	psig	5.48
18. Saturation temperature at PT1, finish	◦F	249.00
19. Temperature of condensate, finish	◦F	234.55
20. Temperature difference, saturation temperature & RTD1, finish	◦F	14.44
21. Mass of condensate plus barrel, finish	lbm	89.45
22. Time interval	sec	33.08

Capacity and General Calculations

23. Average differential pressure	psig	9.02
24. Average subcooling	◦F	14.27
25. Capacity	lbm/hr	3429.90
26. Average inlet pressure	psig	14.47
27. Average condensate temperature	◦F	234.46

Uncertainty Calculations

28. Mass measurement sensitivity		108.84
29. Mass measurement uncertainty		0.3685
30. Mass measurement contribution (Term 1)		1608.40
31. Time interval sensitivity		103.70
32. Time interval uncertainty		0.0331
33. Time interval contribution (Term 2)		11.76
34. Inlet pressure sensitivity		441.72
35. Inlet pressure measurement uncertainty		0.1447
36. Inlet pressure contribution (Term 3)		4082.60
37. Subcooling sensitivity		-91.67
38. Subcooling measurement uncertainty		0.2508
39. Subcooling contribution (Term 4)		528.42
40. Summation of terms		6231.18
41. Overall uncertainty	lbm/hr	78.94
42. Relative overall uncertainty	%	2.30

Condensate Capacity Test with Uncertainty Analysis

General Data

1. Trial no. 24 PT1=4.49 psig, RTD1=90.00 °C, VP1=46.98 % 2. Test date Mar. 3, 2015 @ 1:27 PM
3. Manufacturer's name Johnson Controls Incorporated
4. Type of trap/actuator VG1245BN/M9106-GGC-2
5. Serial no. T250F RY21430 6. Size 3/4, in.
7. Tested by C. Mercer 8. Calculation by C. Mercer
9. Scales description LC304-100 (serial 208927) NIST calibrated reference & certification - 2691

Test Data		Observed Value
10. Pressure at steam trap inlet, PT1, start	psig	4.53
11. Pressure at steam trap outlet, PT2, start	psig	0.00
12. Saturation temperature at PT1, start	◦F	225.89
13. Temperature of condensate, RTD1, start	◦F	193.67
14. Temperature difference, saturation temperature & RTD1, start	◦F	32.21
15. Mass of condensate plus barrel, start	lbm	71.59
16. Pressure at steam trap inlet, finish	psig	4.55
17. Pressure at steam trap outlet, finish	psig	0.00
18. Saturation temperature at PT1, finish	◦F	225.93
19. Temperature of condensate, finish	◦F	194.22
20. Temperature difference, saturation temperature & RTD1, finish	◦F	31.70
21. Mass of condensate plus barrel, finish	lbm	87.16
22. Time interval	sec	25.45

Capacity and General Calculations

23. Average differential pressure	psig	4.54
24. Average subcooling	◦F	31.96
25. Capacity	lbm/hr	2202.30
26. Average inlet pressure	psig	4.54
27. Average condensate temperature	◦F	193.95

Uncertainty Calculations

28. Mass measurement sensitivity		141.45
29. Mass measurement uncertainty		0.3969
30. Mass measurement contribution (Term 1)		3151.70
31. Time interval sensitivity		86.53
32. Time interval uncertainty		0.0255
33. Time interval contribution (Term 2)		4.85
34. Inlet pressure sensitivity		321.50
35. Inlet pressure measurement uncertainty		0.0454
36. Inlet pressure contribution (Term 3)		213.25
37. Subcooling sensitivity		-19.95
38. Subcooling measurement uncertainty		0.2515
39. Subcooling contribution (Term 4)		25.18
40. Summation of terms		3394.97
41. Overall uncertainty	lbm/hr	58.27
42. Relative overall uncertainty	%	2.65

Condensate Capacity Test with Uncertainty Analysis

General Data

1. Trial no. 25 PT1=14.50 psig, RTD1=120.44 °C, VP1=25.00 % 2. Test date Mar. 4, 2015 @ 10:52 AM
3. Manufacturer's name Johnson Controls Incorporated
4. Type of trap/actuator VG1245BN/M9106-GGC-2
5. Serial no. T250F RY21430 6. Size 3/4, in.
7. Tested by C. Mercer 8. Calculation by C. Mercer
9. Scales description LC304-100 (serial 208927) NIST calibrated reference & certification - 2691

Test Data		Observed Value
10. Pressure at steam trap inlet, PT1, start	psig	14.71
11. Pressure at steam trap outlet, PT2, start	psig	1.28
12. Saturation temperature at PT1, start	◦F	249.22
13. Temperature of condensate, RTD1, start	◦F	246.65
14. Temperature difference, saturation temperature & RTD1, start	◦F	2.57
15. Mass of condensate plus barrel, start	lbm	65.97
16. Pressure at steam trap inlet, finish	psig	14.61
17. Pressure at steam trap outlet, finish	psig	1.32
18. Saturation temperature at PT1, finish	◦F	249.01
19. Temperature of condensate, finish	◦F	246.10
20. Temperature difference, saturation temperature & RTD1, finish	◦F	2.91
21. Mass of condensate plus barrel, finish	lbm	67.99
22. Time interval	sec	24.51

Capacity and General Calculations

23. Average differential pressure	psig	13.36
24. Average subcooling	◦F	2.74
25. Capacity	lbm/hr	295.34
26. Average inlet pressure	psig	14.66
27. Average condensate temperature	◦F	246.38

Uncertainty Calculations

28. Mass measurement sensitivity		146.90
29. Mass measurement uncertainty		0.3349
30. Mass measurement contribution (Term 1)		2420.20
31. Time interval sensitivity		12.05
32. Time interval uncertainty		0.0245
33. Time interval contribution (Term 2)		0.09
34. Inlet pressure sensitivity		80.65
35. Inlet pressure measurement uncertainty		0.1466
36. Inlet pressure contribution (Term 3)		139.78
37. Subcooling sensitivity		-18.96
38. Subcooling measurement uncertainty		0.2508
39. Subcooling contribution (Term 4)		22.61
40. Summation of terms		2582.68
41. Overall uncertainty	lbm/hr	50.82
42. Relative overall uncertainty	%	17.21

Condensate Capacity Test with Uncertainty Analysis

General Data

1. Trial no. 26 PT1=14.50 psig, RTD1=100.05 °C, VP1=25.00 % 2. Test date Mar. 4, 2015 @ 11:19 AM
3. Manufacturer's name Johnson Controls Incorporated
4. Type of trap/actuator VG1245BN/M9106-GGC-2
5. Serial no. T250F RY21430 6. Size 3/4, in.
7. Tested by C. Mercer 8. Calculation by C. Mercer
9. Scales description LC304-100 (serial 208927) NIST calibrated reference & certification - 2691

Test Data		Observed Value
10. Pressure at steam trap inlet, PT1, start	psig	14.50
11. Pressure at steam trap outlet, PT2, start	psig	0.12
12. Saturation temperature at PT1, start	◦F	248.80
13. Temperature of condensate, RTD1, start	◦F	211.64
14. Temperature difference, saturation temperature & RTD1, start	◦F	37.16
15. Mass of condensate plus barrel, start	lbm	49.52
16. Pressure at steam trap inlet, finish	psig	14.55
17. Pressure at steam trap outlet, finish	psig	0.14
18. Saturation temperature at PT1, finish	◦F	248.90
19. Temperature of condensate, finish	◦F	212.37
20. Temperature difference, saturation temperature & RTD1, finish	◦F	36.53
21. Mass of condensate plus barrel, finish	lbm	52.66
22. Time interval	sec	21.59

Capacity and General Calculations

23. Average differential pressure	psig	14.40
24. Average subcooling	◦F	36.85
25. Capacity	lbm/hr	523.36
26. Average inlet pressure	psig	14.52
27. Average condensate temperature	◦F	212.01

Uncertainty Calculations

28. Mass measurement sensitivity		166.77
29. Mass measurement uncertainty		0.2555
30. Mass measurement contribution (Term 1)		1815.10
31. Time interval sensitivity		24.25
32. Time interval uncertainty		0.0216
33. Time interval contribution (Term 2)		0.27
34. Inlet pressure sensitivity		22.92
35. Inlet pressure measurement uncertainty		0.1452
36. Inlet pressure contribution (Term 3)		11.08
37. Subcooling sensitivity		3.21
38. Subcooling measurement uncertainty		0.2508
39. Subcooling contribution (Term 4)		0.65
40. Summation of terms		1827.10
41. Overall uncertainty	lbm/hr	42.74
42. Relative overall uncertainty	%	8.17

Condensate Capacity Test with Uncertainty Analysis

General Data

1. Trial no. 27 PT1=11.56 psig, RTD1=110.28 °C, VP1=72.25 % 2. Test date Mar. 4, 2015 @ 12:04 PM
3. Manufacturer's name Johnson Controls Incorporated
4. Type of trap/actuator VG1245BN/M9106-GGC-2
5. Serial no. T250F RY21430 6. Size 3/4, in.
7. Tested by C. Mercer 8. Calculation by C. Mercer
9. Scales description LC304-100 (serial 208927) NIST calibrated reference & certification - 2691

Test Data		Observed Value
10. Pressure at steam trap inlet, PT1, start	psig	11.69
11. Pressure at steam trap outlet, PT2, start	psig	6.21
12. Saturation temperature at PT1, start	◦F	243.08
13. Temperature of condensate, RTD1, start	◦F	230.15
14. Temperature difference, saturation temperature & RTD1, start	◦F	12.93
15. Mass of condensate plus barrel, start	lbm	66.71
16. Pressure at steam trap inlet, finish	psig	11.49
17. Pressure at steam trap outlet, finish	psig	6.16
18. Saturation temperature at PT1, finish	◦F	242.66
19. Temperature of condensate, finish	◦F	230.33
20. Temperature difference, saturation temperature & RTD1, finish	◦F	12.33
21. Mass of condensate plus barrel, finish	lbm	118.11
22. Time interval	sec	25.66

Capacity and General Calculations

23. Average differential pressure	psig	5.40
24. Average subcooling	◦F	12.63
25. Capacity	lbm/hr	7210.50
26. Average inlet pressure	psig	11.59
27. Average condensate temperature	◦F	230.24

Uncertainty Calculations

28. Mass measurement sensitivity		140.29
29. Mass measurement uncertainty		0.4621
30. Mass measurement contribution (Term 1)		4201.80
31. Time interval sensitivity		280.98
32. Time interval uncertainty		0.0257
33. Time interval contribution (Term 2)		51.99
34. Inlet pressure sensitivity		656.20
35. Inlet pressure measurement uncertainty		0.1159
36. Inlet pressure contribution (Term 3)		5784.20
37. Subcooling sensitivity		-207.86
38. Subcooling measurement uncertainty		0.2509
39. Subcooling contribution (Term 4)		2719.73
40. Summation of terms		12757.73
41. Overall uncertainty	lbm/hr	112.95
42. Relative overall uncertainty	%	1.57

Condensate Capacity Test with Uncertainty Analysis

General Data

1. Trial no. 28 PT1=5.75 psig, RTD1=98.22 °C, VP1=41.50 % 2. Test date Mar. 4, 2015 @ 1:06 PM
3. Manufacturer's name Johnson Controls Incorporated
4. Type of trap/actuator VG1245BN/M9106-GGC-2
5. Serial no. T250F RY21430 6. Size 3/4, in.
7. Tested by C. Mercer 8. Calculation by C. Mercer
9. Scales description LC304-100 (serial 208927) NIST calibrated reference & certification - 2691

Test Data		Observed Value
10. Pressure at steam trap inlet, PT1, start	psig	5.73
11. Pressure at steam trap outlet, PT2, start	psig	0.20
12. Saturation temperature at PT1, start	◦F	229.08
13. Temperature of condensate, RTD1, start	◦F	208.34
14. Temperature difference, saturation temperature & RTD1, start	◦F	20.75
15. Mass of condensate plus barrel, start	lbm	100.92
16. Pressure at steam trap inlet, finish	psig	5.76
17. Pressure at steam trap outlet, finish	psig	0.15
18. Saturation temperature at PT1, finish	◦F	229.17
19. Temperature of condensate, finish	◦F	208.70
20. Temperature difference, saturation temperature & RTD1, finish	◦F	20.47
21. Mass of condensate plus barrel, finish	lbm	113.41
22. Time interval	sec	28.63

Capacity and General Calculations

23. Average differential pressure	psig	5.57
24. Average subcooling	◦F	20.61
25. Capacity	lbm/hr	1571.00
26. Average inlet pressure	psig	5.74
27. Average condensate temperature	◦F	208.52

Uncertainty Calculations

28. Mass measurement sensitivity		125.75
29. Mass measurement uncertainty		0.5358
30. Mass measurement contribution (Term 1)		4540.20
31. Time interval sensitivity		54.88
32. Time interval uncertainty		0.0286
33. Time interval contribution (Term 2)		2.47
34. Inlet pressure sensitivity		184.03
35. Inlet pressure measurement uncertainty		0.0574
36. Inlet pressure contribution (Term 3)		111.72
37. Subcooling sensitivity		-18.35
38. Subcooling measurement uncertainty		0.2513
39. Subcooling contribution (Term 4)		21.27
40. Summation of terms		4675.66
41. Overall uncertainty	lbm/hr	68.38
42. Relative overall uncertainty	%	4.35

Condensate Capacity Test with Uncertainty Analysis

General Data

1. Trial no. 29 PT1=10.65 psig, RTD1=106.90 °C, VP1=25.00 % 2. Test date Mar. 5, 2015 @ 9:17 AM
3. Manufacturer's name Johnson Controls Incorporated
4. Type of trap/actuator VG1245BN/M9106-GGC-2
5. Serial no. T250F RY21430 6. Size 3/4, in.
7. Tested by C. Mercer 8. Calculation by C. Mercer
9. Scales description LC304-100 (serial 208927) NIST calibrated reference & certification - 2691

Test Data		Observed Value
10. Pressure at steam trap inlet, PT1, start	psig	10.69
11. Pressure at steam trap outlet, PT2, start	psig	0.28
12. Saturation temperature at PT1, start	◦F	240.94
13. Temperature of condensate, RTD1, start	◦F	223.55
14. Temperature difference, saturation temperature & RTD1, start	◦F	17.39
15. Mass of condensate plus barrel, start	lbm	54.56
16. Pressure at steam trap inlet, finish	psig	10.65
17. Pressure at steam trap outlet, finish	psig	0.26
18. Saturation temperature at PT1, finish	◦F	240.84
19. Temperature of condensate, finish	◦F	224.65
20. Temperature difference, saturation temperature & RTD1, finish	◦F	16.18
21. Mass of condensate plus barrel, finish	lbm	58.04
22. Time interval	sec	34.66

Capacity and General Calculations

23. Average differential pressure	psig	10.40
24. Average subcooling	◦F	16.79
25. Capacity	lbm/hr	361.20
26. Average inlet pressure	psig	10.67
27. Average condensate temperature	◦F	224.10

Uncertainty Calculations

28. Mass measurement sensitivity		103.85
29. Mass measurement uncertainty		0.2815
30. Mass measurement contribution (Term 1)		854.56
31. Time interval sensitivity		10.42
32. Time interval uncertainty		0.0347
33. Time interval contribution (Term 2)		0.13
34. Inlet pressure sensitivity		9.99
35. Inlet pressure measurement uncertainty		0.1067
36. Inlet pressure contribution (Term 3)		1.14
37. Subcooling sensitivity		-5.73
38. Subcooling measurement uncertainty		0.2510
39. Subcooling contribution (Term 4)		2.07
40. Summation of terms		857.90
41. Overall uncertainty	lbm/hr	29.29
42. Relative overall uncertainty	%	8.11

Condensate Capacity Test with Uncertainty Analysis

General Data

1. Trial no. 30 PT1=0.50 psig, RTD1=100.94 °C, VP1=47.88 % 2. Test date Mar. 5, 2015 @ 9:35 AM
3. Manufacturer's name Johnson Controls Incorporated
4. Type of trap/actuator VG1245BN/M9106-GGC-2
5. Serial no. T250F RY21430 6. Size 3/4, in.
7. Tested by C. Mercer 8. Calculation by C. Mercer
9. Scales description LC304-100 (serial 208927) NIST calibrated reference & certification - 2691

Test Data		Observed Value
10. Pressure at steam trap inlet, PT1, start	psig	0.79
11. Pressure at steam trap outlet, PT2, start	psig	0.30
12. Saturation temperature at PT1, start	◦F	214.66
13. Temperature of condensate, RTD1, start	◦F	212.55
14. Temperature difference, saturation temperature & RTD1, start	◦F	2.11
15. Mass of condensate plus barrel, start	lbm	83.22
16. Pressure at steam trap inlet, finish	psig	0.58
17. Pressure at steam trap outlet, finish	psig	0.23
18. Saturation temperature at PT1, finish	◦F	213.98
19. Temperature of condensate, finish	◦F	211.64
20. Temperature difference, saturation temperature & RTD1, finish	◦F	2.34
21. Mass of condensate plus barrel, finish	lbm	92.24
22. Time interval	sec	55.49

Capacity and General Calculations

23. Average differential pressure	psig	0.42
24. Average subcooling	◦F	2.23
25. Capacity	lbm/hr	585.37
26. Average inlet pressure	psig	0.69
27. Average condensate temperature	◦F	212.10

Uncertainty Calculations

28. Mass measurement sensitivity		64.88
29. Mass measurement uncertainty		0.4386
30. Mass measurement contribution (Term 1)		809.96
31. Time interval sensitivity		10.55
32. Time interval uncertainty		0.0555
33. Time interval contribution (Term 2)		0.34
34. Inlet pressure sensitivity		282.30
35. Inlet pressure measurement uncertainty		0.0069
36. Inlet pressure contribution (Term 3)		3.78
37. Subcooling sensitivity		-10.00
38. Subcooling measurement uncertainty		0.2522
39. Subcooling contribution (Term 4)		6.36
40. Summation of terms		820.45
41. Overall uncertainty	lbm/hr	28.64
42. Relative overall uncertainty	%	4.89

Condensate Capacity Test with Uncertainty Analysis

General Data

1. Trial no. 31 PT1=14.50 psig, RTD1=90.00 °C, VP1=37.38 % 2. Test date Mar. 5, 2015 @ 9:56 AM
3. Manufacturer's name Johnson Controls Incorporated
4. Type of trap/actuator VG1245BN/M9106-GGC-2
5. Serial no. T250F RY21430 6. Size 3/4, in.
7. Tested by C. Mercer 8. Calculation by C. Mercer
9. Scales description LC304-100 (serial 208927) NIST calibrated reference & certification - 2691

Test Data		Observed Value
10. Pressure at steam trap inlet, PT1, start	psig	14.79
11. Pressure at steam trap outlet, PT2, start	psig	0.11
12. Saturation temperature at PT1, start	◦F	249.37
13. Temperature of condensate, RTD1, start	◦F	192.57
14. Temperature difference, saturation temperature & RTD1, start	◦F	56.80
15. Mass of condensate plus barrel, start	lbm	67.51
16. Pressure at steam trap inlet, finish	psig	14.79
17. Pressure at steam trap outlet, finish	psig	0.13
18. Saturation temperature at PT1, finish	◦F	249.37
19. Temperature of condensate, finish	◦F	193.67
20. Temperature difference, saturation temperature & RTD1, finish	◦F	55.70
21. Mass of condensate plus barrel, finish	lbm	84.59
22. Time interval	sec	31.32

Capacity and General Calculations

23. Average differential pressure	psig	14.67
24. Average subcooling	◦F	56.25
25. Capacity	lbm/hr	1963.20
26. Average inlet pressure	psig	14.79
27. Average condensate temperature	◦F	193.12

Uncertainty Calculations

28. Mass measurement sensitivity		114.94
29. Mass measurement uncertainty		0.3802
30. Mass measurement contribution (Term 1)		1909.80
31. Time interval sensitivity		62.68
32. Time interval uncertainty		0.0313
33. Time interval contribution (Term 2)		3.85
34. Inlet pressure sensitivity		72.23
35. Inlet pressure measurement uncertainty		0.1479
36. Inlet pressure contribution (Term 3)		114.16
37. Subcooling sensitivity		-7.68
38. Subcooling measurement uncertainty		0.2511
39. Subcooling contribution (Term 4)		3.72
40. Summation of terms		2031.53
41. Overall uncertainty	lbm/hr	45.07
42. Relative overall uncertainty	%	2.30

Condensate Capacity Test with Uncertainty Analysis

General Data

1. Trial no. 32 PT1=0.50 psig, RTD1=90.76 °C, VP1=25.00 % 2. Test date Mar. 5, 2015 @ 11:46 AM
3. Manufacturer's name Johnson Controls Incorporated
4. Type of trap/actuator VG1245BN/M9106-GGC-2
5. Serial no. T250F RY21430 6. Size 3/4, in.
7. Tested by C. Mercer 8. Calculation by C. Mercer
9. Scales description LC304-100 (serial 208927) NIST calibrated reference & certification - 2691

Test Data		Observed Value
10. Pressure at steam trap inlet, PT1, start	psig	0.49
11. Pressure at steam trap outlet, PT2, start	psig	0.06
12. Saturation temperature at PT1, start	◦F	213.66
13. Temperature of condensate, RTD1, start	◦F	195.14
14. Temperature difference, saturation temperature & RTD1, start	◦F	18.52
15. Mass of condensate plus barrel, start	lbm	76.07
16. Pressure at steam trap inlet, finish	psig	0.53
17. Pressure at steam trap outlet, finish	psig	0.09
18. Saturation temperature at PT1, finish	◦F	213.78
19. Temperature of condensate, finish	◦F	194.77
20. Temperature difference, saturation temperature & RTD1, finish	◦F	19.01
21. Mass of condensate plus barrel, finish	lbm	76.56
22. Time interval	sec	22.18

Capacity and General Calculations

23. Average differential pressure	psig	0.43
24. Average subcooling	◦F	18.77
25. Capacity	lbm/hr	79.77
26. Average inlet pressure	psig	0.51
27. Average condensate temperature	◦F	194.96

Uncertainty Calculations

28. Mass measurement sensitivity		162.29
29. Mass measurement uncertainty		0.3816
30. Mass measurement contribution (Term 1)		3834.90
31. Time interval sensitivity		3.60
32. Time interval uncertainty		0.0222
33. Time interval contribution (Term 2)		0.01
34. Inlet pressure sensitivity		91.52
35. Inlet pressure measurement uncertainty		0.0051
36. Inlet pressure contribution (Term 3)		0.22
37. Subcooling sensitivity		105.70
38. Subcooling measurement uncertainty		0.2522
39. Subcooling contribution (Term 4)		710.64
40. Summation of terms		4545.76
41. Overall uncertainty	lbm/hr	67.42
42. Relative overall uncertainty	%	84.52

Condensate Capacity Test with Uncertainty Analysis

General Data

1. Trial no. 33 PT1=14.50 psig, RTD1=120.44 °C, VP1=86.13 % 2. Test date Mar. 6, 2015 @ 9:14 AM
3. Manufacturer's name Johnson Controls Incorporated
4. Type of trap/actuator VG1245BN/M9106-GGC-2
5. Serial no. T250F RY21430 6. Size 3/4, in.
7. Tested by C. Mercer 8. Calculation by C. Mercer
9. Scales description LC304-100 (serial 208927) NIST calibrated reference & certification - 2691

Test Data		Observed Value
10. Pressure at steam trap inlet, PT1, start	psig	14.80
11. Pressure at steam trap outlet, PT2, start	psig	12.81
12. Saturation temperature at PT1, start	◦F	249.39
13. Temperature of condensate, RTD1, start	◦F	247.93
14. Temperature difference, saturation temperature & RTD1, start	◦F	1.46
15. Mass of condensate plus barrel, start	lbm	60.85
16. Pressure at steam trap inlet, finish	psig	15.00
17. Pressure at steam trap outlet, finish	psig	13.22
18. Saturation temperature at PT1, finish	◦F	249.77
19. Temperature of condensate, finish	◦F	247.93
20. Temperature difference, saturation temperature & RTD1, finish	◦F	1.84
21. Mass of condensate plus barrel, finish	lbm	106.89
22. Time interval	sec	37.16

Capacity and General Calculations

23. Average differential pressure	psig	1.89
24. Average subcooling	◦F	1.65
25. Capacity	lbm/hr	4459.50
26. Average inlet pressure	psig	14.90
27. Average condensate temperature	◦F	247.93

Uncertainty Calculations

28. Mass measurement sensitivity		96.87
29. Mass measurement uncertainty		0.4193
30. Mass measurement contribution (Term 1)		1650.20
31. Time interval sensitivity		120.00
32. Time interval uncertainty		0.0372
33. Time interval contribution (Term 2)		19.89
34. Inlet pressure sensitivity		880.96
35. Inlet pressure measurement uncertainty		0.1490
36. Inlet pressure contribution (Term 3)		17234.77
37. Subcooling sensitivity		-379.73
38. Subcooling measurement uncertainty		0.2507
39. Subcooling contribution (Term 4)		9065.47
40. Summation of terms		27970.32
41. Overall uncertainty	lbm/hr	167.24
42. Relative overall uncertainty	%	3.75

Condensate Capacity Test with Uncertainty Analysis

General Data

1. Trial no. 34 PT1=7.64 psig, RTD1=103.50 °C, VP1=84.25 % 2. Test date Mar. 6, 2015 @ 10:35 AM
3. Manufacturer's name Johnson Controls Incorporated
4. Type of trap/actuator VG1245BN/M9106-GGC-2
5. Serial no. T250F RY21430 6. Size 3/4, in.
7. Tested by C. Mercer 8. Calculation by C. Mercer
9. Scales description LC304-100 (serial 208927) NIST calibrated reference & certification - 2691

Test Data		Observed Value
10. Pressure at steam trap inlet, PT1, start	psig	7.68
11. Pressure at steam trap outlet, PT2, start	psig	4.57
12. Saturation temperature at PT1, start	◦F	233.99
13. Temperature of condensate, RTD1, start	◦F	218.24
14. Temperature difference, saturation temperature & RTD1, start	◦F	15.76
15. Mass of condensate plus barrel, start	lbm	74.86
16. Pressure at steam trap inlet, finish	psig	7.65
17. Pressure at steam trap outlet, finish	psig	4.39
18. Saturation temperature at PT1, finish	◦F	233.94
19. Temperature of condensate, finish	◦F	218.24
20. Temperature difference, saturation temperature & RTD1, finish	◦F	15.70
21. Mass of condensate plus barrel, finish	lbm	137.64
22. Time interval	sec	27.33

Capacity and General Calculations

23. Average differential pressure	psig	3.18
24. Average subcooling	◦F	15.73
25. Capacity	lbm/hr	8270.20
26. Average inlet pressure	psig	7.66
27. Average condensate temperature	◦F	218.24

Uncertainty Calculations

28. Mass measurement sensitivity		131.72
29. Mass measurement uncertainty		0.5313
30. Mass measurement contribution (Term 1)		4897.10
31. Time interval sensitivity		302.60
32. Time interval uncertainty		0.0273
33. Time interval contribution (Term 2)		68.40
34. Inlet pressure sensitivity		723.36
35. Inlet pressure measurement uncertainty		0.0766
36. Inlet pressure contribution (Term 3)		3073.40
37. Subcooling sensitivity		-163.31
38. Subcooling measurement uncertainty		0.2512
39. Subcooling contribution (Term 4)		1682.17
40. Summation of terms		9721.07
41. Overall uncertainty	lbm/hr	98.60
42. Relative overall uncertainty	%	1.19

Condensate Capacity Test with Uncertainty Analysis

General Data

1. Trial no. 35 PT1=5.93 psig, RTD1=108.51 °C, VP1=54.88 % 2. Test date Mar. 6, 2015 @ 12:07 PM
3. Manufacturer's name Johnson Controls Incorporated
4. Type of trap/actuator VG1245BN/M9106-GGC-2
5. Serial no. T250F RY21430 6. Size 3/4, in.
7. Tested by C. Mercer 8. Calculation by C. Mercer
9. Scales description LC304-100 (serial 208927) NIST calibrated reference & certification - 2691

Test Data		Observed Value
10. Pressure at steam trap inlet, PT1, start	psig	5.91
11. Pressure at steam trap outlet, PT2, start	psig	2.30
12. Saturation temperature at PT1, start	◦F	229.57
13. Temperature of condensate, RTD1, start	◦F	226.85
14. Temperature difference, saturation temperature & RTD1, start	◦F	2.72
15. Mass of condensate plus barrel, start	lbm	53.84
16. Pressure at steam trap inlet, finish	psig	5.94
17. Pressure at steam trap outlet, finish	psig	2.28
18. Saturation temperature at PT1, finish	◦F	229.64
19. Temperature of condensate, finish	◦F	227.40
20. Temperature difference, saturation temperature & RTD1, finish	◦F	2.24
21. Mass of condensate plus barrel, finish	lbm	70.65
22. Time interval	sec	27.53

Capacity and General Calculations

23. Average differential pressure	psig	3.64
24. Average subcooling	◦F	2.48
25. Capacity	lbm/hr	2198.30
26. Average inlet pressure	psig	5.93
27. Average condensate temperature	◦F	227.13

Uncertainty Calculations

28. Mass measurement sensitivity		130.76
29. Mass measurement uncertainty		0.3112
30. Mass measurement contribution (Term 1)		1656.40
31. Time interval sensitivity		79.85
32. Time interval uncertainty		0.0275
33. Time interval contribution (Term 2)		4.83
34. Inlet pressure sensitivity		306.78
35. Inlet pressure measurement uncertainty		0.0593
36. Inlet pressure contribution (Term 3)		330.63
37. Subcooling sensitivity		-78.82
38. Subcooling measurement uncertainty		0.2513
39. Subcooling contribution (Term 4)		392.46
40. Summation of terms		2384.32
41. Overall uncertainty	lbm/hr	48.83
42. Relative overall uncertainty	%	2.22

Condensate Capacity Test with Uncertainty Analysis

General Data

1. Trial no. 36 PT1=1.20 psig, RTD1=100.20 °C, VP1=25.00 % 2. Test date Mar. 6, 2015 @ 1:25 PM
3. Manufacturer's name Johnson Controls Incorporated
4. Type of trap/actuator VG1245BN/M9106-GGC-2
5. Serial no. T250F RY21430 6. Size 3/4, in.
7. Tested by C. Mercer 8. Calculation by C. Mercer
9. Scales description LC304-100 (serial 208927) NIST calibrated reference & certification - 2691

Test Data		Observed Value
10. Pressure at steam trap inlet, PT1, start	psig	1.20
11. Pressure at steam trap outlet, PT2, start	psig	0.13
12. Saturation temperature at PT1, start	◦F	215.98
13. Temperature of condensate, RTD1, start	◦F	211.64
14. Temperature difference, saturation temperature & RTD1, start	◦F	4.34
15. Mass of condensate plus barrel, start	lbm	49.02
16. Pressure at steam trap inlet, finish	psig	1.22
17. Pressure at steam trap outlet, finish	psig	0.15
18. Saturation temperature at PT1, finish	◦F	216.04
19. Temperature of condensate, finish	◦F	210.17
20. Temperature difference, saturation temperature & RTD1, finish	◦F	5.87
21. Mass of condensate plus barrel, finish	lbm	51.26
22. Time interval	sec	55.61

Capacity and General Calculations

23. Average differential pressure	psig	1.07
24. Average subcooling	◦F	5.11
25. Capacity	lbm/hr	145.36
26. Average inlet pressure	psig	1.21
27. Average condensate temperature	◦F	210.91

Uncertainty Calculations

28. Mass measurement sensitivity		64.74
29. Mass measurement uncertainty		0.2507
30. Mass measurement contribution (Term 1)		263.38
31. Time interval sensitivity		2.61
32. Time interval uncertainty		0.0556
33. Time interval contribution (Term 2)		0.02
34. Inlet pressure sensitivity		74.47
35. Inlet pressure measurement uncertainty		0.0121
36. Inlet pressure contribution (Term 3)		0.81
37. Subcooling sensitivity		-1.04
38. Subcooling measurement uncertainty		0.2521
39. Subcooling contribution (Term 4)		0.07
40. Summation of terms		264.28
41. Overall uncertainty	lbm/hr	16.26
42. Relative overall uncertainty	%	11.18

Appendix D

Source Code

% Mass flowrate Predication using Incompressible ISA-I model

%Constants

d=0.785; %inside diameter of type L copper pipe (3/4" O.D)
Pc=3206.2; %absolute critial pressure (psia)
Rho0=62.369; % standard density of water @15C (lbm/ft^3)

%Valve Characteristics

Fd=0.98; %valve style modifier (dimensionless)
Xt=0.3; %pressure differential ratio factor (dimensionless)
Fl=0.6; %liquid pressure recovery factor (dimensionless)
Cv=11.7; %flow cofficient for condensate control valve (dimensionless)

%State Properties (user defined)

T1=; %supply temperature (C)
P1=; %inlet gauge pressure (psig)
P2=; %outlet gauge pressure (psig)

% NIST Variables (Liquid)

Rho1L=; %density @ supply pressure and supply temperature (lbm/ft^3)
UvL=; %kitematic viscosity (ft^2/s)

% Numerical Constants for model

N1=1.0; %Q(gpm), deltP (psia)
N2=8.90E2; %d(in)
N4=1.73E4; %Q(gpm), Uv(cS)

% Unit Conversion

T1=273.15+T1; %C to K
T1R=T1*1.8; %K to R
UvL=UvL*92903.04; %ft^2/s to cS
UvV=UvV*92903.04; %ft^2/s to cS
P1=P1+14.467672; %psig to psia
P2=P2+14.467672; %psig to psia
Pv=P1;

deltP=P1-P2; %differential pressure between PT1 and PT2 (psia)
Ff=0.96-0.28*sqrt(Pv/Pc); %liquid critical pressure ratio factor (dimensionless)

```
%Type of Flow for Incompressible Fluid and Turbulent Verification

if (deltP < Fl^2*(P1-Ff*Pv)) %Non-choked flow

   Q=(N1*Cv)/sqrt((Rho1L/Rho0)/deltP); %volumetric flow(USGPM)
   Q=Q*8.0208; %USGPM to ft^3/hr
   Mfi=Q*Rho1L; %mass flowrate (lbm/hr)

   Rei=(N4*Fd*Q)/(UvL*sqrt(Cv*Fl))*((Fl^2*Cv^2)/(N2*d^4)+1)^0.25;

   if (Rei<10000)
      Assumption='false';
   else
      Assumption='true';
   end

   UncompressedFlow={Mfi 'Non-choked' Assumption}

else %Choked flow

   Q=(Cv*N1*Fl)/sqrt((Rho1L/Rho0)/(P1-Ff*Pv)); %volumetric flow(USGPM)
   Q=Q*8.0208; %USGPM to ft^3/hr
   Mfi=Q*Rho1L; %mass flowrate (lbm/hr)

   Rei=(N4*Fd*Q)/(UvL*sqrt(Cv*Fl))*((Fl^2*Cv^2)/(N2*d^4)+1)^0.25;

    if (Rei<10000)
      Assumption='False';
    else
      Assumption='True';
    end

   UncompressedFlow={Mfi 'Choked' Assumption}

end
```

```
% Mass flowrate Predication for HE, HF, HNE, HNE-DS Model

% Note: all models except for HF use Model=2 else use Model=1
% HE: N=1
% HNE: N=0.0001
% HNE-DS: first determine compressibility factor with HE model then calculate boiling
% delay factor N for determination of new compressibility factor with an altered HNE

Model=2;

%State variables and property data

N=1; %boiling delay coefficient model 2
data=xlsread('0.5_M.xlsx'); %Read NIST table
Ncrit=0.22241; %Ncrit for Model 1
gam=data(1,12); %isentropic expoent (gas) model 1
Pin=data(1,2); %inlet pressure (psig)
Tin=data(1,1); %inlet temperature (deg C)
Pout=data(1,13); %outlet pressure (psig)
hg=data(1,6); %vapor latent heat (J/kg)
hf=data(1,5); %liquid latent heat (J/kg)
hfg=hg-hf; %difference between vapor and liquid phase (J/kg)
sh=data(1,9); %specific heat at constant pressure for liquid (J/Kg K)
svg=data(1,4); %specific volumne for inlet vapor (m^3/kg)
svl=data(1,3); %specific volumne for inlet liquid (m^3/kg)
cv=11.7; %valve flow cofficient

if (Model==2)
   x=0.0; %inlet vapor quality (saturated liquid)
else
   x=0.0001;
end

sc=1; %slip correction initilization

%Unit conversion

Pin=(Pin+14.467672)*6894.75728; %psia to pa
Tin=Tin+273.15; %C to K
Pout=(Pout+14.467672)*6894.75728; %psia to pa

%Pressure ratio

Nnot=Pout/Pin; %(dimensionless)
```

```
%Homogeneous specific volume of mixture

Vin=x*svg+(1-x)*svl; %(m^3/kg)

%Compressibility factor (equilibrium condition, N=1)

if (N==1 andand Model==2)
   w=(x*svg)/Vin +((sh*Tin*Pin)/Vin)*((svg-svl)/hfg)^2; %(dimensionless)
%Critical pressure ratio (equilibrium condition, N=1)
if (w<2)
   Ncrit=0.6055+0.1356*log(w)-0.0131*(log(w))^2; %approximated explictly(dimensionless)
end
if (w>=2)
   Ncrit=0.55+0.217*log(w)-0.046*(log(w))^2+0.004*(log(w))^3; %(dimensionless)
end
end

%Compressibility factor (nonequilibrium condition (N<=1)

if (N<1 andand Model==2)
    w=(x*svg)/Vin +sh*(Tin*Pin)/Vin*((svg-svl)/hfg)^2*N; %(dimensionless)
%N=(x+sh*Tin*Pin*((svg-svl)/hfg^2)*log(1/Ncrit))^(3/5); boiling delay determination
%Critical pressure ratio (equilibrium condition, N=1)
if (w<2)
    Ncrit=0.6055+0.1356*log(w)-0.0131*(log(w))^2; %approximated explictly(dimensionless)
end
if (w>=2)
    Ncrit=0.55+0.217*log(w)-0.046*(log(w))^2+0.004*(log(w))^3; %(dimensionless)
end
end

%Expansion coefficient

if (Nnot<=Ncrit) %critical
   n=Ncrit; %(dimensionless)
end
if (Nnot>Ncrit) %subcritical
   n=Nnot; %(dimensionless)
end

fi=sqrt(w*log(1/n)-(w-1)*(1-n))/(w*(1/n-1)+1); %(dimensionless)

%Mass flux for frictionless isentropic flow
```

```
if (Model==1)
   MdotA=1/Vin*(2*x*svg*Pin*(gam/(gam-1))*(1-n^((gam-1)/gam)))^0.5;
else
MdotA=fi*sqrt((2*Pin)/Vin); % (kg/m^2 s)
end

%Discharge coefficient

Kvs=10; % (m^3/hr)
dc=Kvs*sqrt(1000/(2*100000)); % (m^3*s*hr^-1*m^-1)

% %Slip correction

% sc=sqrt(Vin/svl)*(1+x*((svg/svl)^(1/6)-1)*(1+x*((svg/svl)^(5/6)-1)))^(-1/2); %(dimensionless)

%Mass flowrate for frictionless isentropic flow

Mdot=MdotA*dc*sc; % (kg/hr)
Mdot=2.2056*Mdot % (lbm/hr)
```

```
%Experimental Trials with Uncertainty Analysis%

%Input Varibles%

n=33942; %Index pointer
t_sat_start_p1=238.475; %Saturation temperature at trap inlet, deg F (start)
t_sat_finish_p1=238.040; %Saturation temperature at trap inlet, deg F(finish)
s_s=175.5; %Subcooling uncertainty
m=1.385; %Inlet pressure exponent

%Test Data%

p1_start=pressureonecut(1); %Pressure at steam trap inlet (start)
p2_start=pressuretwocut(1); %Pressure at steam trap outlet (start)
t_c_start=temperaturecut(1); %Temperature of condensate (start)
w_c_start=cutfit(1); % Mass of condensate plus barrel (start)
p1_finish=pressureonecut(n); %Pressure at steam trap inlet (finish)
p2_finish=pressuretwocut(n); %Pressure at steam trap outlet (finish)
t_c_finish= temperaturecut(n); %Temperature of condensate (finish)
w_c_finish=cutfit(n); %Mass of condensate plus barrel (finish)
time=timecut(n)-timecut(1); %Time interval

%Condensate Temperature Conversion (F)%
t_c_start=t_c_start*9/5+32;
t_c_finish=t_c_finish*9/5+32;

%Instrument Uncertainty%

lc1=0.005; %Load cell 1 uncertainty
daq1=0.001;%Data acquisition uncertainty
pt1=0.01; %Pressure transducer 1 uncertainty
rtd1=0.25; %Temperature transducer 1 uncertainty

%Capacity and General Calculations%

delt_t_start=t_sat_start_p1-t_c_start; %Temperature difference (start)
delt_t_finish=t_sat_finish_p1-t_c_finish; %Temperature difference (finish)

avg_diff_pressure=(p1_start-p2_start+p1_finish-p2_finish)/2;
avg_subcooling=(delt_t_start+delt_t_finish)/2;
capacity=(w_c_finish-w_c_start)*3600/time;
avg_inlet_pressure=(p1_start+p1_finish)/2;
avg_sat_temperature=(t_sat_start_p1+t_sat_finish_p1)/2;
```

```
%Uncertainty Calculations%

m_m_s=3600/time; %Mass measurement sensitivity
m_m_u=lc1*(w_c_start+w_c_finish)/2; %Mass measurement uncertainty
t_i_s=3600*(w_c_finish-w_c_start)/(time)^2; %Time interval sensitivity
t_i_u=daq1*time; %Time interval uncertainty
i_p_e= m; %Inlet pressue expoent
i_p_s=i_p_e*capacity/avg_inlet_pressure; %Inlet pressure sensitivity
i_p_m_u=pt1*avg_inlet_pressure; %Inlet pressure uncertainty
s_m_u= sqrt(((t_sat_start_p1-t_sat_finish_p1)/(p1_start-p1_finish))^2*pt1^2+rtd1^2); %Subcooling measurment uncertanity

%Propagation of Uncertainity%

term1=m_m_s^2*m_m_u^2;
term2=t_i_s^2*t_i_u^2;
term3=i_p_s^2*i_p_m_u^2;
term4=s_s^2*s_m_u^2;

S=term1+term2+term3+term4;

%Overall Uncertainity%

overall_uncertainty=sqrt(S)

%Relative Overall Uncertainty%

relative_overall_uncertainty=overall_uncertainty/capacity*100 %Percent relative overall uncertainty

T1UA=[p1_start;p2_start;t_sat_start_p1;t_c_start;delt_t_start;
   w_c_start;p1_finish;p2_finish;t_sat_finish_p1;t_c_finish;delt_t_finish;
   w_c_finish;time;0;0;0;avg_diff_pressure;avg_subcooling;capacity;avg_inlet_pressure
   avg_sat_temperature;0;0;0;m_m_s;m_m_u;term1;t_i_s;t_i_u;term2;i_p_e;i_p_s;i_p_m_u;term3;s_s;s_m_u;term4;
   S;overall_uncertainty;relative_overall_uncertainty];

save T1UA.mat;

clear all;
```

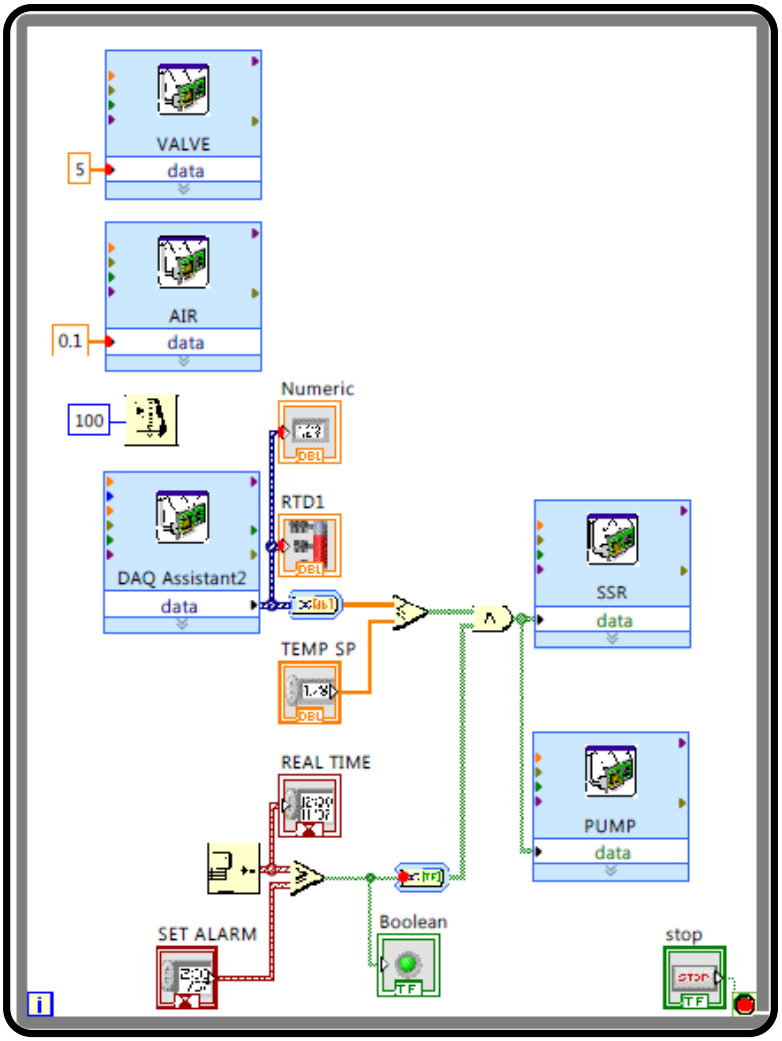

Source Code (Timing Circuit)

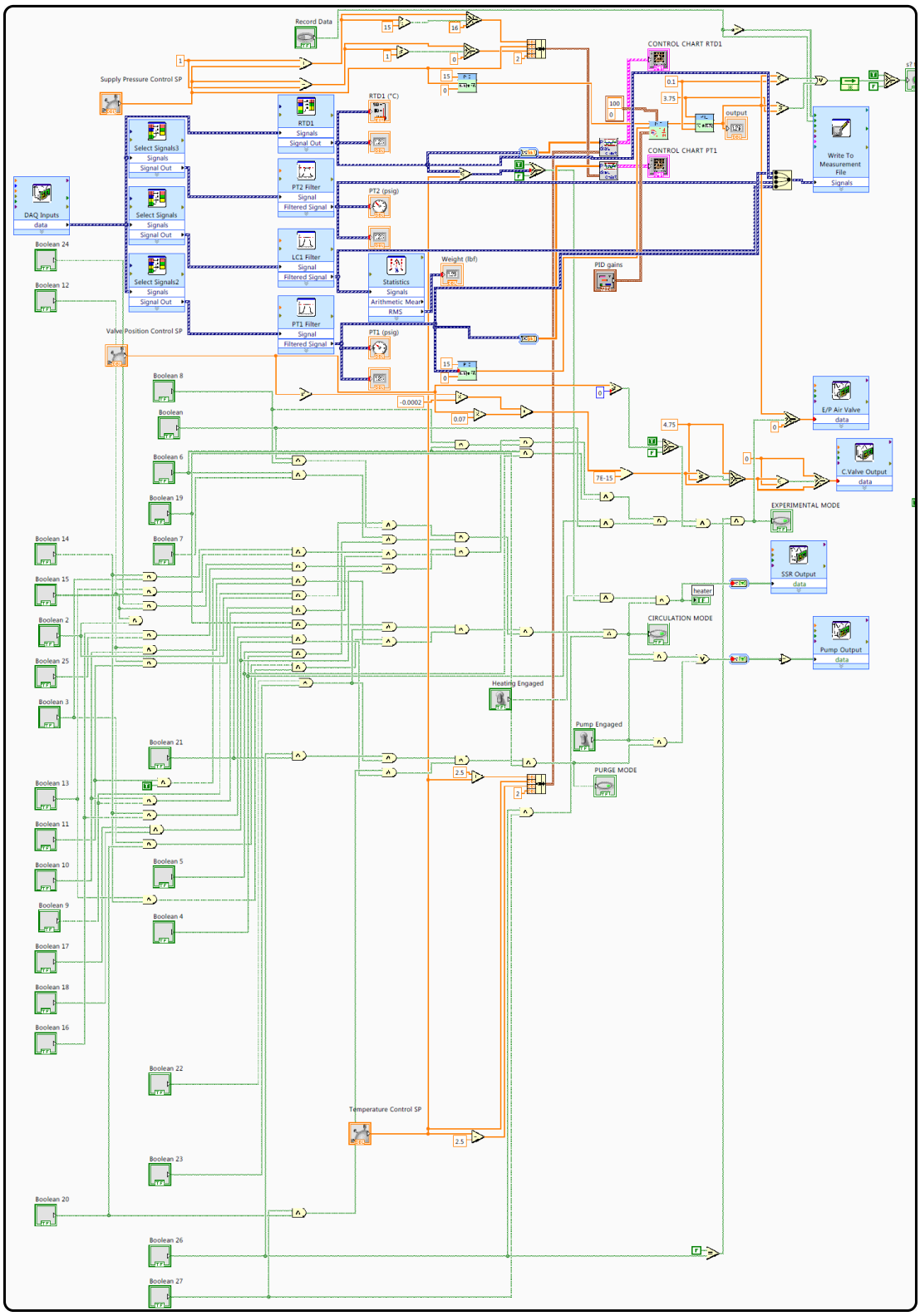

Source Code for Experimental and Confirmation Trials

Appendix E

Experimental and Confirmation Trial Data (Graphical)

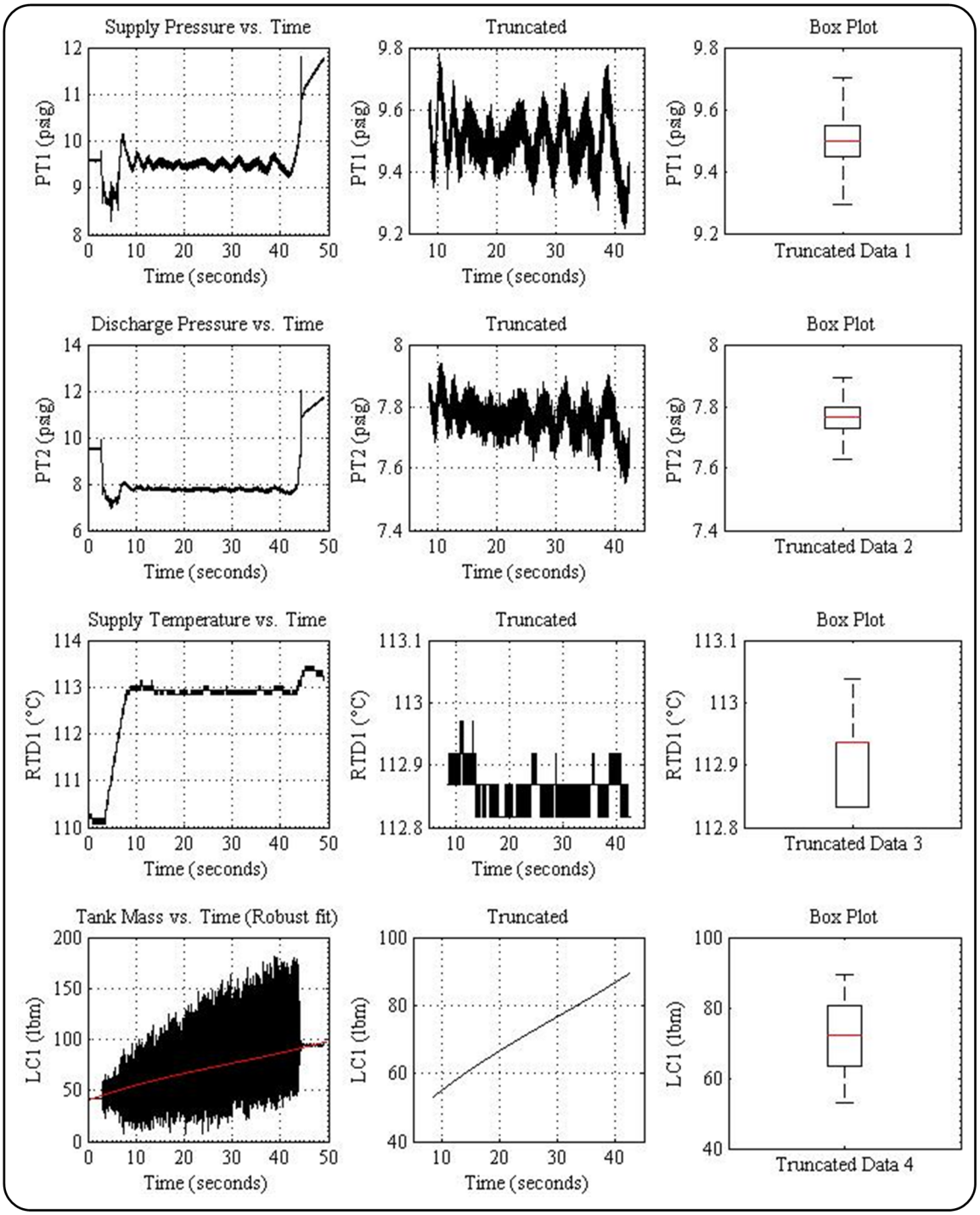

Trial 1

[Pressure = 9.50 psig, Temperature = 112.76°C, Valve Position = 100.0%]

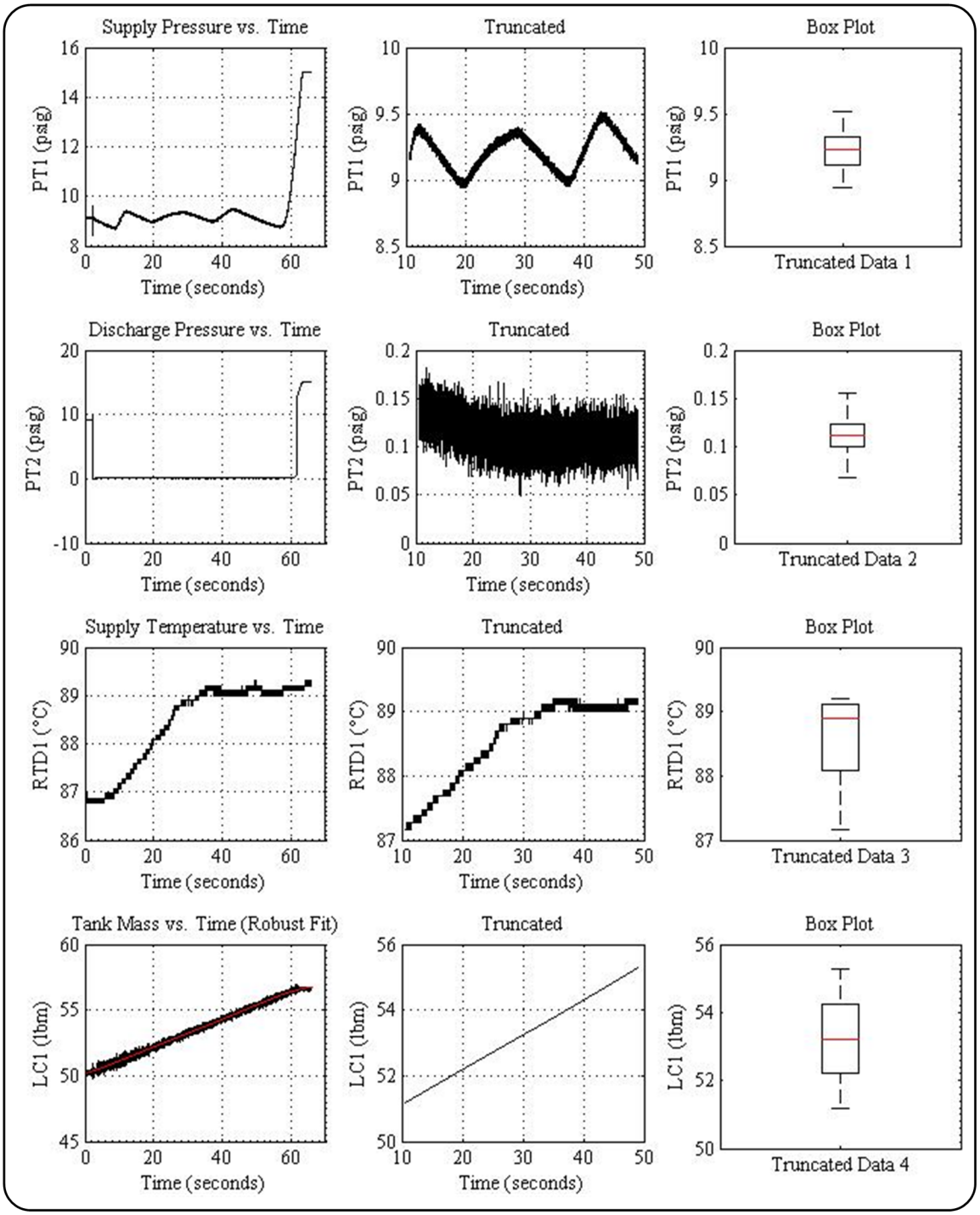

Trial 2

[Pressure = 9.18 psig, Temperature = 90.00°C, Valve Position = 25.00%]

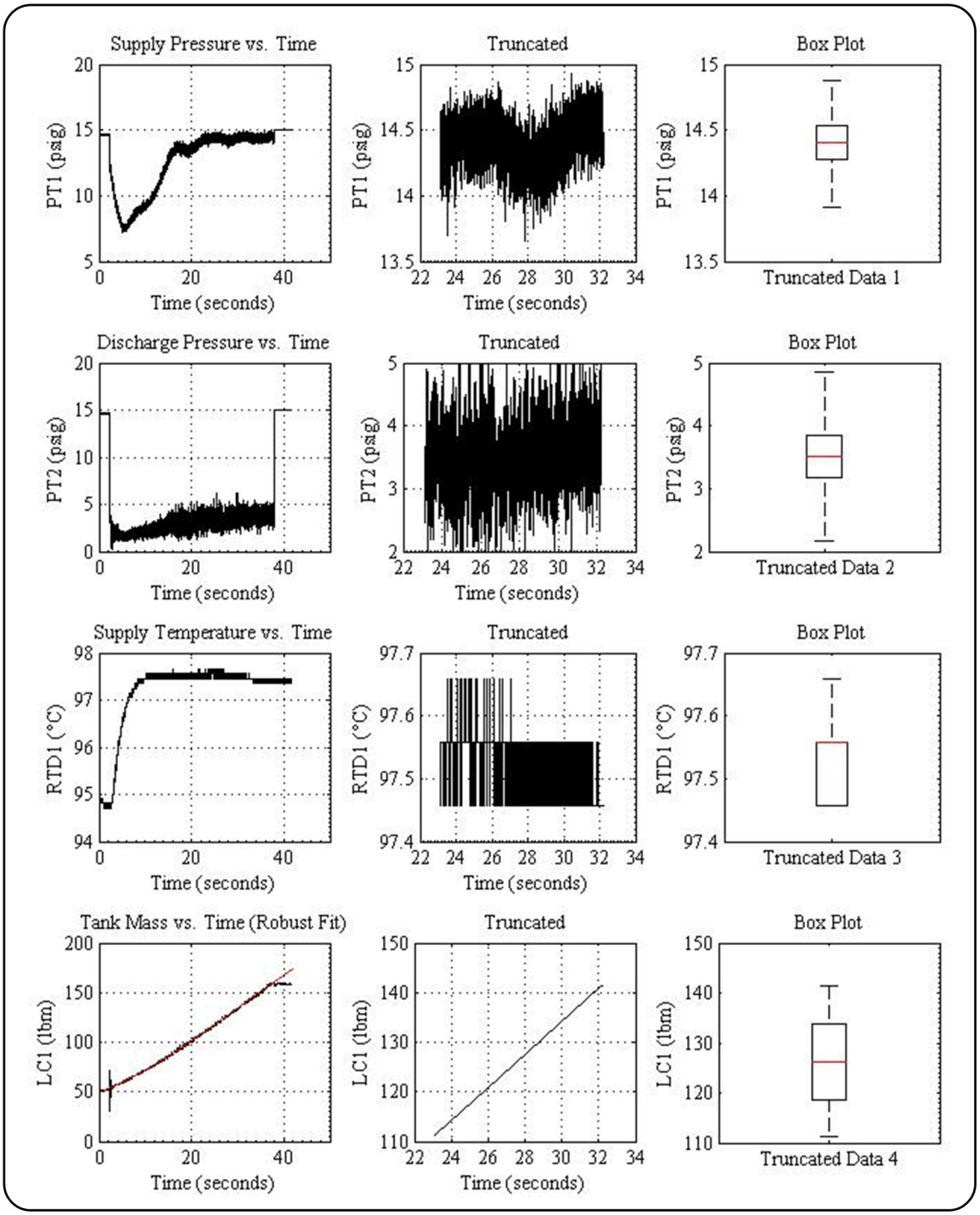

Trial 3

[Pressure = 14.50 psig, Temperature = 97.61°C, Valve Position = 74.88%]

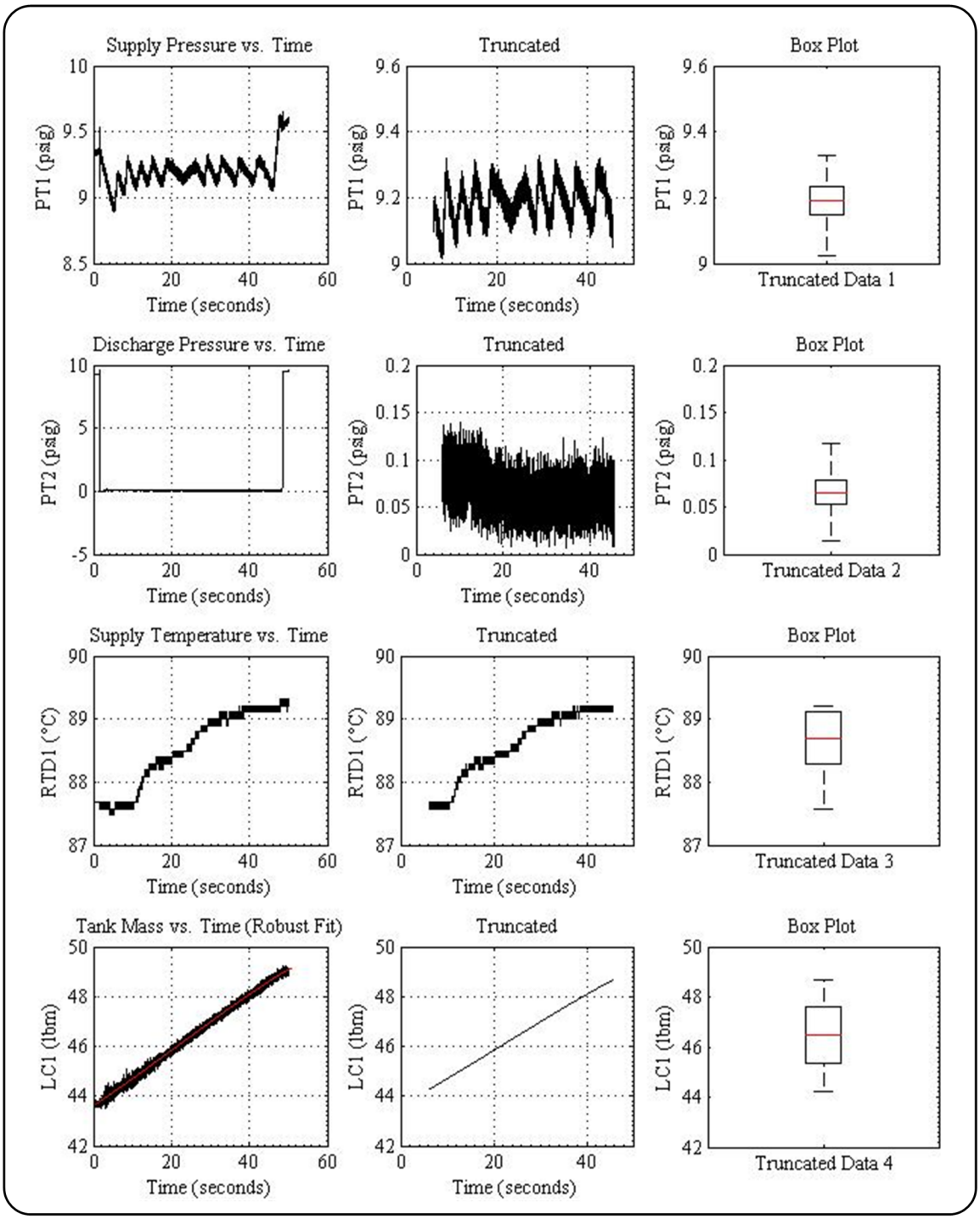

Trial 4

[Pressure = 9.18 psig, Temperature = 90.00°C, Valve Position = 25.00%]

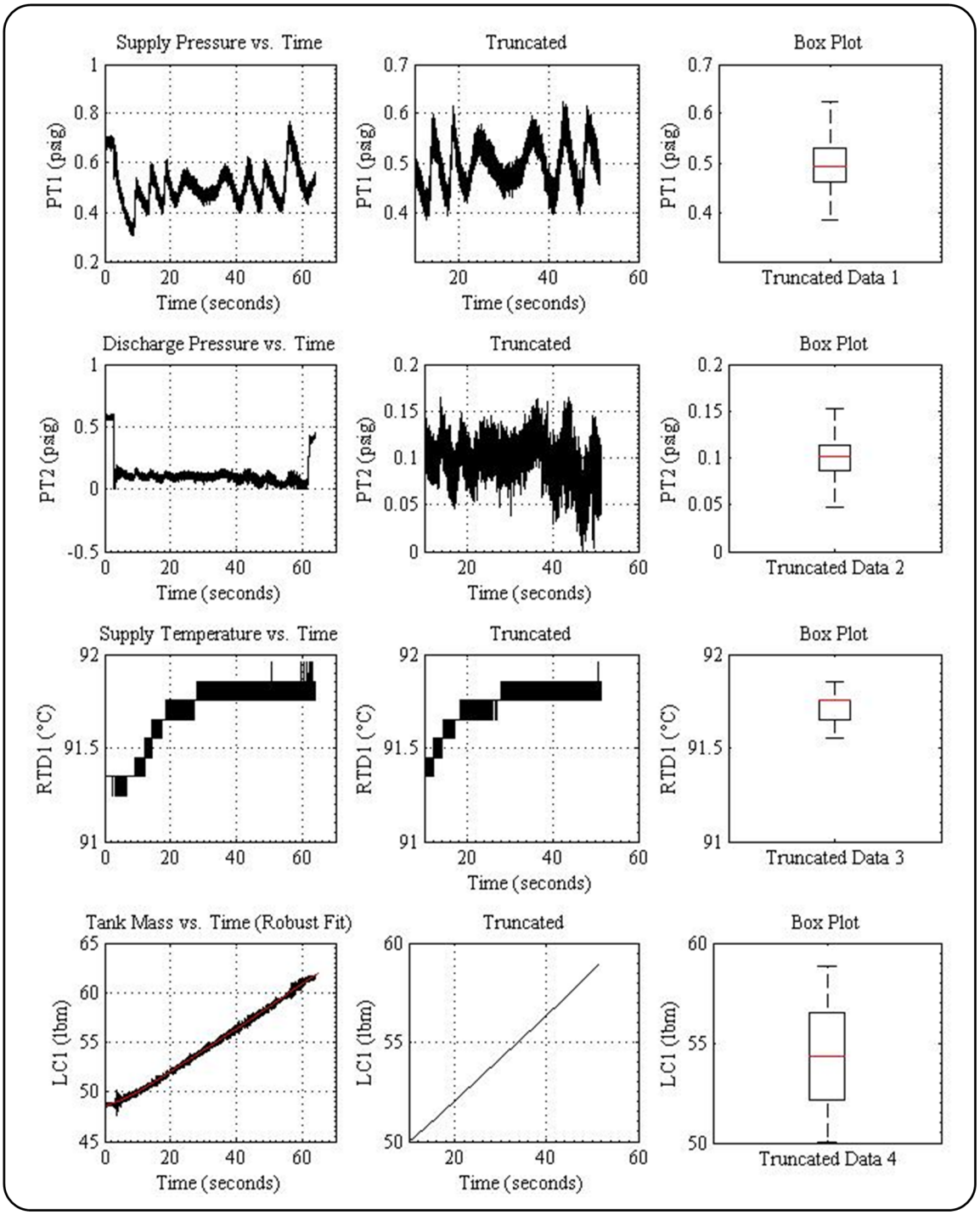

Trial 5

[Pressure = 0.50 psig, Temperature = 92.01°C, Valve Position = 53.50%]

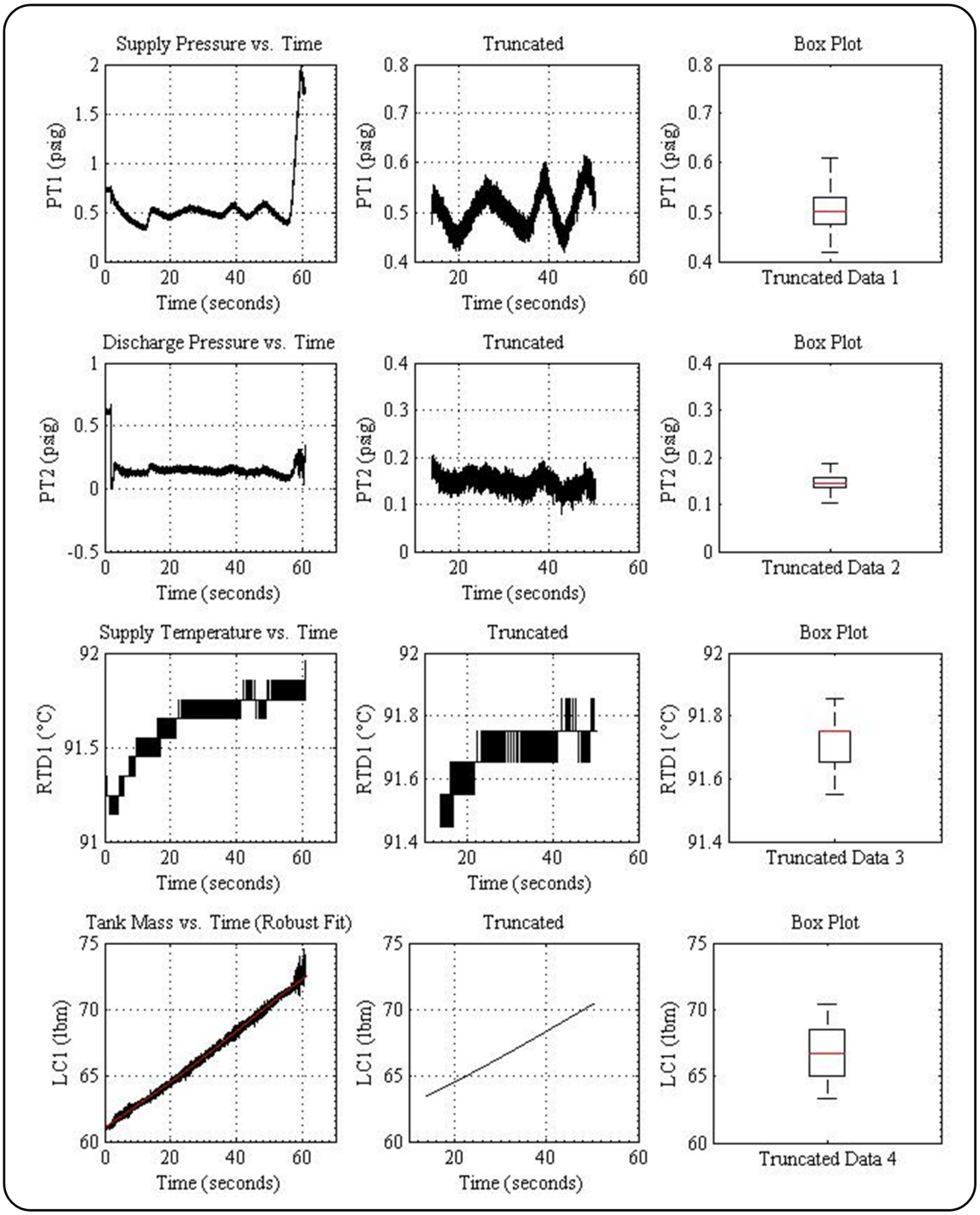

Trial 6

[Pressure = 0.50 psig, Temperature = 92.01°C, Valve Position = 53.50%]

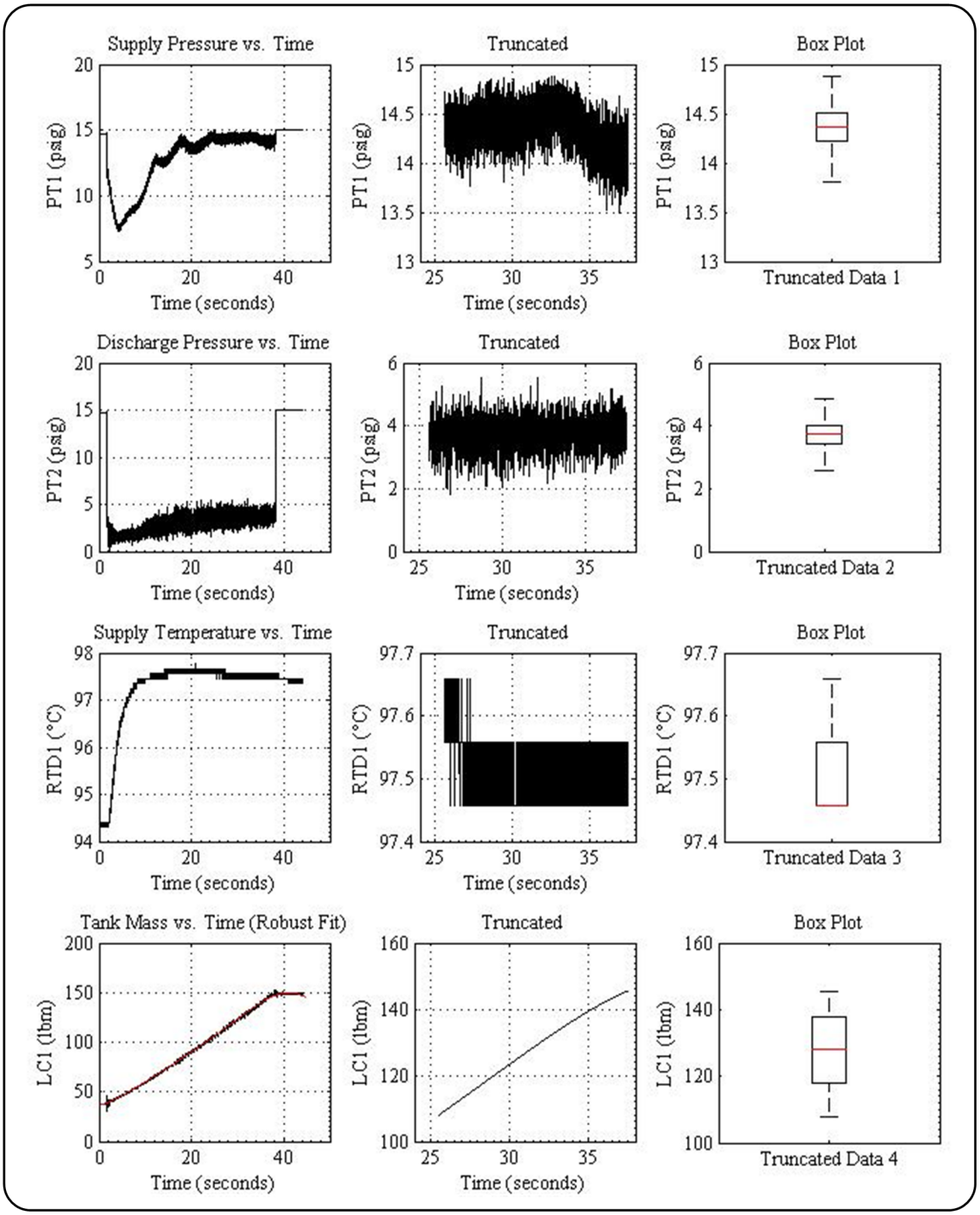

Trial 7

[Pressure = 14.50 psig, Temperature = 97.61°C, Valve Position = 74.88%]

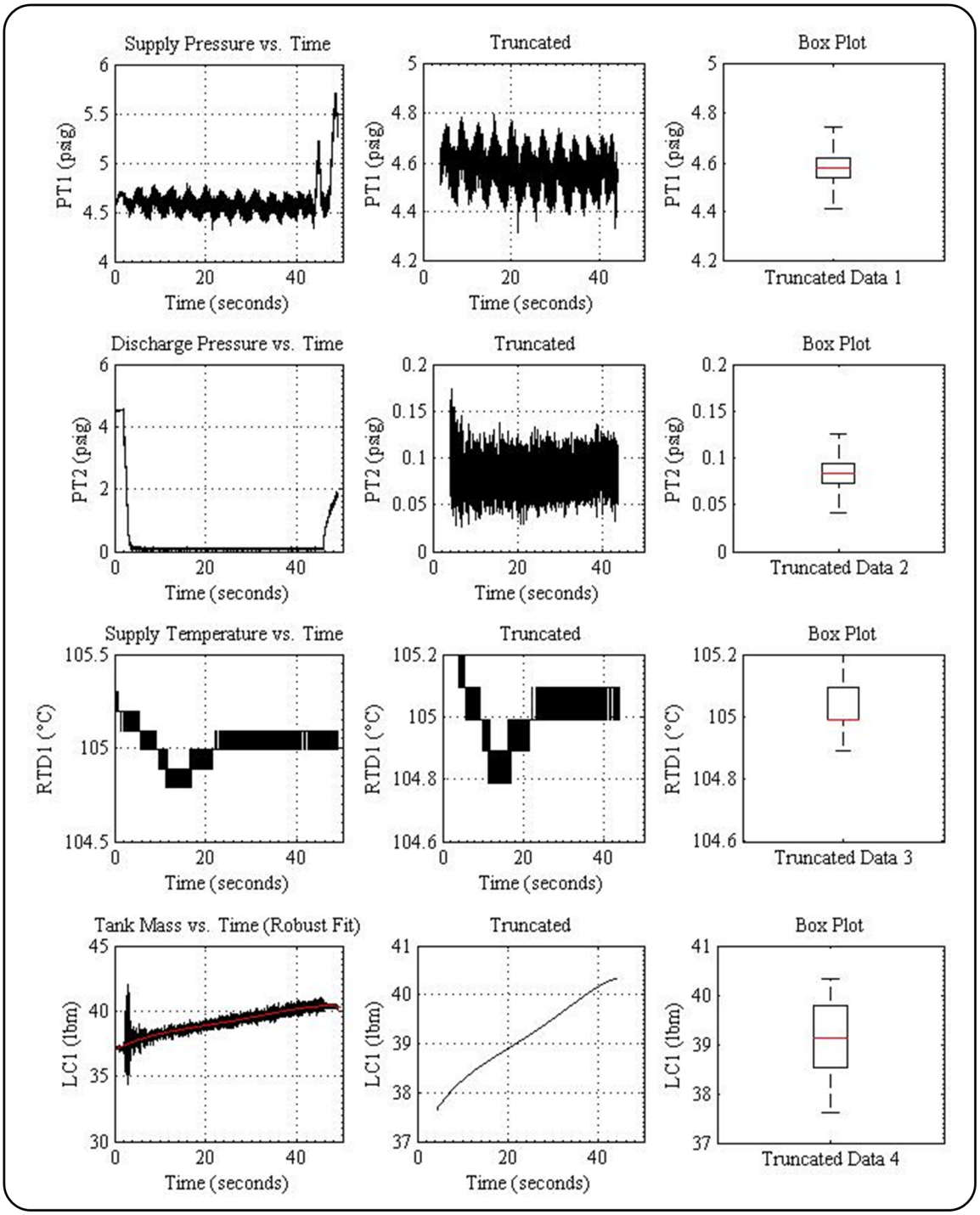

Trial 8

[Pressure = 4.57 psig, Temperature = 106.60°C, Valve Position = 25.00%]

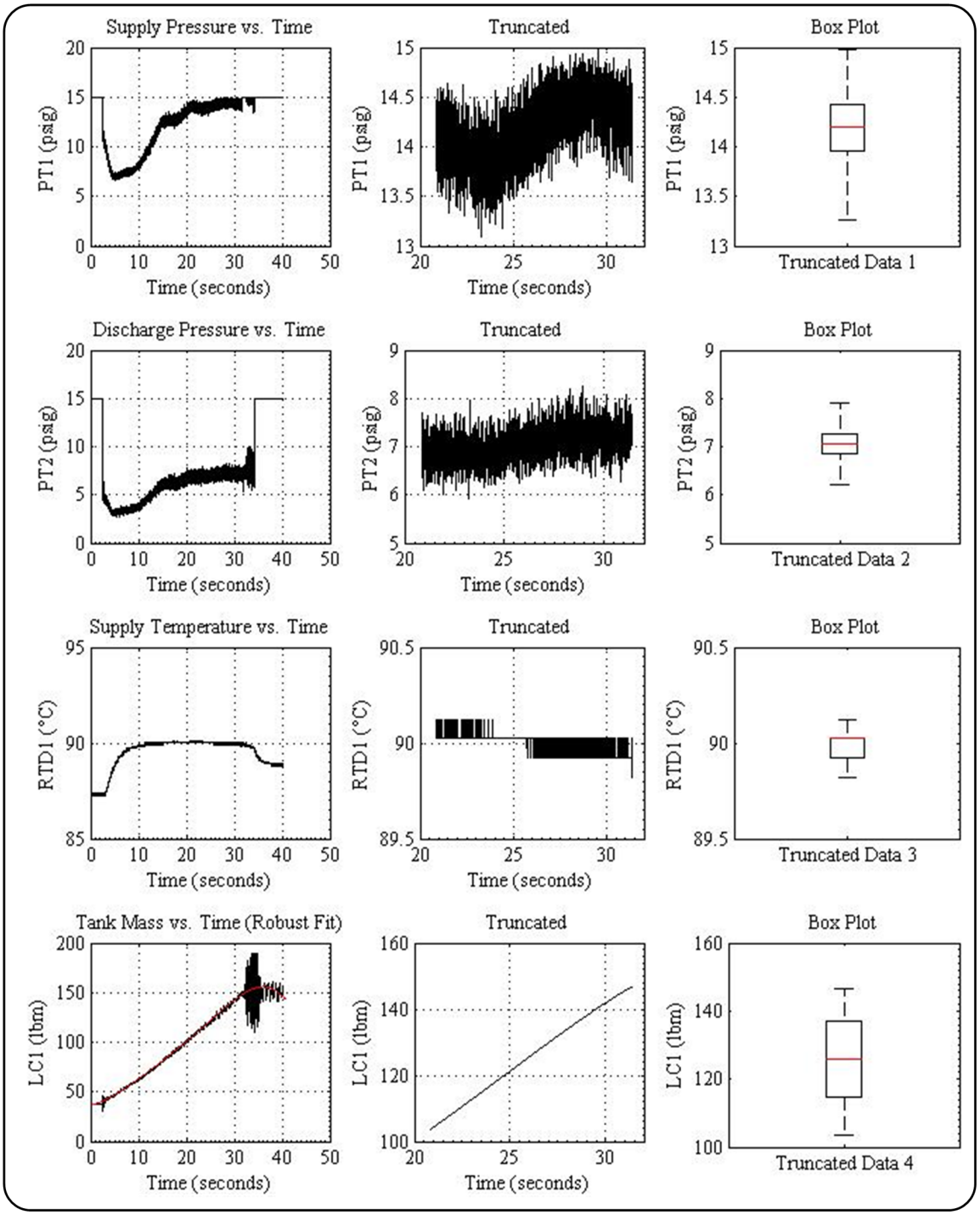

Trial 9

[Pressure = 14.50 psig, Temperature = 90.00°C, Valve Position = 100.00%]

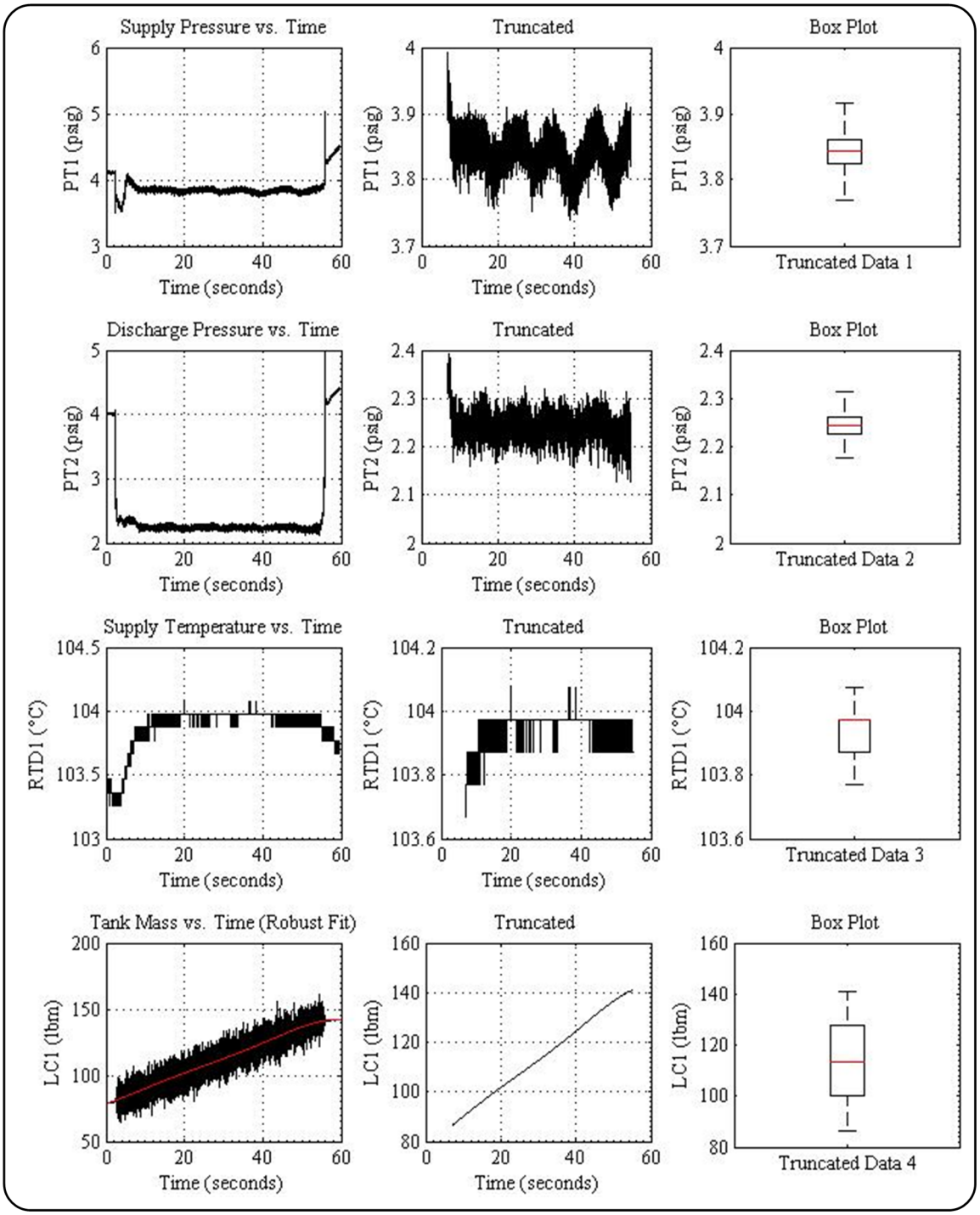

Trial 10

[Pressure = 3.84 psig, Temperature = 105.60°C, Valve Position = 79.38%]

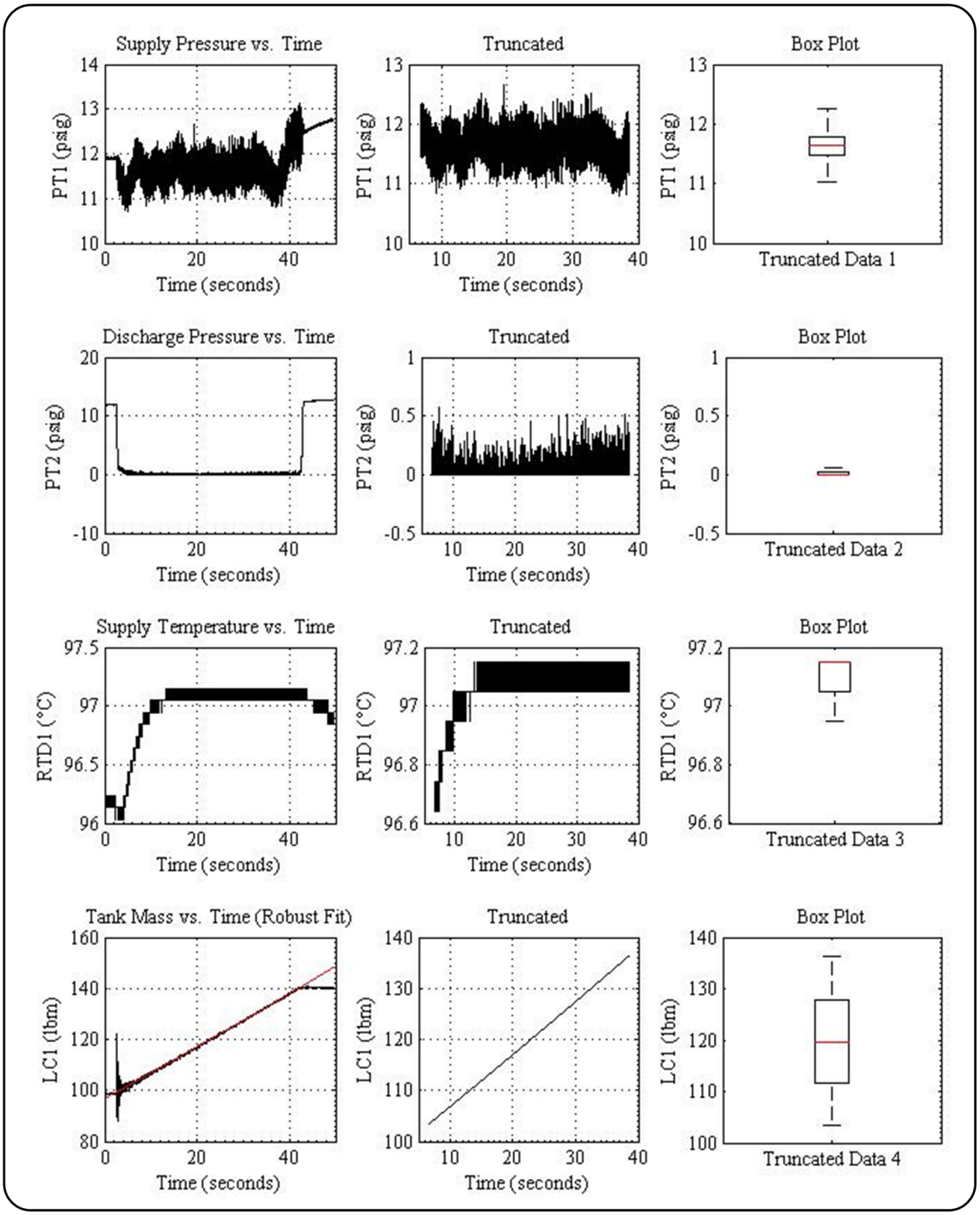

Trial 11

[Pressure = 11.63 psig, Temperature = 96.68°C, Valve Position = 48.63%]

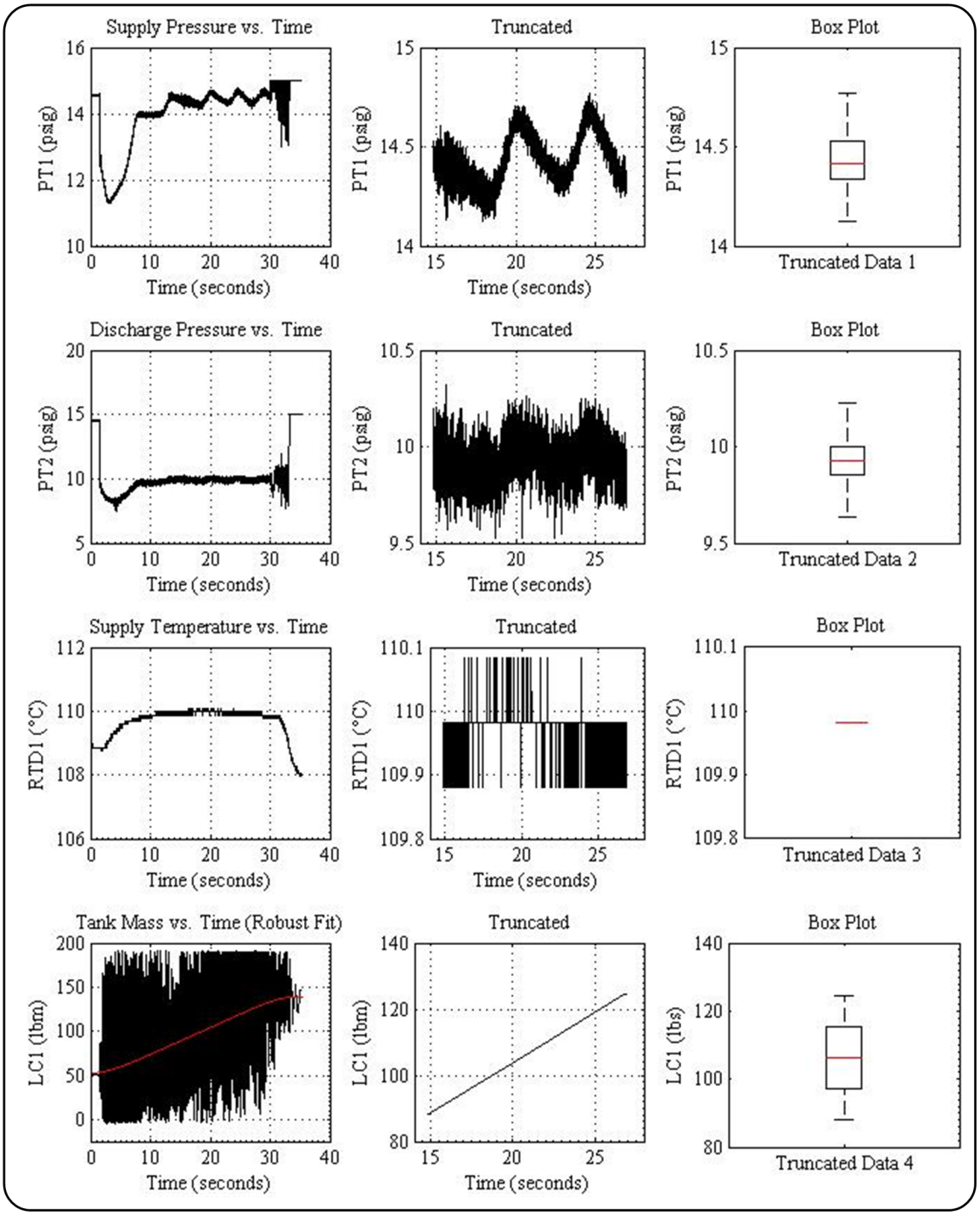

Trial 12

[Pressure = 14.50 psig, Temperature = 109.94°C, Valve Position = 100.00%]

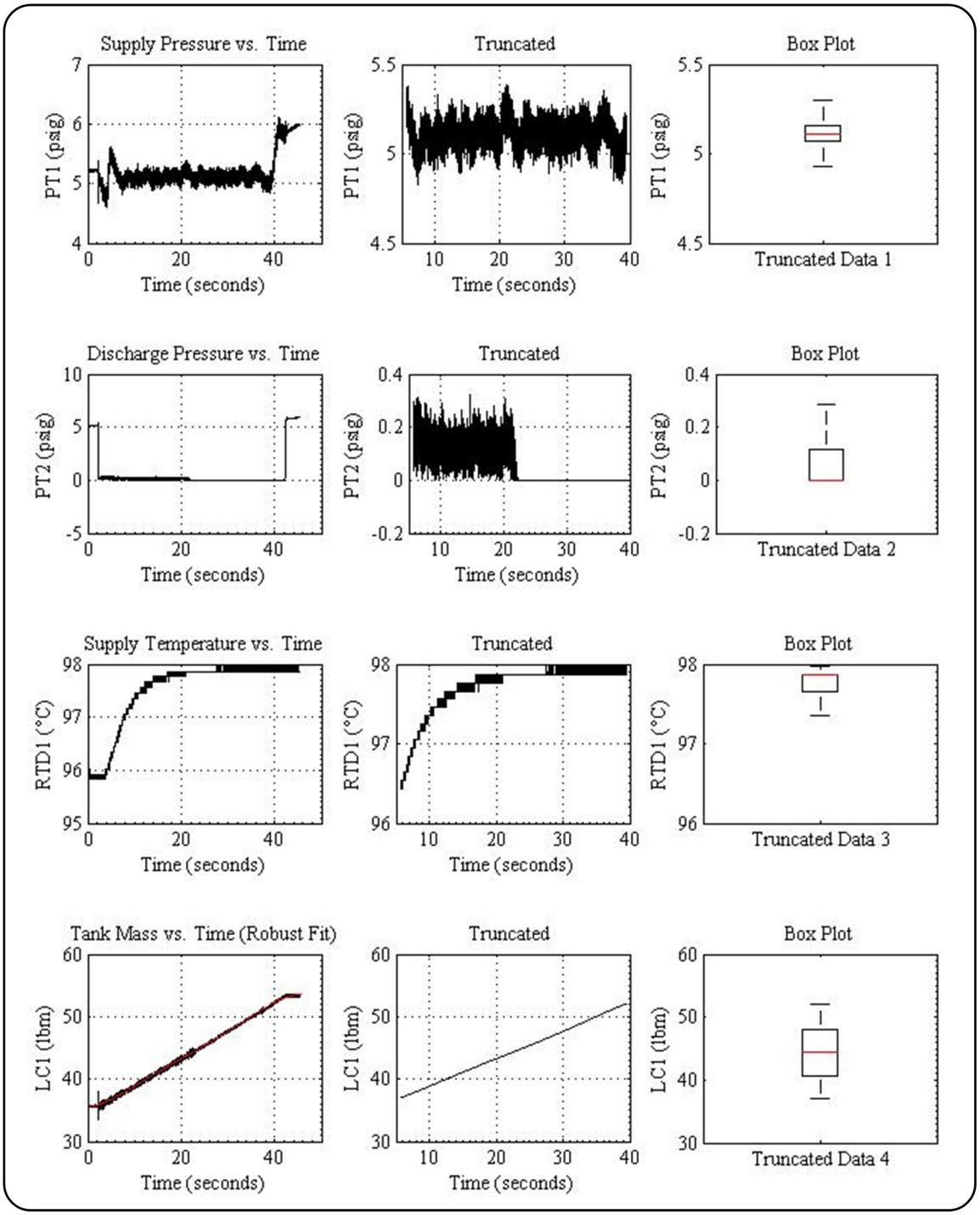

Trial 13

[Pressure = 5.12 psig, Temperature = 97.92°C, Valve Position = 43.00%]

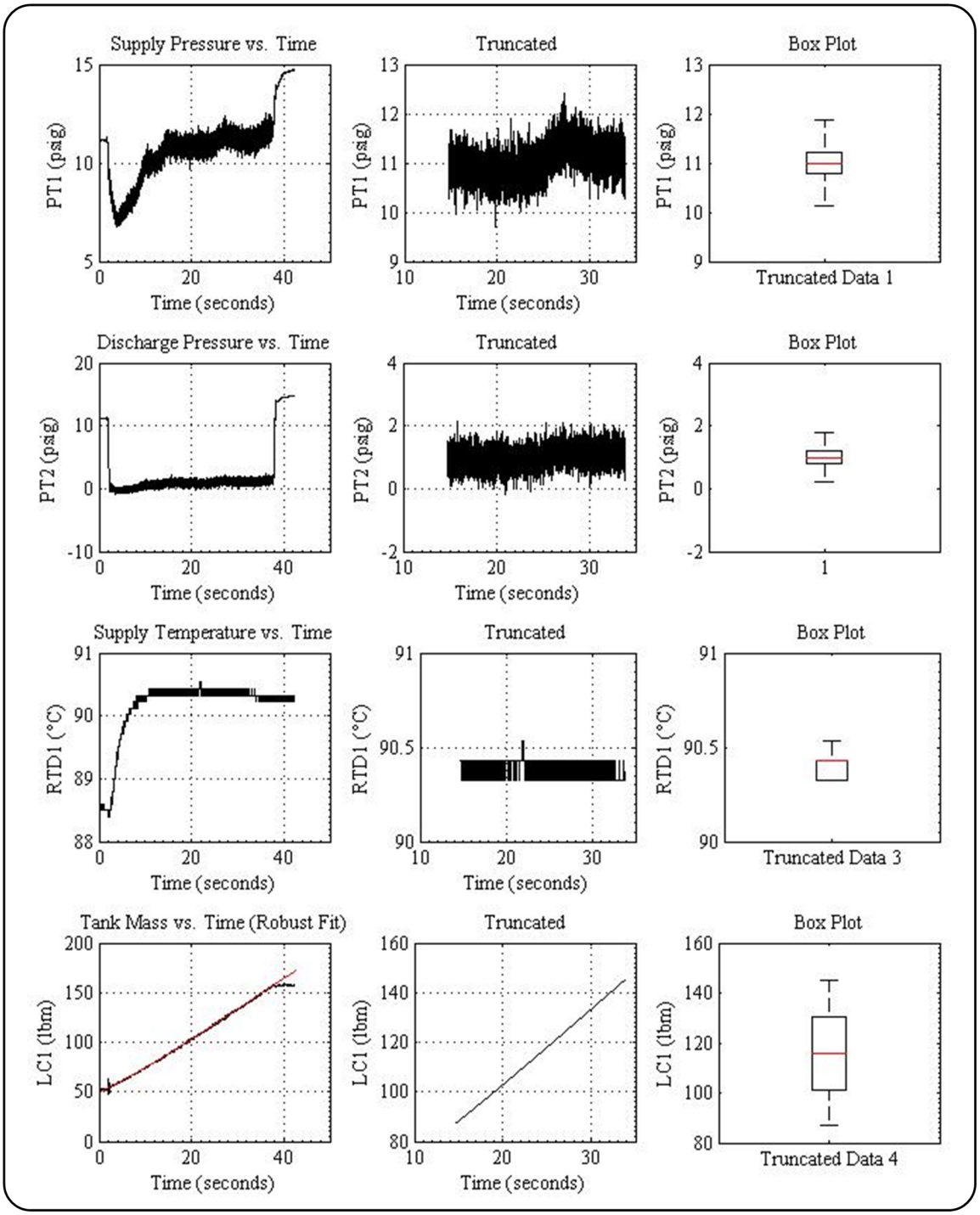

Trial 14

[Pressure = 11.00 psig, Temperature = 90.00°C, Valve Position = 74.50%]

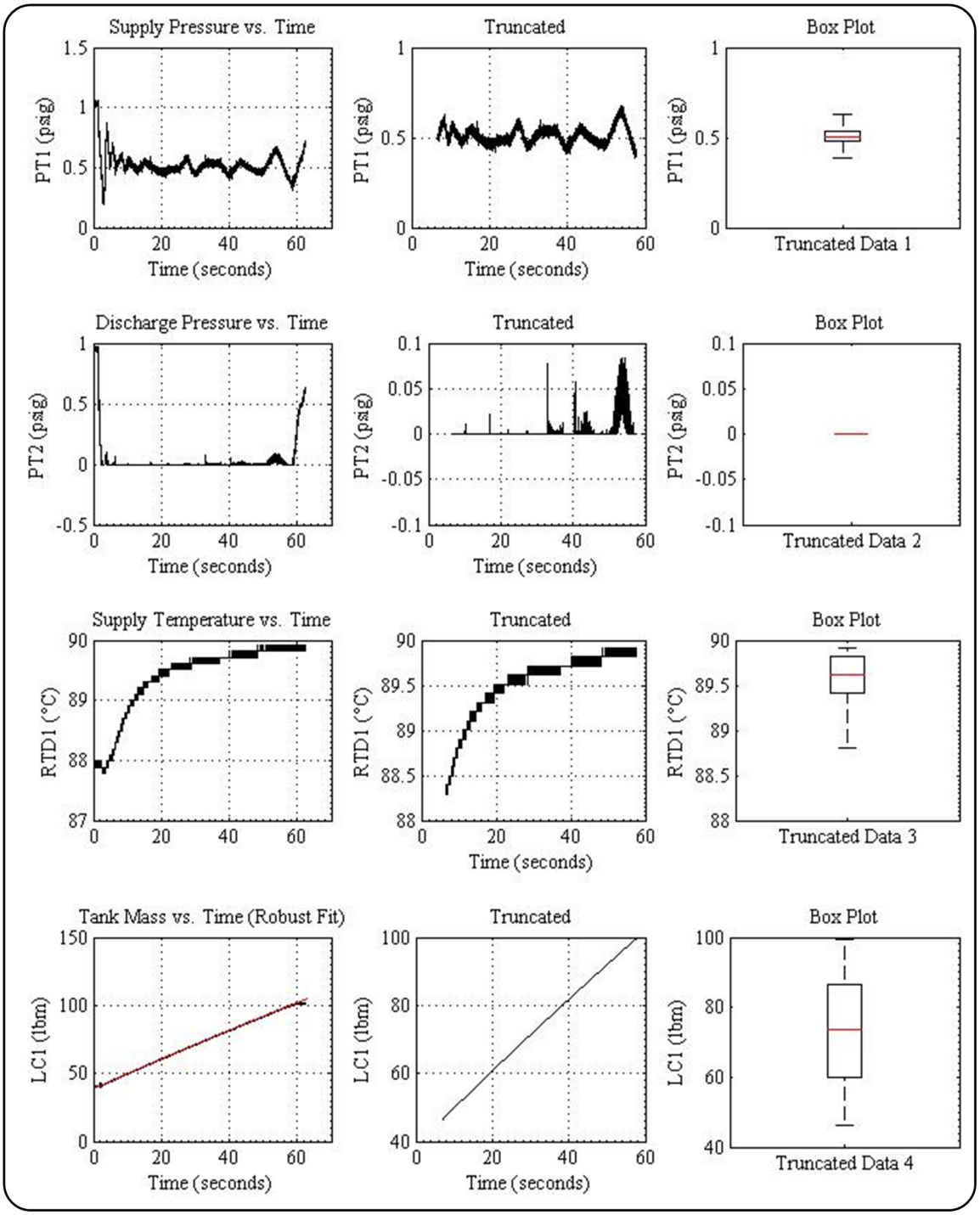

Trial 15

[Pressure = 0.50 psig, Temperature = 90.00°C, Valve Position = 99.25%]

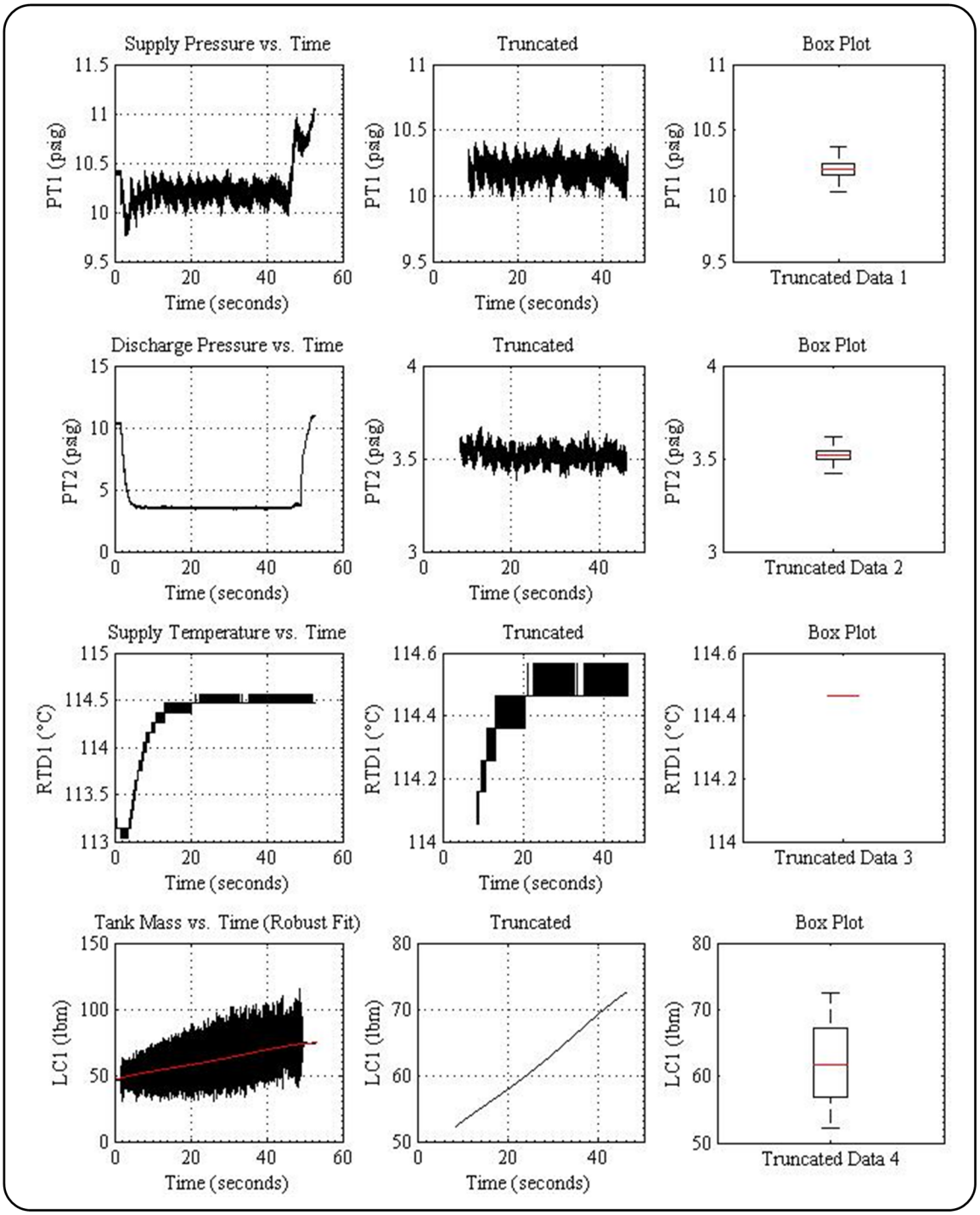

Trial 16

[Pressure = 10.21 psig, Temperature = 114.47°C, Valve Position = 49.00%]

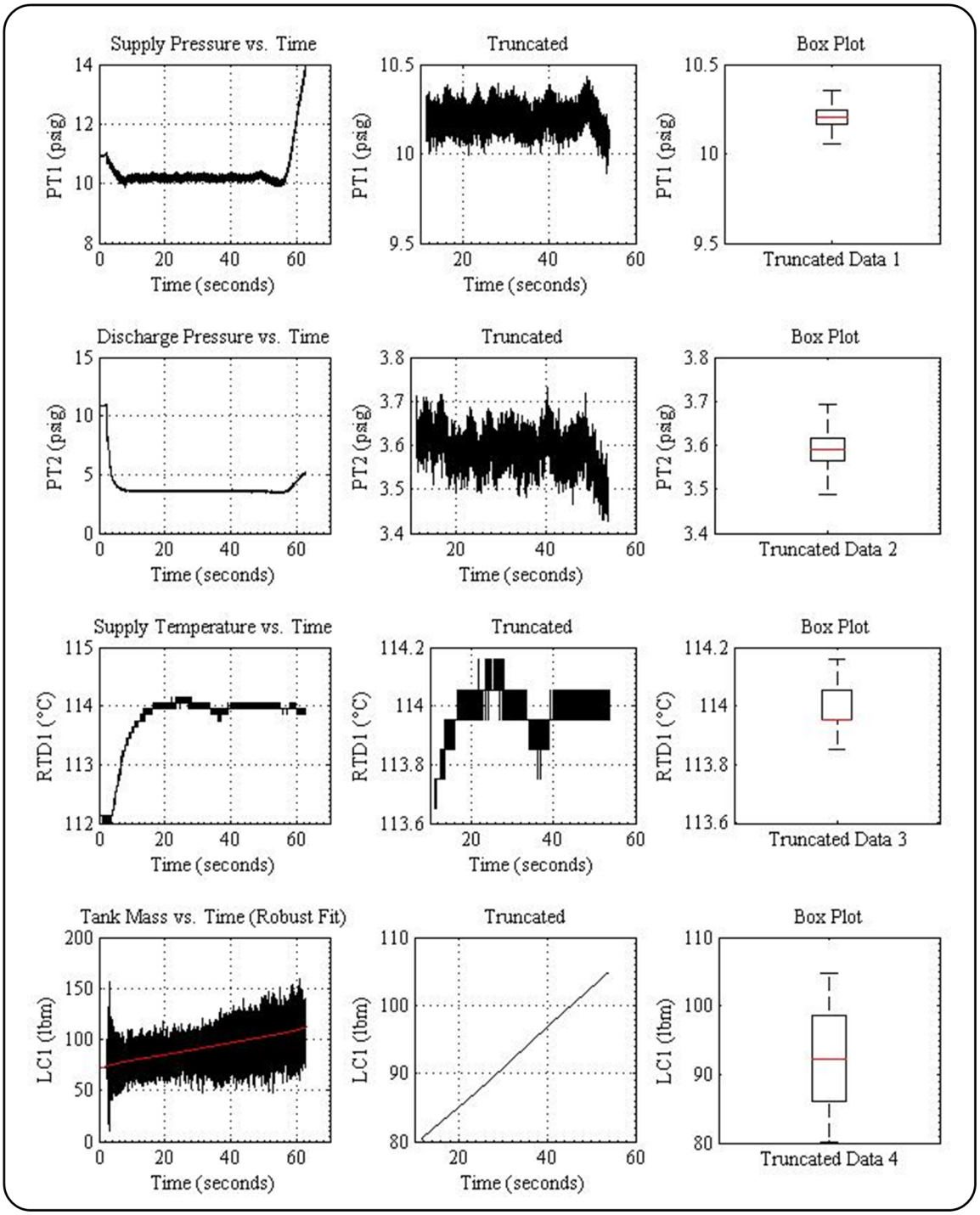

Trial 17

[Pressure = 10.21 psig, Temperature = 114.47°C, Valve Position = 49.00%]

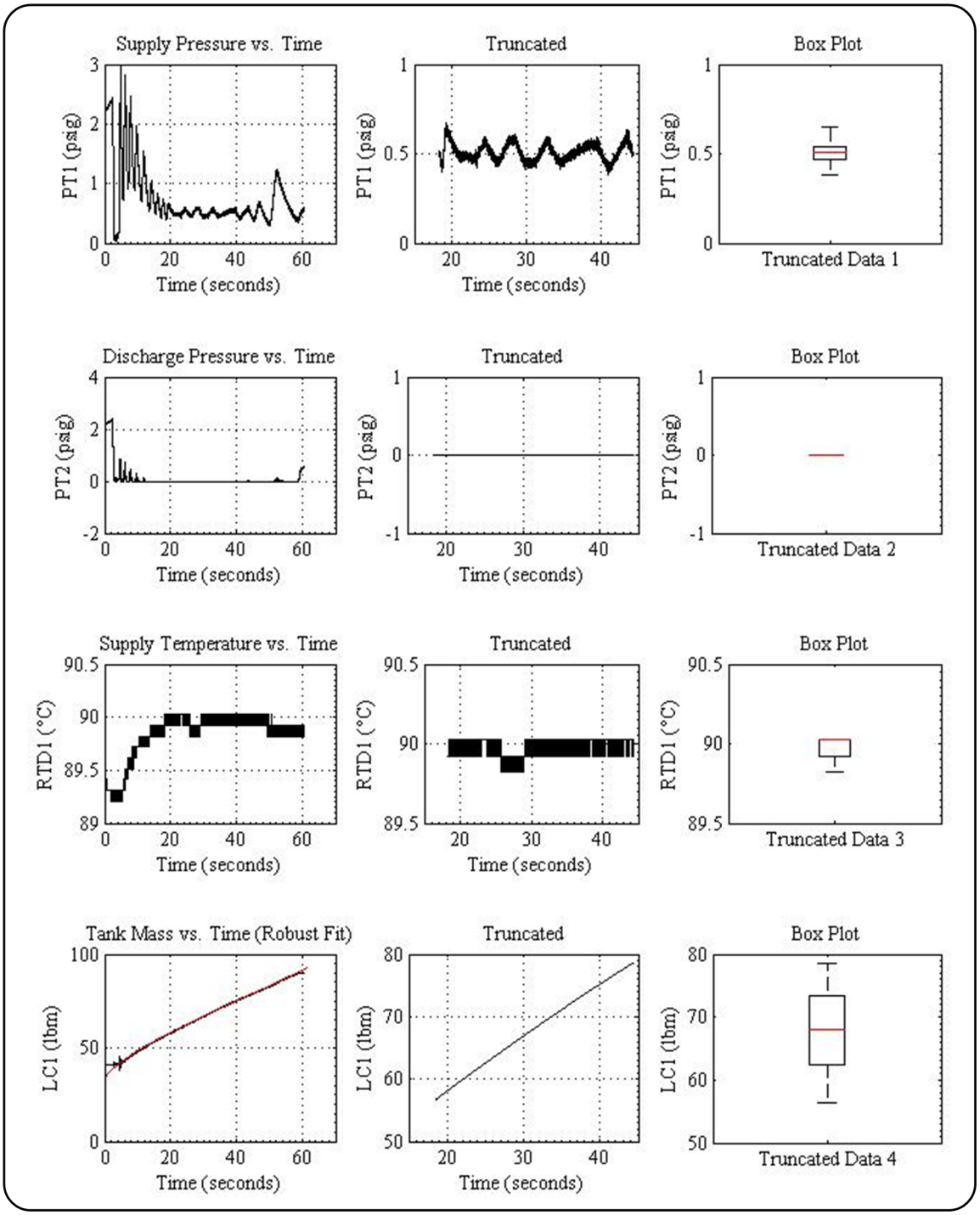

Trial 18

[Pressure = 0.50 psig, Temperature = 90.00°C, Valve Position = 75.63%]

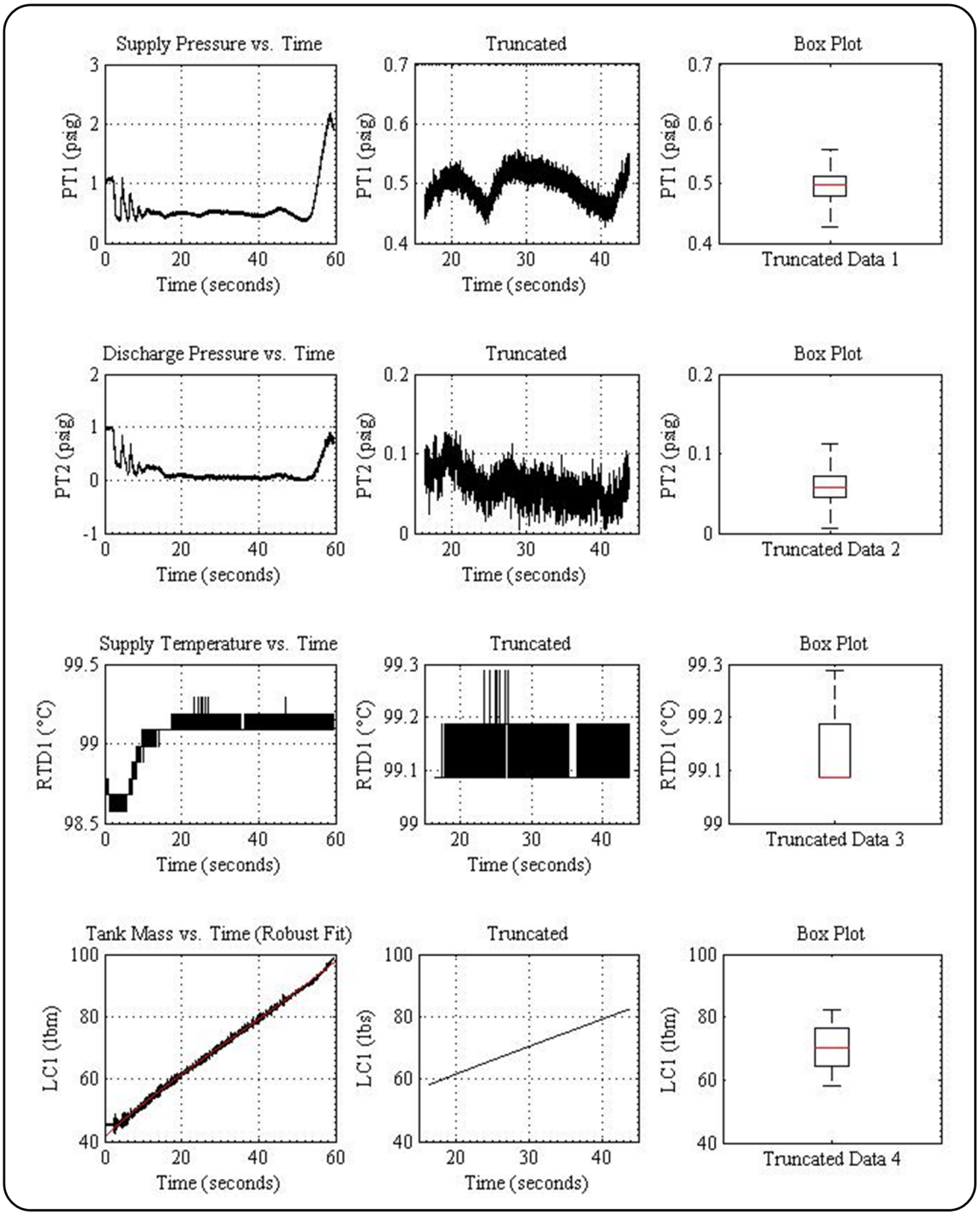

Trial 19

[Pressure = 0.50 psig, Temperature = 99.13°C, Valve Position = 100.00%]

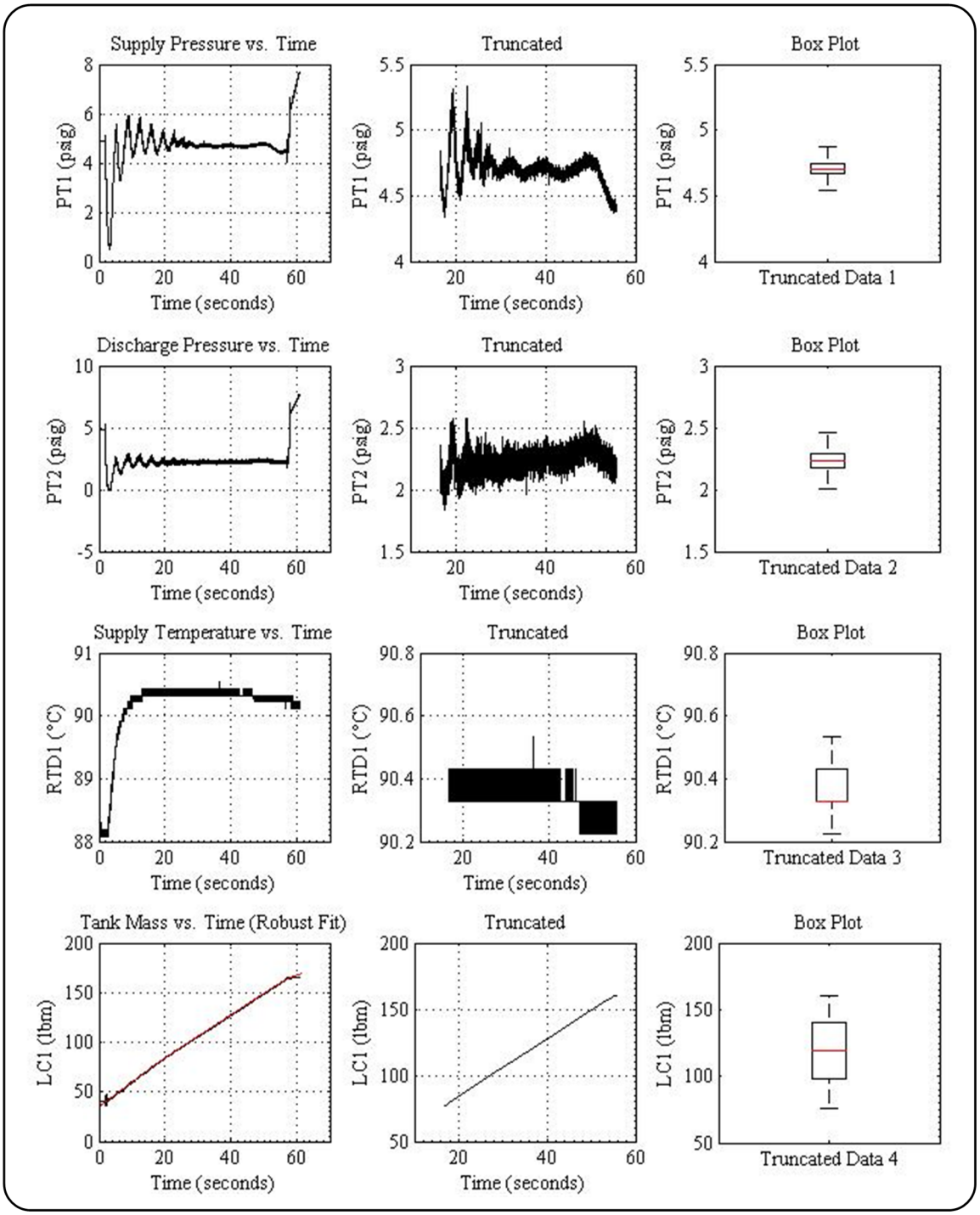

Trial 20

[Pressure = 4.70 psig, Temperature = 90.00°C, Valve Position = 100.00%]

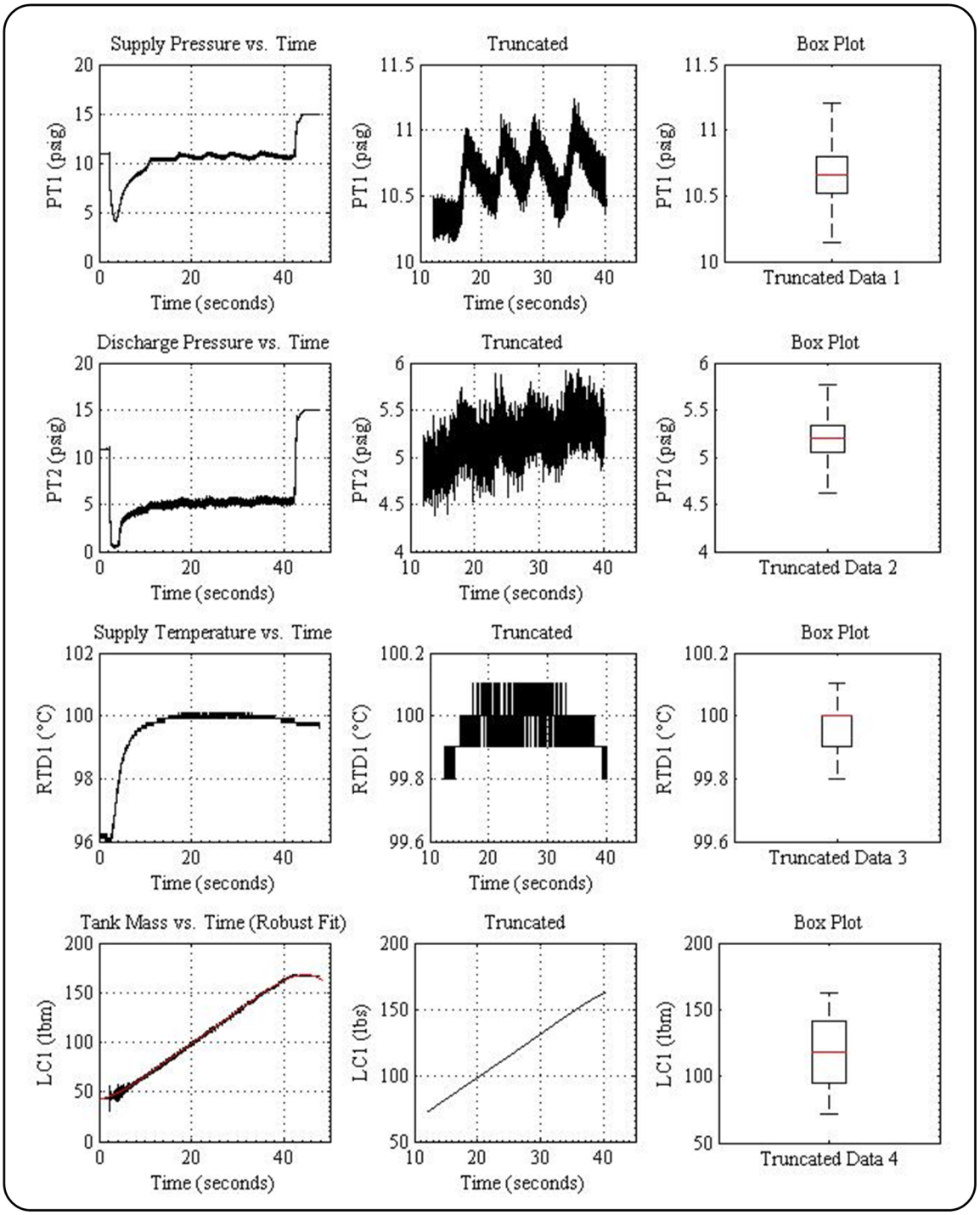

Trial 21

[Pressure = 10.72 psig, Temperature = 98.07°C, Valve Position = 100.00%]

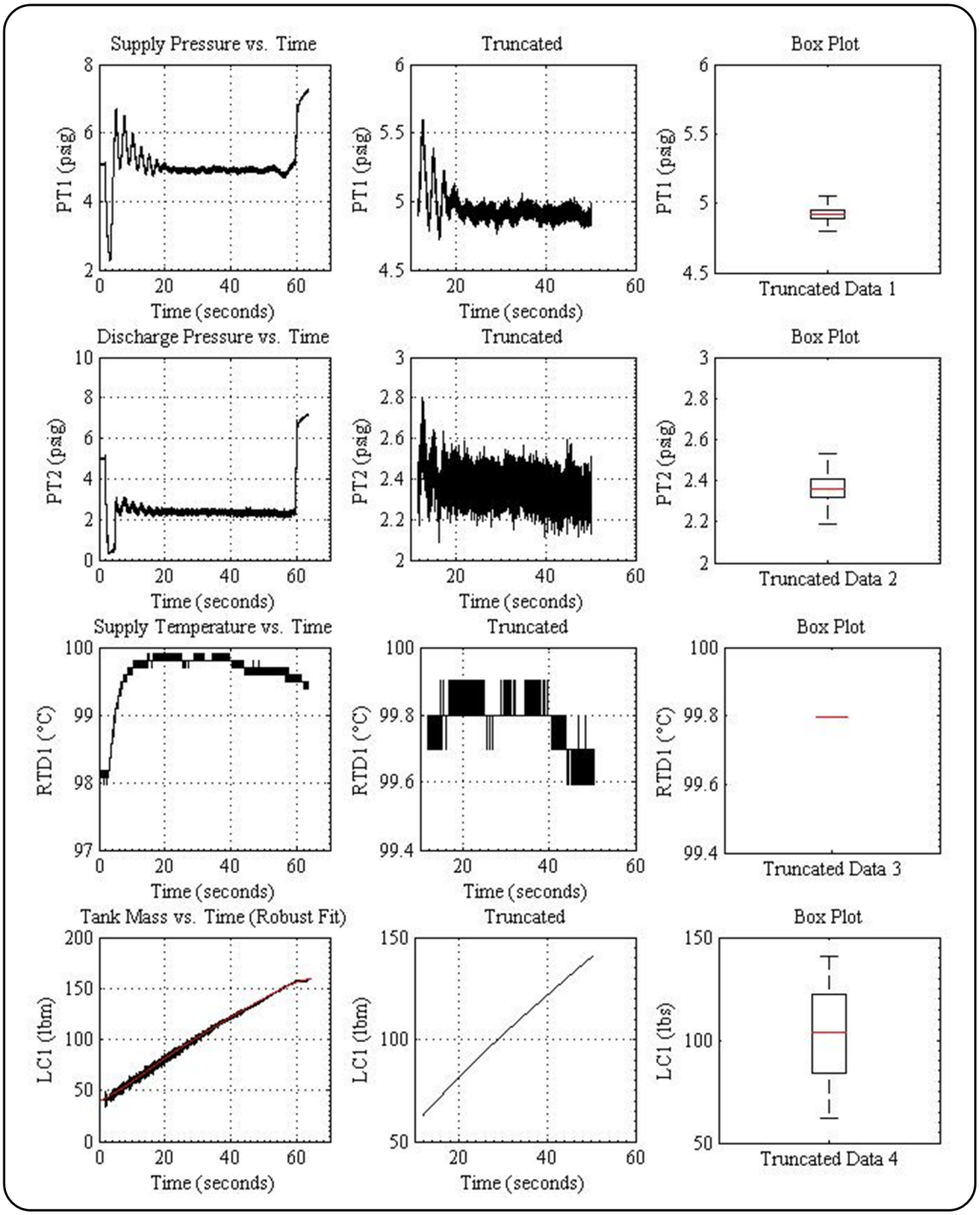

Trial 22

[Pressure = 4.91 psig, Temperature = 99.59°C, Valve Position = 82.38%]

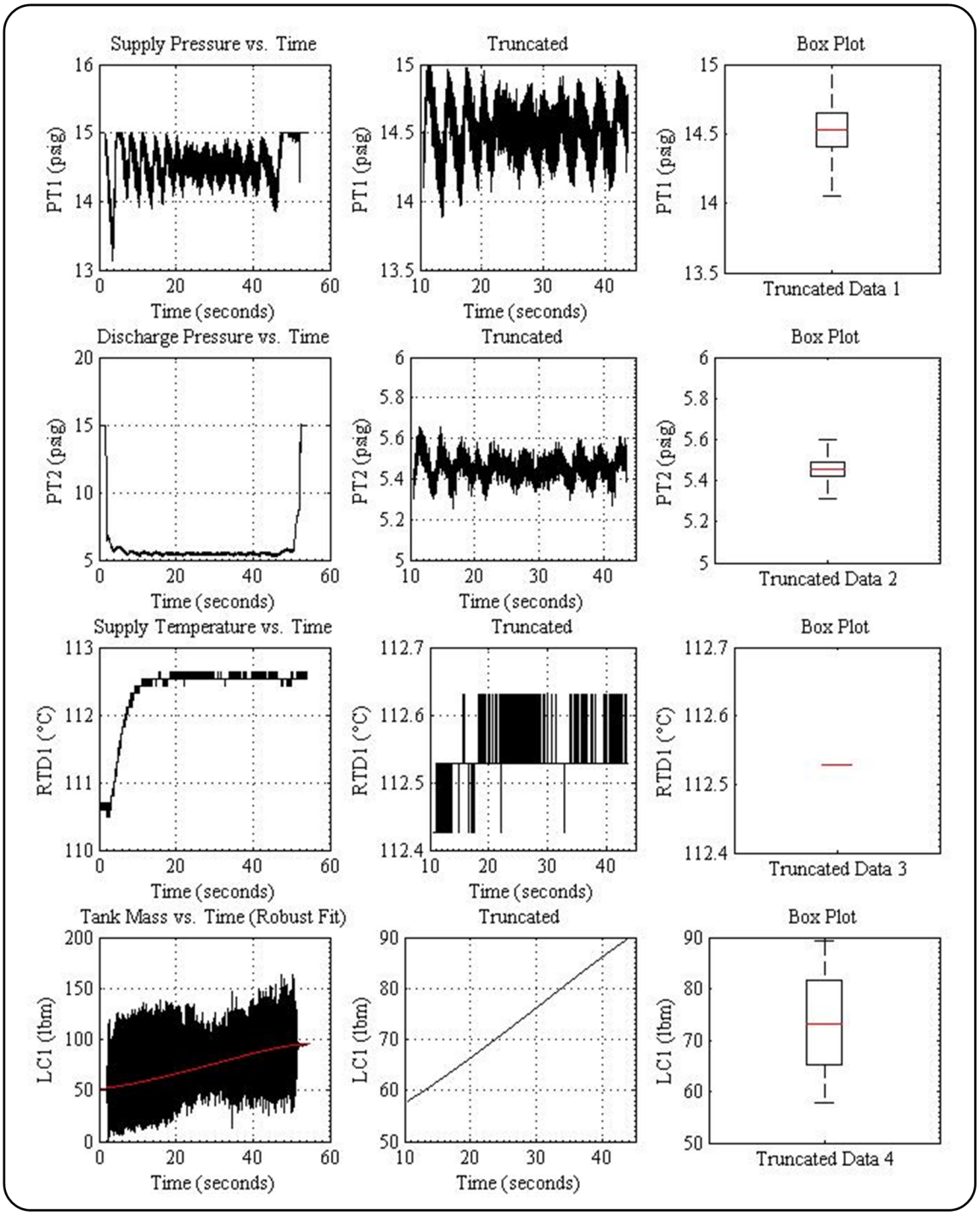

Trial 23

[Pressure = 14.5 psig, Temperature = 112.70°C, Valve Position = 49.00%]

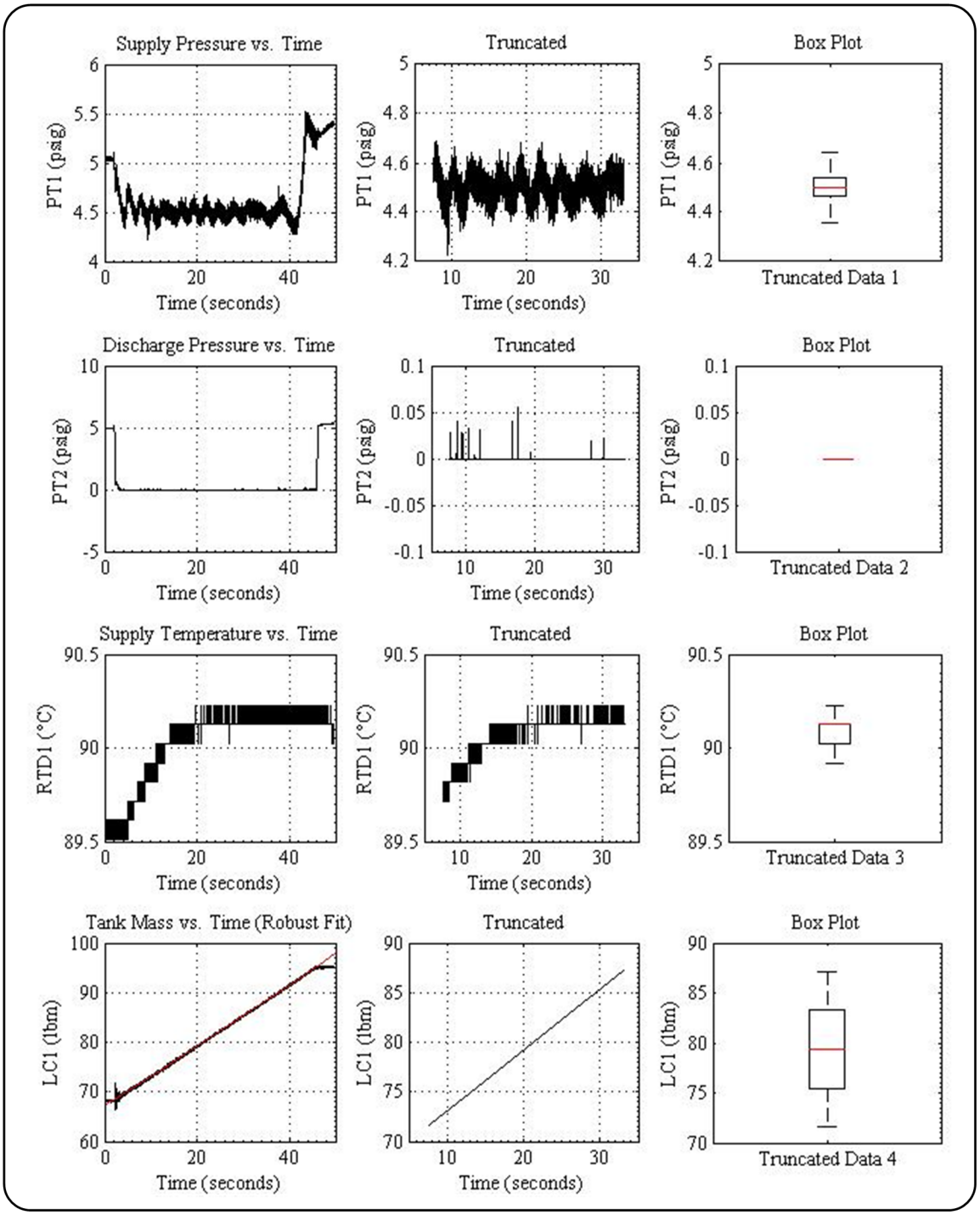

Trial 24

[Pressure = 4.49 psig, Temperature = 90.00°C, Valve Position = 46.98%]

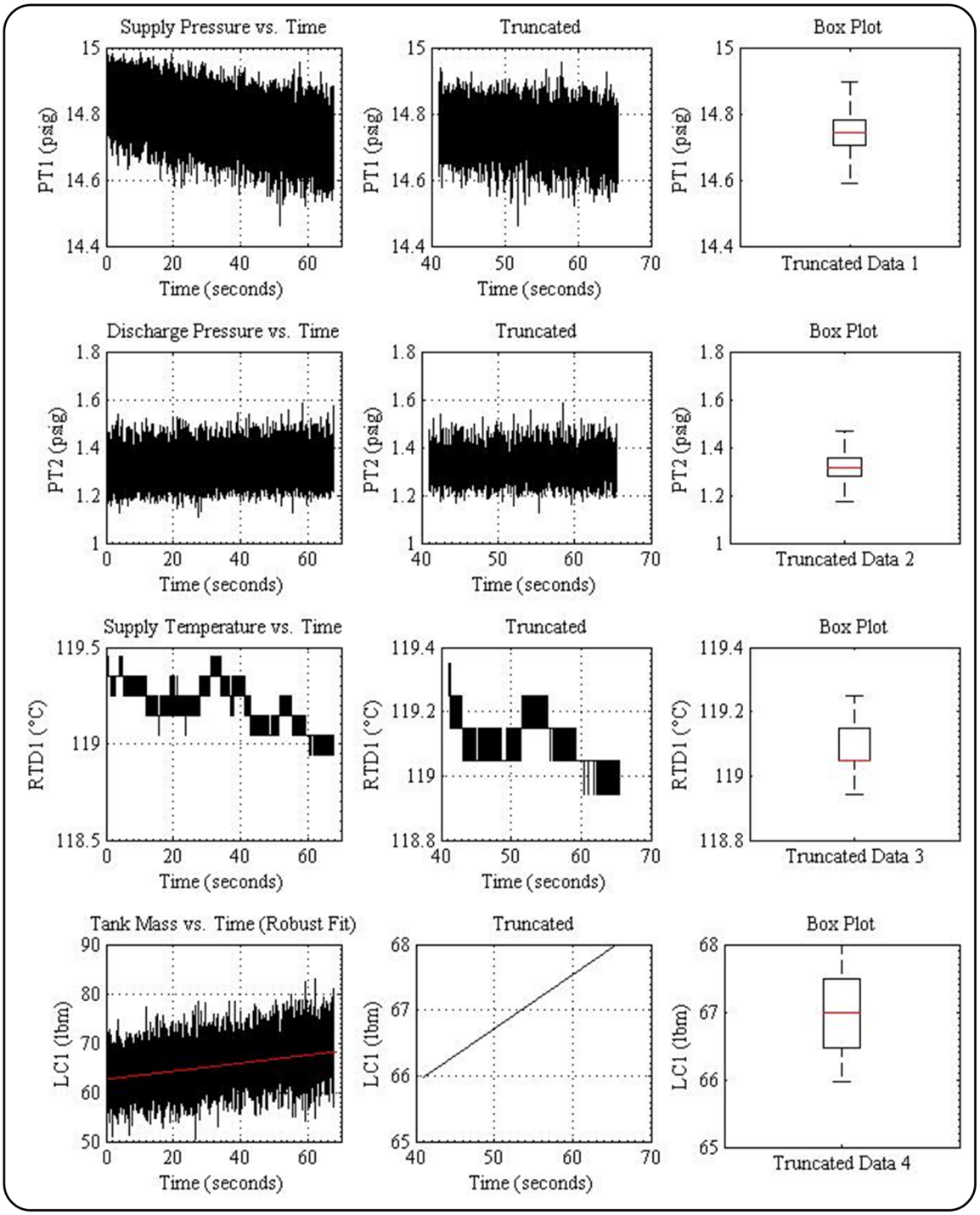

Trial 25

[Pressure = 14.50 psig, Temperature = 120.44°C, Valve Position = 25.00%]

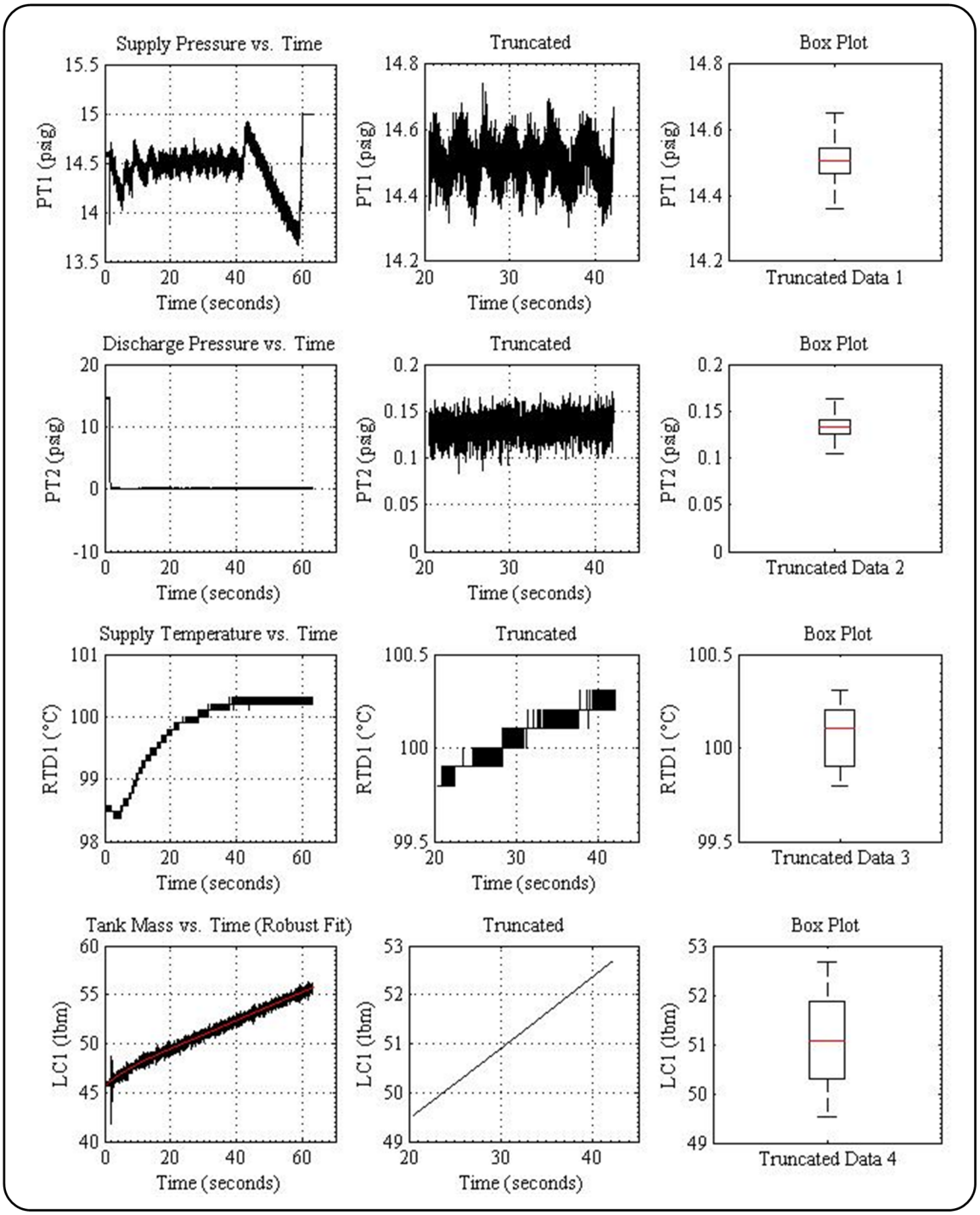

Trial 26

[Pressure = 14.50 psig, Temperature = 100.05°C, Valve Position = 25.00%]

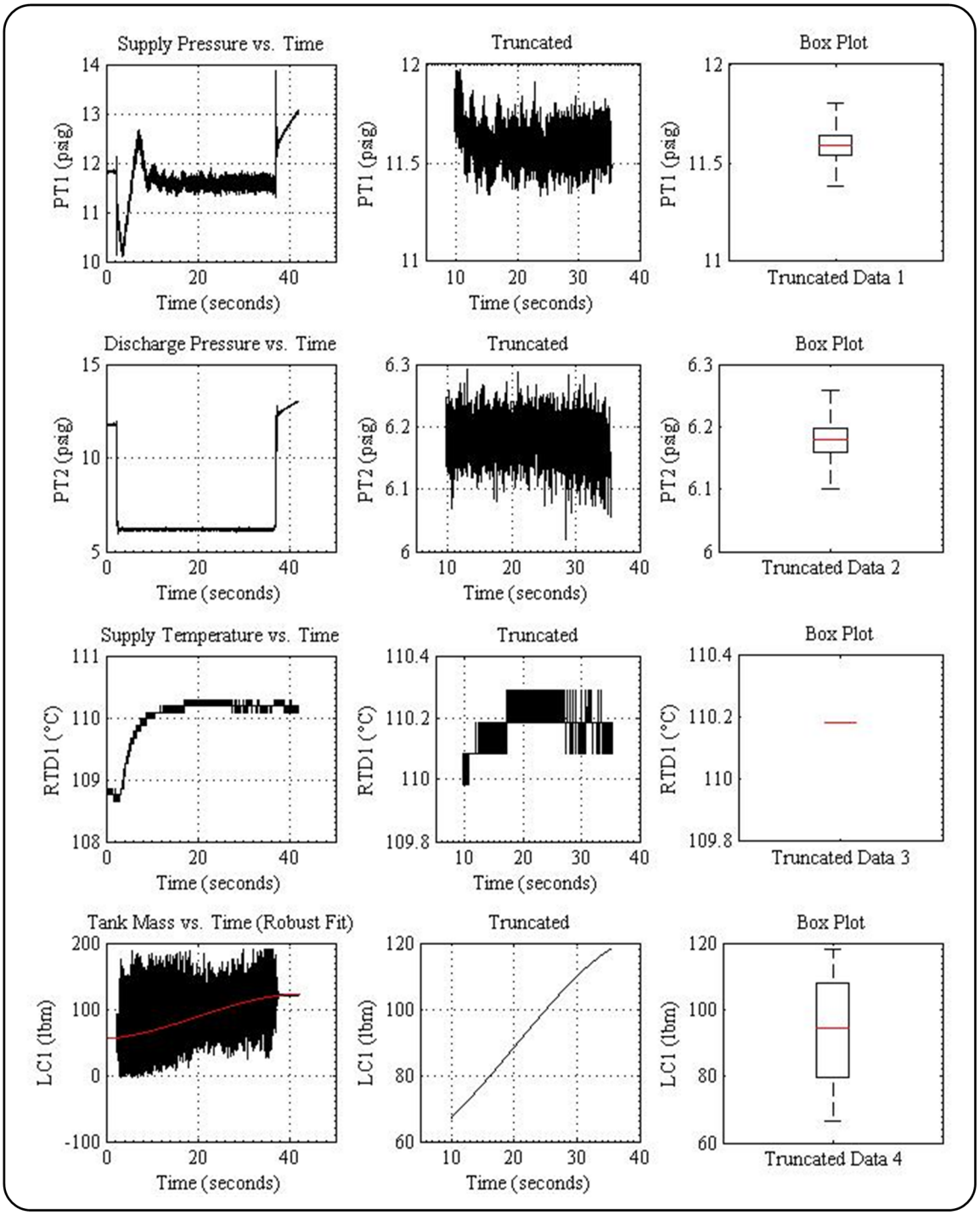

Trial 27

[Pressure = 11.56 psig, Temperature = 110.28°C, Valve Position = 72.25%]

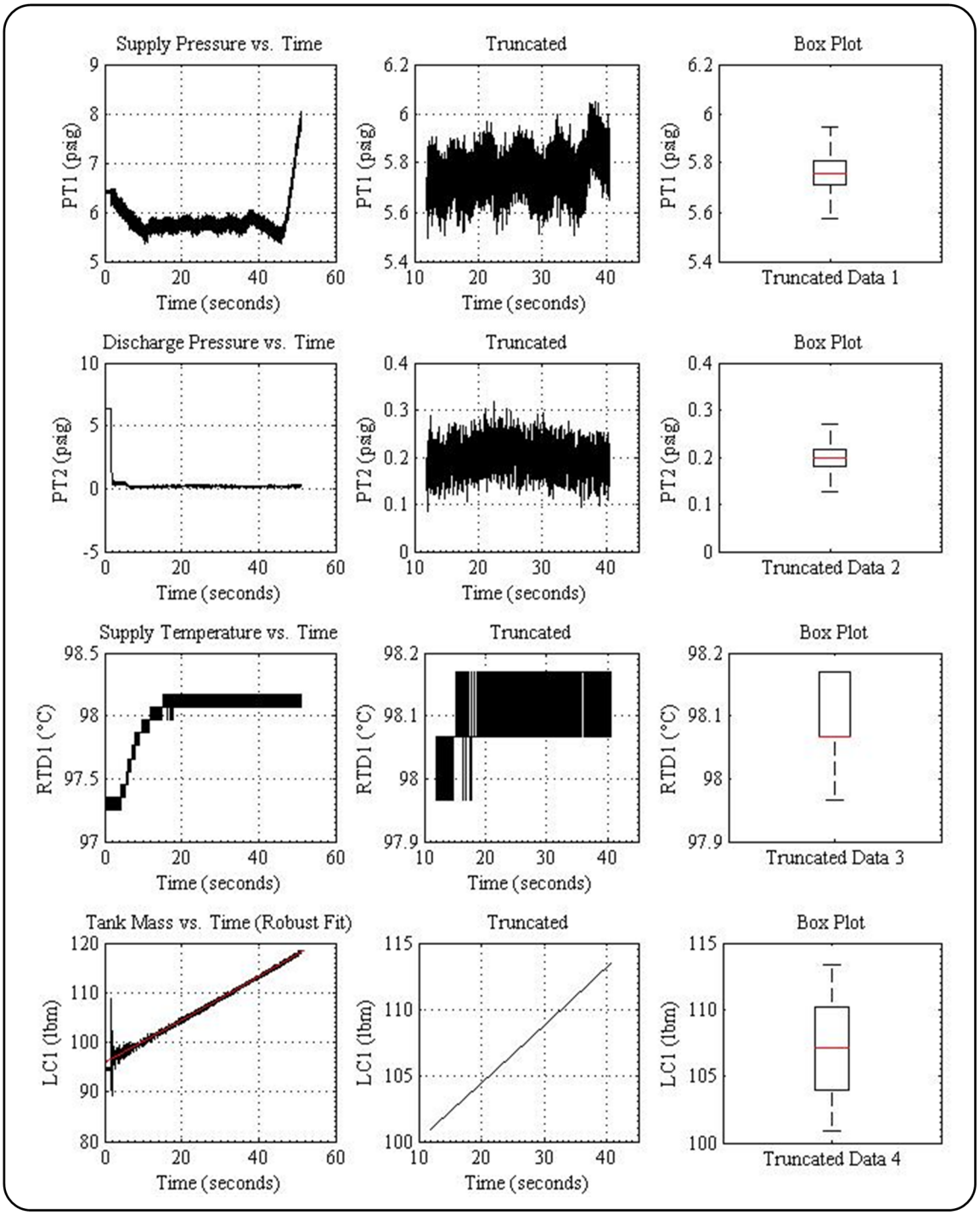

Trial 28

[Pressure = 5.75 psig, Temperature = 98.22°C, Valve Position = 41.50%]

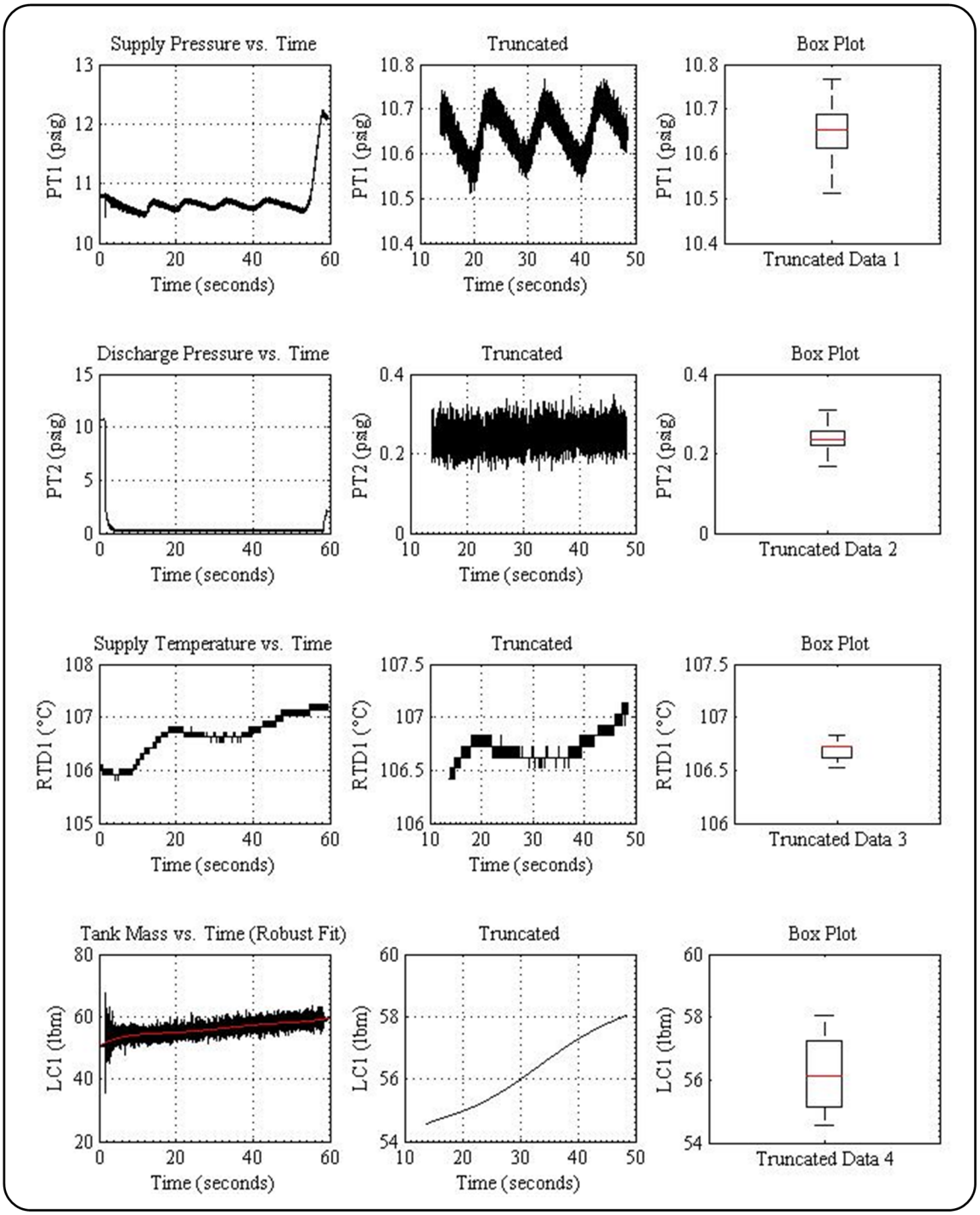

Trial 29

[Pressure = 10.65 psig, Temperature = 106.90°C, Valve Position = 25.00%]

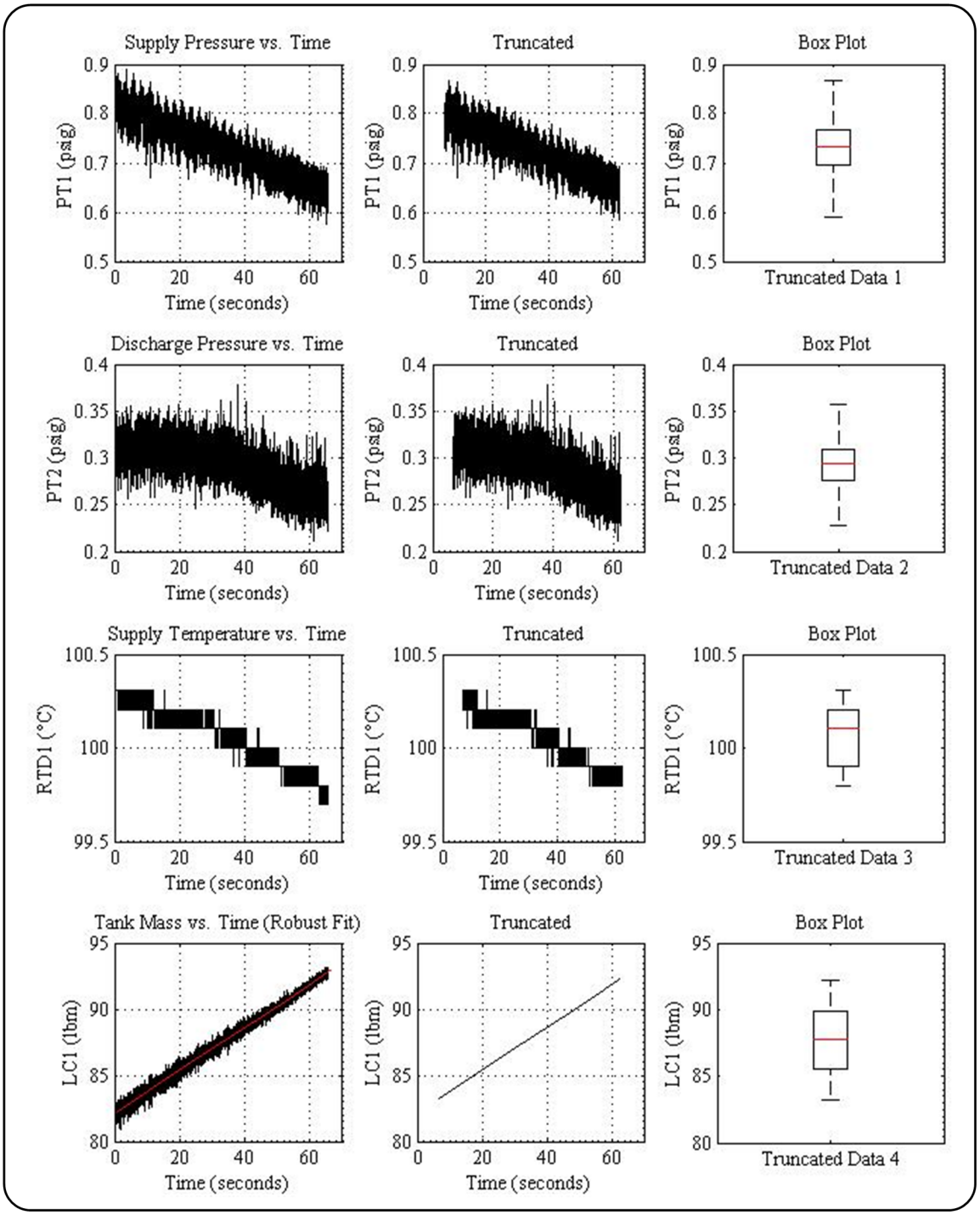

Trial 30

[Pressure = 0.50 psig, Temperature = 100.94°C, Valve Position = 47.8%]

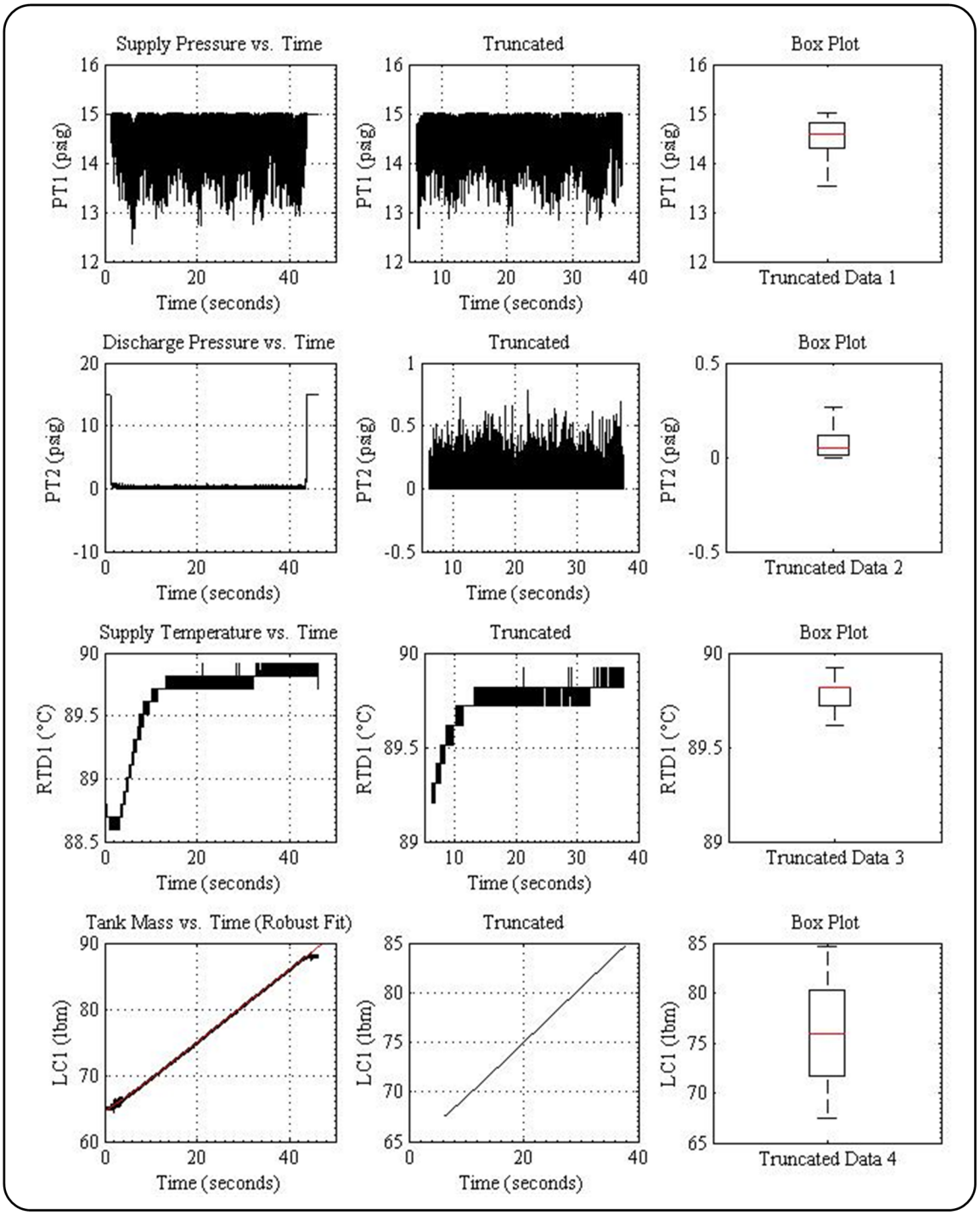

Trial 31

[Pressure = 14.50 psig, Temperature = 90.00°C, Valve Position = 37.38%]

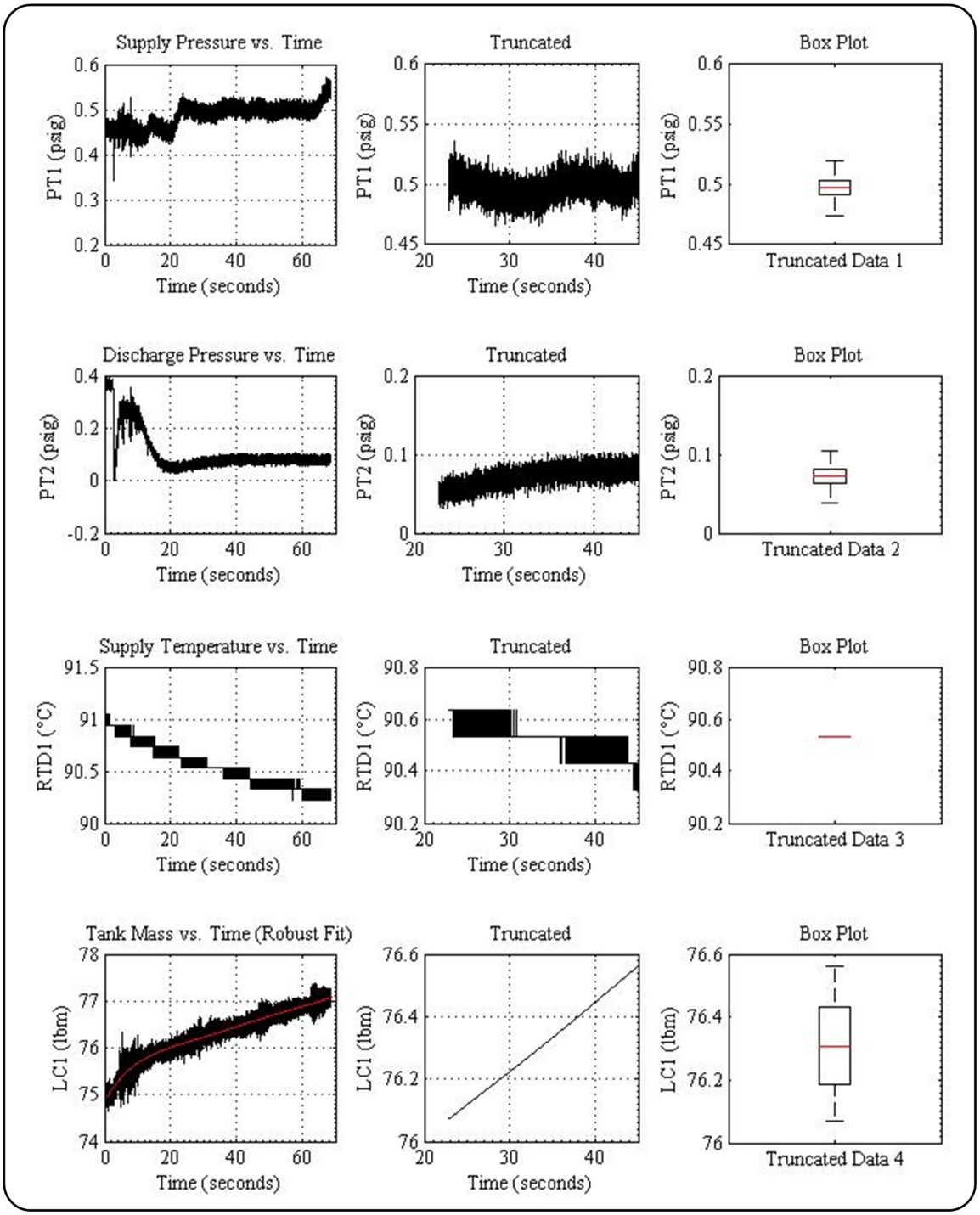

Trial 32

[Pressure = 0.50 psig, Temperature = 90.76°C, Valve Position = 25.00%]

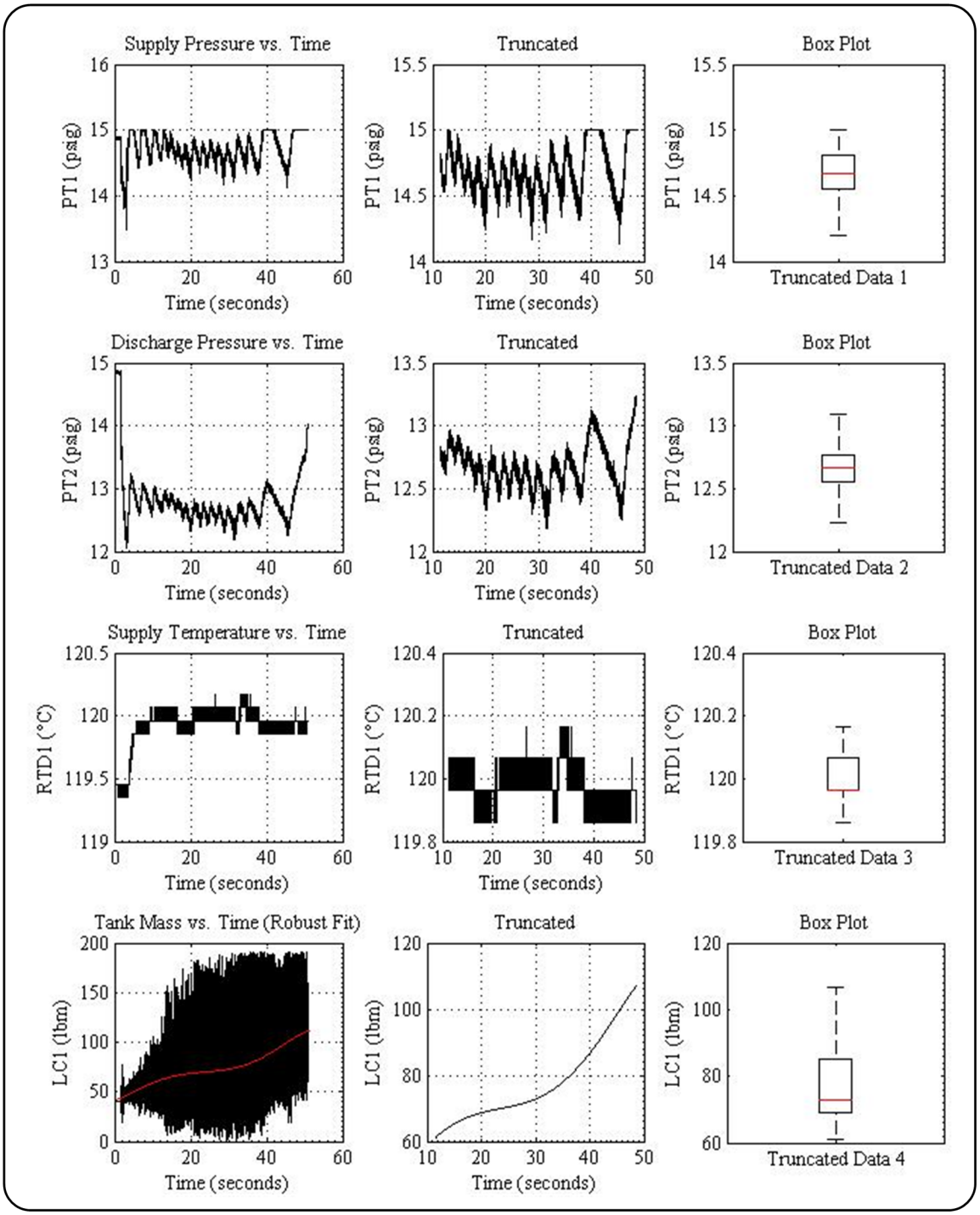

Trial 33

[Pressure = 14.50 psig, Temperature = 120.44°C, Valve Position = 86.13%]

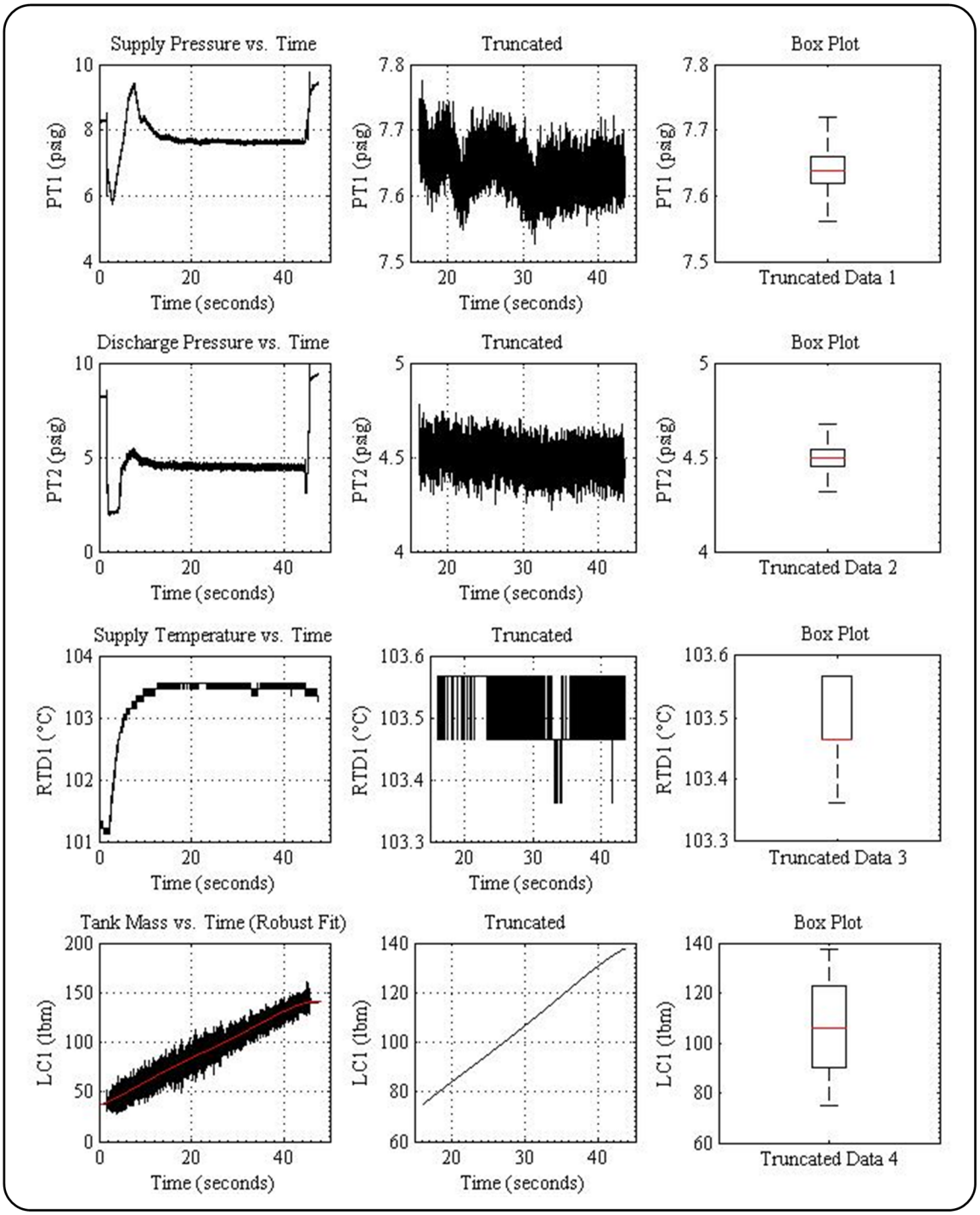

Trial 34

[Pressure = 7.64 psig, Temperature = 103.50°C, Valve Position = 84.25%]

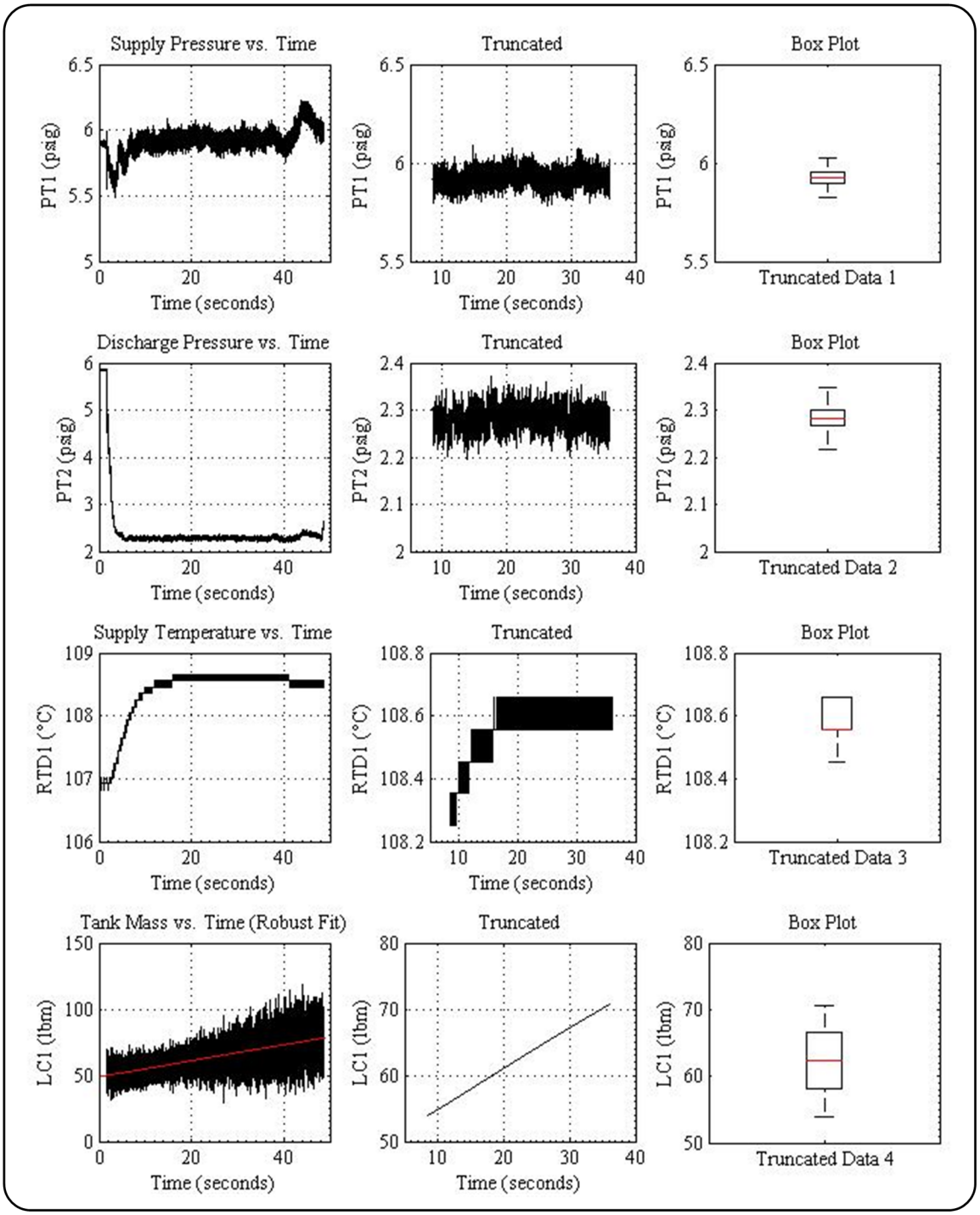

Trial 35

[Pressure = 5.93 psig, Temperature = 108.51°C, Valve Position = 54.88%]

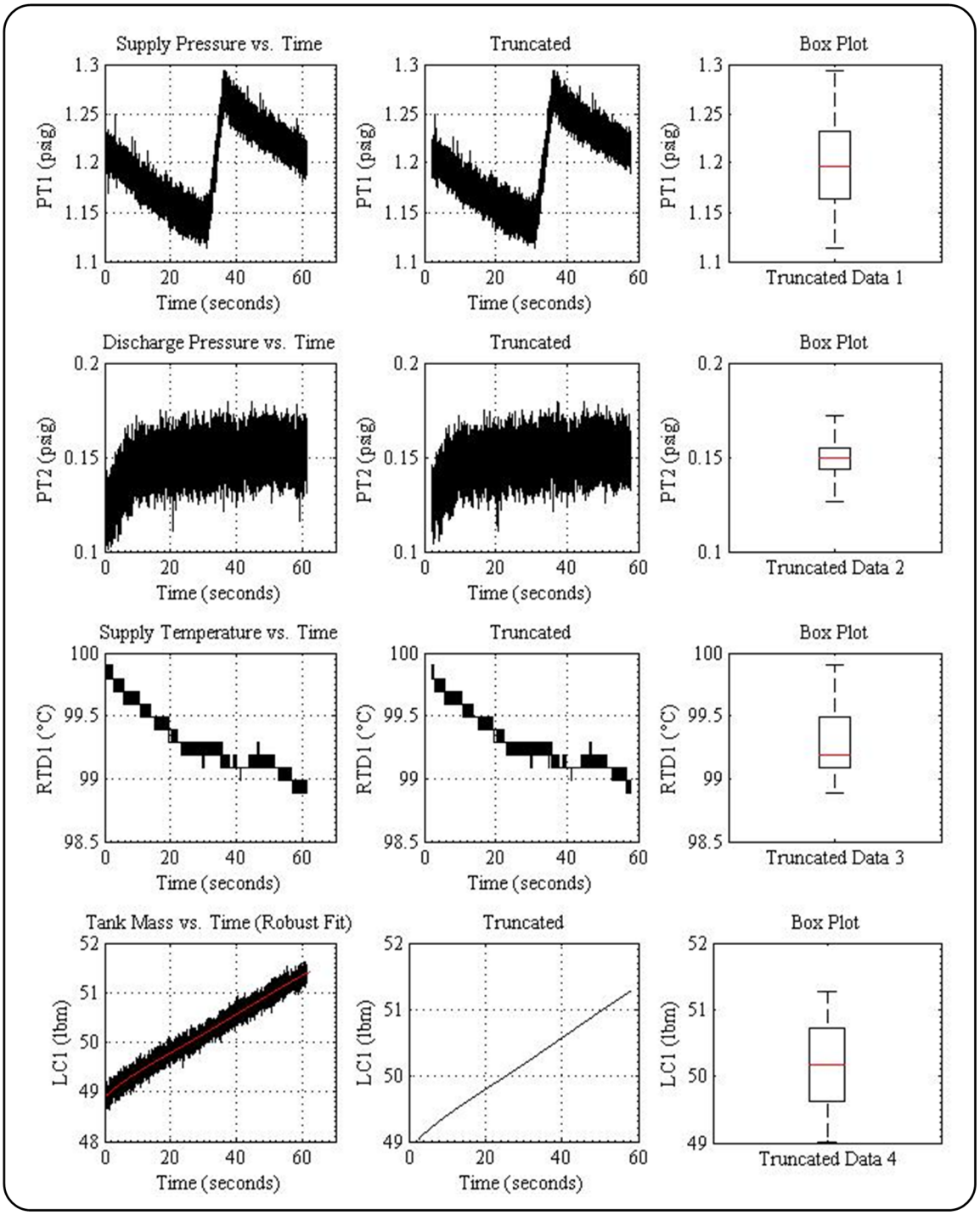

Trial 36

[Pressure = 1.20 psig, Temperature = 100.20°C, Valve Position = 25.00%]

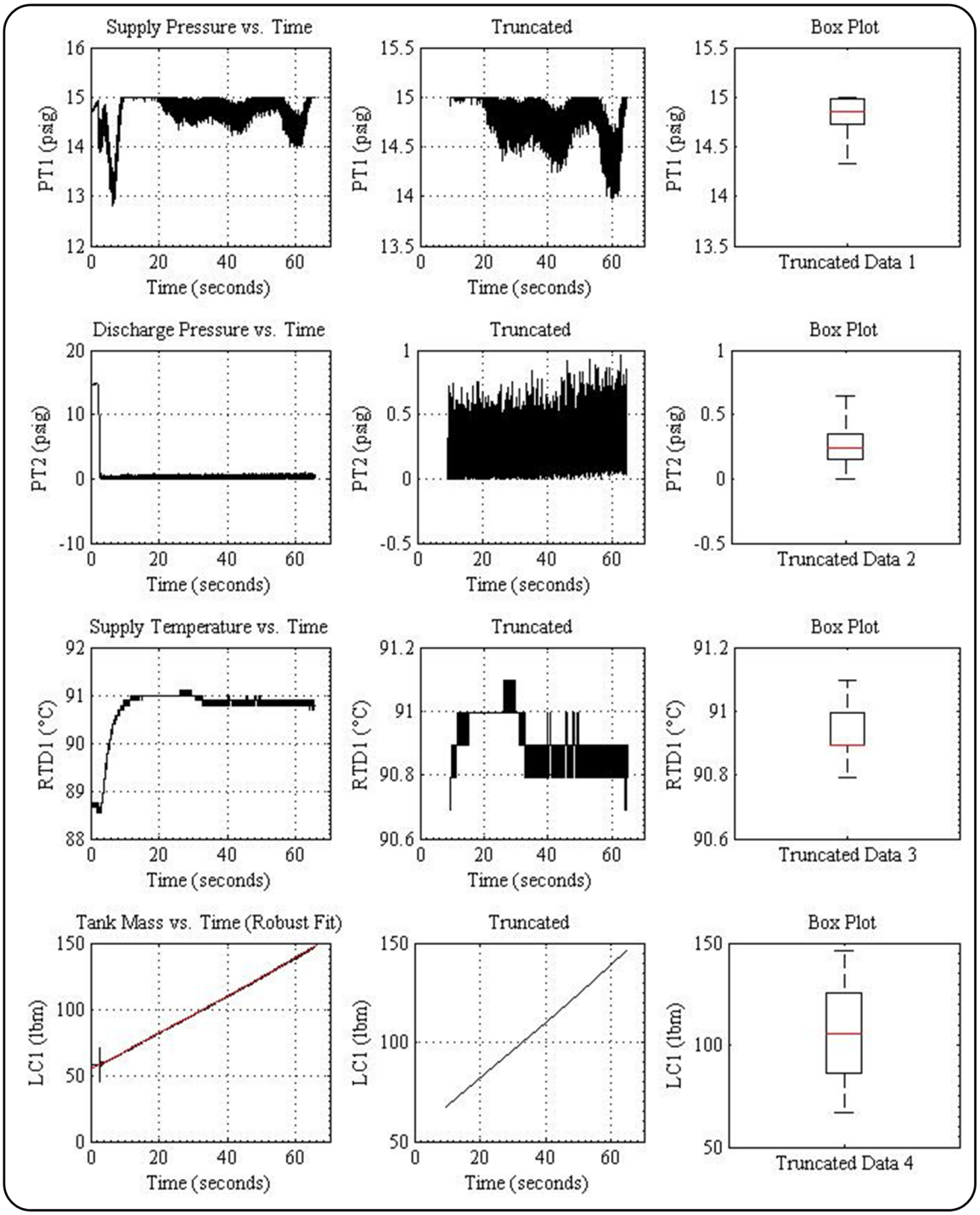

Trial 37

[Pressure = 14.50 psig, Temperature = 90.00°C, Valve Position = 50.00%]

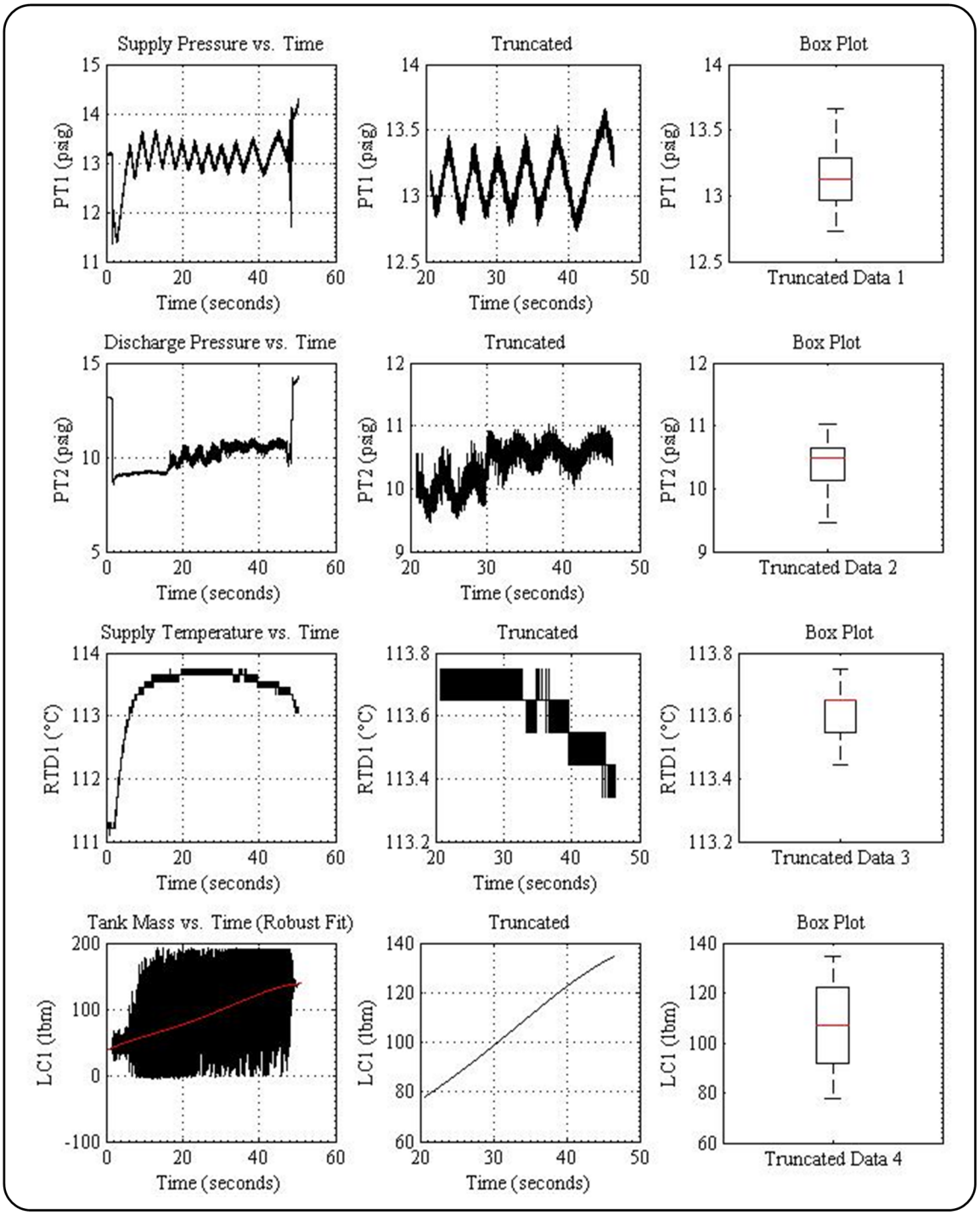

Trial 38

[Pressure = 12.80 psig, Temperature = 113.60°C, Valve Position = 87.00%]

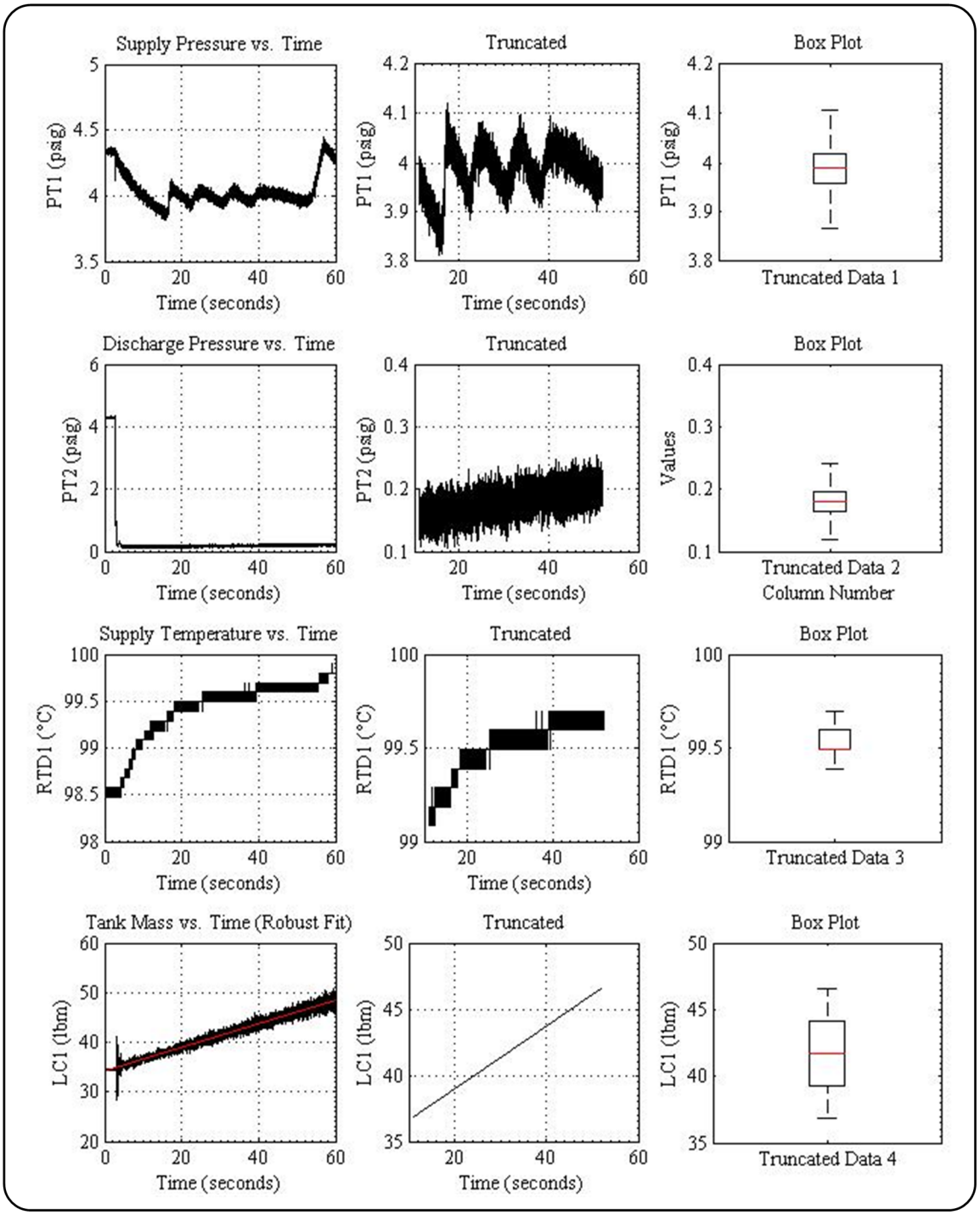

Trial 39

[Pressure = 4.00 psig, Temperature = 99.30°C, Valve Position = 37.00%]

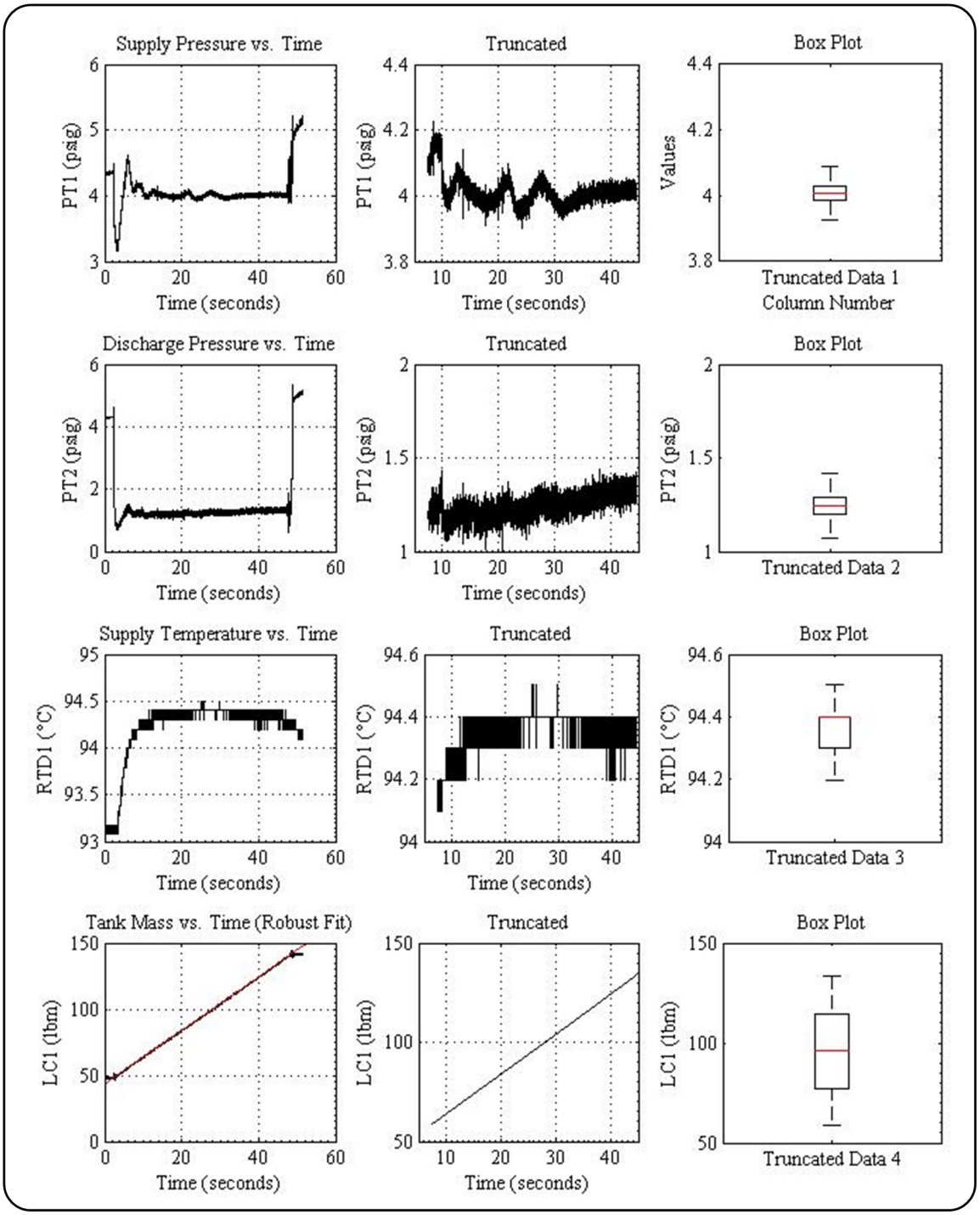

Trial 40

[Pressure = 4.00 psig, Temperature = 94.00°C, Valve Position = 87.00%]

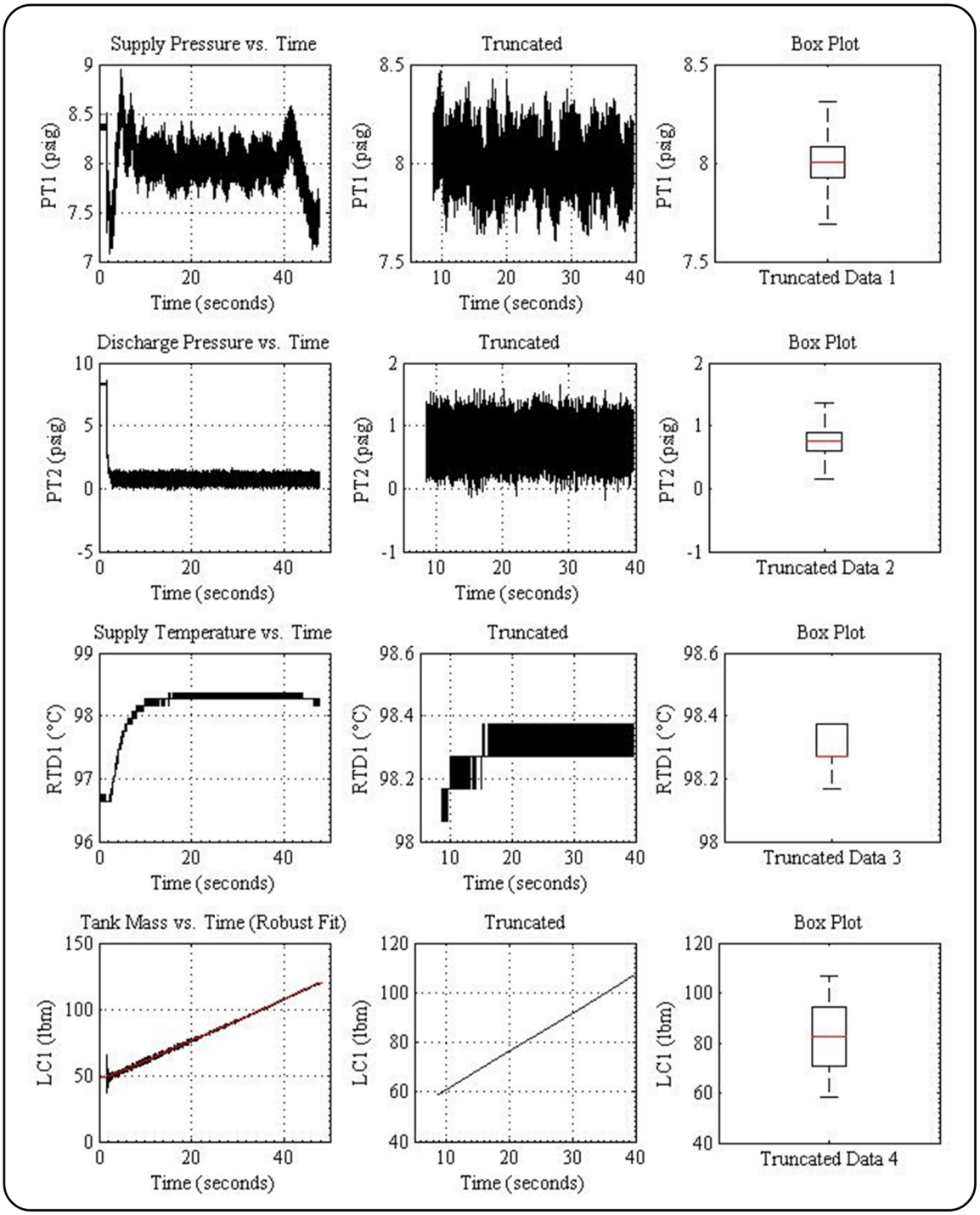

Trial 41

[Pressure = 8.00 psig, Temperature = 98.00°C, Valve Position = 61.70%]

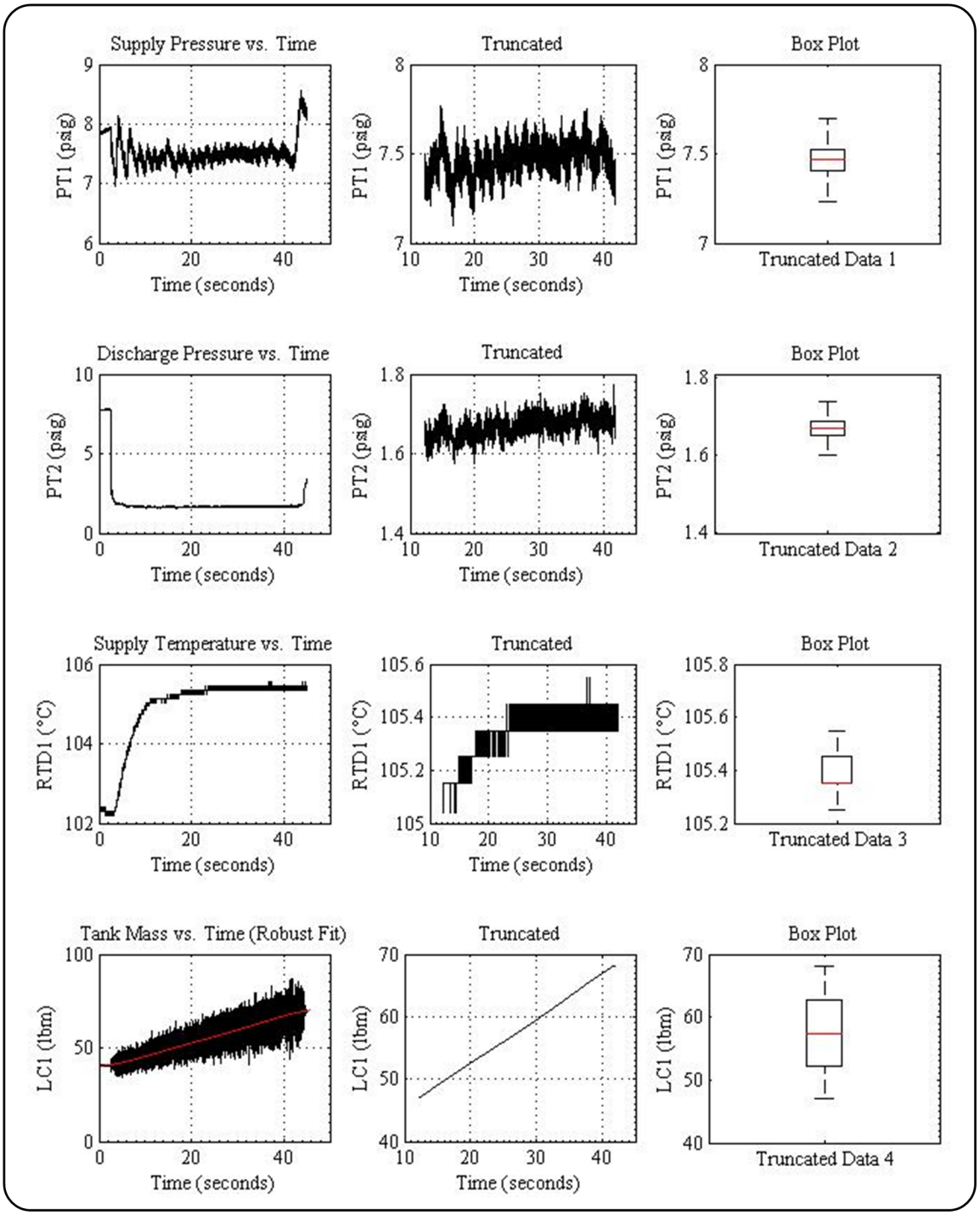

Trial 42

[Pressure = 7.50 psig, Temperature = 105.50°C, Valve Position = 50.00%]

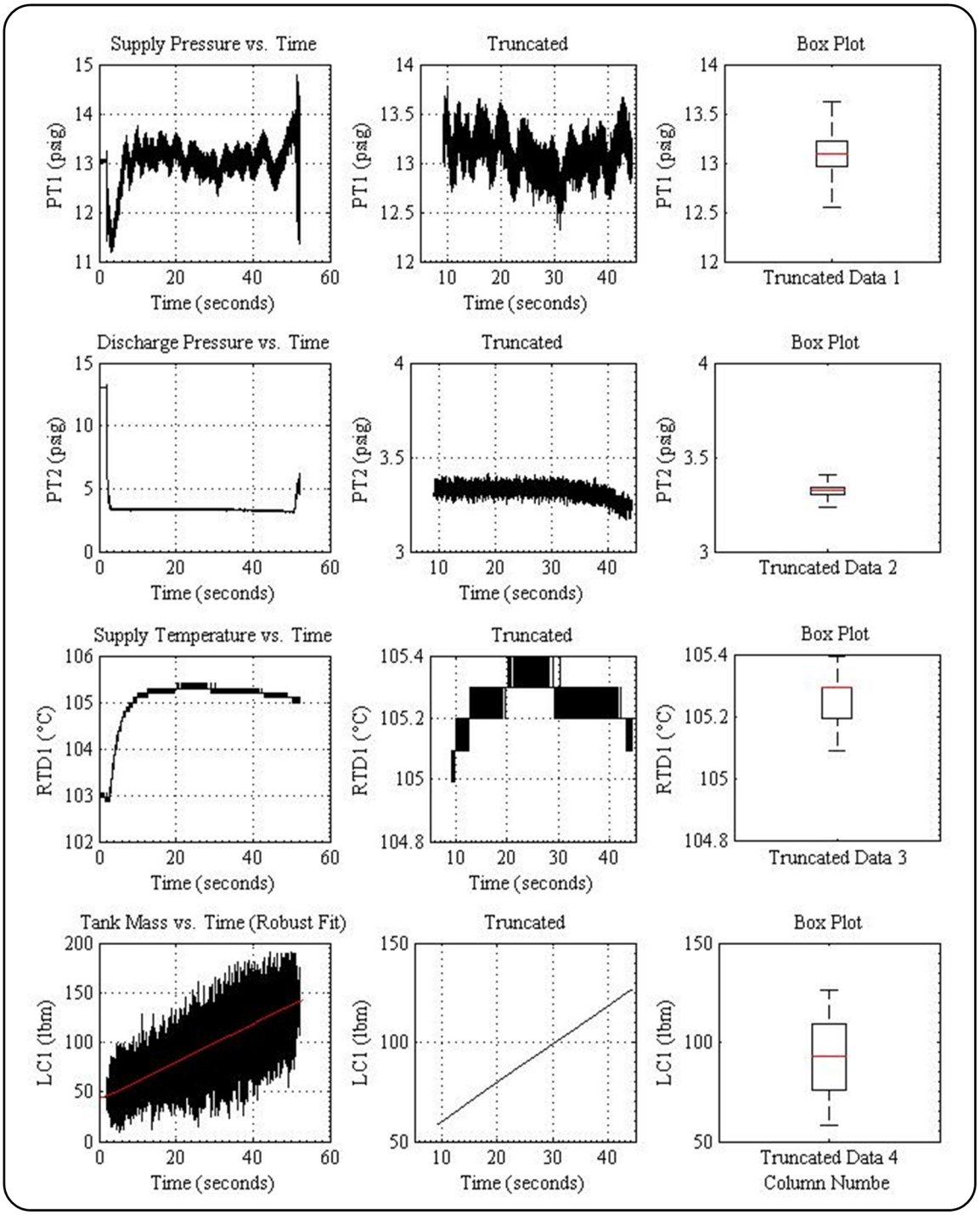

Trial 43

[Pressure = 12.70 psig, Temperature = 105.00°C, Valve Position = 62.00%]

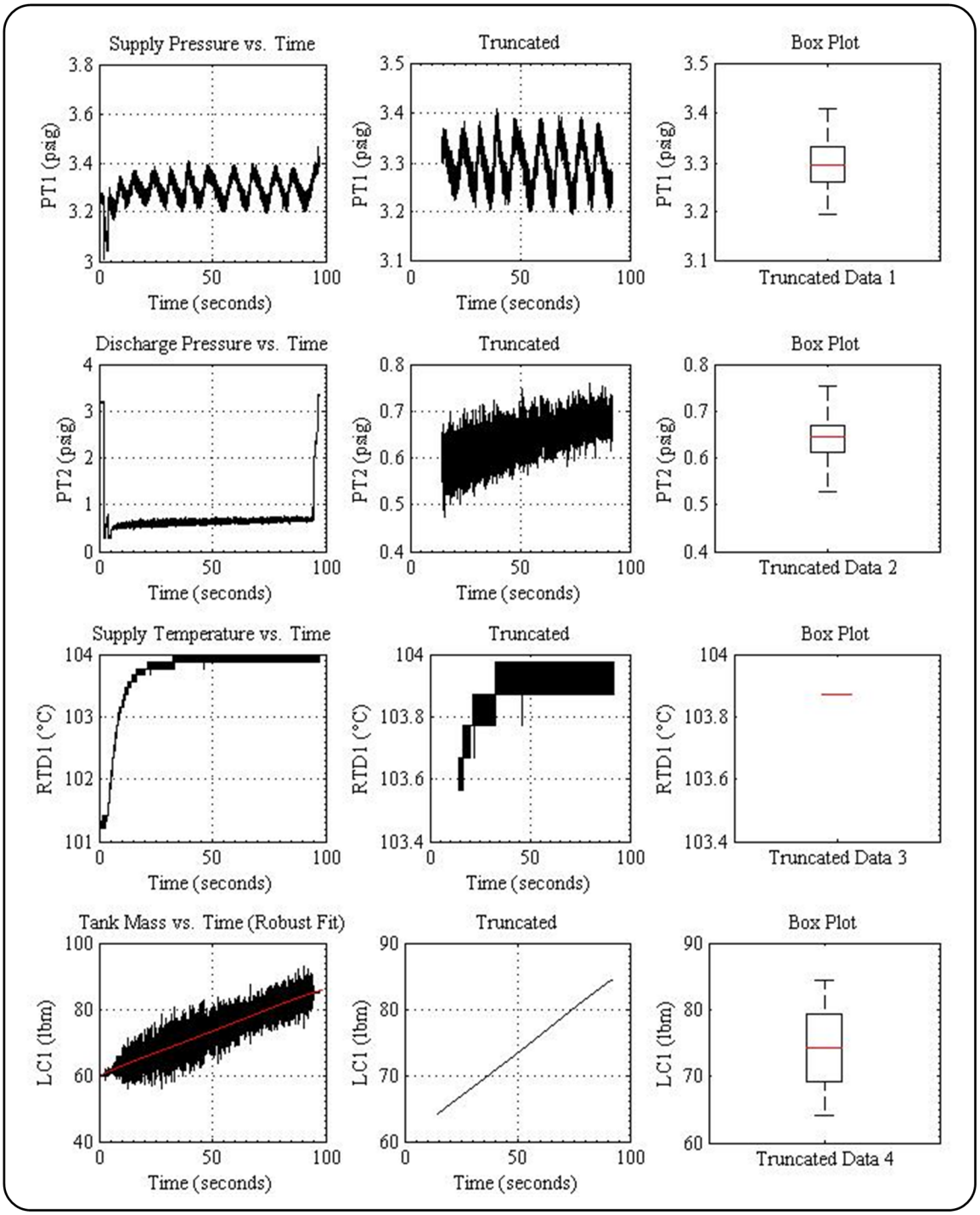

Trial 44

[Pressure = 3.30 psig, Temperature = 103.80°C, Valve Position = 42.00%]

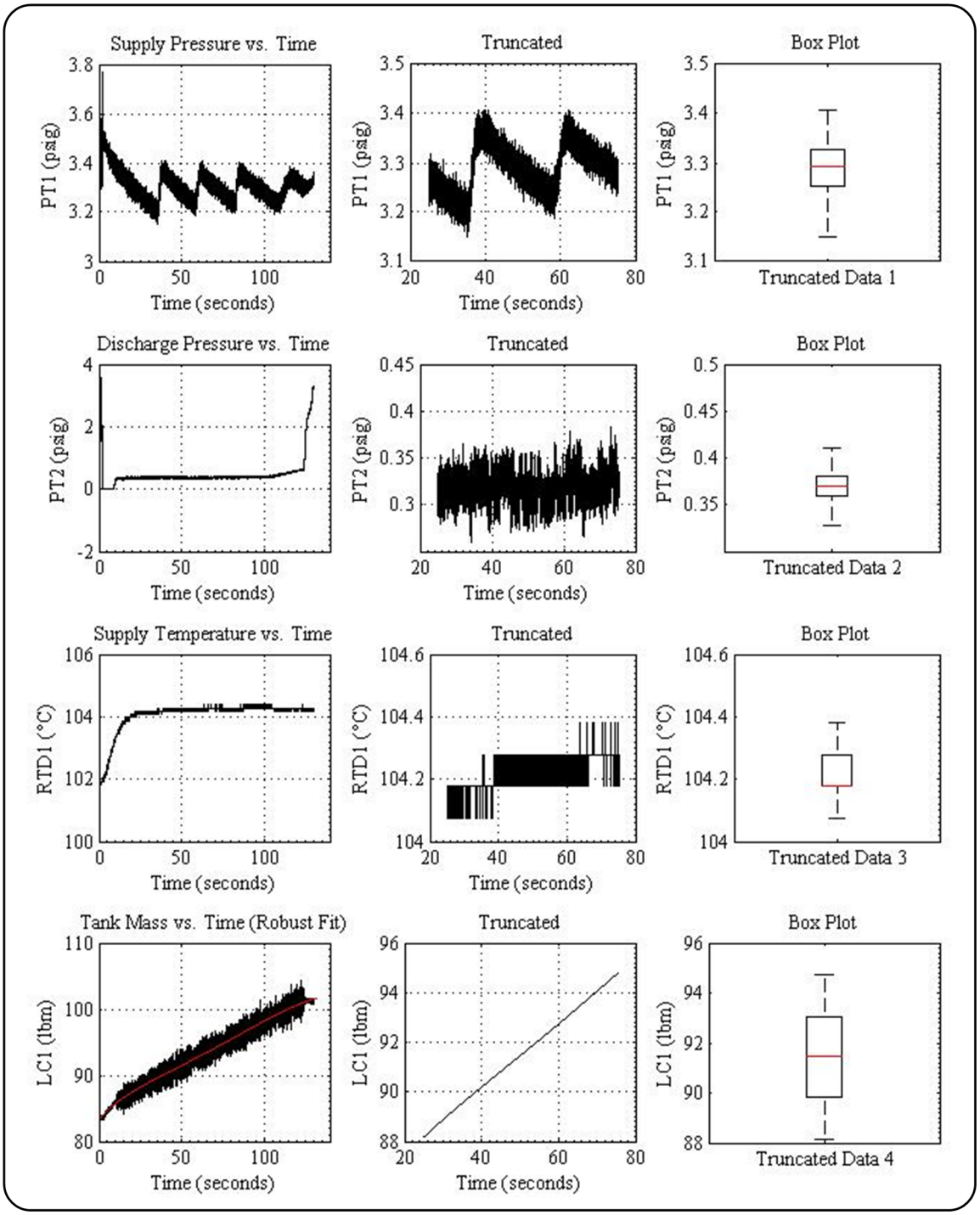

Trial 45

[Pressure = 3.30 psig, Temperature = 104.00°C, Valve Position = 32.00%]

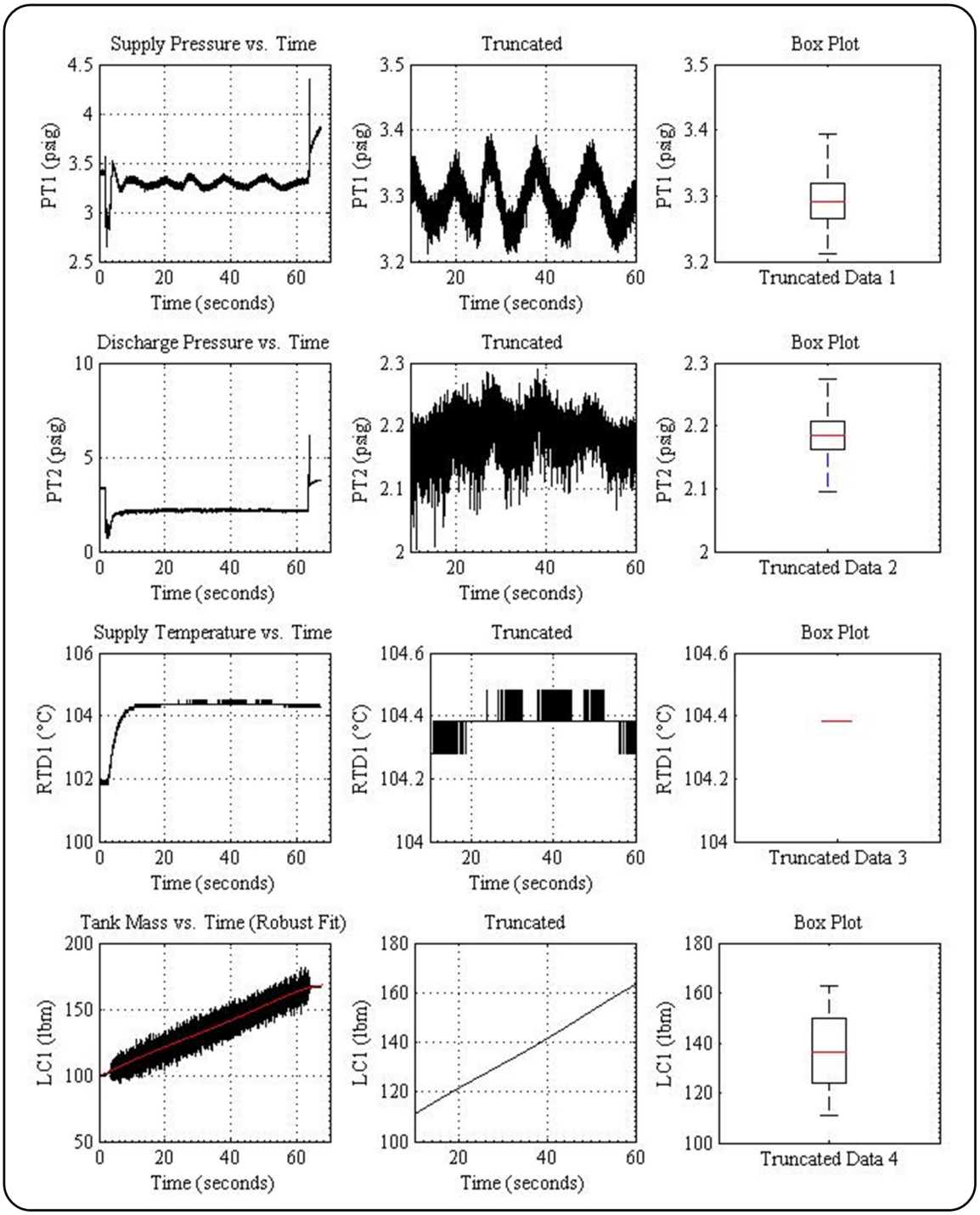

Trial 46

[Pressure = 3.30 psig, Temperature = 104.30°C, Valve Position = 72.00%]

Appendix F

Flow Visualization Apparatus

Discharge Observatory
Supply Observatory


Discharge Observatory